



2014

Society for Thermal Medicine



31st Annual Meeting
Marriott City Center
Minneapolis, MN

Tuesday 6 May		Hour	Wednesday 7 May		Thursday 8 May		Friday 9 May			Saturday 10 May	
		7:00	Breakfast - Ballroom 1 -		Breakfast - Ballroom 1 -		Breakfast - Ballroom 1 -			Breakfast - Ballroom 1 -	
		8:15	Refresher: Thermonutrality Elizabeth Repasky - Ballroom 2 -	Refresher: Radiation Biology Chang Song -Deer/Elk Lake -	Refresher: Current State of Nanotoxicology Christy Haynes - Ballroom 2 -	Refresher: Device Development Satish Ramadhyan & Erik Rudie - Deer/Elk Lake -	Refresher: Cell Death Mechanisms John Pearce - Ballroom 2 -	Refresher: Exercise Physiology Lee Jones - Deer/Elk Lake	Refresher: Japanese Thermal Medicine Update Satoshi Kokura -Pine/Cedar/Birch-	Refresher: HIFU Update Emad Ebbini - Ballroom 2 -	Refresher: Thermoradiotherapy for Cancer Stem Cells Jennifer Yu - Deer/Elk Lake -
		9:15	Advanced Magnetic Resonance Imaging Approaches to Thermal Therapy and Nanomedicine Biodistribution - Ballroom 2 -		Heat Induced Drug Delivery and Monitoring of Release Using Ultrasound - Ballroom 2 -		Local Tumor Ablation plus Immune Stimulation: Towards in situ Cancer Vaccines - Ballroom 2 -			Clinical Update on Thermal Ablation medicine - Ballroom 2 - 9:30 – 11:00	
		9:30									
Finance Committee Meeting - Excelsior - 10:30 - 11:30		10:30	Coffee Break - Ballroom 1 -		Coffee Break - Ballroom 1 -		Coffee Break - Ballroom 1 -				
		10:30									
		10:45	Minnesota nanoparticle and thermal therapy symposium - Ballroom 2 -		Treatment Planning and Guidance - Ballroom 2 -	Physiological/Immunol ogical Aspects of Thermal Medicine -Deer/Elk Lake Room -	Focused Ultrasound in Radiation Oncology - Ballroom 2 -	Thermosensitive and Photothermal Nanomedicine - Deer/Elk Lake Room -		Coffee Break - Atrium -	
		12:15								Heat Generating Nanomedicine - Ballroom 2 - 11:15 – 12:45	
IJH Editorial Board Meeting - Excelsior - 12:00 - 1:30		12:15	Lunch break	New Investigator Luncheon -St. Croix II - 6 th Floor	Lunch break		STM Business Meeting Luncheon - Ballroom 2 -				
		13:45								New Devices & Approaches - Deer/Elk Lake Room - 11:15 – 12:45	
Registration Desk Open - Lobby - 1:00 - 4:40	STM Council Meeting - Excelsior - 2:30 - 4:30	13:45	Common Topics in Thermal Medicine: Computational Methods in Treatment Planning - Ballroom 2 -	Non-Oncological Application of Thermal Medicine -Deer/Elk Lake Room -	Image Guided Thermal Therapy - Ballroom 2 - 1:45 – 3:15		Common Topics Thermal Medicine: Cell Death/ Sensitization - Ballroom 2 -	Metabolism Workshop - Deer/Elk Lake Room -			
		15:45			President's Reception - Ballroom 2 - 3:15 – 3:45		Coffee Break - Ballroom 1 -				
		15:45	Coffee Break - Ballroom 1 -								
		16:00	New Investigator Symposium - Ballroom 2 -		Expanding the Clinical Hyperthermia Experience - Ballroom 2 - 3:45 – 6:15		William Dewey Award: Mark Dewhirst - Ballroom 2 – 4:00-5:00				
Exhibitor Set-Up Poster Hanging - Ballroom 1 - 5:00		18:00	Poster Session & Reception - Ballroom 1 -				J. Eugene Robinson Award Rolf Issels - Ballroom 2 – 5:00-6:30				
Drs. Chang Song and Dennis Leeper: 31 meetings later & Dr. Rosemary Wong: Update on Changes at NIH and NCI - St. Croix II - 6 th floor 5:30 – 6:15		18:00					Robinson Dinner <i>Mason's Restaurant & Barre</i>				
		19:30									
Welcome Reception - St. Croix Prefunction Terrace - 6 th floor 6:30 – 8:00											

Table of Contents

Program Organizing Committee	4
Governing Council	6
Keynote Speakers.....	8 - 9
William Dewey Award	110
J. Eugene Robinson Award.....	11
STM New Investigator Awards	12 - 13
Special Session: NIH Update	14
Refresher Courses.....	15 - 17
Thermoneutrality	
Radiation Biology	
Current State of Nanotoxicology	
Device Development	
Cell Death Mechanisms	
Exercise Physiology in the oncology setting	
Japanese Thermal Medicine Update	
HIFU Update	
Thermoradiotherapy for Cancer Stem Cells	
Conference Program.....	18
Registration Desk Hours	5, 18
Tuesday, May 6th	18
Wednesday, May 7th	20
Thursday, May 8th	30
Friday, May 9th	35
Saturday, May 10th.....	40
Abstracts.....	44 - 188
Wednesday, May 7th	44
Thursday, May 8th	107
Friday, May 9th	136
Saturday, May 10th.....	167
Poster Session.....	77
Author Index	189

31st Annual Meeting of the Society for Thermal Medicine

We thank our sponsors!

Platinum



Gold



Silver



Bronze Sponsors



RADIATION RESEARCH SOCIETY
<http://www.radres.org>



STM 2014 Program Organizing Committee



Committee members:

Chair: Robert J. Griffin, PhD	University of Arkansas for Medical Sciences
Sharon Evans, PhD	Roswell Park Cancer Institute
Dieter Haemmerich, PhD	Medical University of South Carolina
Erik Cressman, MD, PhD	University of Minnesota
Muneeb Ahmed, MD	Beth Israel Medical Center
John Bischof, PhD	University of Minnesota
Timo ten Hagen, PhD	Erasmus Medical Center
P. Jack Hoopes, PhD, DVM	Dartmouth University
Chang W. Song, PhD	University of Minnesota
Jennifer Yu, PhD	Cleveland Clinic
Jason Stafford, PhD	MD Anderson
Nathan Koonce, MS	University of Arkansas for Medical Sciences

Special Thanks to:

Manager **Jeff Mercer** of Allen Press, Inc. and Meeting Planner **Kathryn Harth and team (Nichole Stoddard, Kelli Park Fuhrmann, Tony Ballard)** from Kansas State Conference services, for their assistance with the STM 2014 Annual Meeting. **Nathan Koonce**, PhD candidate at University of Arkansas for Medical Sciences for help with the print program and the meeting prospectus. Graduate students **Harishankar Natesan** (U of MN), **Leoni Rott** (U Hanover/U of MN), **Katie Hurley** (U of MN) and **Nathan Koonce** (UAMS) for helping with audiovisual and operational items during the meeting.

Meeting Information

Registration Desk Hours

HOUR	DAY	LOCATION
1:00 – 4:30 5:00 – 7:30	Tuesday, May 6 th	Atrium (4 th floor) Minnesota room (6 th floor)
7:00 - 11:00 1:00 – 6:30	Wednesday, May 7 th	Atrium (4 th floor)
7:00 - 11:00 1:00 - 6:30	Thursday, May 8 th	Atrium (4 th floor)
7:00 - 11:00 1:00 - 5:00	Friday, May 9 th	Atrium (4 th floor)
7:00 - 11:00	Saturday, May 10 th	Atrium (4 th floor)

Internet Instructions for meeting areas:

Your Conference Code:

STM14

Wired Connection Instructions

1. With your computer turned OFF, connect an Ethernet cable to your computer
2. Turn ON your computer and launch web browser
3. Click on the grey login link to be directed to login page.
4. Follow the on-screen instructions and enter the Conference Code when prompted

Wireless Connection Instructions

1. With your computer turned ON, set your wireless adapter SSID to **Marriott_CONF**.
2. Launch a web browser
3. Click on the grey login link to be directed to login page.
4. Follow the on-screen instructions and enter the Conference Code when prompted



Governing Council Society for Thermal Medicine (2014 – 15)

Mission Statement

The Society for Thermal Medicine is a 501(c)(3), non-profit organization whose mission is to significantly improve patient treatment outcomes by advancing the science, development and application of Thermal Therapy.

Our Society strives to:

- Promote new discovery in thermal biology, physics/engineering, and medicine.
- Sponsor high quality forums for education of medical professionals in the practice of thermal medicine.
- Advocate for increased patient access to appropriate, high quality, thermal therapies.

President: Robert J. Griffin, PhD

University of Arkansas for Medical Sciences
Dept. of Radiation Oncology
Little Rock, AR

Past President: Dieter Haemmerich, PhD, DSc

Medical University of South Carolina
Department of Pediatrics
Charleston, SC

President-elect: Erik Cressman, MD, PhD

University of Texas MD Anderson Cancer Center
Department of Interventional Radiology
Houston, TX

Secretary / Treasurer: Robert Ivkov, MD

Johns Hopkins School of Medicine
Department of Radiation Oncology
Baltimore, MD

Vice President-elect: Jason Stafford, PhD

University of Texas MD Anderson Cancer Center
Department of Imaging Physics
Houston, TX

IJH Editor: Mark W. Dewhirst, PhD, DVM

The International Journal of Hyperthermia
Duke University Medical Center
Department of Radiation Oncology
Durham, NC

Councilors

Councilors: Biology /Chemical Sciences

2014-2015

Nicole Levi-Polyachenko, PhD - Wake Forest University

2013-2014

Stuart Calderwood, PhD - Beth Israel Deaconess Medical Center

Councilors: Clinical/Medical Sciences

2014-2015

Jennifer Yu, MD, PhD - Cleveland Clinic

2013-2014

Barry Wilcox, MD, FACRO - Baylor University Medical Center

Councilors: Engineering/Physical Sciences

2014-2015

Robert McGough, Michigan State

2013-2014

Christopher Brace, PhD, MSEE - University of Wisconsin



Minneapolis Points of Interest

Taste of the Twin Cities <http://tastetwincities.com/>

Select from a variety of tours in downtown Minneapolis, each includes several restaurant stops and a tour guide. Some tours are walking, others provide transportation. Some are outdoors, and some are completely indoors, taking advantage of the 80 miles of skywalks all over downtown Minneapolis.

Minneapolis Convention & Visitors Bureau <http://www.minneapolis.org>

For great suggestions about [where to eat](#)

For information about [local tours and attractions](#)

For a schedule of [local arts and entertainment](#)

Food Trucks on Marquette – A quick and unique lunchtime opportunity!

Just two blocks from the STM conference hotel, food trucks of all varieties that set-up from 11 a.m. to 2 p.m. Monday-Friday to provide lunch to the downtown masses.

Mill City Museum <http://www.millcitymuseum.org/>

A must see for first-time-visitors to the Twin Cities, built into the ruins of what was once the world's largest flour mill, Mill City Museum is located on the historic Mississippi Riverfront. Here, visitors of all ages learn about the intertwined histories of the flour industry, the river, and the city of Minneapolis.

MPLS Warehouse Entertainment District <http://mplwarehouse.com/>

If you're looking for a night out on the town, the Warehouse District is a great place visit, and it's within walking distance of the STM conference hotel.



Mall of America® is located in Bloomington, MN - *only 25 min direct light rail ride from downtown Minneapolis*. As one of the most visited tourist destinations in the world, Mall of America features - 520 stores, 50 restaurants and attractions galore, including Nickelodeon Universe®, the nation's largest indoor theme park. **Plus, there's no sales tax on clothing or shoes!**

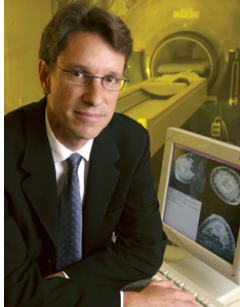
~~~~~  
**SAVE THE DATES!!!!!!**

**2015 STM meeting, April 14-18, Orlando, FL**  
**Buena Vista Palace Hotel and Spa**  
**(next to Downtown Disney)**



## Keynote Speakers

Wednesday, May 7  
9:30 am, Ballroom 2



### Michael Garwood, PhD

Professor  
Center for Magnetic Resonance Research  
University of Minnesota  
Minneapolis, Minnesota

#### **“Advanced Magnetic Resonance Imaging Approaches to Thermal Therapy and Nanomedicine Biodistribution”**

The Garwood laboratory focuses on developing cutting-edge MRI and MR spectroscopy techniques and on exploiting them in studies of tissue function, metabolism, and microstructure. An emphasis has been on identifying and validating quantitative metrics to assess normal and disease states non-invasively with imaging, and on applying them to learn about metabolism, hemodynamics, and tissue micro-environment. On the technical side, the Garwood group has recently made a significant advancement in the way MRI is performed – a technique called SWIFT. With SWIFT, broadband frequency-swept excitation, together with extremely short acquisition delay, make it possible to also preserve frequency-shifted signals in the vicinity of magnetic objects. For example, magnetically-labeled nanoparticles (e.g., SPIOs), which cause signal voids in conventional MR images, give rise to positive contrast (bright spots) in SWIFT images, thus improving the capability to track and quantify targeted contrast agents and molecular therapies, as well as magnetically-labeled cells.

Thursday, May 8  
9:30 am, Ballroom 2



### Katherine Ferrara, PhD

Professor  
Biomedical Engineering  
University of California-Davis  
Davis, California

#### **“Ultrasound-guided drug and gene delivery”**

Prior to her PhD, Dr. Ferrara was a project engineer for General Electric Medical Systems, involved in the development of early magnetic resonance imaging and ultrasound systems. Following an appointment as an Associate Professor in the Department of Biomedical Engineering at the University of Virginia, Charlottesville, Dr. Ferrara served as the founding chair of the Department of Biomedical Engineering at UC Davis. She is currently a Distinguished Professor of Biomedical Engineering at UC Davis. Her laboratory is known for early work in aspects of ultrasonics (e.g. radiation forces and phase inversion techniques) and has more recently expanded their focus to broadly investigate molecular imaging and drug delivery. She is the Director of the Center for Content Rich Evaluation of Therapeutic Efficacy (cCRETE) as part of the UC Davis RISE program. Dr. Ferrara received the Achievement Award from the IEEE Ultrasonics, Ferroelectrics and Frequency Control Society in 2012, which is the top honor of this society. She is a member of the National Academy of Engineering and a fellow of the IEEE, American Association for the Advancement of Science, the Biomedical Engineering Society, the Acoustical Society of America and the American Institute of Medical and Biological Engineering.

## Keynote Speakers

Friday, May 9

9:30 am, Ballroom 2

### **Gosse Adema, PhD**



Professor  
Department of Tumor Immunology  
Radboud University  
Nijmegen, Netherlands

**“Local Tumor Ablation plus Immune Stimulation: Towards in situ Cancer Vaccines”**

Gosse J. Adema obtained his PhD degree in 1991 from the University of Utrecht, working at the department of Physiological Chemistry. He held a post-doc position at the division of Immunology at the Netherlands Cancer Institute (1991-1994) where he discovered the melanocyte differentiation antigen Gp100. In 1994 he moved to the Radboud medical center to start his own research group at the department of Tumor Immunology. In 1996-1997 he was a visiting scientist at DNAX Research Institute, Palo Alto, USA (Dr G. Zurawski and L. Lanier) where he identified the Dendritic cell chemokine DC-CK-1 (CCL18). In 2003 he became a full professor in Molecular Immunology at the department of Tumor Immunology at Radboud. In the same year he became theme leader of Infection, Immunity and Tissue Regeneration (150 scientists). Professor Adema received the Eijkman Winkler Medal of the University of Utrecht (2004), the VICI award from the Netherlands organization for Scientific Research (2006) and the Radboud University Educational Price (2011) for his work in the International Master program Molecular Mechanisms of Disease. Since 2008 he is a member of the board of the Scientific Council of the Dutch Cancer Society. Furthermore, he is a member of the Research Foundation – Flanders (FWO) expert panel for Microbiology and Immunology since 2009 and of the French Cancer Institute (2009).

## 2<sup>nd</sup> William C. Dewey Award & Lecture

Friday May 9, 4 pm in Ballroom 2



The Bill Dewey award is presented to an investigator who has contributed in a significant way to the mentorship and training of new investigators in the field of thermal medicine. This lecture is named in honor of Dr. Bill Dewey who trained many leaders in our field in all three disciplines (physics, biology and clinical/medical). His emphasis on making hyperthermia treatment a quantifiable therapy with a defined method for performing thermal dosimetry has stood the test of time and has influenced how hyperthermia and thermal ablation are practiced today.



**Mark W. Dewhirst, PhD**  
Department of Radiation Oncology  
Duke University

William C. Dewey Lecture: **“The William Dewey Award: Lessons learned and passed forward”**

Mark W. Dewhirst, DVM, PhD is the Gustavo S. Montana Professor of Radiation Oncology and Director of the Radiation Oncology Program of the Duke Comprehensive Cancer Center. He also holds appointments in the Departments of Pathology and Biomedical Engineering at Duke and in the Department of Anatomy Pathology and Radiology at the School of Veterinary Medicine at North Carolina State University. Dr. Dewhirst joined the faculty of Duke University in 1984 and was promoted to Full Professor in 1993. He received an endowed professorship in 2002. A recipient of the 2001 Wayne Rundles Award from the Duke Comprehensive Cancer Center, and the Failla Award and Lecture from the Radiation Research Society in 2008, Dr. Dewhirst has well over 400 peer-reviewed publications, book chapters and reviews. He has been a Visiting Professor at numerous institutions, has given named lectures at the University of Western Ontario, the New Zealand Cancer Society and Thomas Jefferson University. He currently serves on the Editorial Boards of several journals including Cancer Research, Clinical Cancer Research and the International Journal of Radiation Oncology Biology and Physics. He is also Editor-in-Chief of the International Journal of Hyperthermia. He graduated from the University of Arizona in 1971 with a degree in Chemistry and Colorado State University in 1975 and 1979 with DVM and PhD degrees, respectively.

### Abstract

I was fortunate to have Dr. Dewey on my graduate committee. In many ways, he served as my mentor as much as my primary mentor, Edward Gillette. However, both shaped my career in significant ways. Over the years, I have mentored well over 70 graduate students, postdoctoral fellows medical students, residents and faculty. In 2011, I was named the first Associate Dean for Faculty Mentoring by the Duke University School of Medicine. Mentoring has been my passion throughout my career and I have been fortunate to be mentor to many students who were involved in studies involving hyperthermia. In this lecture, I will review some of their work, but the emphasis will be on the principles that I have attempted to pass forward to this next generation. I am honored to receive this award and hope to make this lecture something that will be remembered in the future, particularly by the young trainees who will be attending the meeting.

## 25<sup>th</sup> J. Eugene Robinson Award & Lecture

Friday May 9, 5 pm in Ballroom 2



The J. Eugene Robinson Award is presented annually to an investigator who has made outstanding contributions to the field of hyperthermic oncology in one or more of the three main disciplines: Medicine/Clinical, Biology/Physiology, and Physics/Engineering. It is the highest and most prestigious award of the Society for Thermal Medicine. The award is named after J. Eugene Robinson who was a pioneer of hyperthermia research from the 1960's through the 1980's and a strong proponent of combined radiation and hyperthermia for cancer therapy.



**Rolf Issels, MD, PhD**  
University Medical Center Grosshadern  
University of Munich Sarcoma Center

J. Eugene Robinson Lecture: **“Regional hyperthermia combined with chemotherapy - from the bench to bedside”**

Rolf Issels, MD, is Professor of Internal Medicine and University Hospital Medical Centre Grosshadern, and head of clinical co-operation, Hyperthermia Group, GDF National Research Centre for Environment and Health, Munich, Germany. His research interests have included multimodality therapy for sarcomas and pancreatic cancer, stem cell transplantation, clinical hyperthermia, thermosensitive drug targeting, heat –shock proteins and related immunology . In addition to STM, Dr. Issels is a member of American Society of Clinical Oncology (ASCO), European Organization for the Research and Treatment of Cancer (EORTC), European Society for Hyperthermic Oncology (ESHO) and European Society for Medical Oncology (ESMO). He received an M.D. from the University of Munich in 1978 and a Ph.D. in biochemistry for the University of Tuebingen in 1980 and did a research fellowship with Harvard University at Massachusetts General Hospital, Boston.

### Abstract

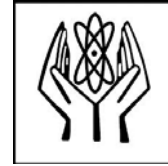
The hallmarks of hyperthermia and its pleiotropic effects are in favor of its combined use with chemotherapy. Preclinical research reveals that for heat killing and synergistic effects the thermal dose is most critical. Thermal enhancement of drug cytotoxicity is accompanied by cellular death and necrosis without increasing its oncogenic potential. The induction of genetically defined stress responses can deliver danger signals to activate the host's immune system. The positive results of randomized trials have definitely established hyperthermia in combination with chemotherapy as a novel clinical modality for the treatment of cancer. Hyperthermia targets the action of chemotherapy within the heated tumor region without affecting systemic toxicity. In specific clinical settings regional hyperthermia (RHT) or hyperthermic perfusion has proved its value and deserve a greater focus and investigation in other malignancies. In Europe, more specialized centers should be created and maintained as network of excellence for hyperthermia in the field of oncology.



## 2014 STM New Investigator Awards

Sponsored by

NCI/NIH R13CA174356 and Radiation Research Society



RADIATION RESEARCH SOCIETY

Twelve New Investigators have earned Travel Awards to the 31<sup>st</sup> Annual Meeting of the Society for Thermal Medicine. \$600 grants will be awarded based on applications and abstracts judged by a Committee of STM members chaired by Dr. Erik Cressman of the University of Texas MD Anderson Cancer Center. The awards are funded in part by the National Institutes of Health through grant R13CA174356 from the National Cancer Institute as well as the Radiation Research Society. These New Investigators will present their abstracts May 7<sup>th</sup> at 4 pm in Minneapolis. STM Officers and guests will also host the New Investigators at a private luncheon on Wed. May 7.



**E Balidemaj - Academic Medical Center, University of Amsterdam, The Netherlands**

"Imaging electric tissue properties using MRI for improved SAR assessment during Hyperthermia Treatment"



**Arlene Leonie Oei - Academic Medical Center, University of Amsterdam, The Netherlands**

"PARP1-inhibition sensitizes combined hyperthermia-radiation and combined hyperthermia-cDDP treatment of cervical carcinoma cells"



**Li Li - Duke University, USA & Erasmus Medical Center, Rotterdam, The Netherlands**

"The effect of heat cycling on intratumoral liposome accumulation and triggered drug release."



**Brogan McWilliams - Kansas State University**

"A directional interstitial antenna for microwave tissue ablation: theoretical and experimental investigation"



**Amy Ku - Roswell Park Cancer Institute**

"Myeloid-Derived Suppressor Cells Subvert the Immunostimulatory Activity of Systemic Thermal Therapy by Blocking T cell Trafficking in the Tumor Microenvironment"



**Gaurav Kumar - Beth Israel Deaconess Medical Center**

"Celecoxib Suppresses Local Inflammatory And Systemic Pro-Oncogenic Effects Of Hepatic Radiofrequency (RF) Ablation In Small Animals"



# 2014 STM New Investigator Awards

Sponsored by  
NCI/NIH R13CA174356 and Radiation Research Society



RADIATION RESEARCH SOCIETY

-----Continued-----



**Matthew Adams - University of California San Francisco**

“Theoretical Design and Evaluation of Endoluminal Ultrasound Applicators for Thermal Therapy of Pancreatic Cancer under Image Guidance”



**Anilchandra Attaluri - Johns Hopkins University School of Medicine**

“Magnetic nanoparticle hyperthermia as a radiosensitizer for locally advanced pancreas cancer: an in-vitro and in-vivo study”



**Jason Chiang - University of Wisconsin-Madison**

“Water Vapor Transport during Microwave Ablations: Numerical Simulation and Experimental Validation”



**Andrew Wong – University of California, Davis**

“Overcoming accelerated blood clearance of CU-doxorubicin nanoparticles with MR guided focused ultrasound thermal ablation”



**Frederik Soetaert - Ghent University**

“Optimal switch-off times of pulsed currents in bipolar radiofrequency ablation”



**Christopher Dillon - University of Utah**

“A novel method for quantifying perfusion-induced energy losses in magnetic resonance-guided focused ultrasound”

## Opening Session: NIH Update

### NIH/NCI Updates 2013/2014



**Rosemary Wong, PhD**  
**National Cancer Institute**  
Radiotherapy Development Branch  
Rockville, MD

The 2013 fiscal year has been a very challenging one for all federal agencies due to 1) operating under two Continuing Resolutions and 2) the implementation of Sequestration started on March 1, 2013 as a Congressional strategy to address the U.S. budget deficit. This budget reduction imposed by Sequestration resulted in a 4-5% budget reduction at the NCI and NIH level resulting not only in an overall budget reduction for all currently funded grants, but also affected the number of new grants awarded in fiscal year 2013.

A number of new NIH policy changes implemented in 2013 and those proposed for 2014 will be highlighted for STM members who, no doubt, could impact the grant application and award process for applicants and their academic institutions.

The NIH is currently operating under a Continuing Resolution through January 15, 2014 at a FY2012 level of funding. The Bipartisan Budget Act of 2013 passed by the House and Senate in December 2013 approved a two-year spending bill that would cancel the sequester cuts in 2014 and 2015, but would extend the sequestration period through 2023. What impact this passage will have on the final appropriated 2014 NIH/NCI budget and subsequent number of NIH/NCI grants funded in 2014 remains to be seen. Additionally, the overall success rate and funding paylines for NIH/NCI applications in all areas of research besides the Hyperthermia and Thermal Medicine research field will be provided for the past few years. Information on new initiatives and funding opportunities including Dr. Varmus' Provocative Question initiative during the past two years will also be discussed.



## Refresher Courses



### Thermoneutrality

**Elizabeth Repasky, PhD**  
**Roswell Park Cancer Institute**  
**Department of Immunology**  
**Buffalo, NY**

Wednesday, May 7, 8.15-9.15 am  
Ballroom 2



### Radiation Biology

**Chang Song, PhD**  
**University of Minnesota**  
**Department of Therapeutic Radiology**  
**Minneapolis, MN**

Wednesday, May 7, 8.15-9.15 am  
Deer/Elk Lake Room



### Assessing Nanoparticle Toxicity

**Christy Haynes, PhD**  
**University of Minnesota**  
**Department of Chemistry**  
**Minneapolis, MN**

Thursday, May 8, 8.15-9.15 am  
Ballroom 2



### Device Development

**Satish Ramadhyani, PhD**  
**Systems Engineer**  
**Gall Medical**

**Eric Rudie, PhD**  
**Rudie Consulting, LLC**  
**Denervx, LLC**

Thursday, May 8, 8.15-9.15 am  
Ballroom 2  
Deer/Elk Lake Room





**Cell Death Mechanisms**  
**John Pearce, PhD**  
**University of Texas - Austin**  
**Austin, TX**

Friday, May 9, 8.15-9.15 am  
Ballroom 2



**The application of the principles of exercise physiology in the oncology setting**  
**Lee Jones, PhD**  
**Memorial Sloan Kettering Cancer Center**  
**New York, NY**

Friday, May 9, 8.15-9.15 am  
Deer/Elk Lake Room



**Japanese Thermal Medicine Update: Efficacy of Gemcitabine combined with Hyperthermia therapy in the treatment of unresectable pancreatic cancer : Phase II study**  
**Satoshi Kokura, MD, PhD**  
**Kyoto Gakuen University**  
**Kyoto, Japan**

Friday, May 9, 8.15-9.15 am  
Pine/Cedar/Birch



**HIFU Update**  
**Emad Ebbini, PhD**  
**University of Minnesota**  
**Department of Electrical Engineering**  
**Minneapolis, MN**

Saturday, May 10, 8.15-9.15 am  
Ballroom 2



**Can thermotherapy improve radiosensitivity of cancer stem cells?**

**Jennifer Yu, MD, PhD**

**Cleveland Clinic**

**Departments of Radiation Oncology and Stem Cell Biology and Regenerative Medicine  
Cleveland, Ohio**

Saturday, May 10, 8.15-9.15 am  
Deer/Elk Lake Room



***STM congratulates the Informa/Yamamoto Editor's Award  
Winners for 2013: International Journal of Hyperthermia***



**BIOLOGY:** **Chelsea Landon** is originally from West Fork, Arkansas and received a BS in Fisheries and Wildlife Biology from Arkansas Tech University in 2005. Chelsea received a PhD in Pathology and certification in Toxicology from Duke in May 2013 under the guidance of Mark Dewhirst, DVM, PhD. Chelsea is currently in veterinary school at NC State and working in the laboratory of Adam Moeser, DVM, PhD, a gastrointestinal biologist studying the effects of stress on gastrointestinal disease.



**ENGINEERING AND PHYSICS:** **Elvis Dervishi** has been a PhD candidate in "Ecole Doctorale de Cancerologie" at the University Paris Sud (Paris XI), Paris, France, since 2010. His research work consists of high intensity focused ultrasound treatment of brain tumours in a rat model, under the supervision of Professor Jean-Yves Delattre and Dr Anne Laure Boch at Paris Sud (Paris XI) University and in collaboration with Jean-Francois Aubry and Mickael Tanter at Institut Langevin (ESPCI ParisTech, CNRS, INSERM). He received a doctor of medicine degree at the University of Tirana, Albania in 2001. He was the author of three publications focusing on transcranial ultrasonic brain ablation during his thesis work.



**ENGINEERING AND PHYSICS:** **Ryan M. Davis's** training is in Engineering and Physics with a research focus on biomedical magnetic resonance imaging (MRI). He received a Bachelor's of Arts in Electrical Engineering and a Bachelor's of Science in Physics from Johns Hopkins University in 2007. Hyperthermia became a primary research interest when he used MR thermometry to study temperature sensitive liposome content release in small animal tumour models. In 2011, he began pursuing a doctorate in Biomedical Engineering in the lab of Warren S. Warren at Duke University and has published peer-reviewed articles in journals ranging from *Nature Physics* to *Free Radicals in Biology and Medicine*.

# Welcome to Minneapolis and STM 2014

## Finance Committee Meeting

**10:30 - 11:30**      **Excelsior Bay (8th floor)**

Private Meeting of the STM Finance Committee. Chaired by Paul Stauffer and Robert Ivkov.

## IJH Editorial Board Meeting

**12:00 - 1:30**      **Excelsior Bay (8th floor)**

Private Luncheon Meeting of the IJH Editorial Board and Staff from Informa.

## Exhibitor & Poster Set-Up

**5:00-**      **Ballroom 1 (4th floor)**

Time for Exhibitor Booth Set-up and hanging of Posters for presentation.

## Registration Desk Open

**1:00 - 4:30, 5:00-7:30** **Atrium (4th floor), Minnesota Room (6th floor)**

Registered attendees can check-in and pickup namebadges and welcome packets. Walk-up registrations can be processed on-site and speakers can upload PowerPoint presentations to laptops to be used during oral presentations.

## STM Governing Council Meeting

**2:30 - 4:30**      **Excelsior Bay (8th floor)**

Private meeting of the Governing Council and Invited Guests. Chaired by STM President Dieter Haemmerich.

## 31 meetings later: History of STM and Update on Changes at NIH and NCI

**5:30 - 6:15**      **Minnesota Room (6th Floor)**      **Chair: Robert J. Griffin**

Drs. Chang Song and Dennis Leeper will provide a brief review of the history of the society - PLUS Rosemary Wong, Program Director at NCI will open the meeting with an overview of NIH and NCI efforts and objectives.

Tu1

Update on the 2013/2014 Changes at NIH and NCI

*Rosemary Wong*

*National Cancer Institute, Rockville, MD 20892, USA*

## Welcome Reception

6:30 - 8:00

Prefunction Terrace (6th Floor)

The welcome reception is open to all registered meeting attendees. The registration desk will be near the entry for any registered guests who have not already picked up welcome bags. Heavy hors d'oeuvres will be served.

### Platinum Sponsor



### Gold Sponsors



### Silver Sponsors



# Wednesday, May 7

**(All rooms on 4th floor unless otherwise indicated)**

## Breakfast

**7:00 - 8:15 Ballroom 1**

A Breakfast buffet for Meeting Registrants. Your name badge is your admission to breakfast.

## Refresher on Thermoneutrality, Elizabeth Repasky, PhD

**8:15 - 9:15 Ballroom 2 Chair: Jeff Hasday**

Featured presentation by Elizabeth Repasky of the Roswell Park Cancer Institute.

Wed.1 Understanding Cancer Therapy in the Context of Thermal Biology: Not Always a Warm Relationship!

Elizabeth A. Repasky

*Roswell Park Cancer Institute, Buffalo, New York, USA*

## Refresher on Radiation Biology, Chang W. Song, PhD

**8:15 - 9:15 Deer/Elk Lake Room Chair: Mark Hurwitz**

Featured presentation by Chang W. Song of the University of Minnesota.

Wed.2 Combination of Hyperthermia with SBRT/SRS

Chang W. Song<sup>1</sup>, Robert J. Griffin<sup>2</sup>

<sup>1</sup>University of Minnesota, Minneapolis, MN, USA, <sup>2</sup>University of Arkansas for Medical Science, Little Rock, AR, USA

## Keynote Address: Advanced Magnetic Resonance Imaging Approaches to Thermal Therapy and Nanomedicine Biodistribution

**9:30 - 10:30 Ballroom 2 Chair: Jack Hoopes**

Featuring Michael Garwood, PhD of the Center for Magnetic Resonance Research at the University of Minnesota.

Wed.3 Advanced Magnetic Resonance Imaging Approaches to Thermal Therapy and Nanomedicine Biodistribution

M. Garwood<sup>1</sup>, J. Zhang<sup>1</sup>, M.L. Etheridge<sup>1</sup>, H.L. Ring<sup>1</sup>, K.R. Hurley<sup>1</sup>, L. Utecht<sup>1</sup>, A. Petryk<sup>2</sup>, S. Jeon<sup>1</sup>, D. Idiyatullin<sup>1</sup>, C. Hogan<sup>1</sup>, C.L. Haynes<sup>1</sup>, J.C. Bischof<sup>1</sup>, P.J. Hoopes<sup>2</sup>

<sup>1</sup>University of Minnesota, Minneapolis, Minnesota, USA, <sup>2</sup>Dartmouth College, Hanover,

New Hampshire, USA

## Coffee Break with Exhibitors

10:30 - 10:45 Ballroom 1

## Symposium: Minnesota Nanoparticle and Thermal Therapy

10: 45 - 12:15 Ballroom 2

Chair: John Bischof

- Wed.4 Characterization of the State of Aggregation of Nanomaterials in Biological Systems  
*Seongho Jeon, Katie Hurley, Michael Etheridge, Thaseem Thajudeen, Michael Garwood, John Bischof, Christy Haynes, Chris Hogan*  
*University of Minnesota, Minneapolis, USA*
- Wed.5 Enhancing Therapeutic Efficacy of Magnetic Hyperthermia Through Designed Aggregation of SPIO Nanoparticles  
*Jayanth Panyam, Tanmoy Sadhukha, Timothy Wiedmann*  
*University of Minnesota, Minneapolis, MN, USA*
- Wed.6 Continuous vs Pulsed Near Infra-red Heating of Hollow Gold Nanoparticles - Implications and Applications  
*Joseph Zasadzinski<sup>1</sup>, Norbert Reich<sup>2</sup>, Gary Braun<sup>3</sup>, Dean Morales<sup>2</sup>, Natalie Forbes<sup>2</sup>, Alessia Pallaoro<sup>2</sup>, Xiao Huang<sup>2</sup>*  
*<sup>1</sup>University of Minnesota, Minneapolis, Minnesota, USA, <sup>2</sup>University of California, Santa Barbara, California, USA, <sup>3</sup>Sanford-Burnham Medical Research Center, La Jolla, California, USA*
- Wed.7 Assessment of preconditioning on LNCaP tumors by a TNF- $\alpha$  nanoparticle construct using MRI  
*Greg Metzger, John Bischof, Jeunghwan Choi, Isabelle Iltis, Manda Vollmers*  
*University of Minnesota, Minneapolis, MN, USA*
- Wed.8 Cytotoxic Interactions of Heat and Salt Exposure using Sodium Acetate in Murine 4T1 Breast Carcinoma Cells  
*Erik Cressman<sup>1</sup>, Robert Griffin<sup>2</sup>, Azemat Jamshidi-Parsian<sup>2</sup>*  
*<sup>1</sup>MD Anderson Cancer Center, Houston, TX, USA, <sup>2</sup>University of Arkansas for Medical Sciences, Little Rock, AR, USA*
- Wed.9 Testing of Cardiac Ablative Devices Employing Visible Heart<sup>®</sup> Methodologies  
*Paul Iaizzo*  
*University of Minnesota, Minneapolis, Minnesota, USA*

## Attendees on their own for lunch

12:15 - 1:45

## New Investigator Luncheon

12:15 - 1:45 St. Croix II - 6th Floor

Private Meal for all New Investigators registered for the meeting and members of the Governing Council

## Workshop on Common Topics in Thermal Medicine: Computational Methods in Treatment Planning

1:45 - 3:45

Ballroom 2

Chair: Yoed Rabin & Gal Shafirstein

- Wed.10 Computerized training of cryosurgery: objectives and prototype development  
*Yoed Rabin, Kenji Shimada, Robert Keelan, Anjali Sehrawat, Hong Zhang*  
*Carnegie Mellon University, Pittsburgh, PA, USA*
- Wed.11 Simulated ultrasound imaging for the purpose of prostate cryosurgery training  
*Robert Keelan, Hong Zhang, Kenji Shimada, Yoed Rabin*  
*Carnegie Mellon University, Pittsburgh, PA, USA*
- Wed.12 Tools and Models for In Silico Investigation of EM- and US-Based Thermal Therapies in Complex Anatomies  
*Esra Neufeld<sup>1</sup>, Adamos Kyriakou<sup>1,2</sup>, Niels Kuster<sup>1,2</sup>*  
*<sup>1</sup>Foundation for Research on Information Technologies in Society (IT'IS), Zurich, Switzerland, <sup>2</sup>Swiss Federal Institute of Technology (ETH), Zurich, Switzerland*
- Wed.13 Numerical Investigation of HIFU Tumor Ablation: Focus Scanning Approaches, Vasculature, and Standing-Waves  
*Adamos Kyriakou<sup>1,2</sup>, Esra Neufeld<sup>1</sup>, Gal Shafirstein<sup>3</sup>, Eduardo Moros<sup>4</sup>, Gabor Szekely<sup>2</sup>, Niels Kuster<sup>1,2</sup>*  
*<sup>1</sup>Foundation for Research on Information Technologies in Society (IT'IS), Zurich, Switzerland, <sup>2</sup>Swiss Federal Institute of Technology (ETH), Zurich, Switzerland, <sup>3</sup>Roswell Park Cancer Institute, Buffalo, New York, USA, <sup>4</sup>H. Lee Moffitt Cancer Center and Research Institute, Tampa, Florida, USA*
- Wed.14 Damage-Dependent Bioheat Transfer Modeling in Thermal Therapy  
*Yusheng Feng<sup>1</sup>, Cliff Zhou<sup>1,2</sup>, Robert Moser<sup>2</sup>*  
*<sup>1</sup>UT San Antonio, San Antonio, USA, <sup>2</sup>UT Austin, Austin, USA*
- Wed.15 A New Algorithm for Light Dosimetry During Interstitial Laser Therapy of Locally Advanced Tumors  
*Emily Oakley, Brian Warzen, Hassan Arshad, Gal Shafirstein*  
*Roswell Park Cancer Institute, Buffalo, NY, USA*

## Workshop: Non-Oncological Applications of Thermal Medicine

1:45 - 3:45

Deer/Elk Lake Room

Chair: Dieter Manstein



- Wed.16 The Physics behind Cryolipolysis  
*Joel Jimenez Lozano, Joe Coakley, George Frangineas*  
*Zeltiq Aesthetics, Inc., Pleasanton, CA, USA*
- Wed.17 Magnetic Resonance Thermography of Soft Tissue Cooling  
*Amir Y. Sajjadi<sup>1,2</sup>, Sara Sprinkhuizen<sup>1</sup>, Dieter Manstein<sup>2</sup>, Stefan A. Carp<sup>1</sup>*  
*<sup>1</sup>Department of Radiology, Harvard Medical School, Charlestown, MA, USA, <sup>2</sup>Cutaneous Biology Research Center, Harvard University, Charlestown, MA, USA*
- Wed.18 Modeling the detectability of brown fat metabolism using microwave radiometry.  
*Dario Rodrigues<sup>1</sup>, Paolo Maccarini<sup>2</sup>, Pedro Pereira<sup>3</sup>, Sara Salah<sup>4</sup>, Erin Colebeck<sup>5</sup>, Aaron Hood<sup>5</sup>, Erdem Topsakal<sup>5</sup>, Paul Stauffer<sup>1</sup>*  
*<sup>1</sup>Thomas Jefferson University, Philadelphia, PA, USA, <sup>2</sup>Duke University, Durham, NC, USA, <sup>3</sup>ISEL, Lisbon, Portugal, <sup>4</sup>ANSYS, Inc., Irvine, CA, USA, <sup>5</sup>Mississippi State University, Mississippi State, MS, USA*
- Wed.19 Photothermal Ablation of Group A Streptococcus Bacteria and Biofilms Using Functionalized Multi-Wall Carbon Nanotubes  
*Nicole Levi-Polyachenko, Christe Young, Christopher MacNeill, Amy Braden, Louis Argenta, Sean Reid*  
*Wake Forest University Health Sciences, Winston Salem, NC, USA*
- Wed.20 Investigation of a Laser-based System as an Alternative Energy Modality for Vessel Sealing During Surgery  
*William Nau<sup>1</sup>, Nicholas Giglio<sup>2</sup>, Thomas Hutchens<sup>2</sup>, William Perkins<sup>2</sup>, Cassandra Latimer<sup>1</sup>, Arlen Ward<sup>1</sup>, Nathaniel Fried<sup>2</sup>*  
*<sup>1</sup>Covidien, Boulder, CO, USA, <sup>2</sup>University of North Carolina-Charlotte, Charlotte, NC, USA*

## Coffee Break with Exhibitors

**3:45 - 4:00 Ballroom 1**

## New Investigator Symposium

**4:00 - 6:00 Ballroom 2**

**Chair: Nathan Koonce & Audrey Glory**

12 New Investigator Travel Award winners present their Abstracts.

- Wed.21 Imaging electric tissue properties using MRI for improved SAR assessment during Hyperthermia Treatment  
*E Balidemaj<sup>1</sup>, J. Trinks<sup>1</sup>, H.P Kok<sup>1</sup>, R.F. Remis<sup>3</sup>, C.A.T. van den Berg<sup>2</sup>, L.J.A. Stalpers<sup>1</sup>, A.J. Nederveen<sup>1</sup>, H. Crezee<sup>1</sup>*  
*<sup>1</sup>Academic Medical Center, Amsterdam, The Netherlands, <sup>2</sup>University Medical Center Utrecht, Utrecht, The Netherlands, <sup>3</sup>Technical University Delft, Delft, The Netherlands*
- Wed.22 PARP1-inhibition sensitizes combined hyperthermia-radiation and combined

hyperthermia-cddp treatment of cervical carcinoma cells

Arlene Leonie Oei<sup>1,2</sup>, H.P. Kok<sup>2</sup>, L.J.A. Stalpers<sup>1,2</sup>, H.M. Rodermond<sup>1,2</sup>, A. Bel<sup>2</sup>, J. Crezee<sup>2</sup>, N.A.P. Franken<sup>1,2</sup>

<sup>1</sup>Academic Medical Center, University of Amsterdam, Laboratory for Experimental Oncology and Radiobiology (LEXOR), Center for Experimental Molecular Medicine, Amsterdam, Noord-Holland, The Netherlands, <sup>2</sup>Academic Medical Center, University of Amsterdam, Department of Radiation Oncology, Amsterdam, Noord-Holland, The Netherlands

- Wed.23 The effect of heat cycling on intratumoral liposome accumulation and triggered drug release.  
Li Li<sup>1,2</sup>, Timo ten Hagen<sup>2</sup>, Martin Hossann<sup>3</sup>, Gerard van Rhoon<sup>2</sup>, Thomas Soullie<sup>2</sup>, Gerben Koning<sup>2</sup>  
<sup>1</sup>Duke University, Durham, NC, USA, <sup>2</sup>Erasmus MC, Rotterdam, The Netherlands, <sup>3</sup>University Hospital of Munich, Munich, Germany
- Wed.24 A directional interstitial antenna for microwave tissue ablation: theoretical and experimental investigation  
Brogan McWilliams, Emily Schnell, Punit Prakash  
Kansas State University, Manhattan, Kansas, USA
- Wed.25 Myeloid-Derived Suppressor Cells Subvert the Immunostimulatory Activity of Systemic Thermal Therapy by Blocking T cell Trafficking in the Tumor Microenvironment  
Amy Ku, Jason Muhitch, Scott Abrams, Sharon Evans  
Roswell Park Cancer Institute, Buffalo, NY, USA
- Wed.26 Celecoxib suppresses local inflammatory and systemic pro-oncogenic effects of hepatic radiofrequency (RF) ablation in small animals  
Gaurav Kumar<sup>1</sup>, S.Nahum Goldberg<sup>1,2</sup>, Marwan Moussa<sup>1</sup>, Yuanguo Wang<sup>1</sup>, Lana Gourevich<sup>2</sup>, Muneeb Ahmed<sup>1</sup>  
<sup>1</sup>Beth Israel Deaconess Medical Center, Boston, MA, USA, <sup>2</sup>Hadassah Hebrew University Medical Center, Jerusalem, Israel
- Wed.27 Theoretical Design and Evaluation of Endoluminal Ultrasound Applicators for Thermal Therapy of Pancreatic Cancer under Image Guidance  
Matthew Adams<sup>1</sup>, Serena Scott<sup>1</sup>, Vasant Salgaonkar<sup>1</sup>, Graham Sommer<sup>2</sup>, Chris Diederich<sup>1</sup>  
<sup>1</sup>University of California San Francisco, San Francisco, USA, <sup>2</sup>Stanford University Medical Center, Stanford, USA
- Wed.28 Magnetic nanoparticle hyperthermia as a radiosensitizer for locally advanced pancreas cancer: an in-vitro and in-vivo study  
Anilchandra Attaluri<sup>1</sup>, Haoming Zhou<sup>1</sup>, Toni-rose Guiriba<sup>4</sup>, Yue Liu<sup>5</sup>, Mohammad Hedayati<sup>1</sup>, Yi Zhong<sup>2</sup>, Christine Iacobuzio-Donahue<sup>2</sup>, Eleni Liapi<sup>2</sup>, Joseph Herman<sup>3</sup>, Theodore DeWeese<sup>1</sup>, Robert Ivkov<sup>1</sup>

<sup>1</sup>Department of Radiation Oncology & Molecular Radiation Sciences, Johns Hopkins University School of Medicine, Baltimore, MD, USA, <sup>2</sup>Departments of Oncology and Pathology, The Sol Goldman Pancreatic Cancer Research Center, Sidney Cancer Center; Johns Hopkins University School of Medicine, Baltimore, MD, USA, <sup>3</sup>Department of Radiology and Radiological Sciences, Johns Hopkins Hospital, Baltimore, MD, USA, <sup>4</sup>Whiting School of Engineering, Johns Hopkins University, Baltimore, MD, USA, <sup>5</sup>School of Public Health Peking, University Health Science Center,, Beijing, China

- Wed.29 Water Vapor Transport during Microwave Ablations: Numerical Simulation and Experimental Validation  
Jason Chiang<sup>1</sup>, Sohan Birla<sup>2</sup>, Jeyam Subbiah<sup>2</sup>, David Jones<sup>2</sup>, Christopher Brace<sup>1</sup>  
<sup>1</sup>University of Wisconsin-Madison, Madison, USA, <sup>2</sup>University of Nebraska-Lincoln, Lincoln, USA
- Wed.30 Overcoming accelerated blood clearance of cu-doxorubicin nanoparticles with mr guided focused ultrasound thermal ablation  
Andrew Wong, Katherine Watson, Brett Fite, Yu Liu, Jai Seo, Lisa Mahakian, Sarah Tam, Azadeh Kheirloomoom, Katherine Ferrara  
University of California, Davis, Davis, CA, USA
- Wed.31 Optimal switch-off times of pulsed currents in bipolar radiofrequency ablation  
Frederik Soetaert, Guillaume Crevecoeur, Luc Dupré  
Ghent University, Ghent, Belgium
- Wed.32 A novel method for quantifying perfusion-induced energy losses in magnetic resonance-guided focused ultrasound  
Christopher Dillon, Robert Roemer, Dennis Parker, Allison Payne  
University of Utah, Salt Lake City, Utah, USA

## Poster Session & Reception

### 6:00 - 7:30 Ballroom 1

Posters accepted for presentation will be on display with presenting authors ready to discuss their efforts and findings. Light refreshments will be served.

- Po.1 Heating ability of magnetic nanoparticles evaluated from their magnetization curves under alternating field  
Satoshi Ota<sup>1</sup>, Kosuke Nakamura<sup>1</sup>, Asahi Tomitaka<sup>2</sup>, Tsutomu Yamada<sup>1</sup>, Yasushi Takemura<sup>1</sup>  
<sup>1</sup>Yokohama National University, Yokohama, Japan, <sup>2</sup>University of Washington, Seattle, WA, USA
- Po.2 Heat-Mediated Drug Release from Mesoporous Silica-Coated Iron Oxide Nanoparticles  
Katie Hurley, Hattie Ring, Michael Garwood, John Bischof, Christy Haynes  
University of Minnesota, Minneapolis, USA

- Po.3 Tissue Response to Ablative Modalities  
*Ashish Singal<sup>1</sup>, Charles Soule<sup>1</sup>, John Ballard<sup>1</sup>, Erik Cressman<sup>2,1</sup>, Paul Iaizzo<sup>1</sup>*  
*<sup>1</sup>University of Minnesota, Minneapolis, Minnesota, USA, <sup>2</sup>University of Texas, Houston, Texas, USA*
- Po.4 Determining magnetic nanoparticle distribution within cryogenic biological systems using CT imaging for improved regenerative medicine approaches  
*Leoni Rott<sup>1,2</sup>, Michael Etheridge<sup>1</sup>, Almer Meinken<sup>2</sup>, Birgit Glasmacher<sup>2</sup>, John Bischof<sup>1</sup>*  
*<sup>1</sup>University of Minnesota, Minneapolis/MN, USA, <sup>2</sup>Leibniz Universität Hannover, Hannover, Germany*
- Po.5 Thermal therapy for improvement of laser-based tumor ablation strategies  
*Klressa Barnes, Robert Griffin*  
*University of Arkansas for Medical Sciences, Little Rock, USA*
- Po.6 Accessing Higher IONP Concentrations for MRI Contrast  
*Hattie Ring, Katie Hurley, Michael Etheridge, Jinjin Zheng, John Bischof, Christy Haynes, Micheal Garwood*  
*University of Minnesota, Minneapolis, MN, USA*
- Po.7 Thermal Conductivity Measurement of Thin Cardiac Tissues  
*Harishankar Natesan<sup>1</sup>, Jeunghwan Choi<sup>1</sup>, Sean Lubner<sup>2</sup>, Chris Dames<sup>2</sup>, John Bischof<sup>1</sup>*  
*<sup>1</sup>University of Minnesota, Minneapolis, Minnesota, USA, <sup>2</sup>University of California, Berkeley, California, USA*
- Po.8 A novel miniature ablation system for studies in small animals  
*Christian Rossmann, Dieter Haemmerich*  
*Medical University of South Carolina, Charleston, SC, USA*
- Po.9 Modulated electro-hyperthermia applied as monotherapy for various cases having no other options  
*Taesig Jeung<sup>1</sup>, Sunyoung Ma<sup>1</sup>, Jesang Yu<sup>1</sup>, Sangwook Lim<sup>1</sup>, Oliver Szasz<sup>2</sup>*  
*<sup>1</sup>Kosin University College of Medicine, Department of Radiation Oncology, Busan, Republic of Korea, <sup>2</sup>Szent Istvan University, Department of Biotechnics, Godollo, Hungary*
- Po.10 Modulated electro-hyperthermia therapy combined with gold-standard therapies for primary, recurrent and metastatic sarcomas  
*Taesig Jeung<sup>1</sup>, Sunyoung Ma<sup>1</sup>, Jesang Yu<sup>1</sup>, Sangwook Lim<sup>1</sup>, Oliver Szasz<sup>2</sup>*  
*<sup>1</sup>Kosin University College of Medicine, Department of Radiation Oncology, Busan, Republic of Korea, <sup>2</sup>Szent Istvan University, Department of Biotechnics, Godollo, Hungary*
- Po.11 HIFU Hepatic Tumor Ablation: Modeling of Focusing and Motion Tracking Approaches  
*Adamos Kyriakou<sup>1,2</sup>, Esra Neufeld<sup>2</sup>, Frank Preiswerk<sup>3</sup>, Bryn Lloyd<sup>1</sup>, Philippe Cattin<sup>3</sup>, Gabor Szekely<sup>2</sup>, Niels Kuster<sup>1,2</sup>*  
*<sup>1</sup>Foundation for Research on Information Technologies in Society (IT<sup>2</sup>IS), Zurich, Switzerland, <sup>2</sup>Swiss Federal Institute of Technology (ETH), Zurich, Switzerland, <sup>3</sup>*

<sup>3</sup>University of Basel, Basel, Switzerland

- Po.12 Combined radiotherapy and thermal ablation for advanced solid tumors  
Robert Griffin<sup>1</sup>, Beata Przybyla<sup>1</sup>, Nathan Koonce<sup>1</sup>, Klressa Barnes<sup>1</sup>, Gal Shafirstein<sup>2</sup>  
<sup>1</sup>University of Arkansas for Medical Sciences, Little Rock, AR, USA, <sup>2</sup>Roswell Park Cancer Institute, Buffalo, NY, USA
- Po.13 Focusing and Aberration Correction for Transcranial Focused Ultrasound  
Adamos Kyriakou<sup>1,2</sup>, Esra Neufeld<sup>1</sup>, Beat Werner<sup>3</sup>, Gabor Szekely<sup>2</sup>, Niels Kuster<sup>1,2</sup>  
<sup>1</sup>Foundation for Research on Information Technologies in Society (IT<sup>2</sup>IS), Zurich, Switzerland, <sup>2</sup>Swiss Federal Institute of Technology (ETH), Zurich, Switzerland, <sup>3</sup>University Children's Hospital, Zurich, Switzerland
- Po.14 Deep RF Phase Array Numerical Optimization Study  
Paul Turner, Mark Hagmann  
BSD Medical Corp, Salt Lake City, UT, USA
- Po.15 Multiple intratumoral magnetic nanoparticle injections enhances the heat delivery in murine sarcoma model  
Harley Rodrigues, Francielli Mello, Luis Branquinho, Gustavo Capistrano, Elisângela Silveira-Lacerda, Andris Bakuzis  
Universidade Federal de Goiás, Goiânia, Goiás, Brazil
- Po.16 Magnetic Resonance guided Thermo Chemical Ablation  
Florian Maier, Christopher J. MacLellan, David T. Fuentes, R. Jason Stafford, John D. Hazle, Erik N. K. Cressman  
The University of Texas MD Anderson Cancer Center, Houston, USA
- Po.17 Assessment of a QA phantom after multiple heatings and remolding  
Alexis Farrer, Allison Payne, Douglas Christensen  
University of Utah, Salt Lake City, UT, USA
- Po.18 Modeling and Validation of Thermochemical Ablation (TCA) in ex-vivo Bovine Liver  
Martin Jones, Florian Maier, Christopher MacLellan, Jason Stafford, Erik Cressman, David Fuentes  
University of Texas MD Anderson Cancer Center, Houston, TX, USA
- Po.19 The role of transcription factor Nrf2 in mild thermotolerance induced at 40°C  
Audrey Glory, Diana Averill  
UQAM, Montreal, Quebec, Canada
- Po.20 Gold nanoparticle-bound TNF and combined radiotherapy to prime tumors for thermal therapy  
Nathan A. Koonce<sup>1</sup>, Judy Dent<sup>1</sup>, Matt E. Hardee<sup>1</sup>, Matthew C. Quick<sup>2</sup>, Robert J. Griffin<sup>1</sup>  
<sup>1</sup>University of Arkansas for Medical Sciences-Department of Radiation Oncology, Little Rock, AR, USA, <sup>2</sup>University of Arkansas for Medical Sciences-Department of Pathology, Little Rock, AR, USA

- Po.21      Thermo-chromic phantom for characterization of HIFU thermal therapy  
*Andrew S. Mikhail<sup>1</sup>, Ayele H. Negussie<sup>1</sup>, Ari Partanen<sup>2,1</sup>, Pavel Yarmolenko<sup>1</sup>, Nadine Abi-Jaoudeh<sup>1</sup>, Bradford J. Wood<sup>1</sup>, Aradhana Venkatesan<sup>1</sup>*  
*<sup>1</sup>Center for Interventional Oncology, Radiology and Imaging Sciences, Clinical Center, National Institutes of Health, Bethesda, MD, USA, <sup>2</sup>Philips Healthcare, Cleveland, OH, USA*
- Po.22      Investigating magnetic nanoparticle frequency spectra  
*Fridon Shubitidze<sup>1</sup>, Robert Stigliano<sup>1</sup>, Benjamin Barrowes<sup>2</sup>, Katerina Kekalo<sup>1</sup>, Jack Hoopes<sup>3,1</sup>*  
*<sup>1</sup>Thayer School of Engineering at Dartmouth, Hanover, NH, USA, <sup>2</sup>U.S. Army CRREL, Hanover, NH, USA, <sup>3</sup>Geisel School of Medical at Dartmouth, Hanover, NH, USA*
- Po.23      Evaluation of hyperthermia and radiotherapy for the treatment of patients with locally advanced pelvic tumors: Preliminary findings  
*Michael Payne, Doug Kelly, David Simon, Tyler Gutschenritter, James Flynn, Oneita Taylor, Matt Weaver*  
*Cancer Treatment Centers of America, Tulsa, OK, USA*
- Po.24      Modulating DNA Repair Mechanisms to Enhance Hyperthermic Radiosensitization of Breast Cancer Cells  
*Nicholas B. Dye<sup>1</sup>, Rishabh Chaudhari<sup>2</sup>, Juong G. Rhee<sup>1</sup>, Zeljko Vujaskovic<sup>1</sup>*  
*<sup>1</sup>University of Maryland School of Medicine, Baltimore, MD, USA, <sup>2</sup>The George Washington University School of Medicine and Health Sciences, Washington, DC, USA*
- Po.25      Hsp-90 inhibitor enhances heat sensitivity of human breast cancer cells including stem-like cells  
*Juong G. Rhee<sup>1</sup>, Rishabh Chaudhari<sup>2</sup>, Nicholas B. Dye<sup>1</sup>, Seog-Young Kim<sup>3</sup>, Yong J. Lee<sup>3</sup>, Zeljko Vujaskovic<sup>1</sup>*  
*<sup>1</sup>University of Maryland School of Medicine, Baltimore, MD, USA, <sup>2</sup>The George Washington University School of Medicine and Health Sciences, Washington, DC, USA, <sup>3</sup>University of Pittsburgh, Pittsburgh, PA, USA*
- Po.26      Pancreatic Electroporation  
*Derek West*  
*University of Texas at Houston, Houston, Texas, USA*
- Po.27      Nanotechnology for hyperthermia: the pros and cons of using nanoheaters for local temperature handling.  
*Gerardo Goya*  
*Institute of Nanoscience of Argon, University of Zaragoza, Spain*
- Po.28      A new MR pulse sequence for accurate temperature imaging in red bone marrow  
*Ryan Davis<sup>1</sup>, Viola Rieke<sup>2</sup>, Eugene Ozhinski<sup>2</sup>, Misung Han<sup>2</sup>, Sharmilla Majumdar<sup>2</sup>, John Kurhanewicz<sup>2</sup>, Warren Warren<sup>1</sup>*  
*<sup>1</sup>Duke University, Durham, NC, USA, <sup>2</sup>University of California San Francisco, San*

Francisco, CA, USA

Po.29 Effects of physiological temperature changes on Wnt signaling in primary human small airway epithelial cells (SAEC)

Ratnakar Potla, Sergei Atamas, Mohan E Tulapurkar, Ishwar Singh, Jeffrey D Hasday  
University of Maryland Baltimore, Baltimore, USA

### Bronze Sponsors



# Thursday, May 8

## Breakfast

**7:00 - 8:15 Ballroom 1**

A Breakfast buffet for Meeting Registrants. Your name badge is your admission to breakfast.

## Refresher on Assessing Nanoparticle Toxicity, Christy Haynes, PhD

**8:15 - 9:15 Ballroom 2 Chair: John Bischof**

Featuring Christy Haynes, PhD of the Department of Chemistry at the University of Minnesota

- Th.1 Assessing Nanoparticle Toxicity  
*Katie Hurley, Yu-Shen Lin, Melissa Maurer-Jones, Donghyuk Kim, Victoria Szlag, Joseph Buchman, Solaire Finkenstaedt-Quinn, Sam Egger, Christy Haynes*  
*University of Minnesota, Minneapolis, MN, USA*

## Refresher on Device Development: Satish Ramadhyani, PhD/ Erik Rudie, PhD

**8:15 - 9:15 Deer/Elk Lake Room Chair: Christopher Brace**

Featuring Satish Ramadhyani & Erik Rudie

- Th.2 Microwave Tissue Ablation – The Basics  
Eric Rudie<sup>1,2</sup>  
<sup>1</sup>Rudie Consulting, LLC, Maple Grove, MN, USA, <sup>2</sup>Denervx, LLC, Maple Grove, MN, USA
- Th.3 A Review of Cryoablation Systems for Minimally Invasive Treatment of Tumors  
Satish Ramadhyani  
*Galil Medical, Arden Hills, Minnesota, USA*

## Keynote Address: Heat Induced Drug Delivery and Monitoring of Release Using Ultrasound

**9:30 - 10:30 Ballroom 2 Chair: Chris Diederich**

Featuring Katherine W. Ferrara, PhD of the Biomedical Engineering Department at the University of California, Davis.

- Th.4 Ultrasound-guided drug and gene delivery  
Katherine Ferrara, Azadeh Kheirloomoom, Brett Fite, Josquin Foiret, Yu Liu, Andrew Wong, Elizabeth Ingham, Lisa Even, Sarah Tam, Charles Caskey, Jai Seo, Dustin Kruse  
*University of California Davis, Davis, CA, USA*



## Coffee Break with Exhibitors

10:30 - 10:45 Ballroom 1

## Symposium: Treatment Planning and Guidance

10:45 - 12:15 Ballroom 2

Chair: Punit Prakash & Martin Arthur

- Th.5 FEM Numerical Models of Magnetic Nanoparticle Heating Facilitate Treatment Planning and Analysis  
*John Pearce<sup>1</sup>, Alicia Petryk<sup>2</sup>, Jack Hoopes<sup>2</sup>*  
<sup>1</sup>The University of Texas at Austin, Austin, TX, USA, <sup>2</sup>Dartmouth College, Hanover, NH, USA
- Th.6 Nonlinear Simulations of Transient and Continuous Wave Ultrasound in FOCUS  
*Xiaofeng Zhao, Robert J. McGough*  
Michigan State University, East Lansing, MI, USA
- Th.7 Interactive Approximation of High-Intensity Focused Ultrasound Simulation for Arbitrary Transducer Configurations  
*Christian Schumann<sup>1</sup>, Eike Mücke<sup>2</sup>, Daniel Demedts<sup>1</sup>, Joachim Georgii<sup>1</sup>, Caroline von Dresky<sup>1</sup>, Tobias Preusser<sup>1,3</sup>*  
<sup>1</sup>Fraunhofer MEVIS, Bremen, Bremen, Germany, <sup>2</sup>University of Applied Sciences, Bremerhaven, Bremen, Germany, <sup>3</sup>Jacobs University, Bremen, Bremen, Germany
- Th.8 Comparison of single- and multiple-antenna ablation at 915 MHz and 2.45 GHz: a simulation and experimental investigation  
*Mohammed Taj-Eldin, Punit Prakash*  
Kansas State University, Manhattan, KS, USA
- Th.9 Inverse problem statistics of optical parameter inference in brain MR-guided laser induced thermal therapy.  
*Samuel Fahrenholtz<sup>1,2</sup>, R. Jason Stafford<sup>1,2</sup>, Florian Maier<sup>1</sup>, Anil Shetty<sup>3</sup>, David Fuentes<sup>1,2</sup>*  
<sup>1</sup>The University of Texas MD Anderson Cancer Center, Houston, Texas, USA, <sup>2</sup>The University of Texas Graduate School of Biomedical Sciences at Houston, Houston, Texas, USA, <sup>3</sup>Visualase Inc., Houston, Texas, USA
- Th.10 Real-Time Ultrasonic Thermometry Based on the Change in Backscattered Energy  
*R. Martin Arthur, Charles D. Holmes*  
Washington University in St. Louis, St. Louis, MO 63130, USA
- Th.11 Towards on-line adaptive hyperthermia treatment planning: correlation between measured and simulated SAR changes caused by phase steering in patients

*Petra Kok<sup>1</sup>, Silvia Ciampa<sup>2</sup>, Rianne de Kroon-Oldenhof<sup>1</sup>, Eva Steggerda-Carvalho<sup>1</sup>, Gerard van Stam<sup>1</sup>, Paul Zum Vorde Sive Vording<sup>1</sup>, Lukas Stalpers<sup>1</sup>, Debby Geijssen<sup>1</sup>, Fernando Bardati<sup>2</sup>, Arjan Bel<sup>1</sup>, Hans Crezee<sup>1</sup>*

<sup>1</sup>*Department of Radiation Oncology, Academic Medical Center, University of Amsterdam, Amsterdam, The Netherlands, <sup>2</sup>Department of Civil Engineering and Computer Science, University of Rome Tor Vergata, Rome, Italy*

## Symposium: Physiological/Immunological Aspects of Thermal Medicine

**10:45 - 12:15 Deer/Elk/Lake room**

**Chair: Michael Borrelli & Steven Fiering**

- Th.12 Using iron oxide -nanoparticle/AMF mediated hyperthermia to stimulate antitumor immune response against metastatic disease  
*Lei Chen<sup>1</sup>, Jose Conejo-Garcia<sup>2</sup>, P. Jack Hoopes<sup>1</sup>, Mary Jo Turk<sup>1</sup>, Seiko Toraya-Brown<sup>1</sup>, Steven Fiering<sup>1</sup>*  
<sup>1</sup>*Geisel School of Medicine at Dartmouth, Lebanon, NH, USA, <sup>2</sup>Wistar Cancer Center, Philadelphia, PA, USA*
- Th.13 Targeting Vascular Checkpoints in Tumor Immunity by Thermal Medicine: A Tale of Two Niches  
*Sharon Evans<sup>1</sup>, Daniel Fisher<sup>1</sup>, Jason Muhitch<sup>1</sup>, Fumito Ito<sup>1,2</sup>*  
<sup>1</sup>*Roswell Park Cancer Institute, Buffalo, NY, USA, <sup>2</sup>University of Michigan Health Systems, Ann Arbor, MI, USA*
- Th.14 Radiofrequency Ablation Amplifies the Efficacy of Adoptive T Cell Transfer Therapy in the Generation of Antitumor Immunity  
*Mark Bucsek<sup>1</sup>, Fumito Ito<sup>2</sup>, Jason Muhitch<sup>1</sup>, Ashwin Ajith<sup>1</sup>, Sharon Evans<sup>1</sup>*  
<sup>1</sup>*Roswell Park Cancer Institute, Buffalo, New York, USA, <sup>2</sup>University of Michigan Health System, Ann Arbor, Michigan, USA*
- Th.15 Abscopal effect by modulated electro-hyperthermia  
*Csaba Kovago<sup>1</sup>, Nora Meggyeshazi<sup>2</sup>, Gabor Andocs<sup>3</sup>, Oliver Szasz<sup>4</sup>*  
<sup>1</sup>*Szent Istvan University, Pharmacology and Toxicology Department, Faculty of Veterinary Science, Budapest, Hungary, <sup>2</sup>Semmelweis University, 1st Department of Pathology and Experimental Cancer Research, Budapest, Hungary, <sup>3</sup>Tottori University, Department of Veterinary Clinical Medicine, Faculty of Veterinary Science, Tottori, Japan, <sup>4</sup>Szent Istvan University, Department of Biotechnics, Godollo, Hungary*
- Th.16 Assessment of Hemoglobin Saturation In and Around Microwave Thermal Ablation by Optical Spectroscopy  
*Mariajose Bedoya, David Campos, Christopher Brace*  
*University of Wisconsin-Madison, Madison, WI, USA*
- Th.17 Membrane-Targeting Approaches for Enhanced Cancer Cell Destruction with Irreversible Electroporation  
*Chunlan Jiang, Zhenpeng Qin, John Bischof*

University of Minnesota, Minneapolis, MN, USA

## Attendees on their own for lunch

12:15 - 1:45

## President's symposium: Image Guided Thermal Therapy

1:45 - 3:15 Ballroom 2 Chair: Dieter Haemmerich

### Session sponsored by PHILIPS

- Th.18 Precision Noninvasive Thermal Lesion Formation Using Dual-mode Ultrasound  
*Emad Ebbini, Dalong Liu*  
University of Minnesota, Minneapolis, MN, USA
- Th.19 Image-Guided Thermal Therapy: Cryoablation  
*John Baust<sup>1</sup>, Thomas Polascik<sup>2</sup>*  
<sup>1</sup>State University of New York, Binghamton, NY, USA, <sup>2</sup>Duke University Medical Center, Durham, NC, USA
- Th.20 How to improve chemotherapy  
*Timo L.M. ten Hagen*  
Erasmus MC, Rotterdam, The Netherlands
- Th.21 Computer Modeling of Temperature-Sensitive Liposomes on Micro- and Macroscopic scales  
*Dieter Haemmerich*  
MUSC, Charleston, USA

## President's Reception

3:15 - 3:45 Ballroom 2

Please join us as we recognize Past-Presidents of the Society for Thermal Medicine. Sponsored by ZELTIQ and CoolSculpting.

## Workshop: Expanding the Clinical Hyperthermia Experience

3:45 - 6:15 Ballroom 2 Chair: Paul Stauffer & Zeljko Vujaskovic

### Session sponsored by BSD

- Th.22 Low dose re-irradiation & thermography controlled wIRA hyperthermia in extended recurrent breast cancer  
*Markus Notter<sup>1</sup>, Helmut Piazena<sup>2</sup>, Werner Müller<sup>3</sup>, Peter Vaupel<sup>4</sup>*  
<sup>1</sup>HNE La Chaux-de-Fonds, La Chaux-de-Fonds, Switzerland, <sup>2</sup>Charité Medical University, Berlin, Germany, <sup>3</sup>Wetzlar, Wetzlar, Germany, <sup>4</sup>Dep. Radiooncology and Radiotherapy University Medical Center, Mainz, Germany

- Th.23      Regional deep hyperthermia treatment (RHT) for children and adolescents with refractory or recurrent rhabdomyosarcoma (RMS) and RMS-like tumors  
*Ruediger Wessalowski*  
*Clinic of Pediatric Oncology, Hematology and Immunology, Center for Child and Adolescent Health, Medical Faculty, Heinrich-Heine-University Duesseldorf, Duesseldorf, Germany*
- Th.24      Regional Hyperthermia and Radiation Therapy for Cervical Carcinoma  
*Douglas Kelly, Michael Payne, Edwin Watts, James Flynn, David Simon, Tyler Gutschenritter, Matt Weaver*  
*Cancer Treatment Centers of America, Tulsa, OK, USA*
- Th.25      How can we make certain that Thermal Therapy will play a significant role in the future of oncology?  
*Joan Bull*  
*The University of Texas Medical School at Houston, Houston, TX, USA*
- Th.26      Development of the Center for Hyperthermia  
*Jennifer Yu, Andrew Godley*  
*Cleveland Clinic, Cleveland, OH, USA*
- Th.27      Coming full circle: Thermal Oncology Program at the University of Maryland  
*Zeljko Vujaskovic*  
*University of Maryland, Baltimore, USA*
- Th.28      Atzelsberg Circle clinical trials working group: better together  
*Gerard van Rhoon<sup>1</sup>, Oliver Ott<sup>2</sup>, Rolf Sauer<sup>2</sup>*  
*<sup>1</sup>Erasmus MC Cancer Institute, Rotterdam, The Netherlands, <sup>2</sup>University Erlangen-Nuremberg, Erlangen, Germany*

# Friday, May 9

## Breakfast

**7:00 - 8:15 am Ballroom 1**

A Breakfast buffet for Meeting Registrants. Your name badge is your admission to breakfast.

## Refresher on Cell Death Mechanisms, John Pearce, PhD

**8:15-9:15 Ballroom 2 Chair: Michael Graner**

Fri.1 Mathematical Models of Intrinsic and Extrinsic Cell Death Processes

John Pearce

*The University of Texas at Austin, Austin, TX, USA*

## Refresher on Exercise Physiology in the Oncology Setting, Lee Jones, PhD

**8:15 - 9:15 Deer/Elk Lake Room Chair: Pavel Yarmolenko**

Fri.2 The application of the principles of exercise physiology in the oncology setting

Lee Jones

*Memorial Sloan Kettering Cancer Center, NY, NY, USA*

## Refresher: Update on Japanese Thermal Medicine, Satoshi Kokura, MD

**8:15 - 9:15 Pine/Cedar/Birch Chair: Chang W. Song**

Fri.3 Efficacy of Gemcitabine combined with Hyperthermia therapy in the treatment of unresectable pancreatic cancer : Phase II study

Satoshi Kokura<sup>1,2</sup>, Takeshi Ishikawa<sup>2</sup>, Manabu Okajima<sup>2</sup>, Tatsuzo Matsuyama<sup>2</sup>, Naoyuki Sakamoto<sup>2</sup>, Yoshito Ito<sup>1</sup>

<sup>1</sup>Kyoto Gakuen University, Kameoka, Japan, <sup>2</sup>Kyoto Prefectural University of Medicine, Kyoto, Japan

## Keynote Address: Local Tumor Ablation Plus Immune Stimulation: Towards in situ Cancer Vaccines

**9:30 - 10:30 Ballroom 2 Chair: Sharon Evans**

featuring Gosse Adema, PhD from Radboud Institute for Molecular Life Sciences, Radboud University, Nijmegen, The Netherlands

Fri.4 Local Tumor Ablation plus Immune Stimulation: Towards in situ Cancer Vaccines

Gosse Adema

*RadboudUMC, RIMLS, Nijmegen, The Netherlands*

## Coffee Break with Exhibitors

10:30 - 10:45 Ballroom 1

## Symposium: Focused Ultrasound in Radiation Oncology

10:45 - 12:15 Ballroom 2

Chair: Jason Stafford

### **Session sponsor:**

### **Focused Ultrasound Surgery Foundation**

- Fri.5 Focused Ultrasound Therapy in Radiation Oncology: FUS Foundation Perspective  
Jessica Foley  
*Focused Ultrasound Foundation, Charlottesville, VA, USA*
- Fri.6 Magnetic Resonance Guided Focused Ultrasound: Bone Metastases and Beyond  
Mark Hurwitz  
*Thomas Jefferson University, Philadelphia, PA, USA*
- Fri.7 Focused Ultrasound Opportunities in Radiation Oncology  
Sunil Krishnan  
*MD Anderson Cancer Center, Houston, TX, USA*
- Fri.8 Therapeutic Ultrasound as an in situ tumor vaccine and other possibilities  
Chandon Guha  
*Albert Einstein College of Medicine, Bronx, NY, USA*
- Fri.9 MR-guided pulsed high intensity focused ultrasound enhancement of chemotherapeutic agents combined with radiotherapy for prostate cancer treatment  
Lili Chen<sup>1</sup>  
*<sup>1</sup>Fox Chase Cancer Center, Philadelphia, USA, <sup>2</sup>Temple University, Philadelphia, USA*
- Fri.10 MRI Assessment of Effective Ablated Volume Following High Intensity Focused Ultrasound  
Brett Fite<sup>1</sup>, Andrew Wong<sup>1</sup>, Yu Liu<sup>1</sup>, Lisa Mahakian<sup>1</sup>, Sarah Johnson<sup>1</sup>, Olulanu Aina<sup>1</sup>, Neil Hubbard<sup>1</sup>, Robert Cardiff<sup>1</sup>, Erik Dumont<sup>2</sup>, Katherine Ferrara<sup>1</sup>  
*<sup>1</sup>University of California, Davis, CA 95616, USA, <sup>2</sup>Image Guided Therapy, Pessac, France*

## Symposium: Thermosensitive and Photothermal Nanomedicine

10:45 - 12:15 Deer/Elk Lake Room

Chair: Timo ten Hagen

- Fri.11 Breast Cancer Cell Response to Silver Nanoparticle and Photothermal Therapy  
Edreca Thompson<sup>1</sup>, Michelle Alimpich<sup>3</sup>, Christopher MacNeill<sup>1</sup>, Elizabeth Graham<sup>1</sup>, George Donati<sup>2</sup>, Bradley T. Jones<sup>2</sup>, Nicole Levi-Polyachenko<sup>1</sup>  
*<sup>1</sup>Wake Forest University Health Sciences, Winston-Salem, USA, <sup>2</sup>Wake Forest University, Winston-Salem, USA, <sup>3</sup>College of Charleston, Charleston, USA*

- Fri.12 A novel theranostic approach to prostate cancer using gold nanoparticle directed photoacoustic imaging and photothermal therapy  
*Jung Choi, Eduardo Moros*  
*H. Lee Moffitt Cancer Center and Research Institute, Tampa, FL, USA*
- \*Fri.14 Soft Template Synthesis of Donor-Acceptor Conjugated Polymer Nanoparticles: Structural Effects, Stability and Photothermal Studies  
*Christopher MacNeill, Elizabeth Graham, Nicole Levi-Polyachenko*  
*Wake Forest University Health Sciences, Winston Salem, NC, USA*
- \*Fri.13 CXCR4 Targeted Polymer Nanoparticles for Enhanced Photothermal Ablation of the Brain Metastasis of Breast Cancer *In Vitro*  
*Elizabeth Graham, Christopher MacNeill, Nicole Levi-Polyachenko*  
*Wake Forest University, Winston-Salem, NC, USA*
- Fri.15 Cyclopentadecanolide Nanoemulsion promotes Heat-Induced Drug and Nanoparticle penetration throughout Tissues and Sensitizes Tissues to Thermal Ablation and Irreversible Electroporation.  
*Michael Borrelli, Wolf Heberlein, Jakob Szewedo, Jonah Wu*  
*University of Arkansas for Medical Sciences, Little Rock, AR, USA*
- Fri.16 Novel ultrasound imageable low temperature sensitive liposomes for use with ultrasound-guided high intensity focused ultrasound  
*Danny Maples, Ryan Newhardt, Ashish Ranjan*  
*Center for Veterinary Health Sciences, Oklahoma State University, Stillwater, Oklahoma, USA*
- Fri.17 Increasing ablation times boost local drug deposition during combination therapy with thermo-sensitive liposomal doxorubicin  
*Christian Rossmann, Dieter Haemmerich*  
*Medical University of South Carolina, Charleston, SC, USA*
- Fri.18 Hyperthermia improves drug delivery to solid tumors.  
*Timo L.M. ten Hagen*  
*Erasmus MC, Rotterdam, The Netherlands*

## STM Business Meeting Luncheon

12:15 - 1:45 Ballroom 2

## Workshop on Common topics in Thermal Medicine: Cell Death and Sensitization

1:45 - 3:45

Ballroom 2

Chair: John Baust

- Fri.19 Mechanisms of Cancer Cell Death Following Cryoablation  
*John G. Baust<sup>1</sup>, Anthony Robilotto<sup>1,2</sup>, William Corwin<sup>1,2</sup>, Robert Van Buskirk<sup>1,2</sup>, Andrew*

*Gage<sup>3</sup>, John M. Baust<sup>2</sup>*

*<sup>1</sup>SUNY Binghamton, Binghamton, NY, USA, <sup>2</sup>CPSI Biotech, Inc., Owego, NY, USA, <sup>3</sup>SUNY Buffalo, Buffalo, NY, USA*

- Fri.20 Arrhenius Models for Cell Death Revisited: Adding a Delay Significantly Improves Predictive Accuracy  
*John Pearce*  
*The University of Texas at Austin, Austin, TX, USA*
- Fri.21 Heat shock and endoplasmic reticulum stress-do they enhance the activity of HSP90 inhibitors?  
*Michael Graner<sup>1</sup>, Justin Hellwinkel<sup>1</sup>, Jasmina Redzic<sup>1</sup>, Alexandra Graner<sup>1</sup>, Helen Madsen<sup>1</sup>, Alex Lencioni<sup>1</sup>, Laura Epple<sup>1</sup>, Lynne Bemis<sup>2</sup>*  
*<sup>1</sup>University of Colorado Anschutz Medical Campus, Neurosurgery, Aurora, Colorado, USA, <sup>2</sup>University of Minnesota Duluth, Duluth, MN, USA*
- Fri.22 Magnetic Nanoparticle Heating in Cancer Hyperthermia and Cryopreservation Applications  
*Michael Etheridge<sup>1</sup>, Katie Hurley<sup>1</sup>, Jinjin Zhang<sup>1</sup>, Seongho Jeon<sup>1</sup>, Yi Xu<sup>1,2</sup>, Jeunghwan Choi<sup>1</sup>, Chris Hogan<sup>1</sup>, Christy Haynes<sup>1</sup>, Michael Garwood<sup>1</sup>, John Bischof<sup>1</sup>*  
*<sup>1</sup>University of Minnesota, Minneapolis, MN, USA, <sup>2</sup>University of Shanghai for Science & Technology, Shanghai, China*
- Fri.23 Lonidamine Induces Intracellular Tumor Acidification and ATP Depletion in Human Melanoma, Breast, Prostate and Ovarian Cancer Xenografts  
*Dennis Leeper<sup>1</sup>, Kavindra Nath<sup>2</sup>, David Nelson<sup>2</sup>, Rong Zhou<sup>2</sup>, Jerry Glickson<sup>2</sup>*  
*<sup>1</sup>Thomas Jefferson University, Philadelphia, PA, USA, <sup>2</sup>University of Pennsylvania, Philadelphia, PA, USA*

## Workshop on Metabolism and Bioenergetics

**1:45 - 3:45**

**Deer/Elk Lake Room**

**Chair: Elizabeth Repasky**

- Fri.24 Modulation of tumor physiology by exercise: implications for cancer progression and therapeutic response  
*Lee Jones*  
*Memorial Sloan Kettering Cancer Center, NY, NY, USA*
- Fri.25 Standard housing temperature for laboratory mice results in mild chronic cold stress which is sufficient to significantly alter host immune responses following bone marrow transplantation  
*Kathleen M. Kokolus, Nicholas D. Leigh, Jingxin Qiu, George L. Chen, Philip L. McCarthy, Xuefang Cao, Elizabeth A. Repasky*  
*Roswell Park Cancer Institute, Buffalo, NY, USA*
- Fri.26 Activation Energy As A System Specific Signature Of Thermal Protein Denaturation At Molecular And Cellular Scales



Zhenpeng Qin<sup>1</sup>, Saravana Kumar Balasubramanian<sup>1</sup>, Willem F. Wolkers<sup>2</sup>, John A. Pearce<sup>3</sup>, John C. Bischof<sup>1</sup>

<sup>1</sup>University of Minnesota, Minneapolis, MN, USA, <sup>2</sup>Leibniz Universität Hannover, Hannover, Germany, <sup>3</sup>University of Texas at Austin, Austin, TX, USA

Fri.27 Effects of moderate hypothermia and hyperthermia on microRNA expression pattern  
Jeffrey Hasday<sup>1,2</sup>, Ratnakar Potla<sup>1</sup>, Sergei Atamas<sup>1,2</sup>, Mohan Tulapurkar<sup>1</sup>, Ishwar Singh<sup>1</sup>  
<sup>1</sup>University of Maryland, Baltimore, MD, USA, <sup>2</sup>Baltimore VA Medical Center, Baltimore, MD, USA

Fri.28 Bioenergetics: Warburg, Apoptosis and Cytochrome C  
John Pearce<sup>1</sup>, Michael Graner<sup>2</sup>  
<sup>1</sup>The University of Texas at Austin, Austin, TX, USA, <sup>2</sup>The University of Colorado at Denver, Denver, CO, USA

### Coffee break in Atrium

**3:45 - 4:00 Atrium**

### William Dewey Award: Lessons Learned and Passed Forward

**4:00 - 5:00 Ballroom 2 Chair: Robert J. Griffin**

Fri.29 William Dewey Award: Lessons learned and passed forward  
Mark Dewhirst  
Duke University, Durham, NC 27710, USA

### J. Eugene Robinson Award: Regional Hyperthermia Combined with Chemotherapy - From the Bench to Bedside

**5:00 - 6:30 Ballroom 2 Chair: Gerard van Rhoon**

Fri.30 Regional hyperthermia combined with chemotherapy - from the bench to bedside  
Rolf D. Issels<sup>1,2</sup>  
<sup>1</sup>University Medical Center Grosshadern, Munich, Germany, <sup>2</sup>University of Munich Sarcoma Center, Munich, Germany

### Robinson Dinner

**7:00 - 9:00 Mason's Restaurant & Barre, 528 Hennepin Ave.**

Advance reservations are required for this private event. \$85 per person.

This year's dinner will be held at [Mason's Restaurant & Barre](#) in downtown Minneapolis on Friday, May 9. Ticket price includes a 3-course meal with salad or soup, entree, dessert, wine, coffee/tea, and gratuity.

# Saturday, May 10

## Breakfast

**7:00 - 8:15**     **Ballroom 1**

## Refresher on HIFU, Emad Ebbini, PhD

**8:15 - 9:15**     **Ballroom 2**                             **Chair: Ashish Ranjan**

Sat.1             Monitoring and Control of Focused Ultrasound in Thermal Therapy  
Emad Ebbini  
*University of Minnesota, Minneapolis, MN, USA*

## Refresher on Thermotherapy and Radiosensitization of Cancer Stem Cells, Jennifer Yu, MD, PhD

**8:15 - 9:15**     **Deer/Elk Lake Room**                     **Chair: Nicole Polyachenko**

Sat.2             Can thermotherapy improve radiosensitivity of cancer stem cells?  
Jennifer Yu  
*Cleveland Clinic, Cleveland, OH, USA*

## Symposium: Clinical Update on Thermal Ablation Medicine

**9:30 - 11:00**     **Ballroom 2**                             **Chair: Erik Cressman & Muneeb Ahmed**

Sat.3             Clinical Development of Laser Interstitial Thermal Therapy (LITT) For Brain Tumors: Experience and Evidence  
Alireza Mohammadi<sup>1</sup>, Ammar Hawasli<sup>2</sup>, Analiz Rodriguez<sup>3</sup>, Jason Schroeder<sup>1</sup>, Adrian Laxton<sup>3</sup>, Symeon Missios<sup>1</sup>, Paul Elson<sup>1</sup>, Stephen Tatter<sup>3</sup>, Gene Barnett<sup>1</sup>, Eric Leuthardt<sup>2</sup>  
<sup>1</sup>Cleveland clinic, Cleveland, Ohio, USA, <sup>2</sup>Washington University, St. Louis, USA, <sup>3</sup>Wake Forest University, Winston-Salem, USA

Sat.4             Analysis of spatial accuracy and precision of a dedicated breast MR-HIFU system during ablation of breast tumors in patients  
Roel Deckers<sup>1</sup>, Gerald Schubert<sup>2</sup>, Laura G. Merckel<sup>1</sup>, Floor M. Knuttel<sup>1</sup>, Thijs van Dalen<sup>3</sup>, Nicky H.G.M. Peters<sup>1</sup>, J.M.H.H van Gorp<sup>4</sup>, Maurice A.A.J. van den Bosch<sup>1</sup>, Chrit T.W. Moonen<sup>1</sup>, Lambertus W. Bartels<sup>1</sup>  
<sup>1</sup>Imaging Division, University Medical Center Utrecht, Utrecht, The Netherlands, <sup>2</sup>Philips Healthcare, Vantaa, Finland, <sup>3</sup>Department of Surgery, Diakonessenhuis, Utrecht, The Netherlands, <sup>4</sup>Department of Pathology, Diakonessenhuis, Utrecht, The Netherlands

Sat.5             Laser Interstitial Thermal Therapy in Brain Tumors: Predictive Value of Overlap between Hyper-Thermic Field and Corticospinal Tract as Manifested in Post-Op Motor Deficit  
Mandana Behbahani, Jeffrey Mullin, Gene Barnett, Alireza Mohammadi

*Cleveland Clinic, Cleveland, USA*

- Sat.6 Alternative therapies to thermal ablation: complementary and competitive approaches  
Ron Gaba  
*University of Illinois Hospital and Health Sciences System, Chicago, IL, United States*  
*Minor Outlying Islands*
- Sat.7 Combinational Oncological Therapies in Interventional Radiology  
Derek West  
*University of Texas Health Sciences Center at Houston, Houston, Texas, USA*
- Sat.8 Overview of Image-Based Monitoring of Thermal Therapies  
R. Jason Stafford  
*The University of Texas MD Anderson Cancer Center, Houston, TX, USA*
- Sat.9 MR-guided Cryoablation of Prostate Adenocarcinoma Recurrences: 6 month follow-up  
Lance Mynderse, David Woodrum  
*Mayo Clinic, Rochester, MN, USA*

## Coffee break in Atrium

**11:00 - 11:15 Atrium**

## Symposium: Heat Generating Nanomedicine

**11:15 - 12:45 Ballroom 2**

**Chair: Robert Ivkov & Elisangela Silveira-Lacerda**

- Sat.10 Magnetic nanoparticle hyperthermia cancer treatment: the road from material science to patients.  
Andrew Giustini<sup>1,2</sup>, Alicia Petryk<sup>1,2</sup>, Robert Stigliano<sup>1,2</sup>, Fridon Shubitidze<sup>2</sup>, Jinjin Zhang<sup>3</sup>, Michael Garwood<sup>3</sup>, Thomas Sroka<sup>1</sup>, Lesley Jarvis<sup>1</sup>, Eunice Chen<sup>1</sup>, Lionel Lewis<sup>1</sup>, Peter Kaufman<sup>1</sup>, P. Jack Hoopes<sup>1,2</sup>  
<sup>1</sup>Geisel School of Medicine at Dartmouth, Hanover, NH, USA, <sup>2</sup>Thayer School of Engineering at Dartmouth, Hanover, NH, USA, <sup>3</sup>Center for Magnetic Resonance Research at the University of Minnesota, Minneapolis, MN, USA
- Sat.11 Real-time thermography during magnetic nanoparticle hyperthermia and numerical simulations suggest a surface shell like heat source around the tumor  
Harley Rodrigues, Francielli Mello, Gustavo Capistrano, Carolina Martins, Sônia Santos, Nicholas Zufelato, Rafael Veloso, Elisângela Silveira-Lacerda, Andris Bakuzis  
*Universidade Federal de Goiás, Goiânia, Goiás, Brazil*
- Sat.12 Magnetic Nanoparticle Hyperthermia for Treatment of Bladder Cancer: A Summary of Large Animal Studies and Remaining Challenges  
Alireza Mashal, Martin Huisjen, Kate McNerny, Karl Frantz, Mike Susedik, Carolyn Adams, Andrew Updegrave, Marvin Ross, Dan McKenna  
*Actium Biosystems, Boulder, CO, USA*

- Sat.13 Toxicity and genotoxicity in cells of the peripheral blood of Swiss mice exposed to non-uniform magnetic field  
*Francielly Mello, Harley Rodrigues, Wanderson Costa, Luis Branquinho, Andris Bakuzis, Elisangela Silveira-Lacerda*  
*Universidade Federal de Goias, Goiania, Goias/Central, Brazil*
- Sat.14 Influence of in-vivo tumor model on outcomes with magnetic nanoparticle hyperthermia  
*Robert Ivkov, Anilchandra Attaluri, Sri Kamal Kandala, Jianan Wang, Michele Wabler, Michael Armour, Haoming Zhou, Christine Cornejo, Yonggang Zhang, Theodore DeWeese, Cila Herman*  
*Johns Hopkins University, Baltimore, MD, USA*
- Sat.15 Imaging and Treatment Planning for Magnetic Nanoparticle Hyperthermia  
*Alicia Petryk<sup>1</sup>, Robert Stigliano<sup>2</sup>, Fridon Shubitidze<sup>2</sup>, Hattie Ring<sup>3</sup>, Michael Garwood<sup>3</sup>, P. Jack Hoopes<sup>1,2</sup>*  
*<sup>1</sup>Geisel School of Medicine, Dartmouth College, Hanover, NH, USA, <sup>2</sup>Thayer School of Engineering, Dartmouth College, Hanover, NH, USA, <sup>3</sup>Center for Magnetic Resonance Research, University of Minnesota, Minneapolis, MN, USA*
- Sat.16 Mitigation of eddy current heating during magnetic nanoparticle hyperthermia therapy  
*Robert Stigliano, Fridon Shubitidze, Jack Hoopes*  
*Dartmouth College, Hanover, NH, USA*

### Symposium: New Devices & Approaches

**11:15-12:45 Deer/Elk/Lake room Chair: Eduardo Moros**

- Sat.17 Integrating Infrared Hyperthermia with Ionizing Radiation in Treatment of Cancer  
*Edward Abraham<sup>1,2</sup>, Van Woo<sup>1</sup>, Cheryl Harlin-Jones<sup>1,2</sup>, Mark Pomper<sup>3</sup>, Anja Heselich<sup>4</sup>, Florian Frohns<sup>4</sup>*  
*<sup>1</sup>Artesian Cancer Centers, Claremore, OK, USA, <sup>2</sup>Hyperthermia Associates, Claremore, OK, USA, <sup>3</sup>Horizon Medical Services, Tamarac, FL, USA, <sup>4</sup>Darmstadt University of Technology, Darmstadt, Germany*
- Sat.18 Recent Progress on a Focused Microwave Therapy System with Integrated Real-Time Microwave Thermal Monitoring  
*John Stang, Mark Haynes, Guanbo Chen, Mahta Moghaddam*  
*University of Southern California, Los Angeles, USA*
- Sat.19 Real-time Temperature Control using Dual Mode Ultrasound Array System  
*Dalong Liu, Alyona Haritonova, Kamlesh Shroff, Mahdi Bayat, Rajagopal Aravalli, Efrosini Kokkoli, Emad Ebbini*  
*University of Minnesota, Minneapolis, USA*
- Sat.20 Evaluation of tissue-mimicking gelatin phantoms for use with MRgHIFU  
*Alexis Farrer, Joshua de Bever, Brittany Coats, Douglas Christensen, Allison Payne*

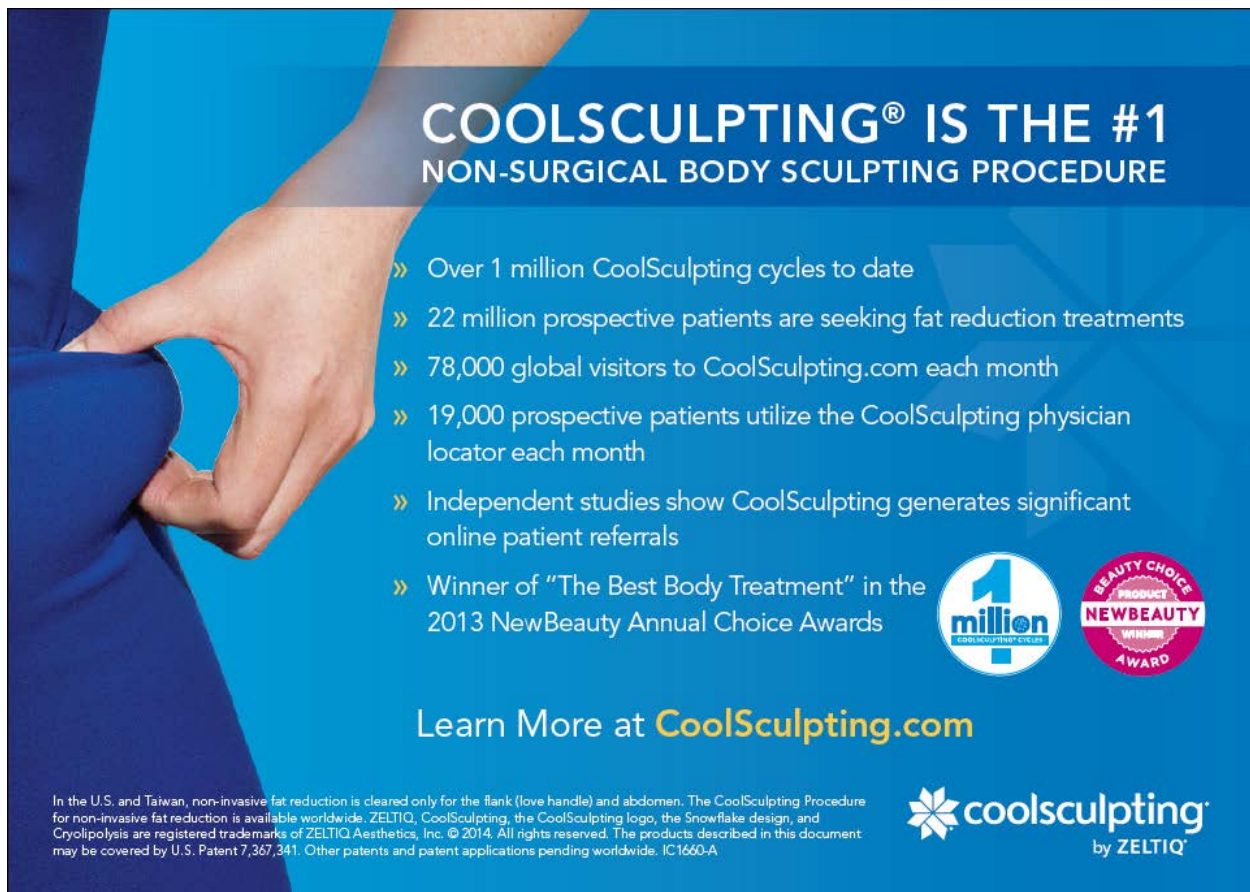
*University of Utah, Salt Lake City, UT, USA*

Sat.21 A New Energy Source For Thermal Medicine: Convective Thermal Water Vapor

Michael Hoey<sup>1</sup>, Christopher Dixon<sup>2,1</sup>

<sup>1</sup>NxThera Inc, Maple Grove, MN, USA, <sup>2</sup>Lenox Hill Hospital, NY, NY, USA

# Abstracts for Wednesday, May 7th






**COOLSCULPTING® IS THE #1  
NON-SURGICAL BODY SCULPTING PROCEDURE**

- » Over 1 million CoolSculpting cycles to date
- » 22 million prospective patients are seeking fat reduction treatments
- » 78,000 global visitors to CoolSculpting.com each month
- » 19,000 prospective patients utilize the CoolSculpting physician locator each month
- » Independent studies show CoolSculpting generates significant online patient referrals
- » Winner of “The Best Body Treatment” in the 2013 NewBeauty Annual Choice Awards

Learn More at [CoolSculpting.com](http://CoolSculpting.com)

In the U.S. and Taiwan, non-invasive fat reduction is cleared only for the flank (love handle) and abdomen. The CoolSculpting Procedure for non-invasive fat reduction is available worldwide. ZELTIQ, CoolSculpting, the CoolSculpting logo, the Snowflake design, and Cryolipolysis are registered trademarks of ZELTIQ Aesthetics, Inc. © 2014. All rights reserved. The products described in this document may be covered by U.S. Patent 7,367,341. Other patents and patent applications pending worldwide. IC1660-A

  
by ZELTIQ

**Wed.1****Understanding Cancer Therapy in the Context of Thermal Biology: *Not Always a Warm Relationship!***

Elizabeth A. Repasky

*Roswell Park Cancer Institute, Buffalo, New York, USA*

Research mice are housed under mildly cool, sub-thermoneutral ambient temperatures, a condition which activates thermoregulatory increases in norepinephrine driven heat production. The goal of this “Refresher” presentation is to review information from the fields of thermal biology and physiology which prepares the audience to appreciate the ramifications of this metabolic stress and understand how the interpretation of experimental data is impacted. I will discuss research by others which has shown that the degree of metabolic effort associated with heat production can significantly impact data interpretation in several fields of study. I will also highlight some of our own recent data regarding the relationships between thermoregulation and tumor growth control by the immune system which suggests that the balance between pro-tumorigenic immunosuppressive cells and anti-tumor effector immune cells is highly sensitive to adrenergic stress in tumor bearing mice. Additionally, I will present new data on the potential for adrenergic stress to impact the therapeutic efficacy of cytotoxic therapies including radiation and chemotherapy. Finally, I will discuss hypotheses concerning the potential for this research to improve our understanding of heterogeneity among human cancer patients with regard to treatment outcome and overall survival.

**Wed.2****Combination of Hyperthermia with SBRT/SRS**

Chang W. Song<sup>1</sup>, Robert J. Griffin<sup>2</sup>

<sup>1</sup>University of Minnesota, Minneapolis, MN, USA, <sup>2</sup>University of Arkansas for Medical Science, Little Rock, AR, USA

Thermal medicine is a medical practice that manipulates tissue or body temperature, i.e. heating or cooling, for the treatment of diseases such as cancer. While ablative heating of tumors to higher than 50°C or cryosurgery to cool tissues to cytotoxic temperature are usually used alone, conventional local hyperthermia, which selectively elevates tumor temperature to about 40-43°C, is used in combination with radiotherapy or chemotherapy. Whole-body hyperthermia at fever range temperatures has been known to elevate immunity and also increase the efficacy of some anti-cancer drugs. For the effective combination of thermal medicine, particularly local hyperthermia, in combination with radiotherapy, it is important to fully comprehend the biological principles of radiotherapy. A recent development in radiotherapy is the increased use of stereotactic body radiation therapy (SBRT) and stereotactic radiosurgery (SRS) which deliver a radiation dose of 20-50 Gy in 1-5 fractions to target tumors. These hypofractionated radiotherapy regimens have been demonstrated to be highly effective for the control of various tumors. However, a simple calculation based on classical radiobiology would suggest that SBRT and SRS with 20-50 Gy in 1-5 fractions are not supposed to be able to directly kill all the tumor cells in clinically identifiable tumors: 1 gm tumors contain  $10^8$ - $10^9$  viable tumor cells. Indications are that high-dose per fraction SBRT and SRS cause vascular damage leading to deterioration of the intratumor microenvironment towards a hypoxic, acidic and nutrient deficient state. Such a chaotic environment appears to kill the tumor cells which survived the direct effect of radiation. The massive release of antigen from the necrotic tumor cells may enhance anti-tumor immune reactions leading to additional cell death. When tumors are treated with high-dose SBRT/SRS and then subjected to local hyperthermia, the vascular damages caused by SBRT-SRS would hinder heat dissipation, thereby improving tumor heating. Furthermore, the acidic and nutritionally deprived intratumor microenvironment caused by SBRT/SRS may sensitize surviving tumor cells to subsequent heating. In addition, mild heating may potentiate the immune reactions caused by SBRT/SRS. Combination of SBRT/SRS with local hyperthermia may be a potent approach for control of tumors.



**Wed.3****Advanced Magnetic Resonance Imaging Approaches to Thermal Therapy and Nanomedicine Biodistribution**

M. Garwood<sup>1</sup>, J. Zhang<sup>1</sup>, M.L. Etheridge<sup>1</sup>, H.L. Ring<sup>1</sup>, K.R. Hurley<sup>1</sup>, L. Utecht<sup>1</sup>, A. Petryk<sup>2</sup>, S. Jeon<sup>1</sup>, D. Idiyatullin<sup>1</sup>, C. Hogan<sup>1</sup>, C.L. Haynes<sup>1</sup>, J.C. Bischof<sup>1</sup>, P.J. Hoopes<sup>2</sup>

<sup>1</sup>University of Minnesota, Minneapolis, Minnesota, USA, <sup>2</sup>Dartmouth College, Hanover, New Hampshire, USA

In spite of preliminary clinical trials in Europe and promising preclinical studies, the successful use of magnetic nanoparticle (mNP) hyperthermia cancer treatment will depend on many factors, including: 1) A safe and adaptable nanoparticle platform; 2) A non-toxic, targetable, nanoparticle-activating alternating magnetic field (AMF); 3) Non-invasive *in vivo* nanoparticle imaging; 4) Relevant and translatable pre-clinical studies; 5) Thermal dosimetry and *in vivo* validated computational models allowing for nanoparticle-AMF treatment planning; 6) Understanding interactions of mNP hyperthermia with conventional adjuvant therapies; 7) Well planned, early-phase clinical studies in humans.

One of the most critical aspects of performing successful and sophisticated mNP-AMF based hyperthermia treatment is the generation of an accurate radiologic-based mNP and anatomic imaging system which can not only assess tumor and normal tissue anatomy and geometry but can detect and quantify the mNPs (Fe) levels and biodistribution in a spatially accurate, sensitive and robust manner. CT imaging is capable of detecting and quantifying mNPs at levels above 10 mg/gram tissue (tumor); unfortunately this level is unlikely to be clinically achievable in most situations. Conventional gradient-echo MRI methods are also capable of detecting mNPs/Fe, although only when mNP/Fe levels are below the grossly quantifiable therapeutic hyperthermia threshold (~ 0.1 mg Fe/gm tissue/tumor when using dextran coated 60-100 nm ferromagnetic NPs). Recently, we solved this problem by using a new MRI technology called SWIFT (SWEEP Imaging with Fourier Transformation). With SWIFT, mNPs in aqueous environments can be visualized clearly with positive contrast (ie, images display hyperintensity in regions where mNPs are located). Furthermore, the concentrations of the mNP/Fe visualized in SWIFT images can be quantified by measuring the longitudinal relaxation time  $T_1$  of the water protons. Experiments on dispersed mNPs in gels show  $1/T_1$  to be linearly proportional to Fe concentration up to at least 3 mg Fe/mL (Zhang et al, *Magn Reson Med*, in press). Such high concentration exceeds that measured in previous MRI studies by roughly an order of magnitude. Of particular note, the measured  $1/T_1$  values of both dispersed and aggregated mNPs in gels were found to be predictive of AMF heating (SAR) (Etheridge et al, submitted). *In vitro* and *in vivo* (mouse tumor model) SWIFT studies and the future of SWIFT imaging in clinical mNP cancer treatment trials, will be discussed.

**Wed.4****Characterization of the State of Aggregation of Nanomaterials in Biological Systems**

Seongho Jeon, Katie Hurley, Michael Etheridge, Thaseem Thajudeen, Michael Garwood, John Bischof, Christy Haynes, Chris Hogan

*University of Minnesota, Minneapolis, USA*

The pH and ionic strengths of inter- and intracellular matrices not ideal for nanomaterials to remain stable in suspension. Therefore, nanomaterials in biological suspensions typically persist as aggregates, i.e. interconnected structures composed individual nanomaterials (nanoparticles). The structures of aggregates may strongly influence the resulting effect nanomaterials have on a biological system. Unfortunately, techniques to characterize three dimensional structures of aggregates are lacking, and this has precluded clear examination of the influence of aggregation on nanomaterial behavior.

Motivated by this issue, we have developed an image processing method to predict 3D-structural information of aggregates from 2D cryo-electron microscopy images, which may be used to examine aggregate morphology in inter- and intracellular matrices. Specifically, we develop computational approaches to determine 4 observable parameters for 2D aggregate projections– the perimeter, the projected area, the longest end to end distance in an aggregate, and the aggregate's two-dimensional radius of gyration. These four parameters from images are compared to the expected values for computationally generated quasifractal aggregates of prescribed properties, i.e. aggregates composed of point contacting primary spheres where the number of primary spheres (N) is proportional to the 3-D radius of gyration raised to a power (the fractal dimension). The most probable number of primary particles and the fractal dimension of an observed aggregate are inferred through this comparison.

We specifically apply this method to iron (II, III) –oxide aggregates in ionic solutions (Phosphate Buffered solutions (PBS)) and protein solutions (Fetal Bovine Serum (FBS)). These solutions are prepared with varying ionic concentration (1.0 ~ 2.0) and protein amount (25% ~ 100%). At least 20 aggregates are analyzed for each suspension. It is found that number of primary particles in aggregates increases with increasing dissolved solute concentration (both ionic solutes and proteins). The fractal dimensions of aggregates in PBS suspensions are found to be ~1.9-2.0 under most conditions, while those in FBS suspensions are in the ~1.7-1.8 range. Iron oxide aggregates are additionally imaged in inter- and intracellular matrices, revealing that intercellular aggregates are significantly smaller than those in intracellular matrices (which are found primarily in endosomes) with fractal dimension of 1.6-2.0, while those in intracellular matrices have fractal dimensions of 1.9-2.1.

**Wed.5**

**Enhancing Therapeutic Efficacy of Magnetic Hyperthermia Through Designed Aggregation of SPIO Nanoparticles**

Jayanth Panyam, Tanmoy Sadhukha, Timothy Wiedmann

*University of Minnesota, Minneapolis, MN, USA*

Particle size is a key determinant of biological performance of sub-micron size delivery systems. Previous studies investigating the effect of particle size have primarily focused on well-dispersed nanoparticles. However, inorganic nanoparticles are prone to aggregation in biological environments. In our studies, we examined the consequence of aggregation on superparamagnetic iron oxide (SPIO) nanoparticle-induced magnetic hyperthermia. Here we show that the extent and mechanism of hyperthermia-induced cell kill is highly dependent on the aggregation state of SPIO nanoparticles. Well-dispersed nanoparticles induced apoptosis, similar to that observed with conventional hyperthermia. Sub-micron size aggregates, on the other hand, induced temperature-dependent autophagy through generation of oxidative stress. Micron size aggregates caused rapid membrane damage, resulting in acute cell kill. Overall, this work highlights the potential for developing highly effective anticancer magnetic hyperthermia modalities through designed aggregation of SPIO nanoparticles.

**Wed.6****Continuous vs Pulsed Near Infra-red Heating of Hollow Gold Nanoparticles - Implications and Applications**

Joseph Zasadzinski<sup>1</sup>, Norbert Reich<sup>2</sup>, Gary Braun<sup>3</sup>, Dean Morales<sup>2</sup>, Natalie Forbes<sup>2</sup>, Alessia Pallaoro<sup>2</sup>, Xiao Huang<sup>2</sup>

<sup>1</sup>University of Minnesota, Minneapolis, Minnesota, USA, <sup>2</sup>University of California, Santa Barbara, California, USA, <sup>3</sup>Sanford-Burnham Medical Research Center, La Jolla, California, USA

Hollow gold nanoparticles strongly absorb near infra red light in the range from 700-900 nm depending on their diameter to shell thickness ratio. However, the conversion of this light energy to heat depends on how the light is delivered – as a continuous wave or as pico- to femtosecond pulses. For continuous wave irradiation, a steady state temperature gradient is rapidly established and the HGN temperature is likely less than 5 – 10 C above the background. The irradiated HGN act as a local heat source, raising the overall temperature of the material with time, proportional to the light intensity. We have used this property of HGN to induce rapid, but controlled release of doxorubicin from thermosensitive liposomes chemically tethered to the HGN that have a permeability transition at 41 C. The combination of doxorubicin and local heating provides a synergistic effect resulting in enhanced cancer cell toxicity. The local heating effects of the HGN on the cell membrane induce the permeability transition even when the bulk temperature is not increased. This allows for drug release even at low concentrations of HGN, as no collective heating effect is necessary.

Pico to femto-second pulsed laser irradiation at similar total energy input, induces a much different temperature response of the HGN. The laser pulses deposit energy in the HGN faster than thermal processes (nano to micro-seconds) can dissipate energy to the surrounding fluids, so all of the energy of the pulse first heats the HGN to sufficient temperatures that annealing or melting of the HGN can take place. The HGN temperature is sufficient that gold-thiol bonds between genetic materials such as DNA, RNA, or proteins and the HGN can be thermalized and broken, thereby releasing therapeutic molecules to the surroundings. As energy is dissipated into the surrounding fluid, usually water, vapor bubbles are formed whose sizes depend on the energy input to the HGN. These vapor bubbles then grow and collapse, similar to cavitation bubbles produced by ultrasound, and can tear apart endosomes, cell membranes, or liposomes. Surprisingly, these dramatic events occur without damaging the DNA, RNA or proteins attached to the HGN. We have used pulsed lasers and HGN to deliver siRNA to target the polo-like kinase gene selectively to cancer cells displaying the neuropilin-1 epitope. Release of the siRNA from the nanoparticles and efficient endosomal escape within the cell result from pulsed laser irradiation. As a result, our approach requires ten-fold less material than standard nucleic acid transduction materials, and is significantly more efficient than other particle based methods. We have also developed a HGN for the cytosolic delivery of nickel-chelated poly-histidine tagged proteins. The method can be used to rapidly deliver protein to an entire cell culture with high efficiency and low toxicity, or, by taking advantage of targeting ligands, address only a chosen cell type in a mixed culture. When used with light supplied by a two-photon microscope, the method is capable of real-time targeting of individual cells with resolution similar to microinjection techniques.

**Wed.7****Assessment of preconditioning on LNCaP tumors by a TNF- $\alpha$  nanoparticle construct using MRI**

Greg Metzger, John Bischof, Jeunghwan Choi, Isabelle Iltis, Manda Vollmers

*University of Minnesota, Minneapolis, MN, USA*

The outcome of systemic and local therapies (e.g., chemotherapy, radiotherapy, surgery, focal ablation) for prostate cancer can be significantly improved by using tumor-specific adjuvants prior to treatment (“preconditioning”). We propose to use dynamic contrast enhanced magnetic resonance imaging (DCE-MRI) to monitor the in vivo response of a mouse model of prostate cancer treated with a vascular disruptive agent, TNF- $\alpha$ , delivered on a gold nanoparticle (NP-TNF). Six male nude mice bearing 4-5 weeks old LNCaP tumors were scanned at 9.4T. DCE-MRI was performed two days before and 4-5 hours after treatment with NP-TNF. An intraperitoneal bolus of Gadolinium-DTPA (Gd) was administered and contrast enhancement was measured for 90 minutes. Concentration time curves of Gd were calculated and the area under the Gd curve (AUGC) was determined pre and post treatment. NP-TNF treatment caused an increase in contrast uptake in tumors. Interestingly, the early concentration (10 minutes post Gd bolus i.p.) was similar in both untreated and treated conditions; however, 90 minutes after injection, [Gd] was 3.4 times higher after treatment compared to before. AUGC doubled from  $11 \pm 6$  [Gd]  $\times$  min before treatment to  $22 \pm 9$  [Gd]  $\times$  min after treatment. An increase in signal enhancement was also observed in the muscle but to a lesser degree. We also evaluated the kinetics of intravenous gadolinium administration in mice bearing a jugular vein catheter to mimic the delivery method used in clinical trials. The overall treatment effects were independent of the delivery pathway of the contrast agent. In conclusion, we show that DCE-MRI is suitable to detect changes associated with a vascular disruptive agent in a mouse model of prostate cancer. The ability to characterize the effects of nanoparticle therapy in vivo with non-destructive methods is important as such compounds, in combination with treatment strategies, progress towards clinical trials.

**Wed.8****Cytotoxic Interactions of Heat and Salt Exposure using Sodium Acetate in Murine 4T1 Breast Carcinoma Cells**

Erik Cressman<sup>1</sup>, Robert Griffin<sup>2</sup>, Azemat Jamshidi-Parsian<sup>2</sup>

<sup>1</sup>MD Anderson Cancer Center, Houston, TX, USA, <sup>2</sup>University of Arkansas for Medical Sciences, Little Rock, AR, USA

**Background**

The mechanism of how thermochemical ablation (TCA) kills cells and what factors are most important in this process are unknown. In one variant of TCA, heat is evolved from a neutralization reaction and sodium acetate is produced as a salt in high concentrations local to the site of administration. We report on the initial assessment of the relationship between exposure time, heat shock, and salt concentration as they affected cell viability in culture.

**Methods**

Triplicate samples in two separate cell culture experiments were performed with increasing concentrations of sodium acetate, the salt product of thermochemical ablation using acetic acid and sodium hydroxide ranging up to 800 mMol/L. Temperature and time exposure variables (37, 41, 50, and 60 °C, 3 and 24h) were tested in 4T1 murine breast carcinoma cells followed by viability assessment using the CellTiter-Glo viability assay.

**Results**

Low temperatures, short exposure times, and low concentrations did not significantly affect cell survival. As these variables were increased, survival quickly decreased. The salt was sufficiently toxic at higher exposures (above 200 mMol/L) that only lower concentrations at short exposure durations could potentially demonstrate added effects of hyperthermia.

**Conclusion**

At low concentrations and low temperatures such as could be expected in systemic exposure or at the extreme periphery of a lesion, sodium acetate is not appreciably toxic to cells. Intralesional concentrations produced in the technique are orders of magnitude higher at the center and remain elevated for quite some distance from the point of injection. This bodes well for thermochemical ablation as a technologic platform, but further work to more clearly define the generality of these observations across different cell types, the distribution of agents, thermal exposure histories, cytotoxic parameters, and interaction of salt products with hyperthermia is warranted.

**Wed.9**

**Testing of Cardiac Ablative Devices Employing Visible Heart® Methodologies**

Paul Iaizzo

*University of Minnesota, Minneapolis, Minnesota, USA*

The Visible Heart® Laboratory has been reanimating large mammalian hearts, including human, for over 17 years. The patented methodologies include the use of a clear perfusate so to allow for direct internal visualization using endoscopes: i.e., while at the same time permitting comparative imaging with echocardiography or fluoroscopy. Hence, we have unique abilities to study the device-tissue interface in totally functional hearts, those in native sinus rhythm or those being paced. We have employed this approach to investigate commonly employed and developing means to administer cardiac ablative therapies. More recently, we have reanimated heart/lung blocs, which provides the unique opportunity to study pulmonary vein ablations within native anatomies.

**Wed.10**

**Computerized training of cryosurgery: objectives and prototype development**

Yoed Rabin, Kenji Shimada, Robert Keelan, Anjali Sehrawat, Hong Zhang

*Carnegie Mellon University, Pittsburgh, PA, USA*

Cryosurgery practices have evolved over the years in close relationship with concurrent technology developments. With the development of cryosurgery as a minimally invasive procedure about two decades ago, additional technical challenges have emerged, such as visualization of the process, correlating medical imaging with the thermal history, optimizing the geometry and the cooling capability of the cryoprobes, and optimizing the total number of cryoprobes and their layout. Recent developments in computer hardware and software technologies are enabling computer simulations of complete cryosurgery cases in a matter of seconds—two orders of magnitude faster than the actual procedure. This accelerated runtime enables projection of multiple scenarios in order to improve clinical decision making. The current presentation aims at recent developments in computation tools for the purpose of cryosurgery training, while discussing training objectives and prototype development of an intelligent tutoring system.



**Wed.11**

**Simulated ultrasound imaging for the purpose of prostate cryosurgery training**

Robert Keelan, Hong Zhang, Kenji Shimada, Yoed Rabin

*Carnegie Mellon University, Pittsburgh, PA, USA*

As a part of an ongoing program to develop computerized training tools for cryosurgery, this presentation addresses three key elements of development: (i) a method to simulate ultrasound imaging in a virtual cryosurgery setup, (ii) a training interface, and (iii) a framework for rapid bioheat transfer simulation. The need for ultrasound simulations stems from the fact that frozen tissue and metallic objects have higher acoustic impedances than the surrounding soft tissue—the target of ultrasound imaging. The presence of these elements in the imaging field creates artifacts ranging from signal distortion to complete shadowing. A new method is displayed in the current presentation to effectively capture those artifacts for the physical simulation of the procedure. The need for a rapid simulation framework originates from the computationally intensive nature of computerized training, combining geometric modelling and phase-change effects. Benchmark studies on a newly developed GPU-based framework is displayed in this presentation, with a typical simulation runtime of 2 seconds for a cryosurgery operation of 5 minutes. Finally, a training interface is displayed to integrate imaging and thermal simulations.

**Wed.12****Tools and Models for In Silico Investigation of EM- and US-Based Thermal Therapies in Complex Anatomies**

Esra Neufeld<sup>1</sup>, Adamos Kyriakou<sup>1,2</sup>, Niels Kuster<sup>1,2</sup>

<sup>1</sup>Foundation for Research on Information Technologies in Society (IT<sup>2</sup>S), Zurich, Switzerland,

<sup>2</sup>Swiss Federal Institute of Technology (ETH), Zurich, Switzerland

Thermal medicine, including hyperthermic oncology, radiofrequency-, microwave-, and focused ultrasound ablation, as well as cryo-ablation, requires *in silico* modelling for treatment planning and optimization, to elucidate the underlying physical, biological and physiological mechanisms, to develop novel technologies, quality assurance guidelines and methods, and for visualization and teaching. The modelling task is further complicated because of: i) the necessity of considering the impact of perfusion and thermoregulation, ii) the importance of the complex anatomy, particularly when the energy is administered externally and needs to be focused deeply, and iii) the need to include physiological and biological factors, e.g., factors related to effect and outcome prediction. Given these requirements, a segmentation tool, detailed anatomical models, and an image-based multiphysics simulation platform, suitable for modelling physical and biological processes in complex anatomies, have been developed and experimentally validated.

To generate detailed, potentially patient-specific, anatomical models, a segmentation tool is required that can handle large numbers of tissues which need to be distinguished, the wide range of treatment regions of interest, and local distortions in the anatomy that typically result from tumors and other pathological conditions. Such constraints often inhibit the use of automatic segmentation techniques. Therefore, a toolbox has been generated that allows to flexibly combine automatic segmentation techniques with semi-automatic, interactive ones and with fully manual approaches. The platform has also been used to generate a set of ten detailed reference anatomical models (Virtual Population, ViP), ranging from children to elderly and covering a wide range of body shapes. Some of these models are poseable and morphable, which extends the population coverage, and they have been used by more than 300 research groups world-wide.

The novel simulation platform was devised to ideally integrate medical image data (to define geometry, distributed parameters, and boundary conditions) and complex anatomical models such as the ViP. Besides other solvers, it comprises full-wave and low frequency EM solvers as well as full-wave and fast hybrid angular spectrum US solvers to determine and optimize the energy deposition for thermal therapies. A thermal solver is available that accounts for perfusion, including discrete vasculature, and local as well as whole-body thermoregulation. It can model effects such as coagulation, cell-water evaporation, and phase transitions. Thermal dose and tissue damage modelling is available to estimate the treatment effect and the platform supports post-processing- and FEM-based approaches to treatment outcome prediction, including modelling of disease evolution.

**Wed.13****Numerical Investigation of HIFU Tumor Ablation: Focus Scanning Approaches, Vasculature, and Standing-Waves**

Adamos Kyriakou<sup>1,2</sup>, Esra Neufeld<sup>1</sup>, Gal Shafirstein<sup>3</sup>, Eduardo Moros<sup>4</sup>, Gabor Szekely<sup>2</sup>, Niels Kuster<sup>1,2</sup>

<sup>1</sup>Foundation for Research on Information Technologies in Society (IT<sup>2</sup>IS), Zurich, Switzerland,

<sup>2</sup>Swiss Federal Institute of Technology (ETH), Zurich, Switzerland, <sup>3</sup>Roswell Park Cancer Institute, Buffalo, New York, USA, <sup>4</sup>H. Lee Moffitt Cancer Center and Research Institute, Tampa, Florida, USA

High intensity focused ultrasound offers advantages over conventional modalities in the ablation of solid malignancies, due to the prospect of achieving precise lesions in an otherwise noninvasive procedure. However, the long treatment times resulting from the necessity to overlap multiple such lesions for good tumor coverage can be limiting, particularly when treating large tumors. In this study, SonoKnife, a line-focused transducer, is modeled to investigate the impact of scanning approaches and of various factors potentially complicating the ablation process.

A head and neck squamous cell carcinoma was positioned in the immediate vicinity of the vertebral column and the mandible of an image-based anatomical model, surrounding the jugular vein and lying in close proximity to the carotid artery. A 450 elements array (1 MHz) was modeled. Acoustic simulations in water were successfully compared against measurements and simulations with FOCUS. Acoustic and thermal simulations of tumor ablation were performed in which beam steering via analytical and simulated time-reversal approaches was applied to the array to overlap multiple focal regions and ensure coverage of the entire tumor. Multiple ablation approaches, including sequential volume scanning and volumetric ablation were investigated. In addition, the treatment parameters, i.e., sonication duration and intensity, pause duration between sonications, scanning order etc., were varied and their impact on the treatment outcome was quantified by calculating CEM43 to delimit damaged/ablated regions.

Analytically calculated phase steering resulted in a prominent distortion and shift of the focal region, which could be improved using time-reversal techniques. Improper choice of the acoustic window can occasionally lead to collateral damage due to standing wave effects from unavoidable reflections at the bones (and skin). For sequential scanning, the scanning order had only a minimal impact, but volumetric ablation approaches resulted in similar treatment quality within reduced treatment time and with less damage to the overlaying tissues. The presence of major vasculature in the vicinity of the treated volume resulted in non-ablated tumor areas close to the vessel walls.

To maximize tumor exposure while sparing healthy tissue, treatment parameters optimization (potentially including frequency) may be necessary on a per-sonication basis. Challenging targets in the vicinity of bone structures can require the definition of alternative acoustic windows. High-resolution acoustic and thermal simulations allow for the detailed modeling of ablation processes. Treatment parameters can be easily optimized, while full-wave modeling permits for adverse secondary effects to be predicted and possibly compensated for.

**Wed.14**

**Damage-Dependent Bioheat Transfer Modeling in Thermal Therapy**

Yusheng Feng<sup>1</sup>, Cliff Zhou<sup>1,2</sup>, Robert Moser<sup>2</sup>

<sup>1</sup>UT San Antonio, San Antonio, USA, <sup>2</sup>UT Austin, Austin, USA

In thermal therapeutic treatment planning and optimization, it is essential to characterize tissue properties in order to bioheat transfer. However, it is a challenge to determine thermal conductivity and perfusion parameter when these properties are evolving due to thermal damage of tissues. In this talk, we present a damage-dependent perfusion model, where capillary perfusion field changes as thermal damage accumulates, based on a general model we have developed using the continuum mixture theory. The permeability and heat coefficient of tissue are assumed to be dependent on the state of tissue damage. Also in this model, the inter- and intra-patient variations of the tissue porosity and blood flow rate due to different physiological states and pathological conditions are also considered. The results show that the temperature fields are quite different between damage-dependent bioheat transfer model and traditional models with considering parameter changes due to thermal damage. Moreover, we will present critical model parameters so that the damage-dependency has large effect on perfusion, which in turn will affect the reliability of treatment planning based on traditional modelling methodology.

Wed.15

### **A New Algorithm for Light Dosimetry During Interstitial Laser Therapy of Locally Advanced Tumors**

Emily Oakley, Brian Warzen, Hassan Arshad, Gal Shafirstein

*Roswell Park Cancer Institute, Buffalo, NY, USA*

**Background and Objectives:** Interstitial laser therapy is being accomplished by delivering laser light through one or more laser fibers inserted into the target tumor. To date, magnetic resonance imaging and intensive computer simulations are being used to deliver the prescribed light dose into the tumor. Therefore, this technology has been limited to few selected medical centers. The objective of this work was to develop an algorithm to calculate light dose distribution within tumors with standard laptop computers.

**Methods:** A geometry that represents the target tumor and margins is reconstructed from two-dimensional scans obtained from computed tomography (CT) imaging, prior to therapy. The laser fibers are represented with an array of cylinders. The entire geometry (fibers and tumor) is imported into a finite element modeling software (COMSOL 4.3b, Comsol AB Stockholm, Sweden). Our previously developed and verified diffusion model is used to calculate light propagation. The calculation time is minimized by optimizing the mesh size. The light distribution is being measured with a dosimetry system, during therapy. These measurements are used to verify the simulation and calculate the optical properties of the treated tumor. An optimization procedure is employed to deliver the prescribed light dose to the target tumor.

**Results:** The algorithm was verified in phantoms mimicking tissue optical properties. CT scans from patients with locally advanced head neck cancer were used to test the algorithm in clinical settings. Tumor geometries and surrounding anatomical structures were segmented to reconstruct the three-dimensional computer model. The geometries are successfully meshed for performing the finite element analysis. The simulation enables the visualization of the light dose distribution in 3D and in cross-sectional layers along the tumor. The effects of potential overtreatment and undertreatment are readily visualized.

**Conclusion:** This light dosimetry algorithm can be utilized to monitor interstitial laser therapy with readily available laptop computers. The method has the potential to assist physicians in administering prescribed light doses to target tumors.

Wed.16

### The Physics behind Cryolipolysis

Joel Jimenez Lozano, Joe Coakley, George Frangineas

*Zeltiq Aesthetics, Inc., Pleasanton, CA, USA*

**Background and Objectives:** Cryolipolysis® non-invasively reduces subcutaneous fat in a treated region. Cryolipolysis is safe and effective when performed using non-invasive applicators to extract energy (cooling). Previous studies have investigated clinical safety, efficacy, and tolerability, biological processes, and clinical experiences. The underlying thermal physics during Cryolipolysis treatment, however, are not yet well understood.

**Materials and Methods:** A finite element method was used to model three-dimensional, time-dependent heat transfer from the applicator to tissue (skin, fat, and muscle) during a cooling treatment. Tissue cooling using the family of vacuum and surface (non-vacuum) applicators (CoolSculpting by ZELTIQ Aesthetics, Pleasanton, CA) was studied. The mathematical model was compared with *in vivo* experimental data at fixed implanted probe locations. Cooled tissue volume was quantified for each applicator.

**Results:** Tissue temperature distributions demonstrated targeted cooling delivery. Heat flux shows energy transfer directionality from tissue to cooling plates. There is good correlation between model and experimental data. Cooled tissue volume is dependent on applicator size, configuration, and skin contact cooling area. Immediate post-treatment stiffened tissue (“butter stick”) pliancy is dependent upon the amount of cooled tissue and parallel cooling plate separation (simultaneously cooling a fold of tissue from both sides). Alternately, the surface applicator effectively cools subcutaneous fat that cannot be drawn into a conventional vacuum applicator.

**Conclusion:** Tissue temperatures using both vacuum and surface applicators are maintained below Cryolipolysis temperature within treatment regions to avoid damage of surrounding tissue. Cooled tissue volume can be maximized by ensuring appropriate applicator fit and tissue draw to enhance contact with cooling plates. Greater cooled fat volume increases adipocyte apoptosis, which gradually manifests in fat reduction. A better understanding of thermal physics during treatment ensures enhanced clinical outcomes.

**Wed.17**

**Magnetic Resonance Thermography of Soft Tissue Cooling**

Amir Y. Sajjadi<sup>1,2</sup>, Sara Sprinkhuizen<sup>1</sup>, Dieter Manstein<sup>2</sup>, Stefan A. Carp<sup>1</sup>

<sup>1</sup>Department of Radiology, Harvard Medical School, Charlestown, MA, USA, <sup>2</sup>Cutaneous Biology Research Center, Harvard University, Charlestown, MA, USA

The objective of this study is to evaluate the feasibility of magnetic resonance (MR) thermography for non-invasive monitoring of cooling of tissue. There is a need to improve the dosimetry and modeling of cold-assisted treatments, in particular as novel cold-assisted therapies, e.g. selective cryolipolysis, emerge. Skin tissue phantoms were heated up to 40°C and MR Thermography was performed on skin tissue while localized cooling was applied to the tissue. First, anatomic data sets are acquired to capture the structural image of the skin tissue, and then three different MR sequences are used to acquire temperature-sensitive data sets. MR temperature distributions are derived from changes in phase differences of phase images acquired from proton-resonance frequency shift methods during cooling procedure. Changes in gradient of temperature provide insight into the thermal propagation mechanism in skin tissue directly exposed to heat and cooling. Post processing of the dynamic changes of phase images is required to improve the quality of the temperature maps and remove the errors from rapping phase images.

**Wed.18****Modelling the detectability of brown fat metabolism using microwave radiometry.**

Dario Rodrigues<sup>1</sup>, Paolo Maccarini<sup>2</sup>, Pedro Pereira<sup>3</sup>, Sara Salahi<sup>4</sup>, Erin Colebeck<sup>5</sup>, Aaron Hood<sup>5</sup>, Erdem Topsakal<sup>5</sup>, Paul Stauffer<sup>1</sup>

<sup>1</sup>Thomas Jefferson University, Philadelphia, PA, USA, <sup>2</sup>Duke University, Durham, NC, USA, <sup>3</sup>ISEL, Lisbon, Portugal, <sup>4</sup>ANSYS, Inc., Irvine, CA, USA, <sup>5</sup>Mississippi State University, Mississippi State, MS, USA

**Background:** Brown adipose tissue (BAT) plays an important role in whole body metabolism and could potentially mediate weight gain and insulin sensitivity. Although some imaging techniques allow BAT detection, there are currently no viable methods for continuous acquisition of BAT energy expenditure. We present the modelling efforts to study the feasibility of using a passive, low-cost and non-invasive technique for long term monitoring of BAT metabolism – microwave radiometry.

**Methods:** A 3D computational model of the human neck and chest was created in HFSS. A BAT region was segmented in the supraclavicular region with a volume of 2-6 cm<sup>3</sup> underlying a superficial layer of 1.5 mm skin and 3-10 mm layer of subcutaneous white adipose tissue (WAT). The model also accounted for relevant bone and muscle structures. The dielectric properties of BAT used in this model were measured in rats over the microwave range 0.5-10 GHz. Measurements were carried out in situ and post mortem in six female rats of approximately 200 g. We used a single-pole Cole-Cole model to fit the experimental data into a frequency dependent parametric model. The anatomical model was coupled to a log-spiral antenna design, which was optimized to maximize radiometric reception of thermal emissions from the BAT target. The power absorption patterns calculated in HFSS were superimposed on simulated thermal distributions computed in COMSOL to predict radiometric signal collected by an ultra-low-noise microwave radiometer. The power received by the antenna was characterized as a function of frequency and different levels of BAT metabolism under cold stimulation (environment temperature at 15°C).

**Results:** The dielectric properties of BAT are higher than WAT, in accordance with the higher water content. The optimized radiometric receive band was 1.1-1.7 GHz, with average antenna efficiency of 20%. The simulated total received power increased 4-15 mdBm during the cold stimulus, corresponding to 15-fold increase in BAT metabolism. Note that the minimum radiometric signal variation required to be detected by the microwave radiometer is 1 mdBm.

**Conclusions:** We present a mathematical model that allows studying the feasibility of non-invasive monitoring of brown fat metabolism with microwave radiometry. Results demonstrate our ability to detect thermal radiation from small volumes (2-6 cm<sup>3</sup>) of BAT located up to 12 mm deep and to monitor small changes (0.5°C) in BAT temperature associated with increased metabolism during cold exposure. The developed miniature radiometric antenna design appears suitable for non-invasive long term monitoring of small changes in BAT metabolism.



**Wed.19**

**Photothermal Ablation of Group A Streptococcus Bacteria and Biofilms Using Functionalized Multi-Wall Carbon Nanotubes**

Nicole Levi-Polyachenko, Christe Young, Christopher MacNeill, Amy Braden, Louis Argenta, Sean Reid

*Wake Forest University Health Sciences, Winston Salem, NC, USA*

Multi-wall carbon nanotubes (MWNT) have been covalently functionalized with an antibody (Ab) to Group A *Streptococcus* (GAS) and used for photothermal ablation of planktonic and biofilm residing GAS. The concentration of GAS-Ab-MWNT bound to populations of GAS was determined to be 15µg/ml. This amount of MWNT was found to be capable of generating temperatures in excess of 70°C upon exposure to 5W of 800nm light for 30 seconds. Compared to carboxylated MWNT (MWNT-COOH), GAS-Ab-MWNT had a 30% enhancement in GAS killing in both planktonic and biofilm GAS. GAS-Ab-MWNT without infrared exposure can decrease GAS in planktonic form, but appeared to increase the growth of GAS in biofilm. Analysis of GAS photothermally ablated in direct contact with *ex vivo* porcine skin shows that the hyperthermia sufficient for killing GAS remains localized and does not cause collateral damage in tissue adjacent to the treated area. The results of this study support the premise that carbon nanotubes may be effectively utilized as highly localized photothermal agents with vast potential for translation into the clinical treatment of bacterial infections of the soft tissue.

Wed.20

### Investigation of a Laser-based System as an Alternative Energy Modality for Vessel Sealing During Surgery

William Nau<sup>1</sup>, Nicholas Giglio<sup>2</sup>, Thomas Hutchens<sup>2</sup>, William Perkins<sup>2</sup>, Cassandra Latimer<sup>1</sup>, Arlen Ward<sup>1</sup>, Nathaniel Fried<sup>2</sup>

<sup>1</sup>Covidien, Boulder, CO, USA, <sup>2</sup>University of North Carolina-Charlotte, Charlotte, NC, USA

Energy-based, electrosurgical and ultrasonic devices are often used to replace sutures and mechanical clips to provide rapid hemostasis in surgical procedures such as colectomy, nephrectomy, thyroidectomy, and hysterectomy. These devices deliver thermal energy to denature proteins and reform structural collagen to rapidly seal blood vessels and fuse tissue structures. In some devices, a mechanical blade is then deployed to transect the tissue. The goal of this study was to investigate the use of an infrared laser as an alternative energy source for vessel sealing applications. A variable power (0-110 W), 1470 nm laser source was coupled to a fiber and beam shaping optics to produce a linear beam 3.0 mm by 9.5 mm for sealing, and 1.1 mm by 9.6 mm for cutting (FWHM). A bench top system designed to mimic the tissue contacting aspects of a surgical instrument was used to seal and transect isolated, *ex vivo* porcine renal arteries up to 8.5 mm in diameter in a two-step process. Seal and cut times were 1.0 second each. A burst pressure system consisting of a pressure meter, infusion pump, and an iris clamp measured resulting seal strengths. Gross and histologic (hematoxylin and eosin (H&E) stain) measurements of thermal damage were also recorded. All blood vessels tested ( $n = 55$ ) were sealed and cut, with total irradiation times of 2.0 seconds at <90 W. Mean burst pressures measured  $1305 \pm 783$  mmHg (compared to normal systolic blood pressure of 120 mmHg), and collateral thermal coagulation zones measured  $0.94 \pm 0.48$  mm. Hand-held prototypes were then fabricated to enable testing on vessels in an *in vivo* porcine model. The optical-based vessel sealing devices were evaluated for hemostasis after sealing isolated and bundled vasculature of the abdomen and hind leg (mesentery, mesometrium, gastrosplenic, gastroepiploic, iliac, femoral, and saphenous vessels), as well as liver and lung parenchyma. Samples of the sealed vessels were collected for histological analysis (H&E and picosirius red staining methods) of lateral thermal damage. Data obtained from two *in vivo* experiments indicated a hemostasis Pass/Fail rate rate of 63% with collateral thermal damage zone of  $1.40 \pm 0.65$  mm, and a hemostasis Pass/Fail rate of 77% with a thermal damage zone of  $1.55 \pm 1.10$  mm in a second experiment. This study demonstrated the feasibility of an optical-based system for sealing and cutting a wide range of vessel sizes and tissue types.

Wed.21

### Imaging electric tissue properties using MRI for improved SAR assessment during Hyperthermia Treatment

E Balidemaj<sup>1</sup>, J. Trinks<sup>1</sup>, H.P Kok<sup>1</sup>, R.F. Remis<sup>3</sup>, C.A.T. van den Berg<sup>2</sup>, L.J.A. Stalpers<sup>1</sup>, A.J. Nederveen<sup>1</sup>, H. Crezee<sup>1</sup>

<sup>1</sup>Academic Medical Center, Amsterdam, The Netherlands, <sup>2</sup>University Medical Center Utrecht, Utrecht, The Netherlands, <sup>3</sup>Technical University Delft, Delft, The Netherlands

**Background:** Reliable Hyperthermia Treatment Planning (HTP) requires the true tissue electrical conductivity ( $\sigma$ ), the main determinant for RF energy absorption. Currently, a fixed tissue conductivity is assumed for all patients and tumour sites, however, inter-patient variations of 30-50% are common and tumor conductivity is mostly unknown. Earlier studies have shown that conductivity uncertainties can lead to more than 2°C lower tumor temperatures. Additionally, inaccurate conductivity values lead to poor prediction of treatment limiting hot spots. Measurement of accurate patient-specific conductivity values is thus essential for reliable HTP. Our aim is to acquire pelvic tissue conductivity using 3 Tesla MRI. Earlier studies have demonstrated the performance of the presented method for phantom measurements. In this work, we focus on in vivo MRI simulations and measurements.

**Methods:** In vivo simulations and measurements were performed to demonstrate the presented algorithm. This algorithm uses the  $B_1^+$  field that is measurable by standard MRI systems. Based on the  $B_1^+$  distribution this method reconstructs the tissue dielectric properties in an iterative fashion based on the Contrast Source Inversion method. In vivo simulations (Ella & Duke) have been used to compare the reconstructed dielectric values to the actual model. Gaussian noise (SNR 20) was added to the simulated fields. Furthermore, in vivo MRI measurements of a female volunteer and cervical carcinoma patient (age: 85, Stage: IVA) have been used for  $\sigma$ -reconstruction. Tumor delineation was performed by a radiation oncologist.

**Results:** The presented algorithm shows a good performance for in vivo simulations. The dielectric properties are reconstructed with high accuracy (mean deviation: 4%). Using in vivo measurements we are able to reconstruct  $\sigma$ -maps which are in good agreement with the  $\sigma$  values known from literature. Mean deviation of conductivity for muscle and fat were approx. 10-17% compared to literature values. Furthermore, an electrical conductivity of  $1.16 \pm 0.40$  S/m was observed for the delineated tumor volume.

**Conclusions:** The in vivo simulations and measurements demonstrated the ability to measure quantitatively the  $\sigma$ -value of healthy tissue and tumors. We have shown a good correlation between the reconstructed  $\sigma$ -values and expected values based on literature for a wide range of  $\sigma$ -values. In vivo simulations demonstrated the ability of the presented method to reconstruct dielectric values with high accuracy of 4%. In vivo measurements showed a mean deviation of approx. 10-17% compared to literature values. Future studies will focus on the effect of more accurate dielectric models on SAR and temperature distribution during Hyperthermia Treatment.

Wed.22

**PARP1-inhibition sensitizes combined hyperthermia-radiation and combined hyperthermia-cddp treatment of cervical carcinoma cells**

Arlene Leonie Oei<sup>1,2</sup>, H.P. Kok<sup>2</sup>, L.J.A. Stalpers<sup>1,2</sup>, H.M. Rodermond<sup>1,2</sup>, A. Bel<sup>2</sup>, J. Crezee<sup>2</sup>, N.A.P. Franken<sup>1,2</sup>

<sup>1</sup>Academic Medical Center, University of Amsterdam, Laboratory for Experimental Oncology and Radiobiology (LEXOR), Center for Experimental Molecular Medicine, Amsterdam, Noord-Holland, The Netherlands, <sup>2</sup>Academic Medical Center, University of Amsterdam, Department of Radiation Oncology, Amsterdam, Noord-Holland, The Netherlands

**Background:** Ionizing radiation causes single and double strand breaks (SSBs and DSBs). DSBs are among the most critical DNA lesions and can be repaired via either non-homologous end joining (NHEJ) in which PARP1, Ku70 and DNA-PKcs are important, or homologous recombination (HR), where BRCA2 and Rad51 are essential. Hyperthermia disturbs HR by temporary inactivation of BRCA2. Cisplatin disrupts NHEJ and PARP1-inhibitor blocks Poly-[ADP-ribose]-polymerase-1, which is important in SSB repair, NHEJ and backup-NHEJ. Our goal is to investigate the additional effectiveness of cDDP and PARP1-inhibition in combination with radiotherapy and/or hyperthermia.

**Methods:** Cervical carcinoma cells (SiHa) were treated at different temperature levels (39-45°C), gamma-irradiation doses (0-8Gy), cDDP and PARP1-inhibitor (NU1025). Clonogenic assays were carried out to measure survival and γH2AX staining was used to visualize DSBs. To elucidate mechanisms of action expression levels of different DNA repair proteins BRCA2, Ku70, Rad51 and DNA-PKcs were investigated after 42.5°C (1 h) using western blot.

**Results:** Combined hyperthermia and radiation resulted in an increased number of γH2AX foci as compared to radiation alone. Hyperthermia treatment in combination with cDDP and PARP1-inhibitor and with radiation and PARP1 inhibitor significantly decreased cell survival. Western blot demonstrated a decreased expression of BRCA2 protein at 30 min after hyperthermia treatment.

**Discussion/Conclusion:** Adding PARP1-inhibitor significantly improves the effectiveness of combined hyperthermia-radiotherapy and combined hyperthermia-cDDP treatment on cervical carcinoma cells. Hyperthermia affects DNA-DSB repair as is indicated by increased γH2AX foci numbers and decreased BRCA2 expression.

**Wed.23****The effect of heat cycling on intratumoral liposome accumulation and triggered drug release.**

Li Li<sup>1,2</sup>, Timo ten Hagen<sup>2</sup>, Martin Hossann<sup>3</sup>, Gerard van Rhoon<sup>2</sup>, Thomas Soullie<sup>2</sup>, Gerben Koning<sup>2</sup>

<sup>1</sup>Duke University, Durham, NC, USA, <sup>2</sup>Erasmus MC, Rotterdam, The Netherlands, <sup>3</sup>University Hospital of Munich, Munich, Germany

Nanomedicine in cancer treatment can help reduce the systemic side-effects of chemotherapy, with the potential to enhance therapeutic efficacy through active drug release. The aim of this study was to combine mild hyperthermic heat cycling and thermosensitive liposomes (TSL) to increase intratumoral liposomal drug accumulation and actively trigger drug release. We defined hyperthermia treatment of tumors at 42 °C for 5 minutes followed by 10 minutes without HT as one heat cycle, and repeat for 5 cycles. We compared heat cycling induced liposome extravasation in 4 tumor models by intravital confocal microscopy. We captured heat cycling triggered content release of carboxyfluorescein (CF) and doxorubicin (Dox) from TSL. The therapeutic efficacy of Dox-TSL under heat cycling for tumor growth control of subcutaneous tumors in mice were compared to Dox-TSL under continuous hyperthermia at 42 °C for 1 hour, and quantified liposome extravasation through permeable tumor vasculature, with deeper and more liposome penetration after each cycle. Heat cycling also effectively triggered content release from CF-TSL and Dox-TSL. Mice bearing subcutaneous human BLM melanoma had tumor growth delay of over 20 days after a single treatment of hyperthermia plus Dox-TSL, which was as efficient as after a single treatment of continuous mild hyperthermia plus Do-TSL. These heat on-off pulses mimic the situation upon applying energy at small focus points to maintain mild hyperthermia in tissues. In conclusion, heat cycling can induce liposome extravasation and trigger content release from TSL and is an attractive alternative to continuous hyperthermia for nanoparticle-mediated drug delivery to solid tumors.

**Wed.24****A directional interstitial antenna for microwave tissue ablation: theoretical and experimental investigation**

Brogan McWilliams, Emily Schnell, Punit Prakash

*Kansas State University, Manhattan, Kansas, USA*

**Background:** Interstitial microwave antennas are in clinical use for thermal ablation of tumors and benign disease. Currently available antennas have axially symmetric radiation patterns and do not provide a means for controlling heating along the angular expanse. Antennas with directional radiation patterns may provide a means for limiting thermal damage to critical structures in proximity to ablation targets. The objective of this study was to design and experimentally assess the feasibility of a directional interstitial antenna for microwave tissue ablation.

**Methods:** To create a directional radiation pattern, a conductive reflector was positioned behind a conventional coaxial monopole antenna, minimizing microwave propagation in that direction. 3D finite element method simulations were employed to investigate the radiation pattern of directional antenna designs at 2.45 GHz. Initial simulations indicated a suitable antenna-reflector spacing to be approximately a quarter wavelength, thus a water-cooled design was explored to minimize applicator diameter. Simulations were used to determine dimensions that optimized the antenna's reflection coefficient and directionality. Proof-of-concept applicators were fabricated and experimentally evaluated with ablations in *ex vivo* porcine muscle. Fiber-optic temperature measurements and extents of visible tissue discoloration were used to characterize dimensions and directionality of experimental ablation zones.

**Results:** Simulations identified an optimal monopole-based design with a reflection coefficient of -23 dB at 2.45 GHz, capable of creating ablation zones measuring 19 mm (width) x 14 mm (radial depth) and 23 mm x 16 mm, when powered with 30 W and 50 W, respectively. Reflection coefficients of the fabricated water-cooled antennas (3.8 mm OD) were in good agreement with simulations (minimum -23.1 dB at 2.35 GHz). Experimental ablations at 30 W ( $n = 3$ ) yielded ablation zones measuring  $18.7 \pm 2.1$  mm x  $15.3 \pm 2.1$  mm, restricted to  $\sim 180^\circ$  of the angular expanse. The temperature elevation measured 1 cm from the applicator in the reverse direction remained under 1 °C, and visibly ablated regions were restricted to within 2 mm of the catheter, indicating directional control. At 50 W ( $n = 4$ ), experimental ablation zones measured  $24 \pm 4.9$  mm x  $17.7 \pm 2.8$  mm. Simulations indicated the potential of high dielectric materials to reduce applicator diameter and increase ablation zone dimensions.

**Conclusion:** This study was undertaken to design and assess the feasibility of creating directional ablation zones with an interstitial microwave antenna. The presented applicator may provide a practical means for limiting thermal damage to critical structures in proximity to ablation targets.

**Wed.25****Myeloid-Derived Suppressor Cells Subvert the Immunostimulatory Activity of Systemic Thermal Therapy by Blocking T cell Trafficking in the Tumor Microenvironment**Amy Ku, Jason Muhitch, Scott Abrams, Sharon Evans*Roswell Park Cancer Institute, Buffalo, NY, USA*

The success of chemotherapy, radiotherapy, and thermal therapy hinges on cytotoxic CD8<sup>+</sup> T cells gaining access to neoplastic cellular targets within the tumor microenvironment. These observations prompted interest in strategies to improve CD8<sup>+</sup> effector T cell trafficking to tumors although the mechanisms that positively or negatively regulate entry at tumor vascular checkpoints are poorly understood. We have previously shown that IL-6-dependent preconditioning regimens including systemic thermal therapy (STT; 39.5 ± 0.5°C for 6 h) convert tumor vessels from T cell-low to -high recruitment sites in multiple implantable and autochthonous murine neoplastic models (i.e., B16 melanoma, CT26 colorectal carcinoma, EMT6 mammary carcinoma, and RIP-Tag5 pancreatic islet cancer). Enhanced T cell trafficking depends on upregulation of the prototypical trafficking molecule, intercellular adhesion molecule-1 (ICAM-1), on tumor vessels. Here, we report on a subset of tumors (mammary 4T1, polyoma middle T-transgenic, and AT-3; pancreatic Pan02) in which STT or recombinant IL-6 preconditioning therapy failed to boost CD8<sup>+</sup> T cell trafficking as determined by real-time live imaging and immunofluorescence histology. A unifying characteristic of thermally-refractive tumors is the preferential expansion of immature CD11b<sup>+</sup>Gr-1<sup>+</sup> myeloid-derived suppressor cell (MDSC) populations, which have been clinically linked to worse prognoses in advanced breast cancer patients. In contrast, the proportion of other immunosuppressive cell types such as CD4<sup>+</sup>Foxp3<sup>+</sup> regulatory T cells and CD11b<sup>+</sup>F4/80<sup>+</sup> macrophages are indistinguishable in thermally-sensitive and -resistant tumors. Further analysis of thermally-refractive tumors revealed that failure to induce vascular ICAM-1 expression is temporally and inversely correlated with intratumoral expansion of MDSC. The causal relationship between MDSC and poor effector T cell trafficking was investigated by admixing thermally-sensitive tumor cells (EMT6, CT26 or B16) with syngeneic MDSC isolated from spleens of tumor-bearing mice at a 2:1 ratio, thus mimicking the high MDSC burden detected in thermally-refractive tumors. Although the number of infiltrating CD11b<sup>+</sup>Gr-1<sup>+</sup> MDSC expanded ~ 80-fold during outgrowth of admixed tumors in vivo, there was no impact on vessel density or baseline expression of ICAM-1 on tumor vessels. However, vessels in admixed tumors became refractory to ICAM-1 induction by STT or IL-6 preconditioning therapy. These findings provide the first evidence that MDSC negatively impact T cell trafficking across tumor vascular gateways, thereby conferring resistance to thermal therapy. These findings further provide the foundation for future identification of the mechanisms underlying resistance to thermal therapy and immunotherapy in tumors with high MDSC burden. Supported by the NIH (CA79765, CA085183) and the Jennifer Liscott Tietgen Family Foundation.

**Wed.26****Celecoxib suppresses local inflammatory and systemic pro-oncogenic effects of hepatic radiofrequency (RF) ablation in small animals**

Gaurav Kumar<sup>1</sup>, S.Nahum Goldberg<sup>1,2</sup>, Marwan Moussa<sup>1</sup>, Yuanguo Wang<sup>1</sup>, Lana Gourevich<sup>2</sup>, Muneeb Ahmed<sup>1</sup>

<sup>1</sup>Beth Israel Deaconess Medical Center, Boston, MA, USA, <sup>2</sup>Hadassah Hebrew University Medical Center, Jerusalem, Israel

**Background:** To determine the effect of celecoxib, a selective COX-2 inhibitor on hepatic radiofrequency ablation (RFA)-induced periablational cellular infiltration and stimulation of distant subcutaneous tumor growth in small animal models.

**Methods:** This study was performed in two different phases. First, we studied the effect of celecoxib on periablational cellular infiltration. C57BL mice were randomized to receive standardized RFA to liver (21g electrode, 1cm active tip, tip temperature 70°Cx5min) or RFA with adjuvant intraperitoneal (I.P.) celecoxib (SC58635) administered daily after procedure. Animals were sacrificed and liver tissues harvested at 3d and 7d post-treatment. Immunohistochemistry was performed for different cell types (F4/80: macrophages,  $\alpha$ -SMA: activated stellate cells), and cellular proliferation (CDC47). Next, we studied the effect of celecoxib on RFA-induced distant tumor growth. Fisher 344 rats (n=41) with single R3230 adenocarcinoma subcutaneous (SC) tumors were randomized (at tumor size = 10-11mm) to RFA or sham procedure without and with adjuvant I.P. celecoxib (50 mg/kg, daily). Animals were sacrificed and tumors harvested 7d post-treatment. Tumor growth analysis (absolute diameter, change in diameter, and growth curve slope) was performed.

**Results:** Hepatic RFA resulted in increased macrophage and stellate cell accumulation in the periablational rim at 3-7d post-RFA which is significantly reduced by adjuvant IP celecoxib at both time points (3d: 24±9mm vs. 12.3±9mm, p<0.03, 7d: 49.7±30mm vs. 21.8±8mm, p<0.01). Similarly, with RFA of normal liver in F344 rats, distant SC tumors were significantly larger at 7d compared to sham (17±2mm vs. 13.8±0.9mm, p<0.001), which were reduced by celecoxib (13.4±0.8mm, p<0.001) to sham levels (p=0.35). Additionally, the higher growth rates in RFA compared to sham (slopes: 0.88±0.23 vs. 0.38±0.16, p<0.001) were also brought down by celecoxib (0.34±0.1mm, p<0.001) to the baseline sham group (p=0.54).

**Conclusion:** Stimulation of distant subcutaneous tumor growth after hepatic RF ablation is, in part, inflammation-mediated and can be successfully suppressed with an adjuvant COX-2 inhibitor.



**Wed.27**

**Theoretical Design and Evaluation of Endoluminal Ultrasound Applicators for Thermal Therapy of Pancreatic Cancer under Image Guidance**

Matthew Adams<sup>1</sup>, Serena Scott<sup>1</sup>, Vasant Salgaonkar<sup>1</sup>, Graham Sommer<sup>2</sup>, Chris Diederich<sup>1</sup>

<sup>1</sup>University of California San Francisco, San Francisco, USA, <sup>2</sup>Stanford University Medical Center, Stanford, USA

**Introduction:** This study's objective is to evaluate the feasibility of targeted thermal therapy of pancreatic tumors using an endoluminal ultrasound applicator within the duodenal lumen.

**Methods:** Patient-specific 3D anatomical models were created based on CT scans of patients with tumors in the head of the pancreas. Nearby anatomical structures surrounding the tumor (average diameter ~20 mm) were segmented and finite element meshes were generated using Mimics Innovation Suite. The applicator, surrounded by a water-cooled balloon, was positioned in the duodenum near the tumor. 3D acoustic pressure and power deposition fields were calculated using the rectangular radiator method for three individual 20x10 mm transducer configurations: planar, weakly focused (curvilinear along width), and strongly focused (curvilinear along length). For each patient model and transducer configuration, transient 3D bioheat transfer FEM models were solved using COMSOL Multiphysics, with integrated PI feedback control of the maximum temperature to simulate control under MRTI guidance. Parametric studies were performed to determine the effects of transducer configuration and frequency (2-5 MHz) on lesion size, penetration depth, and sparing of non-targeted tissues. These studies' results were used to assess the feasibility of full tumor treatment, both via ablation ( $t_{43}>240$  min), performed with multiple applicator orientations over a 15-20 min period, and hyperthermia ( $T>40^{\circ}\text{C}$ ), performed using planar or tubular transducers.

**Results:** Parametric studies showed that highest penetration and specificity in targeted tissue ablation were achieved using strongly focused transducers at 2 MHz. Weakly and strongly focused transducers demonstrated greater penetration (up to 31 mm & 40 mm, respectively, from inner duodenal wall) and duodenal sparing compared to planar transducers (max temperatures  $\sim 5^{\circ}\text{C}$  &  $\sim 2^{\circ}\text{C}$  lower), along with comparatively smaller lesion volumes. For tumors within 25 mm of the duodenal wall, >90% of the tumor volume could be ablated ( $t_{43}>240$  min) in under 20 min without duodenal damage ( $t_{43}<20$  min) by rotating a weakly focused or planar 2 MHz applicator. For hyperthermia applications with a 100<sup>o</sup> sectored tubular transducer, 90% of the tumor volume was 40-45<sup>o</sup>C at steady-state. For tumors extending ~30 mm from the duodenal wall, the translation and rotation of applicators with strongly focused 2 MHz transducers could ablate >80% of the tumor volume in <20 min without damage to non-targeted structures.

**Conclusion:** Biothermal simulations illustrate the feasibility of thermal ablation and hyperthermia in ~20 mm diameter tumors in the pancreatic head within 30-40 mm from the duodenal wall using an endoluminal ultrasound applicator. (NIH P01 CA159992)

Wed.28

**Magnetic nanoparticle hyperthermia as a radiosensitizer for locally advanced pancreas cancer: an *in-vitro* and *in-vivo* study**

Anilchandra Attaluri<sup>1</sup>, Haoming Zhou<sup>1</sup>, Toni-rose Guiriba<sup>4</sup>, Yue Liu<sup>5</sup>, Mohammad Hedayati<sup>1</sup>, Yi Zhong<sup>2</sup>, Christine Iacobuzio-Donahue<sup>2</sup>, Eleni Liapi<sup>2</sup>, Joseph Herman<sup>3</sup>, Theodore DeWeese<sup>1</sup>, Robert Ivkov<sup>1</sup>

<sup>1</sup>Department of Radiation Oncology & Molecular Radiation Sciences, Johns Hopkins University School of Medicine, Baltimore, MD, USA, <sup>2</sup>Departments of Oncology and Pathology, The Sol Goldman Pancreatic Cancer Research Center, Sidney Cancer Center; Johns Hopkins University School of Medicine, Baltimore, MD, USA, <sup>3</sup>Department of Radiology and Radiological Sciences, Johns Hopkins Hospital, Baltimore, MD, USA, <sup>4</sup>Whiting School of Engineering, Johns Hopkins University, Baltimore, MD, USA, <sup>5</sup>School of Public Health Peking, University Health Science Center, Beijing, China

**Background:** Concurrent chemoradiation (CRT) is a standard option for locally advanced pancreatic cancer (LAPC) but has significant toxicity. Localized hyperthermia produced by magnetic iron oxide nanoparticles may enhance efficacy enabling reduced dosing of CRT to minimize toxicity. Local control is inversely related to tumor size for radiation therapy whereas larger tumors can be ideal candidates for magnetic nanoparticle hyperthermia (MNPH).

**Methods:** Human pancreas cancer MiaPaCa-02 cells were cultured for both *in-vitro* screening and development of subcutaneous tumor models in mice. *In-vitro* screening of toxicity from combinations of MIONs (0.2 mg/ml, 4 hour incubation), 43°C in water bath for 30 min, and radiation (4Gy) were performed to guide experimental design of *in-vivo* experiments. MiaPaCa-02 xenografts were obtained by injecting  $5 \times 10^6$  cells suspended in matrigel on the right thigh of 4-6 week old female mice. Mice were anesthetized and MIONs (5.5 mgFe/cc of tumor) or PBS was directly injected into the tumors once they reached a prerequisite volume. To assess radiotherapy enhancement with MNPH mice bearing small ( $0.15 \pm 0.03 \text{ cm}^3$ ) and large ( $0.3 \pm 0.06 \text{ cm}^3$ ) tumors were randomly assigned to control (MION-no AMF or PBS-AMF), AMF (18kA/m,  $160 \pm 5 \text{ kHz}$ , for 20 min), radiation (5Gy), and combination (AMF-18kA/m + 5Gy) groups. Motivated by the intent to provide image-guided delivery of MIONs to LAPC, MIONS were added to Lipiodol (CT contrast agent) to yield a stable formulation. **Results:** MiaPaCa-02 cells treated at 43°C for 30 minutes showed a slightly reduced viability ( $91 \pm 1\%$ ) compared to controls. MION, 4Gy, MION+4Gy at 43°C have significantly reduced viabilities ( $25 \pm 6$ ,  $8 \pm 3$ , and  $1 \pm 1$  vs  $97 \pm 1$ ,  $71 \pm 5$ , and  $48 \pm 14$ ) compared to ones at 37°C. In the *in-vivo* studies, large tumors treated with AMF-18kA/m showed better tumor control compared to smaller tumors ( $16 \pm 3$  vs  $10 \pm 2$  days to 2X initial volume). For small tumors, 5Gy group showed significant tumor growth delay ( $25 \pm 2$  days to 4X) while AMF-18kA/m group was modest ( $17 \pm 4$  days to 4X) compared to control ( $12 \pm 1$  days to 4X). Combination treatment showed significant tumor control ( $52 \pm 11$  days to 4X) than 5Gy or AMF-18kA/m alone. Radiosensitization studies for large tumors are ongoing. The MION-Lipiodol formulation retained heating and imaging abilities. **Conclusion:** Preliminary results are promising and suggest that MNPH enhances therapeutic effects of radiation therapy both *in-vitro* and *in-vivo*. Large tumors have better therapeutic response compared to small tumors when treated with tumor volume normalized iron dose and fixed AMF amplitude. The tested MION-Lipiodol formulation can be a potential theranostic agent.

**Wed.29**

**Water Vapor Transport during Microwave Ablations: Numerical Simulation and Experimental Validation**

Jason Chiang<sup>1</sup>, Sohan Birla<sup>2</sup>, Jeyam Subbiah<sup>2</sup>, David Jones<sup>2</sup>, Christopher Brace<sup>1</sup>

<sup>1</sup>University of Wisconsin-Madison, Madison, USA, <sup>2</sup>University of Nebraska-Lincoln, Lincoln, USA

Microwave ablation has been shown to create larger and hotter ablation zones compared to predecessor technology such as radiofrequency ablation (RFA). These heating advantages have led to improved performances near cooling vasculatures, potentially reducing the risk for tumor recurrence. Numerical simulations of RFA have been useful in optimizing ablation systems and patient-specific treatment planning but analogous heating principles have not been fully applied to microwave ablations. The greater heating efficiency of microwave ablations compared to RFA leads to tissue temperatures far exceeding 100 °C, introducing the formation of water vapor from liquid water and pushing the water vapor into nearby tissue and blood vessels. In this study, we explored the possibility of incorporating mass transfer physics to simulate changes in water vapor concentrations during microwave ablation. The computational results were then validated using computed tomography (CT) imaging.

A numerical approach for the microwave ablation was developed using previously established techniques for heat and mass transport within porous media. The electromagnetic power dissipation rate was derived from Maxwell's equations and combined with heat, mass and the continuity transfer equations using finite-element modeling software. The resulting vapor concentration map was validated against intra-procedural CT images of microwave ablations (100W, 5 minutes) being created inside samples of homogenized liver tissue (n=5). The Jaccard Index, a method of comparing two similar geometries, was used to quantify the similarity between the outer boundary of the ablation zone in the computational moisture map and the CT-derived moisture map at multiple time points.

Comparisons between the boundary of the moisture map ablation zone and the CT-derived ablation boundaries showed reasonable correlation as the ablation was created. The 1% water vapor contour in computational simulations reached diameters of 2.40, 3.20, 3.80, 4.20, and 4.60 cm at 1, 2, 3, 4, and 5 minutes. Similarities between computational and experimental vapor maps were smaller in the early ablation times but increased at the later stages of the ablation, with Jaccard Indices at 0.265, 0.485, 0.612, 0.668, and 0.687, respectively.

This study demonstrated the possibility of incorporating water vapor movement with conventional heating physics associated with microwave ablations. CT-imaging was an effective tool to monitor and validate numerical predictions of water vapor concentration at multiple time points during the ablation procedure. Improved integration and characterization of water vapor dynamics in thermal ablations will lead to more general and realistic models.

**Wed.30****Overcoming accelerated blood clearance of cu-doxorubicin nanoparticles with mr guided focused ultrasound thermal ablation**

Andrew Wong, Katherine Watson, Brett Fite, Yu Liu, Jai Seo, Lisa Mahakian, Sarah Tam, Azadeh Kheiolomoom, Katherine Ferrara

*University of California, Davis, Davis, CA, USA*

**Objective**

Nanoparticle formulations of chemotherapeutic drugs enhance solubility, protect pharmaceuticals from degradation, and improve biodistribution via particle size and charge effects. However, repeated administration of nanoparticles leads to reduced circulation time, the accelerated blood clearance effect. We have previously demonstrated that ultrasound hyperthermia can enhance nanoparticle accumulation. To maintain the therapeutic efficacy of nanoparticle chemotherapies, we hypothesize that magnetic resonance guided focused ultrasound (MRgFUS) thermal ablation can enhance tumor accumulation of nanoparticle drugs.

**Methods**

MRgFUS was performed on a Bruker BioSpec 7T small animal system (Ettlingen, Germany) and 16 element annular FUS transducer (3Mhz center frequency, 300kHz bandwidth, 120 W peak acoustic power, 85° aperture, 48mm diameter, 1 x 1 x 2 mm FWHM focus size) from IMASONIC (Voray sur l'Ognon, France) and positioning system from Image Guided Therapy (Pessac, France). 32 female FVB mice implanted with murine NDL mammary carcinomas were used. 20 mice were followed for four weeks after biweekly treatment with 6 mg/kg copper-doxorubicin long circulating liposomes (CuDox-LCL) and weekly treatment with singlespot MRgFUS (7 s, >70 °C at the focus) then sacrificed for histology. Twelve mice were treated biweekly with CuDox-LCL and weekly singlespot MRgFUS for two weeks, imaged with microPET/CT using <sup>64</sup>Cu-long circulating liposomes (<sup>64</sup>Cu-LCL) at 6, 24, and 48 hours, and then sacrificed for gamma counting and histology.

**Results**

Tumors treated with combination CuDox-LCL and singlespot MRgFUS were below the detection threshold of diagnostic US after four weeks of treatment. While nonenhancing regions on contrast enhanced MRI were observed immediately following ablation and contrast administration, PET/CT of <sup>64</sup>Cu-LCL revealed enhanced accumulation of nanoparticle doxorubicin in MRgFUS tumors as early as 6 hours after therapy ( $8.3 \pm 0.59$  vs.  $4.1 \pm 0.26$  %ID / cc mean  $\pm$  standard error of the mean (SEM) for MRgFUS treated vs. untreated tumors, n = 5, 6). This enhancement at 6 hours persisted after two weeks of treatment ( $8.2 \pm 0.49$  vs.  $6.0 \pm 0.62$  mean  $\pm$  SEM for MRgFUS treated vs. untreated tumors, n = 3, 6). In addition, MRgFUS reduced splenic uptake of nanoparticles ( $8.5 \pm 0.71$  vs.  $10.1 \pm 1.47$  %ID / cc mean  $\pm$  SEM for MRgFUS treated vs. untreated spleens at 6 hrs after therapy, n = 3).

**Conclusions**

MRgFUS ablation of cancer can enhance drug accumulation. Increased intensity or duration of therapy may increase rate of sustained remission.

**Wed.31****Optimal switch-off times of pulsed currents in bipolar radiofrequency ablation**

Frederik Soetaert, Guillaume Crevecoeur, Luc Dupré

*Ghent University, Ghent, Belgium*

Radiofrequency ablation (RFA) heats the tissue by means of electrodes that are subject to radiofrequency voltage differences or that inject radiofrequency currents. Previous studies mainly focus on monopolar RFA devices. In order to treat large tumors, the ablation zone's size needs to increase. This requires multiple sequential ablations to create overlapping ablation zones. Despite all efforts, there is not much freedom regarding the size and shape of the ablation zone. Therefore, we numerically explore the possibility of a bipolar RFA device where two electrodes are driven by a current source.

To optimize the size of the ablation zone, we propose the use of pulsed electromagnetic heat sources. Here, the current is switched on until the maximum temperature in the tissue reaches 80°C. Subsequently, the current is switched off during a fixed period: the switch-off time  $\tau_f$ . Varying  $\tau_f$  alters the governing thermal diffusion processes. The aim is to identify the optimal  $\tau_f$  that induces a temperature build-up in regions that normally survive RFA. To gain insight in the physical phenomena, we implemented a 2D finite element model for pulsed bipolar RFA. The model consists of the solution of two coupled subproblems. The electromagnetic phenomena are described by the Poisson equation with current heat source  $Q$ . The thermal subproblem is based on the Pennes' bioheat model, in which an additional electrical heat source is included.

Our numerical model enables analysis of the effect of the switch-off time on the ablation zone's size. A large  $\tau_f$  does not result in a temperature build-up in the middle between the two needles. In the case of  $\tau_f = 5$  s, a clear temperature build-up arises in this zone. This switch-off time allows the thermal diffusion to reach the center, whereas it prevents a complete spreading of the heat. Therefore, it allows the destruction of the central region which is normally unharmed in bipolar RFA. The optimal switch-off times are typically in the range 5-10 s. This mainly depends on the size of the tumor, the current heat source  $Q$  and the magnitude of the capillary perfusion.

Numerical results confirm that the optimal switch-off time leads to a larger ablation zone in bipolar RFA and thus increases the efficacy of the treatment. Furthermore, this computer-supported treatment planning makes outcome less dependent on the experience of the treating physician. Consequently, the presented concept has the potential to be included in practical RFA treatments.

**Wed.32****A novel method for quantifying perfusion-induced energy losses in magnetic resonance-guided focused ultrasound**

Christopher Dillon, Robert Roemer, Dennis Parker, Allison Payne

*University of Utah, Salt Lake City, Utah, USA*

**Introduction:** Many researchers use the Pennes Bioheat Transfer Equation (PBHTE) to model perfusion-induced energy losses during optimization of magnetic resonance-guided focused ultrasound (MRgFUS) treatments. In spite of its frequent application, only a few attempts have been made to experimentally establish the validity of the PBHTE. This feasibility study uses three-dimensional MR temperature data to quantify perfusion-induced energy losses during MRgFUS for evaluating the PBHTE.

**Methods:** *Theory-* In the PBHTE,  $Q_b$  represents perfusion-induced energy losses ( $W/m^3$ ) and is equal to  $wc_p(T-T_b)$ , where  $w$  is the Pennes perfusion parameter ( $kg/m^3/s$ ),  $c_p$  is the specific heat of blood ( $J/kg/K$ ),  $T$  is the local tissue temperature, and  $T_b$  is the arterial blood temperature. To quantify  $Q_b$ , the temperature profile immediately after turning off the ultrasound power is used as the initial condition for a thermal model, which calculates the temperature decay until the time of the next MR temperature measurement. Based on conservation of energy principles, deviation of the model from the experimental temperatures at that time is used to quantify  $Q_b$  and  $w$ . Estimates of  $Q_b$  and  $w$  are obtained at the time of each MR acquisition during cooling and averaged to mitigate the effects of noise.

*Experimental Protocol-* Experiments were performed in *ex vivo* porcine kidneys, which were perfused with a heparin- $H_2O$  solution in variable flow (0, 20, 40 mL/min) situations. Heating was achieved by electronically steering a phased-array ultrasound transducer (256 elements,  $f=1$  MHz) rapidly in a 10 mm-radius circle for 150 s. MR temperature data were acquired with a 3T Siemens Trio MRI (3D segmented-EPI, TR/TE=35/11 ms, FOV=256x176x30 mm<sup>3</sup>, FA=20°, 752 Hz/pixel, EPI factor=9, 2x2x3 mm<sup>3</sup>, 4.2 second acquisition), and zero-filled interpolated to 0.5-mm isotropic spacing prior to the perfusion analysis. Thermal properties of conductivity and volumetric heat capacity were obtained by a commercially available property analyzer (KD2 Pro, Decagon Devices Inc).

**Results and Discussion:** The average estimated Pennes perfusion values ranged from -0.1–0.8, 9.6–12.4, and 17.9–19.5  $kg/m^3/s$  for 0, 20, and 40 mL/min flow rates, respectively, following anticipated trends with perfusion approximately zero for the no flow case and increasing with flow rate. Future work will include evaluation with a larger range of flow rates and comparison of estimates with other MR techniques for measuring perfusion. This study demonstrates that obtaining perfusion estimates from 3D MR temperature data during MRgFUS is feasible and has the potential to improve and validate biothermal models such as the PBHTE.

# Abstracts for Poster Session: Wed. May 7, 6:00-7:30 pm



## Bronze-Sponsor of the 31<sup>st</sup> STM Annual Meeting

Oncothermia -

Complementary medical therapy in the fight against cancer

Oncothermia is a special kind of hyperthermia and is applied as complementary treatment to cancer therapy options from school medicine. The Oncothermia method has been used successfully for more than 20 years and is available in 31 countries. The treatment can be applied to all tumor types and to all tumor stages and is applied complementary to chemo- and radiotherapy.

The heating of tumor cells with the help of hyperthermia has been used since the ancient world and has been analyzed by science for about 100 years. Oncothermia uses thermal therapy in combination with an electric field. This synergy enables the method to achieve even better results. During the treatment the patient is lying on a therapy bed. A large counter electrode is positioned under the bed. Another electrode is placed on the treated area. The electric field arises between these two electrodes. It supports the exact focusing, the effects of Hyperthermia and tumor cell death. The Oncothermia treatment does not have any side effects. Most patients experience it as comfortable and relaxing.

Oncothermia's treatment goals are the extension of the survival time, the improvement of the quality of life and the minimization of the side effects of chemo- and radiotherapy.

[www.oncotherm.org](http://www.oncotherm.org)



**Po.1****Heating ability of magnetic nanoparticles evaluated from their magnetization curves under alternating field**

Satoshi Ota<sup>1</sup>, Kosuke Nakamura<sup>1</sup>, Asahi Tomitaka<sup>2</sup>, Tsutomu Yamada<sup>1</sup>, Yasushi Takemura<sup>1</sup>

<sup>1</sup>*Yokohama National University, Yokohama, Japan,* <sup>2</sup>*University of Washington, Seattle, WA, USA*

Magnetic nanoparticles (MNPs) are promising heating agents for hyperthermia. It is significant to evaluate their heating ability which depends on field intensity and frequency of an applied ac magnetic field. Temperature rise of the MNPs is usually measured in order to estimate specific loss power (SLP), but it may suffer from uncertainty in surrounding condition and volume, weight or density of samples.

We have succeeded in measuring hysteresis loops of MNPs under an ac magnetic field whose intensity and frequency range were similar to those used in hyperthermia or temperature measurement. It was found that the area of hysteresis loop agreed with the SLP value derived from self-temperature rise of MNPs. In this presentation, magnetic and self-heating properties are discussed in detail using various iron-oxide nanoparticle samples including commercial MNPs and MNPs used for MRI contrast agent. These properties were measured with various sample conditions, fluid, fixed in medium or powder. It is indicated that hysteresis measurement performed with a high frequency field can specify heating properties of MNPs depending on sample condition, density and field condition. As an essential index of magnetic loss of MNPs, SLP and intrinsic loss power (ILP) determined by these experimental results are discussed.



**Po.2****Heat-Mediated Drug Release from Mesoporous Silica-Coated Iron Oxide Nanoparticles**

Katie Hurley, Hattie Ring, Michael Garwood, John Bischof, Christy Haynes

*University of Minnesota, Minneapolis, USA*

Disease diagnosis and treatment benefit greatly from multi-modal approaches. In addition to a range of other benefits, nanoparticles of various compositions can provide these multimodal approaches. For example, nanoparticles can provide treatment through drug delivery along with hyperthermia or photodynamic therapy. Iron oxide nanoparticles (IONPs), which can provide magnetic resonance image contrast and therapeutic heat, are emerging as a key player in this field. Combining these properties with the controlled release of drug further enhances the therapeutic efficacy of the IONP system. However, IONPs on their own are subject to disadvantages such as aggregation and dissolution in biological environments. Additionally, controlled release of drug from IONPs has been limited by low drug loading. In this work, we employ a mesoporous silica coating to confer IONPs with colloidal stability, protection against oxidation and dissolution, and a large pore volume for drug loading, making this platform a valuable tool for multi-modal therapy. In this portion of the study, this platform is used as a controlled-release system whereby IONP-generated heat acts as the controlled release mechanism. Previous work has demonstrated that surface modification with a short polyethylene glycol chain and a hydrophobic chloro-trimethylsilane group allows high loading of a cancer therapeutic, Doxorubicin. Further, the hydrophobic form of this drug can be retained within the particle for over 24 hours without the use of any additional capping agent simply due to hydrophobic-hydrophobic interactions. Herein, we investigate system-wide temperature increases (via IONP-heating or a water bath) as a driver for increased molecular diffusion resulting in drug delivery. The effects of various drug cargoes, pore diameters, heating profiles, and release media will be presented.

**Po.3****Tissue Response to Ablative Modalities**

Ashish Singal<sup>1</sup>, Charles Soule<sup>1</sup>, John Ballard<sup>1</sup>, Erik Cressman<sup>2,1</sup>, Paul Iaizzo<sup>1</sup>

<sup>1</sup>University of Minnesota, Minneapolis, Minnesota, USA, <sup>2</sup>University of Texas, Houston, Texas, USA

**Introduction:** Ablation has secured a prominent place in medicine. Many different ablative modalities are commonly employed in clinical practice to restore normal structure and function. Some of the commonly used ablative modalities are radiofrequency ablation (RFA), cryoablation (Cryo), chemo-ablation, and high intensity focused ultrasound (HIFU). A thorough understanding of tissue response to ablation is necessary to evaluate effectiveness and efficacy of ablation procedure. The purpose of this study is to quantify changes in physiological properties of various tissues (myocardium, diaphragm, and esophagus) in response to different ablative modalities. This information can aid in characterizing device-tissue interaction to minimize ablation related complications.

**Methods:** To investigate the effects of changes in physiological properties, tissue bath studies were performed using clinically available RF and Cryoablation equipment, chemical agents such as hypertonic NaCl, urea, ethyl-alcohol, acetic acid, and a custom designed HIFU setup. Muscle bundles of swine diaphragm, esophagus, and cardiac tissue were prepared (approximate size 25 mm length, 5 mm diameter) and mounted in tissue baths containing Krebs-henseleit buffer at 37°C gassed with 95% oxygen and 5% carbon dioxide to maintain tissue viability. Tissue was stimulated with a pulse width of 1.0 ms to elicit a twitch response that was digitally recorded at a sampling frequency of 250 Hz. Stimulation voltage and length-tension optimization was performed on each muscle bundle before starting the ablation study protocol. Physiological properties such as peak-force, contraction time, baseline shift, were measured pre- and post-ablation. Post-ablation, tissue was allowed to recover for a period of at-least 3 hours to detect signatures of cell damage and recovery caused by different ablation modalities.

**Results:** Typically, peak-forces reduced and baseline-forces increased following treatment with any ablative modality investigated. The percent reductions in peak-forces were dose dependent, i.e. higher reductions in peak-forces were elicited at higher ablation doses. Similarly, percent increases in baseline-forces (contractures or muscle pre-loads) were also found to be dose dependent. Although data was recorded continuously, it was evaluated every 15 minutes for at least 3 hours post-ablation. A signature of recovery was observed during the post-ablation 3 hour period.

**Interpretation:** These results can not only be used in understanding device-tissue interaction to minimize ablation related complications, but also aid in novel medical device design.

**Acknowledgements:** This study was supported in part by “Minnesota Muscle Training Program” NIH 2T32 AR007612.

**Po.4****Determining magnetic nanoparticle distribution within cryogenic biological systems using CT imaging for improved regenerative medicine approaches**

Leoni Rott<sup>1,2</sup>, Michael Etheridge<sup>1</sup>, Almer Meinken<sup>2</sup>, Birgit Glasmacher<sup>2</sup>, John Bischof<sup>1</sup>

<sup>1</sup>University of Minnesota, Minneapolis/MN, USA, <sup>2</sup>Leibniz Universität Hannover, Hannover, Germany

Despite successful vitrification of a range of tissues (including entire organs), practical application of cryopreservation has been limited to small biomaterials due to devitrification and cracking during thaw [2,3]. To overcome these limitations, we propose the use of radiofrequency (RF) excited magnetic nanoparticles (mNPs) for heating vitrified biomaterials. This method has shown much faster and more uniform thawing rates, independent of the sample size [3]. However, successful translation of this approach will require a means to confirm that the mNPs and cryoprotective agents (CPAs) are distributed uniformly within the tissue using a non-invasive imaging method. The aim of this research then is to investigate the use of X-ray computed tomography (CT) to characterize mNP and CPA concentrations in solutions (providing calibration curves) and then demonstrate the approach in tissues. Our recent results show that the addition of mNPs and CPAs cause a density change detectable by X-ray attenuation, reported in Hounsfield Units (HUs) [1,4], as measured on a micro CT device (XT H225, Nikon Inc.). Specifically, we imaged VS55 (a CPA with established success in vitrifying tissues [3]) at concentrations of 4.2M, 6.3M, and 8.4M at 20°C. Further, we imaged iron oxide nanoparticle solutions at concentrations ranging from 1 to 20 mg Fe/ml. The HUs increased linearly from 280 to 560 HU for 4.2M to 8.4M VS55 and from 0 to 590 HU for 0 to 20 mg Fe/ml. Experiments with various combinations of the above mentioned solutions at 20°C and -196°C are underway. Previous work suggests that at -196°C the HUs will maintain their linearity with mNP and CPA concentration [1]. However, the values of the HUs for CPA and CPA+mNP solutions are also dependent on the phase of the solution. Cryogenically cooled solutions will crystallize below a critical CPA concentration, but above this limit and with sufficiently rapid cooling rates they will vitrify to a stable glassy state. This glassy phase is denser than the crystalline phase and therefore the HUs are higher. Continuing research will assess the impact of diffusion loading tissue with known concentrations of mNPs and CPAs, based on the calibration curves characterized in solution. This will provide the capabilities to monitor mNP/CPA concentrations and phase distributions during loading, cryogenic cooling and rescue of vitrified biomaterials, which will be critical to the successful translation of this new mNP, RF thawing technology.

Refs: [1] Bischof JC, et al. ABME 2007; 35(2): pp.292-304.

[2] Fahy GM, et al. Oranogenesis 2009; 5(3): pp.167-175.

[3] Etheridge ML, et al. ASME SBC2013-14334.

[4] Attaluri A, et al. IJH 2011; 27(5): pp.491-502.

**Po.5****Thermal therapy for improvement of laser-based tumor ablation strategies**

Klressa Barnes, Robert J. Griffin

*University of Arkansas for Medical Sciences, Little Rock, USA*

**Introduction:** An emerging approach for recurrent head and neck cancer is systemic injection of laser-active agents to increase laser induced thermal or oxidative damage in the tumor. We have previously determined that mild hyperthermia significantly improves delivery of ICG photothermal dye to solid tumors and translates into increased thermal ablation upon laser exposure. Our current hypothesis is that the delivery and activity of a photosensitizer will also be significantly improved with prior local heating of the tumor. Photofrin-mediated PDT causes irreversible oxidation of cellular components and apoptosis. Applying heat may improve oxygenation and delivery of the photosensitizer and overall therapeutic efficacy. We are currently evaluating the use of conventional hyperthermia to augment the success of clinical grade Photofrin (Pinnacle biologics, LLC) PDT applications.

**Methods:** Hyperthermia was administered to SCCVII and SCK murine tumors at 41-43C for 60-90 min prior to ICG administration i.v. and whole body infrared imaging. Tumor perfusion and damage was assessed by infrared camera assessment of temperature, contrast enhanced ultrasound and histology. Laser was applied with an energy density of 92 J/cm<sup>2</sup> with a beam diameter of 4 mm at 33 ms pulse length. For the current Photofrin studies, we will employ a 635 nm clinical laser using the following parameters in the SCCVII tumor model: 630 ± 10 nm light delivery with a 5 mm core diameter. The output light power will be 35 mW. The hyperthermic conditions found to be most effective with ICG enhanced tumor control with laser will be used.

**Results:** Following 42.5 C for 1 hr, the ICG concentration was increased by 50%, and after 90 minutes of heating the ICG concentration increased an additional 12%, or 62% greater than in unheated tumors. However, the antitumor response in SCCVII tumors (averaging 250 mm<sup>3</sup> in volume) was only slightly enhanced with heat mediated ICG, possibly due to the lack of penetration of the laser. In the ongoing study, we will assess the PDT based anti-tumor effect created by increased delivery of Photofrin and the application of a clinical grade/power laser to maximize therapeutic effects. The results of these studies will be reported.

**Conclusion:** Improved delivery of agents to augment the effects of laser-based therapy (photothermal or photodynamic) using conventional hyperthermia may improve patient treatment options for recurrent, superficial tumors. Increased control of recurrent tumors with laser-based therapy presents an attractive option for patients that have already received previous chemoradiation regimens.

**Po.6****Accessing Higher IONP Concentrations for MRI Contrast**

Hattie Ring, Katie Hurley, Micheal Etheridge, Jinjin Zheng, John Bischof, Christy Haynes, Micheal Garwood

*University of Minnesota, Minneapolis, MN, USA*

Iron-oxide nanoparticles (IONPs) are currently being used for magnetic nanoparticle based cancer hyperthermia due to their heating properties and their use as an imaging contrast agent. Computed tomography (CT) is the conventional method of imaging for this approach, but, the preferred IONP concentration, 1 – 10 mg Fe/mL, is at the lower limit for detection with CT.[1] Magnetic resonance imaging (MRI) has better resolution in soft tissues, however conventional pulse sequences limit the imaging of IONPs to concentrations much lower than those required for clinical hyperthermia. Images of IONPs in at relevant concentrations have been obtained utilizing a recently developed method, sweep imaging with Fourier transformation (SWIFT) MRI.[2]

MRI signal decay can be described by two mechanisms, transverse relaxation ( $T_2^*$ ) and longitudinal relaxation ( $T_1$ ). Quantitative measurements of IONPs with MRI are often made based on the  $T_2^*$  relaxation of the sample. At IONP concentrations above 0.1 mg Fe/mL the signal decays too quickly for conventional methods of detection due to the fast  $T_2^*$  decay. SWIFT creates contrast based on the much longer  $T_1$  relaxation.[2] This approach has recently been enhanced with a  $T_1$  mapping method known as the Look-Locker method, which demonstrated detection of IONP concentrations as high as 3 mg Fe/mL.[3]

Although 3 mg Fe/mL is the highest IONP concentration imaged by MRI to date, clinical hyperthermia will still require imaging at higher concentrations. To facilitate this, one method is to weaken the  $T_2^*$  contrast mechanism of the IONPs without affecting the  $T_1$  mechanism. This effect has been recently demonstrated when IONPs are coated with mesoporous silica, a biocompatible coating which also prevents aggregation. A variety of synthetic parameters and their effects on the  $T_1/T_2^*$  relationship are described. MRI quantification of concentrations as high as 5 mg Fe/mL have been observed to date.

**Po.7****Thermal Conductivity Measurement of Thin Cardiac Tissues**

Harishankar Natesan<sup>1</sup>, Jeunghwan Choi<sup>1</sup>, Sean Lubner<sup>2</sup>, Chris Dames<sup>2</sup>, John Bischof<sup>1</sup>

<sup>1</sup>University of Minnesota, Minneapolis, Minnesota, USA, <sup>2</sup>University of California, Berkeley, California, USA

There is a strong need for accuracy during focal temperature based treatments of thin cardiovascular tissues to improve treatment efficacy while avoiding adjacent tissue complications. One way to achieve this is through prospective modelling of specific therapies using finite element models populated with temperature and hydration dependent thermal property measurements of tissues. For instance, in the treatment of atrial fibrillation, Pulmonary Vein, a thin cardiovascular tissue is focally cooled to very low temperatures of around  $-80^{\circ}\text{C}$ . In this case, it is very important to accurately control the thermal process so as to prevent the freezing of neighbouring tissues such as Phrenic nerve, Lung and Esophagus which may otherwise lead to debilitating complications to the patient. This requires accurate knowledge of thermal properties of thin, multi-layered cardiovascular tissues. Supported 3 omega method, a modification of thermal conductivity measurement technique in the semiconductor industry, has been recently developed to measure thermal conductivity of thin biological tissues. With the help of this method, the current study will focus on building the database for thermal conductivity of very thin cardiac tissues such as Pulmonary vein (~1.5 mm) which have never been measured before. Thermal conductivity of pulmonary vein (N=3) at temperatures  $34.23\pm 0.48$ ,  $22.26\pm 2.25$ ,  $13.94\pm 0.44$ ,  $-9.73\pm 0.54$ ,  $-15.12\pm 2.07$ ,  $-30.54\pm 1.65^{\circ}\text{C}$  are measured to be  $0.59\pm 0.04$ ,  $0.47\pm 0.12$ ,  $0.53\pm 0.08$ ,  $0.80\pm 0.12$ ,  $1.17\pm 0.24$ ,  $1.43\pm 0.16$  W/m. K respectively

**Po.8****A novel miniature ablation system for studies in small animals**

Christian Rossmann, Dieter Haemmerich

*Medical University of South Carolina, Charleston, SC, USA*

Temperatures in the ablative regime (50-100<sup>0</sup>C) are used to treat cancer in liver, lung and bone tissues. Preclinical testing of ablation strategies such as novel therapy combinations (e.g. ablation plus adjuvant drug) require preclinical studies in large cohorts and are often performed in mouse and rat studies. Clinical devices are however not adequate for small ablations as required in small animal studies. In this study we present a miniature ablation system for generation of localized hyperthermia or small thermal lesions and performed experiments in tissue phantoms.

The miniature ablation system consists of an applicator, a Micro-Controller (MC) board and a software tool allowing the user to interact with the system. A thermistor (passive heating element, 1.1mm diameter) was mounted at the tip of the applicator and connected with the MC board. According to a user input, the software tool communicates with the MC which further regulates the thermistor voltage to reach and maintain target temperature. To evaluate the system, 10 minute ablations in agar phantoms were performed with target temperatures between 50-90<sup>0</sup>C.

The maximum temperature reached in the phantom was ~85<sup>0</sup>C (90<sup>0</sup>C target temperature) and strongly decreased with increasing distance from the applicator tip. The 50<sup>0</sup>C iso-thermal zone was spherical and had a maximal diameter of ~4.5mm (90<sup>0</sup>C target temperature). Temperature variations measured at the applicator tip were less than ±1<sup>0</sup>C after reaching the target temperature, providing highly controlled and reproducible tissue exposures not possible with most other devices.

The presented low-cost (<100USD) ablation system is capable of creating spheroidal thermal lesions or hyperthermia zones in small targets and may facilitate preclinical ablation and hyperthermia studies in small animals at precisely controlled temperatures.

**Po.9****Modulated electro-hyperthermia applied as monotherapy for various cases having no other options**

Taesig Jeung<sup>1</sup>, Sunyoung Ma<sup>1</sup>, Jesang Yu<sup>1</sup>, Sangwook Lim<sup>1</sup>, Oliver Szasz<sup>2</sup>

<sup>1</sup>Kosin University College of Medicine, Department of Radiation Oncology, Busan, Republic of Korea, <sup>2</sup>Szent Istvan University, Department of Biotechnics, Godollo, Hungary

**Introduction** Cancer has limited curative possibilities in high-line treatments. Our objective study is modulated electro-hyperthermia (mEHT) [2], as monotherapy, treating patients in advanced stages when other possibilities were not applicable.

**Methods** This study reports 16 patients, treated by mEHT (EHY2000+ device). 3 pancreas, 3 lung adenocarcinoma, 2 gastric, 2 colorectal and 1-1 synovial, bladder, hepatocellular, ovary, renal and cystic cases. mEHT was applied like chronic treatment numerous times (4 - 82 sessions) for a long time (months), 2-3 times a week. Sessions were 60 min. Each 12 sessions in one cycle. The average number of sessions was 33. In most of the cases both the primary and metastatic lesions were treated in independent sessions, or when the metastasis was near then covered both by the large electrode. Control of the cases was made by regular imaging and by the appropriate tumor-markers.

**Results** All patients had benefit from the treatments. Although complete remission was not achieved due to the advanced stages, but good partial remission was very common. Despite of the generally short expected survival in these cases, the long mEHT treatment processes were available, well improving the survival time compared to the historical expectations. Definite reducing of pain (improved quality of life) and no remarkable mEHT related side effect was observed, despite the definite dose escalation. In some cases skin erythema appeared, handled with appropriate cream. It did not terminate any further treatments. In some cases ascites made complications of the treatments, but could be controlled by appropriate medication.

**Conclusion** mEHT was successfully applied as monotherapy in various far advanced cases.

[1] Issels R, et.al, Lancet Oncology, 11:561-570, (2010)

[2] Szasz A, et.al, Oncothermia –Principles and Practices, Springer, (2010)



**Po.10****Modulated electro-hyperthermia therapy combined with gold-standard therapies for primary, recurrent and metastatic sarcomas**

Taesig Jeung<sup>1</sup>, Sunyoung Ma<sup>1</sup>, Jesang Yu<sup>1</sup>, Sangwook Lim<sup>1</sup>, Oliver Szasz<sup>2</sup>

<sup>1</sup>Kosin University College of Medicine, Department of Radiation Oncology, Busan, Republic of Korea, <sup>2</sup>Szent Istvan University, Department of Biotechnics, Godollo, Hungary

**Introduction** After surgery sarcoma has high incidence of local recurrence and distant metastases. It is mostly resistant on radiotherapy and shows only limited response to chemotherapy. Presently a study showed the efficacy of conventional hyperthermia for sarcoma cases [1]. Our objective study is modulated electro-hyperthermia (mEHT) [2], combined with conventional therapies for various sarcomas.

**Methods** 13 sarcoma patients were treated by mEHT (EHY2000+ device). Patients aged between 18–73 years. Histologic type is 2 rhabdomyosarcoma, 2 synovial sarcoma, 2 chondrosarcoma, 1 osteosarcoma, 3 leiomyosarcoma, 1 malignant peripheral nerve sheath tumor, 1 spindle cell sarcoma and 1 malignant fibrous histiocytoma (MFH). Treatment modality was 5 postoperative radiation therapy (RT) and mEHT, 2 combined RT and mEHT for primary lesion, 2 combined RT and mEHT for recurrent sarcoma at original region and 4 combined RT and mEHT for metastatic lesion. mEHT was applied 2–3 times a week. Post-operative RT was applied 50.4 Gy in 28 fractions and other RT was applied 30–39 Gy in 10–13 fractions.

**Results** 5 patients who received post-operative RT and mEHT didn't show local recurrence. One MFH patient received RT 50.4 Gy and 27 times of mEHT and showed good partial remission (PR). Patient with peripheral nerve sheath tumor received RT 30 Gy and tumor mass regressed continuously by 108 sessions of mEHT. One recurrence rhabdomyosarcoma patient received RT 30 Gy and 12 times of mEHT in neck for 1 month with PR. The chondrosarcoma patient who had recurrence at pelvic bone replacement region after surgery, received RT 30 Gy and 50 times of mEHT with PR. 1 patient received RT 30 Gy in 2 weeks and 48 times of mEHT in metastatic lung lesion and showed good PR. Patient with chondrosarcoma had chest-wall metastasis received RT 30 Gy in 10 fractions and 47 times of mEHT showed partial regression. A patient had cervical spine metastasis and received RT 30 Gy and 5 times of mEHT. Patient with osteosarcoma had multiple lung metastasis received chemotherapy and 84 times of mEHT. Metastatic cancer almost disappeared but one lesion that was out of the range of electrode is progressed.

**Conclusion** Primary, recurrent, and metastatic sarcomas well responded to mEHT treatment. Furthermore, mEHT effectively controlled pain and reduced the side effects of the combined therapies.

[1] Issels R, et.al, *Lancet Oncology*, 11:561-570, (2010)

[2] Szasz A, et.al, *Oncothermia –Principles and Practices*, Springer, (2010)

**Po.11****HIFU Hepatic Tumor Ablation: Modeling of Focusing and Motion Tracking Approaches**

Adamos Kyriakou<sup>1,2</sup>, Esra Neufeld<sup>2</sup>, Frank Preiswerk<sup>3</sup>, Bryn Lloyd<sup>1</sup>, Philippe Cattin<sup>3</sup>, Gabor Szekely<sup>2</sup>, Niels Kuster<sup>1,2</sup>

<sup>1</sup>Foundation for Research on Information Technologies in Society (IT<sup>2</sup>S), Zurich, Switzerland,

<sup>2</sup>Swiss Federal Institute of Technology (ETH), Zurich, Switzerland, <sup>3</sup>University of Basel, Basel, Switzerland

A major impediment to high intensity focused ultrasound (HIFU) ablation of hepatic tumors is the respiration-induced organ motion. If unaccounted for, this displacement and the partial obstruction introduced by the thoracic cage and the lung can lead to insufficient energy deposition in the targeted tissue or collateral tissue damage. The impact of motion tracking as well as intercostal targeting and compensation were investigated using acoustic and thermal numerical modeling.

A tumor was implanted behind the ribs of a static anatomical model, which was registered to 4D-MRI images of a respiratory cycle and warped with an automatically derived displacement field to generate a transient model with 14 steps. Acoustic simulations with a randomized phased array transducer (256 elements), were performed for each step of the respiratory cycle with both analytical or simulation-based (time-reversal) steering and compensation. The deposited acoustic energy was then projected back onto the static model and transient thermal simulations of gated and continuous ablation procedures with and without motion compensation were performed.

When compared to their analytical counterparts, simulation-based time-reversal techniques allowed for a significant reduction of pericostal tissue exposure and acoustic shadowing effects induced by the thoracic cage, a visible increase of the deposited acoustic energy in the targeted volume, improved targeting accuracy, enhanced demarcation of the generated lesions, and higher temperature increases. With only distance-based corrections, the focus can shift out of the tumor, the focus strength decreases by a third, and a second focus is occasionally observed close to the primary one. Transient simulations of the dynamic model without motion compensation showed an increased energy build up near the rib and lung, as well as a strongly exposed streak between the intercostal space and the tumor, which is likely due to geometric constraints enhancing focus side-lobes. Moreover, mainly because of slower liver motion at peak ex- and inhalation, the main energy deposition is not evenly distributed along the liver movement magnitude but is mostly observed in two regions that are slightly bigger than the static focus size. The peak temperature increase is reduced by a factor of three. Triggered sonication reduces the heating even further. Modeling of continuous motion compensation is ongoing.

Together with a novel population-based parametric liver motion and drift model, simulations can allow to overcome motion as well as focus distortion issues. Modeling-based optimization permit shortening treatment time, extending the range of treatable cases (locations and tumor size), and reducing collateral damage.

**Po.12****Combined radiotherapy and thermal ablation for advanced solid tumors**

Robert J. Griffin<sup>1</sup>, Beata Przybyla<sup>1</sup>, Nathan A. Koonce<sup>1</sup>, Klressa Barnes<sup>1</sup>, Gal Shafirstein<sup>2</sup>

<sup>1</sup>University of Arkansas for Medical Sciences, Little Rock, AR, USA, <sup>2</sup>Roswell Park Cancer Institute, Buffalo, NY, USA

**Introduction:** Radiotherapy regimens are rapidly evolving towards minimal treatment days, and larger doses/treatment for many tumor types. Thermal ablation is widely used but continues to have recurrences. The logical combination of high dose, stereotactic radiotherapy and a thermal ablation regimen has not been explored. We had originally hypothesized that ablation during or just before radiation may increase oxygenation in the tumor periphery and thus increase radiation sensitivity. It appears that this effect is overshadowed by the stress response at the margin that occurs upon ablation. We were not able to document treatment synergy when radiation was applied immediately before, or simultaneously with, ablation. In the current work, we hypothesized that radiotherapy applied before tumor thermal ablation or at an extended timepoint after ablation would maximize the overall cell kill and tissue destruction caused by the combined treatment.

**Methods:** Radiation was delivered to the entire tumor volume using a faxitron or small animal conformal irradiator developed by our department in a single dose of 20 Gy. Thermal ablation was accomplished using a stainless steel 18 gauge needle with an inserted 805 nm laser fiber which was pulsed at a frequency necessary to maintain a tip temperature between 80-90C when the needle was placed into the center of orthotopically grown MATBIII (rat) or subcutaneous SCK (mouse) breast tumors. Tumor growth was monitored after treatment.

**Results:** In the MATBIII, we performed a study where ablation and single dose, 20 Gy spatially fractionated radiation were separated by 72 h. Here, there was a suggested synergy of treatment effect, with an approximate 60% increase in the number of tumor regressions obtained with combined treatment compared to single modalities. More recently, we observed a marked improvement in tumor control in SCK murine tumors after a regimen where 20 Gy radiation was followed by ablation 30 min later. In this series, the combined treatment was able to stall tumor growth with negligible regrowth in the observation period of approximately 3 weeks. Single modality and control tumors all re-grew and progressed within the same three weeks.

**Conclusion:** Large radiation therapy doses followed by tumor thermal ablation may be an effective approach to allow ablation to sterilize portions of the tumor otherwise resistant to the radiation. This combination can be easily translated into the clinical practice of stereotactic radiation approaches by applying ablation after the last fraction. Supported by NIH CA44114 and the Arkansas Breast Cancer Research Program

**Po.13****Focusing and Aberration Correction for Transcranial Focused Ultrasound**

Adamos Kyriakou<sup>1,2</sup>, Esra Neufeld<sup>1</sup>, Beat Werner<sup>3</sup>, Gabor Szekely<sup>2</sup>, Niels Kuster<sup>1,2</sup>

<sup>1</sup>Foundation for Research on Information Technologies in Society (IT<sup>2</sup>IS), Zurich, Switzerland,

<sup>2</sup>Swiss Federal Institute of Technology (ETH), Zurich, Switzerland, <sup>3</sup>University Children's Hospital, Zurich, Switzerland

Transcranial focused ultrasound (tcFUS) is a noninvasive neurosurgical intervention modality. The efficiency of tcFUS therapy is compromised by the heterogeneous nature and acoustic characteristics of the skull, which induce significant distortion of the acoustic energy deposition, focal shift, and a decrease in thermal gain. Partial compensation of skull-induced aberrations, can be achieved by employing large phased-array transducers with appropriate phase and amplitude corrections. However, precise focusing remains a necessity, especially at high acoustic frequencies. A numerical framework allowing for 3D full-wave, linear and nonlinear acoustic and thermal simulations has been developed and applied to transcranial sonication. Simulations were performed to investigate the impact of skull aberrations, compare different aberration correction approaches to achieve refocusing, extend the treatment envelope of tcFUS therapy, and explore secondary acoustic and thermal treatment effects.

The simulated setup consisted of an idealized model of the commercial tcFUS system ExAblate 4000 (1024 elements operated at 230 kHz) and a detailed anatomical head model. Four different approaches were employed to calculate aberration corrections including an analytical calculation, a semi-analytical ray-casting approach, and two simulation-based time-reversal approaches with and without pressure amplitude corrections. These approaches were evaluated for 22 targets in the brain and their impact on the resulting pressure and temperature distributions was compared. The influence of acoustic nonlinearity and the effect of temperature-dependent perfusion and vascular shut-down were also explored.

Connected-component analyses were conducted on all calculated 3D pressure and temperature distributions to evaluate the acoustic and thermal performance of the different approaches for each target. Those analyses yielded the full-width half-maximum size of the focal regions or thermal lesions, the distance between these regions and the intended target, and the shape and volume of these regions. While the (semi-)analytical approaches failed to induced high pressure values or ablative temperatures in any but the targets in the close vicinity of the geometric focus, the simulation-based approaches allowed for a considerable extension of the treatment envelope, the generation of sharper foci, and an increased targeting accuracy.

This study suggests that employing simulation-based approaches to calculate aberration corrections for tcFUS therapies may significantly extend the envelope of such treatments without the need for patient repositioning as well as predict possible secondary effects, e.g., standing waves and skull heating, and avoid them. The utilization of modern but affordable computer hardware, combined with state-of-the-art high-performance computing techniques, enables realistic acoustic and thermal simulations in complicated setups to be performed within minutes.

**Po.14****Deep RF Phase Array Numerical Optimization Study**

Paul Turner, Mark Hagmann

*BSD Medical Corp, Salt Lake City, UT, USA*

**Introduction-** External phased array RF and microwave hyperthermia applicators have been utilized since the early 1980's, but there have been few publications describing significant further evolution of these applicators.

**Method-** We have developed a numerical model using the COMSOL finite element software to evaluate current and future array design concepts. This study has included changes in the number and sizes of the antennas, the number of channels with phase control, operating frequencies from 60 to 434 MHz, different sizes and media for the bolus, different sizes and shapes for the arrays, and several different tissue characteristics. The model used cylindrical or elliptical homogeneous phantoms to evaluate the focal size, steering of the heating pattern, compare heating of the superficial fat versus that of the deep tissue, and heating efficiency. Several hundred numerical simulations were made. The study primarily focused on the heating of adult torso phantoms. The variables in antenna dipole sizes included 4.04, 5.82, 10.6, and 13 cm. The array diameters included 36 and 60cm. The specific frequencies tested were 60, 75, 100, 140, 175, 250, and 434MHz. The Simulations used arrays of 4, 8, 12, or 24 antennas with couplets or phase control on all of the individual antennas. The bolus widths evaluated were 19, 32, and 48cm.

**Results-**The results of the study demonstrated that frequencies of 100 to 140MHz were suitable for operation with a 12 channel RF control system, but at 175MHz and above 24 or more control channels are required to control the heating pattern and minimize superficial hotspots. At 434MHz there was insufficient central penetration in the large tissue phantoms and there were an increased number of superficial hotspots. Good localization was seen in simulations at frequencies as high as 250MHz with reduced superficial and fat heating and a deep focal zone that was typically 5x5x10 cm. Although the central and steered focus could be significantly reduced in size by using 250 MHz, the superficial heating of fat and other tissue limited the ability to achieve localized heating in the targeted region.

**Conclusion-** Improved targeting for localized heating of a tumor is possible at operating frequencies as high as 250MHz. However, in order to obtain this improvement it would be necessary to increase the complexity of the system to improve the focal targeting and tracking during a treatment by means of pretreatment planning and non-invasive thermometry.

**Po.15****Multiple intratumoral magnetic nanoparticle injections enhances the heat delivery in murine sarcoma model**

Harley Rodrigues, Francielli Mello, Luis Branquinho, Gustavo Capistrano, Elisângela Silveira-Lacerda, Andris Bakuzis

*Universidade Federal de Goiás, Goiânia, Goiás, Brazil*

Cancer treatment with magnetic nanoparticle hyperthermia generally involves the intratumoral injection of magnetic fluids. Indeed, some studies had been showing that the distribution of nanoparticles can be affected by the injection fluid velocity, as well as the number of injection sites. In this work, we compare the hyperthermia efficacy of a group of 3 animals submitted to one single-site injection, with another group of 3 animals, but now, with the same amount of magnetic fluid equally divided into three distinct injection sites. The experiments consisted of a 30-minute magnetic hyperthermia procedure performed at 300kHz in swiss mouse induced tumors by sarcoma S180. Distinct magnetic field amplitudes, ranging from 9.8 up to 13.7 kA/m, were evaluated. The experiments were performed under non-uniform magnetic field configuration conditions, so the field values reported before consist of the value estimated at the center of the tumor. The amplitude of the alternating magnetic fields was obtained from measurements using an AC field probe. Temperature measurements were obtained at the surface by real-time infrared thermal camera, while intratumoral temperature was obtained using a fiber-optic thermometer. In the experiment, 90 microliters of magnetic fluid (2mg of nanoparticles) were injected directly into the center of geometry of the tumor (one site-injection condition), or the same amount of magnetic fluid was equally divided and injected into three symmetrical tumor positions along the major axis of the tumor (one in the same as before and the other two at the corners). The magnetic nanoparticle consisted of citrate-coated manganese-ferrite based nanoparticles. The sample was characterized by several techniques (transmission electron microscopy (TEM), X-ray diffraction (XRD), and vibrating sample magnetometer (VSM)). In particular, for field amplitude of 11.8 kA/m, we found for the one-site injection group a mean maximum intratumoral (surface) temperature of 39.0 (39.3) degrees Celsius. While for the three-injection group, we found an intratumoral (surface) temperature of 42.7 (42.6) degrees Celsius. Increasing the field amplitude resulted, as expected, in higher temperatures. As for instance, for three-sites injection group we found an mean intratumoral temperature increasing to 44.3 degrees Celsius for 13.7kA/m. The higher value of the multiple injection group might be attributed to a better nanoparticle distribution around the tumor. Numerical simulations using COMSOL multiphysics software, under non-uniform field configuration, will be shown in order to compare with our experimental findings.

**Po.16****Magnetic Resonance guided Thermo Chemical Ablation**

Florian Maier, Christopher J. MacLellan, David T. Fuentes, R. Jason Stafford, John D. Hazle, Erik N. K. Cressman

*The University of Texas MD Anderson Cancer Center, Houston, USA*

**Introduction:** Thermochemical ablation (TCA) provides a novel concept in minimally invasive ablative procedures in which two reactive solutions [1], such as an acid and a base, release heat as they react prior to entering the tissue as a hot salt solution. Thermal damage results in surrounding tissue via the released thermal energy. Recently, evaluation studies of TCA were performed using thermal probes to monitor temperature changes during the treatment. However, this allows evaluating temperature at a few positions only. In this work, use of a multi-parametric Magnetic Resonance (MR) pulse sequence for online monitoring of TCA treatments is investigated to provide more detailed insight for effective delivery to advance the understanding of this technology towards clinical translation.

**Methods:** A 2D multiple gradient recalled echo MR pulse sequence [2] was implemented to acquire up to 16 echoes of the same k-space trajectory with different echo times (TE, min = 2.3 ms, max = 28.2 ms, spacing = 1.6 ms). Additionally, the pulse sequence allows for shifted echo trains to get a high temporal resolution of the MR signal decay and therefore a spectral resolution of 0.3 ppm with less aliasing of the peaks. Initial phantom experiments were performed using *ex vivo* rabbit liver and bovine liver inside a clinical 3T MRI scanner. An in-house built MR compatible applicator was used to simultaneously inject Acetic Acid and Sodium Hydroxide. The applicator facilitated acid-base mixing prior to tissue entry. The exothermic reaction started immediately. Multi parametric MR data was acquired during and after the injection using the proposed pulse sequence. Additionally, a thermal probe was placed near the applicator tip.

**Results:** A temperature rise of 19.8 °C was estimated near the tip of the applicator based on the MR data assuming a proton resonance frequency shift of -0.01 ppm/°C. R2\* appeared to change linearly with temperature. The temperature probe observed a temperature rise of 17.4 °C. Post-injection, high resolution spectra revealed additional peaks in the range from -3.1 ppm to -2.8 ppm below the water peak (0 ppm) in regions where the reaction product Sodium Acetate (-2.8 ppm) was expected.

**Conclusion:** This initial assessment of MRgTCA indicates that multi-parametric changes can be used to get a more detailed insight into this novel thermal ablation technique. Temperature measurements and detection of the reaction product seem to be feasible. This will facilitate a platform for the design and optimization of applicators as well as the development and validation of computational models, and progress towards clinical translation.

[1] Cressman ENK, et al. Int J Hyperthermia 2010;26(4):327-337.

[2] Taylor BA, et al. Med Phys. 2008;35(2):793-803.

**Po.17****Assessment of a QA phantom after multiple heatings and remolding**

Alexis Farrer, Allison Payne, Douglas Christensen

*University of Utah, Salt Lake City, UT, USA*

The ATS Laboratories daily quality assurance (DQA) hydrogel phantom is commonly used with MR-guided high intensity focused ultrasound (MRgHIFU) systems. A benefit of the ATS DQA phantom is its ability to be heated to a liquid state and poured into a custom mold. The same volume of ATS DQA phantom can be heated and molded multiple times, increasing its versatility. This study investigates whether the acoustic properties and MR signal are altered after multiple reheatings, and whether any observed changes are reversible.

A control sample was extracted from the original ATS DQA phantom and set aside in a cylindrical tube. The remaining volume of ATS was heated until it was in a uniform liquid state between 45°C and 50°C. After each heating, a portion was poured into a labeled tube indicating the number of heatings the material had undergone; the remaining volume was allowed to re-solidify between each phase change. Five heating cycles were performed, resulting in five sample tubes plus the control tube. To assess whether any potential water loss caused by the multiple heating cycles could be reversed, 2 mL of water was mixed with the ATS phantom in liquid form during the fifth cycle. Each tube was identical and contained an equal volume of phantom material. The control, the remolded tubes, and original volume of ATS were kept refrigerated and in a moist environment between heatings.

A through-transmission technique was used to measure the speeds of sound and attenuation values for all six samples. The typical intra-sample standard deviation, measured sequentially six times for a sample that had been through four heatings, was less than 1 m/s for speed of sound and less than 0.01 dB/cm/MHz for attenuation. A 2-D GRE, high-resolution, proton density-weighted sequence was used with a 3T Siemens MRI to measure the MR signal intensity for all six tubes.

For all six tubes, the speed of sound ( $1585 \pm 5$  m/s) and attenuation ( $0.662 \pm 0.041$  dB/cm/MHz) were measured. The MR signal average ( $544 \pm 28$ ) was measured taking a spatial average over the same circular region of interest for all six samples.

After five reheatings, only minor differences in the acoustic properties or MR signal intensity were observed in the ATS DQA phantom.



**Po.18****Modeling and Validation of Thermochemical Ablation (TCA) in ex-vivo Bovine Liver**

Martin Jones, Florian Maier, Christopher MacLellan, Jason Stafford, Erik Cressman, David Fuentes

*University of Texas MD Anderson Cancer Center, Houston, TX, USA*

**Introduction:** Thermochemical ablation (TCA) presents an appealing multi-functional and minimally invasive technology at a lower overall cost per procedure than existing thermal ablation procedures. It presents an attractive alternative to radiofrequency and laser ablation techniques in treating cancerous tissue of the liver; by-products of the reaction are naturally occurring and may be designed close to physiological pH values within the human body and thus are excreted with little system toxicity. Clinical grade reagents are relatively inexpensive and readily available and, because the energy source is intrinsic to the in-situ chemistry, no base unit or generator is required. The feasibility of TCA technology to rapidly treat single or multiple cancerous lesions *in vivo* in liver has been established; however, it is still a relatively *clinically nascent* technology. The goal of this work is to develop and validate mathematical models of the TCA procedure that will provide an intelligent understanding of the fundamental thermal and chemical processes involved for use in planning the procedure.

**Methods:** A mathematical model that couples Pennes bioheat transfer model to Ficks law for mass transport of the chemical species has been developed. Heat of formation calculations revealed the energy released in the exothermic reaction to be -45 kJ/Mole. Finite element models of the procedure conform to the coaxial needle used to mix and inject the reagents used in the procedure (Sodium Hydroxide and Acetic acid). MR imaging of the ablation region was employed to estimate the distribution of the injectate. The mathematical model was quantitatively compared to MR thermal imaging and fluoroptic probe measurements of TCA induced heating in phantoms and ex-vivo bovine liver.

**Results:** The heat of formation (enthalpy) model of the reagent's exothermic reaction that drives the heat transfer is seen to quantitatively agree with the MR temperature imaging and fluoroptic probe measurements.

**Conclusion:** Initial mathematical modeling of the TCA procedure suggest that the coupled bioheat transfer and mass transfer predictions have potential in developing approaches to planning the procedure as well as in data assimilation techniques for monitoring. Further work is needed in acquiring tissue diffusion parameters for prospectively modeling the procedure.

**Po.19****The role of transcription factor Nrf2 in mild thermotolerance induced at 40°C**

Audrey Glory, Diana Averill

*UQAM, montreal, Quebec, Canada*

Thermotolerance is a phenomenon that allows cells to become resistant to various stresses after being exposed to heat shock. During hyperthermia treatments, the patient's tumor cells can develop thermotolerance, which could lead to a decrease in treatment efficacy. However, since this phenomenon is only transient, its effects are not a real drawback for the clinical use of hyperthermia. That being said, the capacity of a prior heat exposure to protect cells against future exposures is an interesting phenomenon. Thermotolerance can appear either after a short exposure to a high temperature (>43°C) or after a longer exposure to lower temperatures (39-40°C). Our research focuses on this second type, called mild thermotolerance. We have shown that thermotolerance induced during 3h at 40°C protects HeLa cells against apoptosis induced by hyperthermia at 42 or 43°C. There was a decrease in several markers of apoptosis (caspase activation, chromatin condensation) in thermotolerant cells compared to the non-thermotolerant cells, confirming their increased resistance to heat stress. Furthermore, mild thermotolerance protected cells against other forms of stress, for example oxidative stress. To improve understanding of the mechanisms involved in mild thermotolerance at 40°C, we investigated the role of oxidative stress and the NF-E2 related factor 2 (Nrf2) pathway. We showed via FACScan and fluorescence microscopy that the levels of several ROS increased gradually between 5 min and 3h of exposure at 40°C. The level of the Nrf2 protein increased in the nucleus of thermotolerant cells after only 5 min at 40°C, suggesting the activation of this pathway as an early event in the development of mild thermotolerance. To help understand the big picture, the inhibitor of p-53 pifithrin- $\alpha$  and the antioxidant PEG-catalase were added prior to the incubation at 40°C. The improved understanding of thermotolerance and the wider context of its protective effect could lead to its use as a treatment against various stress-related diseases.

**Po.20****Gold nanoparticle-bound TNF and combined radiotherapy to prime tumours for thermal therapy.**

Nathan A. Koonce<sup>1</sup>, Judy Dent<sup>1</sup>, Matt E. Hardee<sup>1</sup>, Matthew C. Quick<sup>2</sup>, Robert J. Griffin<sup>1</sup>

<sup>1</sup>University of Arkansas for Medical Sciences-Department of Radiation Oncology, Little Rock, AR, USA, <sup>2</sup>University of Arkansas for Medical Sciences-Department of Pathology, Little Rock, AR, USA

Hyperthermic insult of tumour tissue can be significantly enhanced with the addition of the cytokine tumour necrosis factor- $\alpha$  (TNF- $\alpha$ ). However, the systemic toxicity associated with TNF- $\alpha$  reduces its clinical utility, giving rise to the need for a selective mechanism of tumour delivery. To this end, a 33-nm polyethylene glycol-coated gold nanoparticle with several hundred TNF- $\alpha$  molecules attached was developed (Cytimmune). Our group and others have previously demonstrated marked vascular targeting and damage in solid tumour models upon systemic treatment with the gold/TNF nanoparticles with reduced systemic toxicity compared to TNF alone. We have previously observed a 1.7-fold tumour growth delay when a single gold/TNF treatment was combined with local hyperthermia in comparison to heat alone. However, recent work in our lab has focused on the combination of gold/TNF and radiation due to extensive publications of the synergistic anti-tumour effect noted when TNF is combined with radiotherapy. In a mouse mammary carcinoma model, 4T1, we found a >2-fold increase in tumour growth delay when gold/TNF was combined with a single dose of 20Gy irradiation. Ongoing efforts are towards understanding the underlying mechanisms responsible for the synergistic antitumor response of gold/TNF and radiation. In addition, work by our lab on combined radiotherapy and ablation indicates a sequence dependence of radiotherapy preceding ablation. Therefore, it seems logical to combine ablation with a gold/TNF and radiation regimen at the end of therapy to kill any remaining radioresistant tumour cells that remain. Overall, this multi-modality approach may provide a method to shrink large bulky tumours to a more treatable size as well as prime the tumour by nanoparticle based anti-vascular treatment for combination with thermal therapy. Supported by NCI CA44114.

**Po.21****Thermochromic phantom for characterization of HIFU thermal therapy**

Andrew S. Mikhail<sup>1</sup>, Ayele H. Negussie<sup>1</sup>, Ari Partanen<sup>2,1</sup>, Pavel Yarmolenko<sup>1</sup>, Nadine Abi-Jaoudeh<sup>1</sup>, Bradford J. Wood<sup>1</sup>, Aradhana Venkatesan<sup>1</sup>

<sup>1</sup>Center for Interventional Oncology, Radiology and Imaging Sciences, Clinical Center, National Institutes of Health, Bethesda, MD, USA, <sup>2</sup>Philips Healthcare, Cleveland, OH, USA

**Introduction:** The efficacy of thermal ablation therapies using laser, radiofrequency, microwave, or ultrasound energy depends on several factors including targeting accuracy and temperature elevation in the target tissue. Although tissue-mimicking phantoms are commonly used as substitutes for biological tissues for a variety of investigative purposes, they typically do not provide absolute measures of temperature elevation. Inclusion of thermochromic material in a tissue-mimicking phantom enables visual confirmation of temperature achieved during therapy, as well as delineates the location and size of ablated regions relative to the treatment plan. The objectives of this research were to 1) develop a novel tissue-mimicking thermochromic phantom; 2) target ablative exposures using high-intensity focused ultrasound (HIFU) under real-time MRI thermometry; and 3) characterize the intensity of thermochromic ink and its distribution post-HIFU in relation to the treatment plan.

**Methods:** A polyacrylamide gel phantom containing thermochromic ink was produced, with a color change temperature threshold of 60°C. A clinical MR-HIFU system (Sonalleve, Philips Healthcare, Vantaa, Finland) was used for HIFU exposures (frequency: 1.2MHz, acoustic power: 100W, duration: 20s) targeted to regions of 4-16mm in diameter. A clinical 1.5T MR scanner (Achieva, Philips Healthcare, Best, the Netherlands) was used for exposure planning, real-time thermometry utilizing the proton resonance frequency shift (PRFS) method, and to visualize and characterize thermal lesions using T2-weighted imaging and quantitative T2 mapping. Post-HIFU, color intensity changes within the phantom were identified and compared to changes in T2 values as well as to MRI temperature maps.

**Results:** Tissue-mimicking thermochromic phantoms were developed and validated for use in thermal therapy applications. HIFU thermal ablations ( $T > 60^{\circ}\text{C}$ ) resulted in permanent color change at targeted locations within the phantom. These color changes corresponded to maximum temperatures recorded using real-time MRI thermometry. In addition, temperature changes were visible on T2-weighted MR images as permanent foci of hypointensity. T2 change was found to be inversely related to temperature change within the region of interest (mean T2 change from  $226 \pm 6\text{ms}$  pre-HIFU to  $93 \pm 13\text{ms}$  post-HIFU).

**Conclusion:** A tissue-mimicking thermochromic phantom was developed to assess the spatial targeting accuracy as well as the precision and uniformity of hyperthermia using a clinical HIFU system. Color changes in the phantom reflected the achieved temperature. Moreover, temperature change correlated with T2 change in MRI. Thermochromic phantoms may be useful in thermal therapy characterization, quality assurance, and user training. Such phantoms could also provide volumetric temperature information in experiments where real-time thermometry is not feasible.

**Po.22****Investigating magnetic nanoparticle frequency spectra**

Fridon Shubitidze<sup>1</sup>, Robert Stigliano<sup>1</sup>, Benjamin Barrowes<sup>2</sup>, Katerina Kekalo<sup>1</sup>, Jack Hoopes<sup>3,1</sup>

<sup>1</sup>Thayer School of Engineering at Dartmouth, Hanover, NH, USA, <sup>2</sup>U.S. Army CRREL, Hanover, NH, USA, <sup>3</sup>Geisel School of Medical at Dartmouth, Hanover, NH, USA

In this paper, magnetic nanoparticle (mNP) frequency spectra are measured and analyzed to better understand the heating mechanism for alternating magnetic field (AMF) hyperthermia. During hyperthermia treatment, AMF energy is converted to heat by the mNPs. This conversion can arise through (1) Néel relaxation, (2) Brownian motion, (3) hysteresis and (4) frictional losses in viscous suspensions. Since all these processes depend on the applied AMF frequencies, there is a need to study mNP frequency spectra to design new mNPs with high heating properties for mNP hyperthermia cancer treatment. This work presents measured wide band electromagnetic signals for interrogation of mNP heating mechanisms. The signals are measured using a wideband frequency domain instrument, which consists of two concentric transmitter (Tx) coils, and three orthogonal receiver loops placed at the Tx coils center. The relation between Tx currents and radii is as  $I_1/I_2 = -R_1/R_2$ , so the total primary transmitter field at the center is zero. The system operates from 30 Hz up to 100 kHz. The In-phase and quadrature component data are collected for Dartmouth and Micromod mNPs. The frequency responses showed that quadrature parts have resonance peaks between 200-300 Hz. The mNP susceptibility is approximated using the Cole-Cole model, and its responses are modeled using the method of auxiliary sources. Comparisons between experimental data and modeled results are illustrated, and mNP heating mechanisms are analyzed.

**Po.23****Evaluation of hyperthermia and radiotherapy for the treatment of patients with locally advanced pelvic tumors: Preliminary findings**

Michael Payne, Doug Kelly, David Simon, Tyler Gutschenritter, James Flynn, Oneita Taylor, Matt Weaver

*Cancer Treatment Centers of America, Tulsa, OK, USA*

The prognosis for patients diagnosed with unresectable, locally advanced pelvic tumors is grim. These tumors are notoriously difficult to treat due to their refractory behavior with current available treatments. As such, novel treatment approaches are needed. Research has demonstrated that combined hyperthermia and radiation therapy can increase overall survival rates in patients with advanced pelvic tumors. This presentation details our hospital's early experience in evaluating patients ( $n = 10$ ) undergoing this combined approach. Patients enrolled in the protocol received hyperthermia one to two times per week after radiation therapy (170-200 cGy/fraction; 4-5 fraction/wk). Hyperthermia treatments were administered using the BSD-2000 Hyperthermia System (BSD Medical Corp. Salt Lake City, Utah, USA). Commonly reported adverse events among patients included pain, cramping, or discomfort in the region of hyperthermia. In most instances, pain could be mitigated by simple adjustments to the heating focus. Two patients receiving palliative therapy ( $n = 4$ ) had noted disease regression, reduced disease related pain, and an increase in performance status following therapy. In four patients receiving curative treatment ( $n = 6$ ) a complete clinical response was observed. Overall, patients tolerated hyperthermia quite well, however several issues served to complicate/delay therapy delivery. Issues of note included elevated pulse and blood pressure rates in some patients, machine malfunction, and hyperthermia accessory availability. In sum, the results of the initial evaluation of this study are encouraging and provide motivation for continual inquiry into the utilization of hyperthermia as an adjuvant standard of care in patients with pelvic tumors.

**Po.24****Modulating DNA Repair Mechanisms to Enhance Hyperthermic Radiosensitization of Breast Cancer Cells**

Nicholas B. Dye<sup>1</sup>, Rishabh Chaudhari<sup>2</sup>, Juong G. Rhee<sup>1</sup>, Zeljko Vujaskovic<sup>1</sup>

<sup>1</sup>University of Maryland School of Medicine, Baltimore, MD, USA, <sup>2</sup>The George Washington University School of Medicine and Health Sciences, Washington, DC, USA

**Introduction:** Hyperthermia is known to increase the radiosensitivity of cancer cells through various mechanisms. Studies have shown that hyperthermia induces degradation of the BRCA2 protein required for repairing DNA double strand breaks (DSB's) through homologous recombination (HR). Loss of HR relegates cells to more error-prone mechanisms of repair resulting in susceptibility to DNA damage. A number of drugs are under investigation to further disrupt a cancer cell's response to DNA damage including heat shock protein (HSP) inhibitors and poly-ADP-ribose polymerase (PARP) inhibitors. If a cancer cell's ability to repair its DNA can be preferentially disrupted using a combination of heat, HSP inhibitors, and PARP inhibitors even the most "radiosensitive" cancer cells may be candidates for successful radiotherapy.

**Methods:** MDA-MB-453 "parent" cells were transfected with a plasmid-encoding GFP under control of the Oct-3/4 promoter to create a "stem-like" phenotype. Parent and stem-like cells were irradiated at 2-6 Gy and subjected to heating (42°C) for 1 hour either before or after irradiation in the presence or absence of the HSP-90 inhibitor AUY-922 and clonal survival was assessed. MDA-MB-231 parent cells were irradiated at 2-6 Gy using combinations of AUY-922 and PARP inhibitor ABT-888 in conjunction with heating (42°C) for 1 hour before or after irradiation and clonal survival was assessed. Caspase-3 and PARP cleavage were used to assess apoptosis.

**Results:** MDA-MB-453 parent and stem-like cells exhibited decreased clonal survival when subjected to heat following irradiation which was enhanced by inhibiting HSP-90. The effect of inhibiting HSP-90 with AUY-922 showed no appreciable effect on clonal survival when used with radiation alone. However, when AUY-922 was combined with radiation followed by heat there was a one log reduction in clonal survival compared to the non-heated group even at the lowest 2 Gy radiation dose. Treated cells showed no increase in Caspase-3 or PARP cleavage 24 hours post treatment.

**Conclusions:** Our results indicate that inhibition of HSP-90 enhances the effects of mild heating on radiosensitization of MDA-MB-453 parent and stem-like cells likely by interfering with the cells ability to repair sublethal DNA damage seen with low dose 2 Gy radiation and not through apoptosis. This is clinically significant as radiation is typically fractionated around 2 Gy per dose. Ongoing studies will determine the additional role of PARP inhibition on radiosensitivity as well as the treatment response in the stem-cell rich cell line MDA-MB-231. These results will be presented at the time of the meeting.

**Po.25****Hsp-90 inhibitor enhances heat sensitivity of human breast cancer cells including stem-like cells**

Juonng G. Rhee<sup>1</sup>, Rishabh Chaudhari<sup>2</sup>, Nicholas B. Dye<sup>1</sup>, Seog-Young Kim<sup>3</sup>, Yong J. Lee<sup>3</sup>, Zeljko Vujaskovic<sup>1</sup>

<sup>1</sup>University of Maryland School of Medicine, Baltimore, MD, USA, <sup>2</sup>The George Washington University School of Medicine and Health Sciences, Washington, DC, USA, <sup>3</sup>University of Pittsburgh, Pittsburgh, PA, USA

**Introduction:** Overexpression of Hsp-90 is reported to cause radio- and heat-resistance. The purpose of this study was to investigate whether an inhibitor of Hsp-90 (AUY-922) plays a role in altering the heat sensitivity of human breast cancer cells, including stem-like cells.

**Methods:** MDA-MB-453 human breast cancer cells (parent cells) were transfected with a plasmid-encoding GFP under the control of Oct-3/4 promoter in order to ensure proper stemness (stem-like cells). The parent and stem-like cells were grown in a DMEM medium supplemented with 10% FBS and antibiotics and heat-treated in a water bath at 42°C for 1 to 5 hours. Multicellular spheroids were also grown in a spinner flask for either parent or stem-like cells and treated in a water bath at 43°C under constant agitation.

**Results:** Flow cytometric analysis revealed that 0.5-1.5% of the parent cells and >95% of the transfected cells were positive for stem-specific surface markers (CD44<sup>high</sup>/CD24<sup>low</sup>). Following an hour of heating at 42°C, the clonogenic survival of the parent and stem-like cells was 61% and 38% respectively, which suggests that the stem-like cells are heat-sensitive. During continuous heating at 42°C for 5 hrs, the cellular level of Hsp-90 increased in the parent cells but not in the stem-like cells, and the parent cells were heat-resistant when compared to the stem-like cells.

The heat-resistant state of the parent cells was confirmed by employing a step-up heating at 44°C (0-90 min) and by observing reduced rates of cell inactivation, which suggests the development of thermotolerance. The extent of thermotolerance was greater for the parent cells than for the stem-like cells. When AUY-922 was used, the heat sensitivity of both the parent and stem-like cells were enhanced, and the difference in thermotolerance between the two cell types was minimized.

Stem-like cells grown in 3D multicellular spheroids following heat treatment showed no change in the level of Hsp-90; however, the Hsp-90 level in the parental spheroids was reduced to 2/3 the level of the monolayer cells. This reduced level of Hsp-90 correlated with an increase in heat sensitivity. The effects of AUY-922 on 3D multicellular spheroids are currently being investigated.

**Conclusion:** The heat sensitivity of breast cancer cells appears to be closely related to the cellular level of Hsp-90. AUY-922 is a potent heat-sensitizer through its inhibition of Hsp-90 for both parental and stem-like breast cancer cells.



**Po.26****Pancreatic Electroporation**Derek West*University of Texas at Houston, Houston, Texas, USA*

Pancreatic Ductal Adenocarcinoma (PDAC) is one of the most lethal forms of cancer, with a 5-year survival of 6%, regardless of its staging. Currently, surgical resection is the only curative treatment, but <20% of patients qualify as surgical candidates. Advanced PDAC, which is surgically unresectable locally advanced adenocarcinoma or metastatic disease, accounts for approximately 80% of the cases at the time of diagnosis.

Almost all currently accepted treatment protocols for locally advanced or metastatic PDAC involve intravenous chemotherapy, most commonly gemcitabine. Despite this, PDAC chemoresistance to gemcitabine has been widely reported, leading to treatment failure and, ultimately, death. While not completely understood, several mechanisms of chemoresistance have been suggested. Among them, desmoplasia has been increasingly seen as a significant contributor to chemoresistance in PDAC. Desmoplasia is a dense stromal reaction seen in many forms of cancer, but is particularly intense in PDAC. The desmoplastic tissue contains extracellular matrix proteins, including collagen, pancreatic stellate cells, immune cells, which are all postulated to aid in growth of PDAC cells. Through elevated interstitial fluid pressures and intrinsic structural characteristics, desmoplasia decreases penetration of macromolecules, such as chemotherapeutic agents, through the tissue.

Electroporation is one such novel approach to overcome chemoresistance. Electroporation is a treatment by which high electrical fields are applied to cells to create cell membrane pores, which transiently or permanently increase cell permeability. Electroporation can be varied by voltage pulse intensity (field strength), time between pulses (pulse interval), number of pulses, and pulse duration. By altering these settings, pore formation in the cellular bi-lipid membrane can be reversible (with associated cell survival) or irreversible (with associated cell death). In the past two decades, the mechanism and practical applications of reversible electroporation have received increasing attention, particularly as a means of introducing a range of drugs, DNA, antibodies and plasmids into cells [11]. In recent clinical developments, irreversible electroporation has been shown promise in the treatment of locally advanced PDAC [7, 8].

Electrochemotherapy is the process by which tumor cells are electroporated during administration of chemotherapeutic agents. Use of electrochemotherapy in the treatment of cutaneous malignancies has shown superior efficacy over chemotherapy alone. As technological advances have been made, irreversible electroporation of pancreatic tumors has been performed with promising results. However, electrochemotherapy for pancreatic tumors has not been explored.

Our studies are preliminary examinations into the feasibility of using electroporation in the treatment of PDAC.

**Po.27****Nanotechnology for hyperthermia: the pros and cons of using nanoheaters for local temperature handling.**Gerardo Goya*Institute of Nanoscience of Aragon, University of Zaragoza, Spain*

Handling local, regional, and whole-body temperatures to treat a series of diseases is an ancient practice with a wide variety of efficacy records. However, in spite of the advancement in this field along the last decade, the impact of temperature changes on molecular mechanisms and cell pathways are still being debated.

For the first time it is possible to produce nanometer-size structures and to deliver them into a small target area to produce local hyperthermia. In theory, these nano-heaters could be delivered into tumour cells/tissue and, through the interaction with an external radiofrequency source, heat can be generated from the inside to ablate the tumour. This non-invasive approach could be potentially useful to treat both superficial and deep-seated tumours.

The usual heating agents are magnetic nanoparticles (MNPs). Engineered MNPs represent a new step for both diagnostic protocols and non-invasive therapies. They can be simultaneously used as intracellular heating agents (known as Magnetic Hyperthermia) as well as contrast agents for magnetic resonance imaging. Bottom line is, for each therapeutic application, precise physical properties are required. In this talk, the physical and chemical specifications for some biomedical application will be discussed in the framework of the synthesis methods required for obtaining each type of biocompatible MNPs, and in connection with their respective therapeutic application. Cell toxicity profiles data of the different MNPs will be presented and discussed based on their final intracellular distribution. Novel approaches for observing new MNP-cell interactions at the single-cell level, involving physical measurements will be presented. The proof of concept of a 'Trojan horse' strategy for immune-related therapies using human-monocyte-derived dendritic cells (DCs) previously loaded with magnetic nanoparticles (MNPs) as heating agents will be presented and the universality of the induced cell death mechanisms will be discussed.

**Po.28****A new MR pulse sequence for accurate temperature imaging in red bone marrow**

Ryan Davis<sup>1</sup>, Viola Rieke<sup>2</sup>, Eugene Ozhinski<sup>2</sup>, Misung Han<sup>2</sup>, Sharmilla Majumdar<sup>2</sup>, John Kurhanewicz<sup>2</sup>, Warren Warren<sup>1</sup>

<sup>1</sup>Duke University, Durham, NC, USA, <sup>2</sup>University of California San Francisco, San Francisco, CA, USA

Prostate and breast cancers are two of the most common types of cancer in the US, and those cancers metastasize to bone in more than two thirds of patients. While radiation and bisphosphonates can temporarily relieve pain from bone fracture, the disease is currently incurable. There is now ample evidence that, in the form of either hyperthermia or ablation, heat could have a powerful place in the treatment of bone cancer. Heat can allow targeted drug delivery to bone, hyperthermia of cancer cells in bone, and palliation of bone pain. However, there is one technical factor that limits many efforts to use heat to treat bone, which is that accurately measuring temperature in red bone marrow is still extremely difficult. This difficulty arises from the amalgamation of bone, adipocytes, and hematopoietic tissue found uniquely in red marrow, which causes broadened and non-Gaussian line-shapes in the NMR spectrum.

The purpose of this study is to compare the temperature accuracy between traditional pulse sequences and a sequence called HOMOGENIZED with off resonance transfer (HOT). Importantly, HOT is fundamentally different from spectroscopic imaging-based approaches that have been used to measure temperature in fatty tissues such as breast or yellow bone marrow. HOT generates magnetization that oscillates at the resonance frequency difference between fat and water (~1kHz) while traditional imaging pulse sequences measure magnetization that oscillates at the Larmor frequency (~100MHz.) Our hypothesis was that measuring the frequency difference between fat and water directly with HOT would provide more accurate temperature images than currently available methods.

The key result is that the temperature coefficient ( $\alpha$ ) was  $1.00e-2 \pm 7e-4$  ppm/°C with HOT and  $2.e-3 \pm 7e-3$  ppm/°C when measured with traditional localized spectroscopy. Given a 5°C temperature increase typical for hyperthermia, the uncertainty in  $\alpha$  propagates to an accuracy of 3.6°C for the currently available techniques and 0.4°C for HOT. Thus the mapping between the resonance frequency of water and temperature is nine times more accurate for HOT than for standard localized spectroscopy. A possible reason for this improvement is that HOT simplifies the NMR spectrum of red marrow by reducing it to one peak. Another reason is that compared to traditional pulse sequences, HOT has on average a 40% smaller full width at half maximum. HOT will thus for the first time allow accurate and quantitative thermal imaging of red marrow.

**Po.29****Effects of physiological temperature changes on Wnt signaling in primary human small airway epithelial cells (SAEC)**

Ratnakar Potla, Sergei Atamas, Mohan E Tulapurkar, Ishwar Singh, Jeffrey D Hasday

*University of Maryland Baltimore, Baltimore, USA*

Human body temperature can vary beyond the normal range during exposure to extreme environmental temperatures, vigorous physical activity and during febrile illnesses. In cardiac arrest survivors, temperature is intentionally lowered (32°C -34°C) (Therapeutic hypothermia (TH)) to minimize neurologic injury and fever is known to increase neurologic injury. Acute respiratory distress syndrome (ARDS) is characterized by acute lung injury that usually leads to a debilitating fibroproliferative process. Work from our own laboratory suggests that Febrile Range Hyperthermia (39.5°C) (FRH) may worsen and TH may mitigate ARDS. To further analyze how TH and FRH may modify ARDS, we studied the effects of clinically relevant hypo- and hyperthermia on miRNA expression in lung epithelium.

We investigated the effects of temperatures representative of TH and fever on the miRNA expression profile in SAECs using miRNA microarray and nCounter miRNA assays with confirmation by qPCR. Surprisingly only eight miRNA were altered under the following clinically relevant conditions: hypothermia (32°C vs 37°C), hyperthermia (39.5°C vs 37°C), therapeutic hypothermia (32°C+TNF $\alpha$  vs 37°C+TNF $\alpha$ ) and fever (39.5°C+TNF $\alpha$  vs 37°C+TNF $\alpha$ ). Of a total of 1018 miRNAs analyzed, we found 4 miRNAs for which levels decreased as temperature increased from 32°C to 37°C and 39.5°C.

*In silico* analysis demonstrated that the four temperature-dependent miRNAs converged on multiple targets that participate in Wnt signaling, which plays a prominent role in lung fibrosis. Consistent with this, we found that 24h pre-incubation at 32°C reduced and 39.5°C incubation increased subsequent expression of canonical WNT- $\beta$  catenin signaling target genes in Wnt-3a-stimulated SAECs and increased activation of the Wnt-responsive TOPFLASH reporter plasmid in Wnt-3a-stimulated HEK293T cells compared with 37°C cells. Overexpression of the relevant miRNA sponge constructs mitigated reduction in Wnt signaling in 32°C-exposed HEK cells while overexpression of the relevant pre-miRNA reversed the increase in Wnt signaling in 39.5°C -exposed HEK cells.


We are currently examining the consequences of the Wnt-signaling-modifying effects of TH- and FRH on the processes leading to post-lung injury fibrosis. These studies may eventually lead to new approaches to improve outcomes in patients with ARDS.

# Abstracts for Thursday, May 8th


Add the  
**Heat of Hyperthermia**  
to Your Cancer Treatment Team



**BSD MEDICAL**



BSD-2000



BSD-500

*See the Difference with BSD Hyperthermia Systems*

Visit [www.BSDMedical.com](http://www.BSDMedical.com) for FDA approved BSD-2000 Hyperthermia System Essential Prescribing Information and BSD-500 Hyperthermia System Indications and Use. | Tel: 801-972-5555

**Th.1****Assessing Nanoparticle Toxicity**

Katie Hurley, Yu-Shen Lin, Melissa Maurer-Jones, Donghyuk Kim, Victoria Szlag, Joseph Buchman, Solaire Finkenstaedt-Quinn, Sam Egger, Christy Haynes

*University of Minnesota, Minneapolis, MN, USA*

Nanoparticle toxicology, an emergent field, works toward establishing the hazard of nanoparticles, and therefore their potential risk, in light of the increased use and likelihood of exposure. Analytical chemists can provide an essential tool kit for the advancement of this field by exploiting expertise in sample complexity and preparation as well as method and technology development. This workshop will include discussion of experimental considerations for performing in vitro nanoparticle toxicity studies, with a focus on nanoparticle characterization, relevant model cell systems, and toxicity assay choices. Additionally, several case studies with candidate biomedical nanoparticles will be included to highlight the important toxicological considerations of these high potential nanoparticles.

**Th.2****Microwave Tissue Ablation – The Basics**

Eric Rudie<sup>1,2</sup>

<sup>1</sup>*Rudie Consulting, LLC, Maple Grove, MN, USA,* <sup>2</sup>*Denervx, LLC, Maple Grove, MN, USA*

Microwave energy is an ideal source for tissue ablation devices. It provides radiant heat generation that does not require direct tissue contact to couple the radiator (antenna) to tissue, thus affording flexibility in the applicator design. Further, microwave heating may be combined with conductive cooling to create a temperature field wherein the body lumen containing the applicator is kept below the temperature threshold for thermal injury and remains viable.

This talk will cover the basics of microwave heat generation within lossy dielectric (tissue). The effects of tissue attenuation, excitation frequency and applicator geometry will be discussed. Examples of microwave applicators will be described and both temperature data and histologic data will be presented. If time permits, basic concepts of antenna resonance, impedance matching and measurement of dielectric constant using a commercially available dielectric probe will be briefly discussed.

**Th.3****A Review of Cryoablation Systems for Minimally Invasive Treatment of Tumors**

Satish Ramadhyani

*Galil Medical, Arden Hills, Minnesota, USA*

The components of cryoablation systems used for the ablation of tumors in the kidney, prostate, liver, lung, and bone will be reviewed. These systems usually utilize the Joule-Thomson effect to create both freezing and thawing temperatures. Freezing is usually achieved by using high-pressure argon gas, while thawing is usually achieved by using helium. Both gases are expended during operation. The presentation will describe how such systems are set up and operated and will point out their advantages and shortcomings. A typical freeze-thaw treatment cycle will be described. An overview of the internal construction of a cryoablation probe will be provided and the thermodynamic processes occurring inside the probe will be briefly reviewed. The presentation will also include a short overview of a new type of cryoablation system, currently under development, that utilizes a different approach to achieve closed-loop operation. This system will minimize the expenditure of argon and eliminate the use of helium.



**Th.4****Ultrasound-guided drug and gene delivery**

Katherine Ferrara, Azadeh Kheiriloom, Brett Fite, Josquin Foiret, Yu Liu, Andrew Wong, Elizabeth Ingham, Lisa Even, Sarah Tam, Charles Caskey, Jai Seo, Dustin Kruse

*University of California Davis, Davis, CA, USA*

Our objective in this presentation is to explore the mechanisms and technologies that are exploited to enhance drug and gene delivery with ultrasound. Physical mechanisms including cavitation, radiation force and hyperthermia can alter the local concentration of the drug or gene, enhance transport across the vascular surface and cell membrane and result in changes in the number or phenotype of immune cells. In addition, we will describe technologies for guiding and assessing delivery, including direct imaging of the therapeutic cargo with positron emission tomography or optical imaging, imaging of temperature elevation, imaging of the mechanical properties of tissue and imaging of tissue perfusion. Finally, we will summarize the delivery vehicle technologies that are showing promise for improving therapeutic efficacy.

Nanostructures, including microRNA, 4x4x14 nm albumin, 15-nm micelles, 100-nm liposomes and micron-diameter microbubbles, have been labeled for nuclear imaging of the shell and in parallel the core of the particle has been imaged with ultrasound, hyperspectral optical methods or magnetic resonance imaging. In pre-clinical models, we find that molecular targeting of particles as large as liposomes can result in rapid (~1 minute) endothelial targeting of cardiac vasculature of ~40% ID/g. The accumulation of targeted microbubbles on tumor endothelium is similarly rapid, although the accumulated particle fraction is substantially smaller. While the accumulation of nanoparticles within cancerous tumors is substantially slower, stable particles typically accumulate to ~5-10% ID/g within 24 hours. Such accumulation can be locally increased 2-3 fold with the application of therapeutic ultrasound. A significant outstanding challenge is the design of therapeutic nanoparticles that remain stable in circulation but are efficacious at the disease site. One approach that we have followed is to form a precipitate complex between copper and doxorubicin within nanoparticles. The advantage of this approach is that the particles are loaded at neutral pH and the copper-doxorubicin complex remains intact until a low pH environment is encountered in a lysosome or tumor or release is facilitated by ultrasound. We find that such a strategy can achieve complete regression of local cancers.

**Th.5****FEM Numerical Models of Magnetic Nanoparticle Heating Facilitate Treatment Planning and Analysis**

John Pearce<sup>1</sup>, Alicia Petryk<sup>2</sup>, Jack Hoopes<sup>2</sup>

<sup>1</sup>The University of Texas at Austin, Austin, TX, USA, <sup>2</sup>Dartmouth College, Hanover, NH, USA

Treatment planning remains a difficult process in magnetic nanoparticle hyperthermia studies. We lack fundamental engineering design methods and criteria that can be used to predict outcomes in experimental studies. Numerical models of existing experimental data help illuminate underlying processes and can be used to quantitatively analyse the relative importance of local heat transfer effects, perfusion effects and the necessary iron oxide nanoparticle loading to achieve adequate tumor heating.

Experiments in MTG-B tumors of varying size on the fore shoulders of C3H mice were heated with injected coated Fe<sub>3</sub>O<sub>4</sub> nanoparticles and heated in 160 kHz magnetic fields of strengths on the order of 34 kA/m (rms). Transient temperatures were recorded with optical probe sensors (FISO, Inc.) and tumor treatment evaluated in histologic studies. The experiments were modelled in realistic ellipsoidal tumor geometries using Comsol Finite Element Method software and the bio-heat equation. A uniform volumetric power density was applied in the tumor and adjusted to match the transient temperature records. The numerical models included three damage models: 1) microvascular disruption, 2) AT-1 cell death, and 3) SN12 cell death. These cell death assays were selected because they follow Arrhenius kinetics very closely and represent a thermally-sensitive (AT-1) and a thermally-robust (SN12) cell type.

The results indicate that for the surface tumor locations studied effective mNP loadings of approximately 1 microgram/mm<sup>3</sup>, or approximately 1 mg/g<sub>tumor</sub>, are required to achieve adequate heating. In a few experiments there is evidence of vascular disruption, which was not reflected in the numerical models even though they included vascular damage-dependent perfusion. This suggests that the mNPs were not evenly distributed in the tumors. The SN12 cells prove remarkably thermally robust when compared to the AT-1 cells in this model space. This observation underlines the necessity of including multiple thermal death / damage processes to obtain a clear picture of effectiveness – single process assays such as CEM can be misleading.

**Th.6****Transient and Continuous Wave Nonlinear Ultrasound Simulations in FOCUS**

Xiaofeng Zhao, Robert J. McGough

*Michigan State University, East Lansing, MI, USA*

FOCUS, the 'Fast Object-oriented C++ Ultrasound Simulator,' was originally developed for rapid and accurate simulations of pressure fields generated by ultrasound hyperthermia and HIFU (high intensity focused ultrasound) transducers. We initially created the FOCUS software for linear simulations of continuous wave and transient pressures generated by single ultrasound transducers and ultrasound phased arrays. Now that the linear ultrasound simulations are established in FOCUS, efforts to incorporate nonlinear propagation routines into FOCUS are underway. Recently developed nonlinear simulation codes compute solutions to the Khokhlov - Zabolotskaya - Kuznetsov (KZK) equation for transient and continuous wave excitations. For transient simulations of the KZK equation, FOCUS employs an adapted version of the approach in [Lee and Hamilton, "Time-domain modeling of pulsed finite-amplitude sound beams," JASA, 1995], and for continuous wave simulations of the KZK equation, FOCUS implements a modified C++ version of the approach described in [Berntsen, "Numerical Calculations of Finite Amplitude Sound Beams," Frontiers of Nonlinear Acoustics:12th ISNA, Elsevier, 1990]. Transient and continuous wave KZK simulations in FOCUS perform these nonlinear calculations with implicit backward Euler and Crank - Nicolson finite difference methods. The transient and continuous wave KZK simulations are implemented in FOCUS for axisymmetric flat circular and spherically focused transducer geometries. Results obtained from these implementations of the KZK equation are compared to linear simulation results calculated with the fast nearfield method (FNM) in FOCUS. The results show that, when the nonlinear terms are neglected, the linear KZK and FNM simulations match in the farfield of the paraxial region for unfocused and mildly focused transducers and are different elsewhere. Results of nonlinear transient and continuous wave KZK simulations are also shown. Continuous wave nonlinear KZK simulations are performed in the frequency domain, and simulated pressure fields corresponding to the first four harmonics are shown for representative transducer geometries. The contributions from these harmonics are superposed in different axial locations, and the simulation results show the evolution of the nonlinear waveforms with increasing propagation distance. Likewise, transient nonlinear KZK results are performed in the time domain, and animations of the simulated results are shown for the same transducer geometries. Transient nonlinear waveforms also demonstrate the development of shock fronts with increasing propagation distance for sufficiently large input pressures in a nonlinear medium. Incorporating these nonlinear KZK simulations into FOCUS therefore enables convenient simulations of nonlinear pressure fields generated by flat circular and spherically focused transducers.

**Th.7****Interactive Approximation of High-Intensity Focused Ultrasound Simulation for Arbitrary Transducer Configurations**

Christian Schumann<sup>1</sup>, Eike Mücke<sup>2</sup>, Daniel Demedts<sup>1</sup>, Joachim Georgii<sup>1</sup>, Caroline von Dresky<sup>1</sup>, Tobias Preusser<sup>1,3</sup>

<sup>1</sup>Fraunhofer MEVIS, Bremen, Bremen, Germany, <sup>2</sup>University of Applied Sciences, Bremerhaven, Bremen, Germany, <sup>3</sup>Jacobs University, Bremen, Bremen, Germany

**Introduction:** Current HIFU simulation techniques incorporate graphics processing units (GPU) to improve the performance tremendously. However, these methods are still not fast enough for immediate feedback during interactive sonication planning. We present a method for high-speed interactive approximation of the ablated volume of a HIFU sonication with given parameters such as focal spot, transducer power and sounding duration. The result is an efficient ellipsoidal visualization of the thermal ablation area. To incorporate the effect of structures in the focused ultrasound beam cone we use techniques of uncertainty visualization.

**Methods:** Our visualization of the approximated sonication consists of three steps. The first step is a pre-processing which has to be executed once for every transducer configuration, since it is independent from patient data. The respective transducer domain is sampled in 5 dimensions: the 3 spatial dimensions, transducer power and sonication duration. For a given sample point in this 5D grid a homogenous GPU based HIFU simulation computes the thermal dose, from which a thresholding yields the ablation volume. Ellipsoidal parameters for this volume including position, scale and rotation are acquired using principle component analysis (PCA) and stored for the sample point. In the second step, an ellipsoid for a given 3D position, duration, and power is visualized during interactive planning. To this end the respective ellipsoid parameters are interpolated based on the pre-processed grid. Finally, to account for patient specific anatomy, the GPU is used to determine the amount of occlusion resulting from anatomical structures between the transducer elements and the target point. The visualization of the ellipsoid is adapted accordingly with respect to color and fuzziness.

**Results and Conclusion:** The presented method has been integrated into a HIFU planning prototype. The approximation including the patient specific uncertainty visualization can be carried out interactively. Hence, a preview of the sonication can be shown while moving the mouse. After definition of multiple sonications the plan can be verified using an accurate heterogeneous simulation. Comparisons of the approximation with the actual simulation show promising results and high potential for the improvement of interactive manual planning of sonication for patient specific HIFU treatment. The duration of the pre-processing step is in the range of minutes to hours, depending on the resolution of the sampling of the 5D parameter space. However, this is not problematic since it has to be computed only once for every FUS device and the results are stored to be reused.

**Th.8****Comparison of single- and multiple-antenna ablation at 915 MHz and 2.45 GHz: a simulation and experimental investigation**

Mohammed Taj-Eldin, Punit Prakash

*Kansas State University, Manhattan, KS, USA*

**Background:** Most currently available clinical systems for microwave ablation operate within the ISM bands of 915 MHz and 2.45 GHz. The optimal operating frequency for rapid, controlled heating is not readily identifiable. While antenna arrays have been studied at lower frequencies for hyperthermia, synchronous and asynchronous arrays operating at 2.45 GHz have not been extensively studied for ablation. The objective of this work is to compare single- and multiple-antenna microwave ablation at 915 MHz and 2.45 GHz, while controlling transmitted power and treatment duration.

**Methods:** A full-wave FEM solver was used to design and simulate the energy deposition pattern from coaxial dipole antennas radiating into liver tissue at 915 MHz and 2.45 GHz. Antenna lengths were calculated to be half the effective wavelength at each frequency, and manually optimized to minimize reflection coefficient and maximize ablation zone diameter. Applied power was adjusted so that 30 W was transmitted into tissue in all cases. Energy deposition patterns from antenna arrays were computed by superposition of electric field (for synchronous arrays) and power deposition patterns (for asynchronous arrays) from individual antennas. Experimental ablations with single- and multiple-antennas were performed in *ex vivo* liver and muscle tissue.

**Results:** Simulations and experiments indicated 25% larger ablation zones at 2.45 GHz compared to 915 MHz ( $37 \pm 1.7$  mm vs.  $29.7 \pm 0.6$  mm). Shorter antenna lengths at 2.45 GHz, yielded shorter (L:  $57 \pm 3.6$  mm vs.  $72.3 \pm 6.4$  mm), more spherical ablation zones. The maximum discrepancy between simulated and experimental ablation zone diameters was 13.3% across all cases. Simulations of dual- and triple-antenna arrays operating at 915 MHz indicated elliptical energy deposition patterns for both synchronous and asynchronous arrays, and larger ablation zones for synchronous arrays. Simulations of a 2.45 GHz dual-antenna synchronous array showed extensions of the ablation zone perpendicular to the array axis, indicating regions of constructive and destructive phase interaction. More spherical experimental ablation zones were observed for synchronous arrays (48 mm x 46 mm) compared to asynchronous arrays (57 mm x 42 mm).

**Conclusions:** For the 30 W, 10 min ablations considered in this study, larger, more spherical ablation zones were achieved with 2.45 GHz antennas. Synchronous equal-phase arrays yielded more spherical ablation zones than asynchronous arrays. These results suggest that larger, more spherical ablation zones may be achieved in liver and muscle with antennas operating at 2.45 GHz. Further study of antennas and arrays operating at higher frequencies appears warranted for controlled tissue ablation.

**Th.9****Inverse problem statistics of optical parameter inference in brain MR-guided laser induced thermal therapy.**

Samuel Fahrenholtz<sup>1,2</sup>, R. Jason Stafford<sup>1,2</sup>, Florian Maier<sup>1</sup>, Anil Shetty<sup>3</sup>, David Fuentes<sup>1,2</sup>

<sup>1</sup>The University of Texas MD Anderson Cancer Center, Houston, Texas, USA, <sup>2</sup>The University of Texas Graduate School of Biomedical Sciences at Houston, Houston, Texas, USA,

<sup>3</sup>Visualase Inc., Houston, Texas, USA

**Introduction:** Multiple post market studies are ongoing to investigate magnetic resonance-guided laser-induced thermal therapy (MRgLITT) as a neurosurgical treatment for oncology and motion disorders. While MRgLITT has powerful real-time guidance of treatment delivery, brain MRgLITT stands to benefit from effective planning to inform physicians' laser fiber placement. Differential equations expressing bioheat mechanisms have been extensively researched for planning, but these models lack reliable patient specific physical parameter data, e.g. optical parameters, thermal conductivity, or microvasculature perfusion. This abstract explores a potential method to improve parameter data via a statistical characterization of optical parameter data obtained from previous MRgLITT procedures.

**Methods:** The inverse problem used to characterize the MRgLITT procedures has three notable components: training data, a physics model, and a parameter-space search algorithm. The training data was MR thermal imaging from 19 MRgLITT (980 nm wavelength) oncological brain ablations in 7 patients. The physics model is a Green's function bioheat model for homogenous tissue. The parameter-space search algorithm is a gradient-based quasi-Newton method. A parameter reduction effectively reduces the search space of the optimizer to the effective optical attenuation. The optimization for the inverse recovery was performed during the heating portion of the therapy. The remaining thermal parameters (*i.e.* conductivity, perfusion, specific heat, mass density) are assumed constant to demonstrate feasibility.

**Results:** To three significant figures, the descriptive statistics for  $\mu_a$  were 2300 m<sup>-1</sup> mean, 2320 m<sup>-1</sup> median, 510 m<sup>-1</sup> standard deviation, 1470 m<sup>-1</sup> minimum and 3130 m<sup>-1</sup> maximum. The standard deviation normalized by the mean was 22.2%. The inverse problem took 27 minutes to optimize all 19 datasets.

**Conclusion:** As expected, the recovered mean is biased by modeling approximations of the underlying physics model. However, the standard deviation adjusted for the bias in the mean is smaller than literature values and indicates an increased accuracy in the characterization of the optical parameters needed to plan MRgLITT procedures. This investigation was designed to run efficiently, but it demonstrates the potential for the optimization and validation of more sophisticated bioheat models that incorporate the uncertainty of the data into the predictions, e.g. stochastic finite element methods.

**Th.10****Real-Time Ultrasonic Thermometry Based on the Change in Backscattered Energy**

R. Martin Arthur, Charles D. Holmes

*Washington University in St. Louis, St. Louis, MO 63130, USA*

**Background:** Thermal therapies from cryosurgery to ablation would benefit from a non-invasive, safe, inexpensive and convenient 3D thermometer to monitor heating patterns. We have shown in predictions, simulations and measurements that ultrasonic change in backscattered energy (CBE) can be used to create temperature images (TI) with 1°C accuracy. CBE is the ratio of energy at a temperature of interest to that at a reference temperature on a pixel-by-pixel basis.

**Methods:** To align images taken at different temperatures, motion between images must be minimized. Motion tracking is the primary limit to real-time operation for CBE TI. Our existing routines for optimal non-rigid motion compensation were simplified for real-time operation. We compared the performance of our optimal routines to those tailored for real-time, to ensure correlation coefficients  $\geq 0.95$  between images after motion compensation. For real-time TI, our phased-array ultrasonic imaging system (Terason 3000) controlled a workstation via a local network, which performed up sampling and cross-correlation-based motion tracking of RF images. After motion compensation, it calculated CBE and displayed TIs. We investigated the use of graphical processing units (GPUs) to reduce computation times. Timing analysis was carried out on a custom-built workstation provided by Lickenbrock Technologies. It had an ASUS P5Q-EM motherboard with an Intel Core 2 Quad Q9300, 2.5 GHz processor and 8 GB of RAM. The video card was a GPU NVidia GTX260 with 896 Mbytes Video RAM.

**Results:** Up sampling was dependent on the image size, not sub-region size. For a 60x38mm image, it took about 6 seconds for the CPU and 0.7 seconds for the GPU. Thus, GPU up sampling was roughly 10 times faster than the CPU. For motion compensation with sub-region sizes of 5x5 and 10x10mm, GPU motion compensation was 66x & 99x faster than the CPU. At 20mm, however, the GPU margin was only 20x better.

**Conclusions:** Our tests using parallel processing on the graphical-processing unit (GPU) test-bed showed a reduction in motion compensation times by about two orders of magnitude. This improvement indicates that we can form 500k-pixel TIs in < 0.5sec. State-of-the-art GPU boards should reduce this time by a factor of 6. The result would be TI with CBE at 1°C accuracy and 25 mm<sup>2</sup> spatial resolution at a 5Hz frame rate.

**Support:** R21-CA90531, R01-CA107558 and the Wilkinson Trust at Washington University, St. Louis.

**Th.11****Towards on-line adaptive hyperthermia treatment planning: correlation between measured and simulated SAR changes caused by phase steering in patients**

Petra Kok<sup>1</sup>, Silvia Ciampa<sup>2</sup>, Rianne de Kroon-Oldenhof<sup>1</sup>, Eva Steggerda-Carvalho<sup>1</sup>, Gerard van Stam<sup>1</sup>, Paul Zum Vorde Sive Vording<sup>1</sup>, Lukas Stalpers<sup>1</sup>, Debby Geijssen<sup>1</sup>, Fernando Bardati<sup>2</sup>, Arjan Bel<sup>1</sup>, Hans Crezee<sup>1</sup>

<sup>1</sup>Department of Radiation Oncology, Academic Medical Center, University of Amsterdam, Amsterdam, The Netherlands, <sup>2</sup>Department of Civil Engineering and Computer Science, University of Rome Tor Vergata, Rome, Italy

**Introduction:** Hyperthermia is a proven radio and chemosensitizer, which significantly improves clinical outcome for several tumor sites. Clinical results can be further improved, since the goal tumor temperature is usually not achieved due to treatment limiting hot spots in normal tissue. Patient specific hyperthermia treatment planning (HTP) can help to avoid these hot spots, but is not yet clinically reliable due to uncertainties in tissue properties and perfusion. The purpose of this study was to investigate whether HTP can be used to predict changes in absorbed power (SAR) after adapting antenna settings during locoregional hyperthermia treatments.

**Methods:** This study included 78 treatment sessions from 15 patients with non-muscle invasive bladder cancer. At the start of treatments temperature rise measurements were performed with three different antenna settings, from which the SAR was derived along the 14-point thermocouple probes. HTP was performed based on a CT scan in treatment position with the bladder catheter *in situ*. Electric field distributions were calculated using the finite difference time domain method. Simulated SAR distributions were calculated from the electric fields and the SAR along the thermocouple tracks was extracted. Correlations between measured and simulated (average) SAR were determined. Next, correlations between the changes in simulated and measured SAR averaged over the thermocouple probe were determined for all three combinations of antenna settings. For the prediction of hot spots, it is important that HTP can estimate the relative amplitude of SAR peaks. Therefore, the ratio between the measured and simulated quotient of maximum and average SAR was analysed.

**Results:** For ~40% of the sessions the correlation coefficient between measured and simulated SAR profiles was higher than 0.5, while ~60% showed a weak correlation ( $R < 0.5$ ). The overall correlation coefficient between measured and simulated average SAR was weak:  $R = 0.31$  ( $p < 0.001$ ). The measured and simulated changes in average SAR after adapting antenna settings correlated much better:  $R = 0.70$  ( $p < 0.001$ ). The ratio between the measured and simulated quotient of maximum and average SAR was  $1.03 \pm 0.26$  (mean  $\pm$  SD), indicating that HTP can also correctly predict the relative amplitude of SAR peaks.

**Conclusion:** HTP can correctly predict SAR changes after adapting antenna settings during locoregional hyperthermia treatments. This allows on-line adaptive treatment planning, assisting the operator in determining antenna settings to increase tumor temperatures.



**Th.12****Using iron oxide -nanoparticle/AMF mediated hyperthermia to stimulate antitumor immune response against metastatic disease**

Lei Chen<sup>1</sup>, Jose Conejo-Garcia<sup>2</sup>, P. Jack Hoopes<sup>1</sup>, Mary Jo Turk<sup>1</sup>, Seiko Toraya-Brown<sup>1</sup>, Steven Fiering<sup>1</sup>

<sup>1</sup>Geisel School of Medicine at Dartmouth, Lebanon, NH, USA, <sup>2</sup>Wistar Cancer Center, Philadelphia, PA, USA

Previous studies from our lab have demonstrated the ability of iron oxide nanoparticles when heated by an alternating magnetic field to stimulate an immune response that inhibits the growth of rechallenged tumors. In order to further investigate the immune mediators of this effect we have extended the studies into detailed analysis of 2 tumors on one mouse, with one tumor treated with hyperthermia. To further clinically model this system we have extended the studies into truly metastatic mouse tumor models. Our studies examine both efficacy and immune effector mechanisms.

**Th.13****Targeting Vascular Checkpoints in Tumor Immunity by Thermal Medicine: A Tale of Two Niches**

Sharon Evans<sup>1</sup>, Daniel Fisher<sup>1</sup>, Jason Muhitch<sup>1</sup>, Fumito Ito<sup>1,2</sup>

<sup>1</sup>Roswell Park Cancer Institute, Buffalo, NY, USA, <sup>2</sup>University of Michigan Health Systems, Ann Arbor, MI, USA

The CD8 T cell-mediated adaptive immune response has emerged as a critical component driving the efficacy of standard cancer therapies chemotherapy and radiotherapy as well as high- and low-temperature thermal modalities. The vasculature functions as a critical checkpoint during the initiation and effector phases of tumor immunity although the mechanisms governing the rate of T cell homing is poorly understood. Generation of an effector pool of tumor-restricted T lymphocytes initially depends on trafficking of naïve/central memory T cells across high endothelial venules (HEVs) in tumor-draining lymph nodes (TdLN). Effector activity requires blood-borne cytotoxic T cells to migrate across tumor vessels in order to access tumor targets. Here, we report that TdLN HEVs and tumor vessels represent significant obstacles to the generation of anti-tumor immunity. Intravital microscopy revealed that the rate of homeostatic CD8 T cell trafficking is reduced ~ 50% in TdLN HEVs and is insufficient in tumor vessels to support tumor cell lysis. Poor trafficking at both vascular sites could surprisingly be overcome by a preconditioning thermal therapy regimen that co-opts the IL-6–dependent pro-trafficking activities occurring during natural fever. In this regard, administration of moderate and high-temperature thermal therapy prior to adoptive T cell transfer strongly promotes CD8 T cell trafficking across TdLN HEVs and tumor vessels in murine melanoma and colorectal cancer models. Taken together, these findings suggest that IL-6–dependent mechanisms can be exploited to create a therapeutic window to boost T cell mediated antitumor immunity and immunotherapy. Supported by NIH CA79765 and AI082039.

**Th.14****Radiofrequency Ablation Amplifies the Efficacy of Adoptive T Cell Transfer Therapy in the Generation of Antitumor Immunity**

Mark Bucsek<sup>1</sup>, Fumito Ito<sup>2</sup>, Jason Muhitch<sup>1</sup>, Ashwin Ajith<sup>1</sup>, Sharon Evans<sup>1</sup>

<sup>1</sup>Roswell Park Cancer Institute, Buffalo, New York, USA, <sup>2</sup>University of Michigan Health System, Ann Arbor, Michigan, USA

Radiofrequency ablation (RFA) has evolved from a palliative therapy to a clinically effective strategy to treat unresectable primary and metastatic tumors. RFA treatment results in coagulative necrosis and catastrophic tumor cell death while sparing normal adjacent tissue. Like chemotherapy and radiation, control of disease following ablation relies on the ability of CD8 effector T cells to enter neoplastic tissues and kill residual tumor targets. Unfortunately, local recurrence occurs frequently following RFA, suggesting that stimulation of the endogenous anti-tumor immune response is not sufficient to prevent tumor relapse despite a robust inflammatory response. The current study addressed the hypothesis that the local inflammatory response induced by RFA provides a favorable environment for immunotherapeutic intervention to aid in the generation of durable anti-tumor immunity. These studies employed a novel combination of adoptive T cell transfer immunotherapy (ACT) after RFA to investigate immune-mediated tumor control in implantable murine models (B16.F10 melanoma or CT26 colorectal tumors). Tumors were treated with a subcurative RFA regimen (90°C, 1 min) followed by adoptive transfer of tumor-antigen specific CD8 effector T cells 6 hours later. Following combination therapy, two anatomically distinct sites required for the development of anti-tumor immunity were assessed: tumor draining lymph nodes (TDLNs) and the residual tumor microenvironment. A profound increase in naïve CD8 T cell trafficking was detected in TDLNs, overcoming the tumor-induced repression in homeostatic extravasation normally observed within gatekeeper blood vessels at this site. RFA also upregulated trafficking of tumor-specific CD8 effector cells across tumor vessels, which are typically poor sites of T cell recruitment. A concomitant reduction was detected in the frequency of Foxp3<sup>+</sup> CD4<sup>+</sup> CD25<sup>+</sup> regulatory T cells (TRegs) in both the tumor and TdLN following preconditioning RFA treatment. The overall increase in the CD8 T cell:TReg ratio was further associated with augmented antigen-restricted apoptosis of tumor cell targets. A significant increase in overall survival without local recurrence was observed > 80 days post-treatment with combination therapy whereas there were no survivors in mice treated with RFA or ACT alone. Further investigation with tumor rechallenge in surviving mice demonstrated that adoptive T cell transfer following RFA elicited a long-lived tumor-specific memory response. Taken together, these studies suggest that in addition to the role of RFA as a direct tumor reductive therapeutic modality, thermal ablation may have clinical potential as an adjuvant therapy to augment the efficacy of T cell-based cancer immunotherapies. Supported by grants from the NIH (CA79765 and AI082039).

**Th.15****Abscopal effect by modulated electro-hyperthermia**

Csaba Kovago<sup>1</sup>, Nora Meggyeshazi<sup>2</sup>, Gabor Andocs<sup>3</sup>, Oliver Szasz<sup>4</sup>

<sup>1</sup>Szent Istvan University, Pharmacology and Toxicology Department, Faculty of Veterinary Science, Budapest, Hungary, <sup>2</sup>Semmelweis University, 1st Department of Pathology and Experimental Cancer Research, Budapest, Hungary, <sup>3</sup>Tottori University, Department of Veterinary Clinical Medicine, Faculty of Veterinary Science, Tottori, Japan, <sup>4</sup>Szent Istvan University, Department of Biotechnics, Godollo, Hungary

**Background:** Modulated electro-hyperthermia (mEHT) is a non-invasive technique for targeted tumor treatment [1]. The signal has time-fractal modulation enhancing the membrane processes by ratchet process [2]. The fractal-noise induced process is working like enzymatic wheel by electric field. The strongly impedance coupled modulated radiofrequency selectively enriches in the extracellular matrix surrounding the malignant cells without harming the non-malignant neighborhood. It is a local treatment. Our objective presents results acting systemically on far distant metastases by treating only the primary lesion.

**Method:** C26 mouse colorectal adeno-carcinoma cell line allograft was applied to both femoral regions of BalbC mice. One of the lesions (right leg) were treated with a single shot mEHT treatment for 30 minutes, the other (left leg) was kept for individual control of every animal. Four groups were formed and sampling was made after 12, 24, 48 and 72h post-treatment. The groups formed for parallel study were: (1) Sham control; (2) injected with 7.5 ml/kg Marsdenia tenacissima [3], intraperitoneal; (3) mEHT treated; (4), combined mEHT and Marsdenia tenacissima injection 30 min before mEHT. Various histomorphologic and immunohistochemical analysis, TUNEL assay were tested in treated and control tissue samples. Results were analyzed using digital microscopy.

**Results:** mEHT, as was shown before, induced a selective tumor death advancing from the tumor centre. The majority of cell-destruction was made by apoptosis, and observed locally on the treated side only. The Marsdenia tenacissima injection was not effective, having identical pictures with the sham treated animals. However, the combined therapy was effective far from the mEHT localization, in both the mEHT treated and untreated lesions in all the time-points. Cytochrome C release was shown in treated and untreated sides after 12 h, while this was observed only the treated side when mEHT was applied alone. Cleaved Caspase3 was shown in both sides in the combined treatment, at 24 h, as well as both were TUNEL positive. The same far-distance effect was seen on HMGB1 which was released into the extracellular matrix in the untreated tumor at combined therapy. These observations are characteristic on apoptosis.

**Conclusion:** mEHT in combination with systemic Marsdenia tenacissima injection can induce abscopal effect in untreated tumor in far distance from the treatment site in the C26 allograft double tumor model.

[1] Szasz A et.al. Oncothermia –Principles and Practices, Springer, (2010)

[2] Westrehoff HV, et.al, Proc. Natl. Acad. Sci. USA, 83:4734-4738 (1986)

[3] Huang Z, et.al, Oncology Letters, 5:917-922, (2013)

**Th.16****Assessment of hemoglobin saturation in and around microwave thermal ablations by optical spectroscopy**

Mariajose Bedoya, David Campos, Christopher Brace

*University of Wisconsin-Madison, Madison, WI, USA*

**Clinical Relevance:** All thermal ablations are characterized by a peripheral zone of sublethal hyperthermic temperatures that can be a common site for local tumor progression. This zone also demonstrates imaging and histologic evidence of inflammation and increased blood perfusion. The increase in oxygenated blood may provide a target for synergistic radiation therapy.

**Purpose:** To determine whether the increase in temperature and imaging evidence of inflammation noted on post-ablation contrast-enhanced imaging correlates to increases in blood oxygenation adjacent to the ablation zone.

**Materials and Methods:** A total of six thermal ablations were performed using a clinical microwave ablation system in swine livers in vivo. Temperature and hemoglobin saturation information were taken during ablation at three different locations (n=2 at each site): inside the ablation, in the ablation periphery and in normal liver. Hemoglobin saturation was monitored using a two-fiber optical spectroscopy technique. Temperatures were monitored 1, 1.5 and 2.5 cm from the microwave antenna by fiberoptic probes. CT data were collected serially during the ablation procedure and biphasic contrast-enhanced CT data were obtained after the ablations. Mean CT numbers from regions of interest (ROIs) corresponding to the three specified locations were measured. Hemoglobin saturation, temperature and attenuation values were compared between the different regions using the serial CT data and values obtained overtime during the ablation.

**Results:** In the normal liver zone, mean temperature was  $40.1 \pm 0.6^\circ\text{C}$ , mean normalized hemoglobin saturation was a constant 47%, and CT number was  $53.7 \pm 61.1$  HU. Inside the ablation zone mean temperatures was  $57.5 \pm 0.6^\circ\text{C}$ , mean hemoglobin saturation was 0% and attenuation values decreased to  $42.5 \pm 61.5$  HU. At the periphery of the ablation, mean temperature was  $45.2 \pm 4.6^\circ\text{C}$ , hemoglobin saturation dropped during from approximately 14% to 0% during the first 60 sec of the ablation, and CT number was  $58.2 \pm 68.3$  HU. While CT number was relatively unchanged from baseline in the ablation periphery, this zone showed marked enhancement consistent with the well-known transient hepatic attenuation difference (THAD) in biphasic imaging.

**Conclusion:** Despite elevated temperatures and imaging evidence of increased arterial blood supply in the peripheral ablation zone, no increased in oxygenation was noted on optical spectroscopy in this zone. However, optical data appeared noisy and irregular during several trials. Additional technique refinement is necessary to accurately measure haemoglobin saturation.

**Th.17****Membrane-Targeting Approaches for Enhanced Cancer Cell Destruction with Irreversible Electroporation**

Chunlan Jiang, Zhenpeng Qin, John Bischof

*University of Minnesota, Minneapolis, MN, USA*

Irreversible electroporation (IRE) is a promising technology to treat local malignant cancer using short, high voltage electric pulses. It offers many advantages over surgery and thermal ablations including that IRE 1) is fast and minimally invasive, 2) destroys the tumor while preserving adjacent connective tissues, and 3) can be delivered to tumors adjacent to major blood vessels without the concern of heat sink effect. Unfortunately, in vivo studies show that IRE suffers from an inability to destroy large volumes of cancer tissue without introduction of cytotoxic agents and/or increasing the applied electrical dose to dangerous levels.

This research will address this limitation by leveraging membrane-targeting mechanisms that increase lethal membrane permeabilization. Methods that directly modify membrane properties or change the pulse delivery timing are proposed that do not rely on cytotoxic agents. Specifically, mechanisms that directly modify membrane properties (i.e., line tension and surface tension) should reduce the voltage threshold for lethal permeabilization and therefore increase the efficacy of cell killing and therefore the volume treated after a given IRE dose. Two methods to achieve these changes are proposed in this study: 1) addition of surfactant (dimethyl sulfoxide, or DMSO) to directly interact with membrane lipids thereby changing membrane line tension and surface tension, and 2) use of pulse timing (i.e., introduction and persistence of defects in the membrane between pulses). Experimental studies were conducted on a human prostate cancer model (LNCaP Pro 5) under both in vitro (cell suspension) and in vivo (dorsal skin fold chamber) conditions, both with multiple viability assessment methods to evaluate and compare the injury levels with or without IRE enhancement.

This work shows that significant enhancement (67–75% more cell destruction in vitro and >100% treatment volume increase in vivo) can be achieved using membrane-targeting approaches for IRE cancer destruction. The methods introduced (DMSO and pulse timing) are low cost, non-toxic, and easy to be incorporated into existing clinical use. Moreover, when needed, these methods can also be combined with electrochemotherapy to further enhance IRE treatment efficacy.

**Th.18****Precision Noninvasive Thermal Lesion Formation Using Dual-mode Ultrasound**

Emad Ebbini, Dalong Liu

*University of Minnesota, Minneapolis, MN, USA*

We have recently introduced and validated the concept of dual-mode ultrasound array (DMUA) system for noninvasive image-guided surgery using HIFU. The advantages of DMUA in imaging the dynamics of lesion formation have been demonstrated in vivo. For example, cavitation due to tissue boiling is reliably detected by DMUA transducers with high spatial and temporal resolutions (on the order of 1 mm and 1 msec). Using this kind of feedback, the DMUA system can be used in forming lesions with precise dimensions and uniform damage patterns, i.e. no tissue desecration due to overexposure. This could be clinically significant in controlling the thermal exposure in a manner that does not produce unintended effects. Furthermore, the DMUA feedback has been shown to provide a means to adjust the exposure levels (or dose) for thermal damage at each target location. This is highly significant since the delivered dose depends on the local absorption of the HIFU beam. We have validated this feedback approach to precision lesion formation experimentally in a variety of tissue samples in addition to in vivo. In this talk, we will describe the imaging and therapeutic capabilities of a prototype DMUA system designed for the application of HIFU treatments in peripheral vascular disease. Experimental results will be shown to demonstrate the precise lesioning capabilities of the system in a number of tissue types, e.g. muscle, cardiac, and liver tissues. Examples of closed-loop vs open-loop controlled lesion formation will also be given and discussed. The results clearly demonstrate the advantages of closed-loop control in formation precision lesions even in the presence of distorting conditions such as tissue heterogeneity and local cooling due to blood flow.

**Th.19****Image Guided Thermal Therapy: Cryoablation**

John Baust<sup>1</sup>, Thomas Polascik<sup>2</sup>

<sup>1</sup>*State University of New York, Binghamton, NY, USA*, <sup>2</sup>*Duke University Medical Center, Durgam, NC, USA*

Image-guided placement of cryoprobes allows for real-time monitoring of an ablative dose when applied to solid tumors. The freezing process is viewed with the aid of intra-operative ultrasound as an advancing hyperechoic rim with a proximal shadow. The 1-2 mm “rim” represents a boundary between non-ablated but chilled tissue and damaged (frozen) tissue with the inner rim having temperatures of approximately -15 °C. In addition post-thaw histology confirms that the lesion size observed operatively (the freeze zone or “ice ball”) does not expand in the days to weeks following.

While diverse tumor sites are subject to cryoablation, urologic tumors of the kidney and prostate provide the greater clinical experience. Recently the use of CT, MRI and MRI – ultrasound methods of real-time visualization show growth. This presentation will review diverse approaches to image-guided cryoablation especially for the treatment of prostate cancer.



**Th.20****How to improve chemotherapy**

Timo L.M. ten Hagen

*Erasmus MC, Rotterdam, The Netherlands*

Failure of chemotherapy can be explained by a multitude of factors which alone or in combination are responsible for the lack of a beneficial effect. While new agents are being investigated and time and money is invested in finding new targets also possibilities exist to make already available compounds (more) effective or effective at all. It is important to better understand what we can do to reach this goal; to improve the efficacy of compounds we can take of the shelf but have been dismissed. Here examples will be given that focus on combining treatment approaches, which by themselves may have none or little effect, but when combined result in tumor response and in improvement of the condition or outlook of the patient. Using combination therapy as a starting point, and focusing on combining hyperthermia and nanocarrier-based drug delivery, opens possibilities to revive or improve certain drugs.

**Th.21****Computer Modeling of Temperature-Sensitive Liposomes on Micro- and Macroscopic scales**Dieter Haemmerich*MUSC, Charleston, USA*

Temperature-sensitive liposomes (TSL) release their contents in response to localized hyperthermia above ~40 °C, and have received increasing attention in the recent past, with first formulations now in clinical trials. This presentation describes the TSL drug transport kinetics based on computational models, identifying relevant properties of drug and TSL that affect delivery, to provide guidelines for development of more effective drug delivery systems. For validation of computational models, results from intravital fluorescence microscopy studies in small animal tumor models are presented in comparison. While several devices are available to locally heat tissue and enable localized TSL drug delivery, one particularly elegant method is via high-intensity focused ultrasound (HIFU). HIFU focuses ultrasound with mm accuracy into deep tissue regions to locally heat tissue non-invasively, while MR thermometry allows monitoring of tissue temperature during HIFU. Computational models and corroborating animal studies of the HIFU+TSL approach are presented showing the ability to facilitate and predict locally targeted drug delivery. TSL thus have the potential to become a clinically relevant drug delivery system for loco-regional cancer treatment.

**Th.22****Low dose re-irradiation & thermography controlled wIRA hyperthermia in extended recurrent breast cancer**

Markus Notter<sup>1</sup>, Helmut Piazena<sup>2</sup>, Werner Müller<sup>3</sup>, Peter Vaupel<sup>4</sup>

<sup>1</sup>HNE La Chaux-de-Fonds, La Chaux-de-Fonds, Switzerland, <sup>2</sup>Charité Medical University, Berlin, Germany, <sup>3</sup>Wetzlar, Wetzlar, Germany, <sup>4</sup>Dep. Radiooncology and Radiotherapy University Medical Center, Mainz, Germany

**Purpose:**

Evaluation of efficacy and side effects of combined re-irradiation and infrared superficial hyperthermia monitored by thermography in previously irradiated recurrent breast cancer. Specifically lymphangiosis carcinomatosa may be very extended and requires large treatment fields.

**Methods:**

Records from 69 heavily pre-irradiated patients with locally advanced recurrent breast cancer treated from 9/2009 – 12/2013 are analyzed. Prior treatments included surgery (100%), radiation (100%), chemotherapy (82%) and hormonal therapy (85%) All patients were re-irradiated to 16 – 24 Gy (median 20 Gy) 1/week always in combination with superficial infra red hyperthermia. Temperature distribution in the treated region was monitored continuously by an infrared thermography camera mounted to the wIRA radiator and remotely controlled by a computer. Visual inspection of the temperature color-coded images was additionally used for guidance in the correct centering of the heated region and to avoid hot spots. Patients and tumor characteristics predictive for actuarial local control and toxicity were studied.

**Results:**

The median follow up was 12 months. 64% CR, 30% PR, 4% NC and 2% PD of 107 treated volumes was achieved. Temperature analysis: maximum skin temperature over lymphangiosis: 42.5 – 43.2°C, minimum 40.2 – 41.9°C. Time intervall between first treatment and first local recurrence, initial stage and number of previous re-treatments of recurrences were most predictive for local control. Only grade 1 and 2 toxicities were noted so far.

**Conclusions:**

Use of thermography-controlled wIRA-hyperthermia combined with low dose re-irradiation provides good local control of heavily pretreated chest wall recurrences. The remissions achieved so far are very promising and correspond to results found in the literature. Real-time, online monitoring and control of local superficial hyperthermia all over the whole treatment field results in very low toxicity.

**Th.23****Regional deep hyperthermia treatment (RHT) for children and adolescents with refractory or recurrent rhabdomyosarcoma (RMS) and RMS-like tumors**Ruediger Wessalowski

*Clinic of Pediatric Oncology, Hematology and Immunology, Center for Child and Adolescent Health, Medical Faculty, Heinrich-Heine-University Duesseldorf, Duesseldorf, Germany*

**Purpose**

For the treatment of rhabdomyosarcomas (RMS) and RMS-like tumors, a multimodal approach is used that consists of systemic and local therapy. The preferred local therapy approach, if possible, is a complete resection without mutilation or loss of function and irradiation in selected cases. However, survival of children and adolescents with refractory or recurrent RMS and RMS-like tumors remains poor. We investigated the efficacy of a platinum-based (platinum/etoposide/ifosfamide, PEI) combination chemotherapy and regional deep hyperthermia in children and adolescents with RMS and RMS-like tumors that had failed to respond to or relapsed after first-line treatment.

**Patients and Methods**

35 patients aged 7-19 years (median, 5;6 years) with refractory or recurrent RMS or RMS-like tumors (24 poor response/non-resectable, 9 first-relapse, 2 multiple relapses) were treated prospectively with PEI (cisplatin 40 mg/m<sup>2</sup> on d1 and d4, etoposide 100 mg/m<sup>2</sup> on d1-4, and ifosfamide 1800 mg/m<sup>2</sup> on d1-4) and simultaneous, 1-hour, regional deep hyperthermia (RHT; 41-43 °C on d1 and d4). Patients received 3-4 treatment courses at 21-day intervals until residual tumor resection was possible; they subsequently received 2-4 additional courses of PEI-RHT. Local radiotherapy was administered for incompletely resected tumors. Chemotherapy and hyperthermia toxicities were assessed with World Health Organization grading.

**Results**

Histology identified embryonal RMS (n=21), alveolar RMS (n=8), undifferentiated sarcoma (n=3), extraosseous Ewing's sarcoma (n=2), synovial sarcoma (n=1). Most patients (74%) responded to treatment; 42.9% achieved 5-year overall survival (Kaplan-Meier plots and log-rank tests). The median follow-up of surviving patients was 64 months (range, 23 -135 months).

**Conclusions**

A multimodal strategy that integrated PEI-RHT with tumor resection with or without radiation can successfully treat children and adolescents with refractory or recurrent RMS and RMS-like tumors. The long-term prognosis of these patients was significantly dependent on the time point of treatment intensification. This strategy merits further investigation in patients with insufficient tumor response to standard chemotherapy in first-line treatment.

**Funding**

Deutsche Krebshilfe eV, Bonn and Elterninitiative Kinderkrebsklinik Düsseldorf eV

**Th.24****Regional Hyperthermia and Radiation Therapy for Cervical Carcinoma**

Douglas Kelly, Michael Payne, Edwin Watts, James Flynn, David Simon, Tyler Gutschenritter, Matt Weaver

*Cancer Treatment Centers of America, Tulsa, OK, USA*

Regional hyperthermia has been found to be beneficial for cervical carcinoma. The Deep Dutch Hyperthermia study randomized patients to radiation therapy (RT) alone, or RT + hyperthermia (HT) for various locally advanced pelvic malignancies. The largest benefit of adding HT was found with cervix cancer. The 12-year local control improved from 37% to 56%, and overall survival improved from 20% to 37%. A Cochrane review of 6 European randomized trials supported the benefit of adding HT to RT for cervix cancer. In Europe, RT + HT has become a standard treatment for cervical cancer, whereas in the US it is RT + chemotherapy. HT has an advantage over chemo in that there is minimal added toxicity. There was an FDA humanitarian device exemption (HDE) granted in 2011 for the BSD-2000 device for use in cervical cancer patients who are ineligible for chemotherapy.

There has been limited research into the combination of RT + HT + chemo, including an attempt at a randomized study in the US which was closed due to poor accrual. Cervix cancer is a rare malignancy, with a less than 1% lifetime incidence. Regional HT use seems to be in limbo in the US, as the number of centers with regional hyperthermia may be too small to conduct a randomized study for cervix cancer, yet the lack of such studies makes full FDA approval difficult, and in turn prevents the user base from expanding. BSD has launched two post-approval registry studies to document the toxicity and efficacy of using hyperthermia with radiation for newly diagnosed cervix cancer as well as recurrent cases, with or without chemotherapy. If all centers with HT in the US participate in this study it could yield some valuable US data.

CTCA in Tulsa has used twice weekly hyperthermia with radiation to treat 5 patients with newly diagnosed and 10 with recurrent cervical cancers over the past three years. Ten received concurrent chemotherapy. Seven patients had prior radiation. Of the evaluable patients, the overall response (CR + PR) was 4/4 for the newly diagnosed and 6/9 for the recurrent cases. The authors have found hyperthermia to be a useful addition to the radiation management of cervical carcinoma.

**Th.25****How Can We Make Certain that Thermal Therapy (TT) Will Play a Role in the Future of Oncology?**

Joan Bull

*The University of Texas Medical School at Houston, Houston, TX, USA*

What must be accomplished in order to project thermal therapy (both local-regional and whole-body thermal therapy), as an important, vital modality to combine with radiation, chemotherapy, immune and targeted therapy? Personalized therapy is clearly the future of oncology. Personalized treatment integrates both diagnosis and therapy. How can we place thermal therapy into a personalized framework? An answer is to investigate the effect of thermal therapy on the driver mutations of cancer stem cells (CSCs), non-stem cancer cells, and cancer stroma with epithelial mesenchymal transition (EMT) by using genomics, to study DNA sequence, epigenetics, transcriptome and/or the metabolome of the tumor before and after thermal therapy. The definition of individual patients' tumor can be identified by genomics, using massively parallel sequencing methods, can be accomplished by examining tissue, blood, urine, CSF, and circulating tumor cells (CTCs). To date, genomic investigations have been only superficially explored in malignant hyperthermia, not in thermal therapy. Thermal therapy analyses await identification in both single and combination modalities. The relative roles of genomics, exomics, and liquid biopsies will be defined and discussed in CSCs, non-stem cancer cells, and cancer stroma. The current and the future status of targeted therapies will also be presented.

**Th.26**

**Development of the Center for Hyperthermia**

Jennifer Yu, Andrew Godley

*Cleveland Clinic, Cleveland, OH, USA*

Hyperthermia and radiation have been shown to improve local control compared to radiation alone in multiple cancers. Despite its benefits, few centers offer this type of treatment. We discuss our experience establishing a Center for Hyperthermia at the Cleveland Clinic.

**Th.27****Coming full circle: Thermal Oncology Program at the University of Maryland**

Zeljko Vujaskovic

*University of Maryland, Baltimore, USA*

The tradition of hyperthermia cancer treatment is deeply rooted in the history of the University of Maryland's Department of Radiation Oncology. The most prestigious award given by the Society for Thermal Medicine is named after J. Eugene Robinson, a pioneer in the field of hyperthermic oncology. Dr. Robinson spearheaded combined radiation and hyperthermia cancer treatment and research at the University of Maryland from his arrival in 1962 until his premature death in 1983. He organized the first hyperthermia meeting, the "International Symposium on Cancer Therapy by Hyperthermia and Radiation", in 1975. With such a rich tradition and clinical experience, the Department of Radiation Oncology at the University of Maryland decided to revive and expand their thermal therapy program. In March of 2013, the department purchased a new BSD 500 hyperthermia device. After completion of commissioning and training, the first patients started treatment in April of 2013. Up to now, 22 patients have received 191 treatments with external thermal therapy (ETT). Effort has now been expanded to initiate treatment with combined brachytherapy and interstitial thermal therapy (ITT). Implementation of ETT and ITT in a University hospital setting will be discussed, particularly as it relates to equipment technical requirements, personnel, reimbursement, patient selection, referrals and treatment protocols.



**Th.28****Atzelsberg Circle clinical trials working group: better together**


Gerard van Rhoon<sup>1</sup>, Oliver Ott<sup>2</sup>, Rolf Sauer<sup>2</sup>

<sup>1</sup>*Erasmus MC Cancer Institute, Rotterdam, The Netherlands,* <sup>2</sup>*University Erlangen-Nuremberg, Erlangen, Germany*

The “Atzelsberg Circle” is an interdisciplinary working group of clinicians and basic research scientists drawn from the German Cancer Society (“Deutsche Krebsgesellschaft e. V.”, DKG) and the German Radiotherapy Society (“Deutsche Gesellschaft für Radioonkologie e. V.”, DEGRO). Since it start in 2007 the group has grown steadily and now representatives of nearly all European Hyperthermia Centers are participating in the meetings. The primary objective of the Group is to promote research on the clinical application of hyperthermia in the form of prospective clinical trials. The success of any clinical trial is critically dependent on appropriate patient accrual. Therefore, the “Atzelsberg Circle” is intended to provide an excellent and stimulating platform for designing clinical protocols in close cooperation to allow participation of as many institutes as possible. A secondary objective of the Group is to guarantee high quality of applied hyperthermia treatment in study protocols. Again, multi-disciplinary cooperation is considered essential for defining appropriate quality control and assurance protocols.

An interesting aspect of the coordinated action of the “Atzelsberg Circle” on quality assurance and excellent documentation is, that its authority helps to obtain financial support for implementation of the study and conduct the required data registration, validation and statistical analyses. At present there are 5 active clinical trials within the “Atzelsberg Circle” and several are in preparation.

# Abstracts for Friday, May 9<sup>th</sup>

 FOCUSED  
ULTRASOUND  
FOUNDATION

Current and Future Applications of  
**Focused Ultrasound 2014**  
4th International Symposium

October 12-16, 2014 | Bethesda, Maryland, USA  
[fusfoundation.org/symposium](http://fusfoundation.org/symposium)

**REGISTER &  
SUBMIT  
ABSTRACTS  
NOW!**

The world's leading forum for  
clinical and scientific experts advancing  
image-guided focused ultrasound

**Fri.1**

**Mathematical Models of Intrinsic and Extrinsic Cell Death Processes**

John Pearce

*The University of Texas at Austin, Austin, TX, USA*

Single step irreversible Arrhenius chemical kinetics models have been used for several decades as an assessment tool in hyperthermia research in the form of Cumulative equivalent Minutes at 43 C, CEM<sub>43</sub> and in the classical form as predictive models for thermal denaturation and cell death. The Arrhenius model is very effective in predicting the denaturation of structural proteins and cell death at higher temperatures — above 55 to 60 C — but uniformly over-predict cell death in the hyperthermic temperature range.

This refresher course will review the fundamental principles underlying the classical Arrhenius chemical kinetic model, and inspect the reasons for its failure in the case of functional protein cascades, with apoptosis as the example process. The lessons of a more detailed biochemical model of the apoptosis decision-making process and of successful kinetic models in the more complex cell death case will be applied to illustrate the sort of features a numerical model must have to get the right answer. Time permitting, a first-order correction to the classical Arrhenius model which makes the predictions much more accurate in the cell survival curve case will be discussed.

**Fri.2****The application of the principles of exercise physiology in the oncology setting**

Lee Jones

*Memorial Sloan Kettering Cancer Center, NY, NY, USA*

Throughout the past 80 years, numerous seminal scientific reports have applied the principles of exercise physiology to the study healthy aging, athletic, and chronic disease populations. These reports have provided sound scientific knowledge of the underlying limitations to exercise tolerance which, in turn, have informed the design of effective exercise training and rehabilitation programs to improve clinical outcomes. In stark contrast, the application of the principles of exercise physiology has received comparably little attention in persons diagnosed with cancer. With the recent increased interest in the application of exercise therapy as a central component of cancer survivorship, it has become increasingly apparent that cancer patients have markedly reduced exercise tolerance, and such reductions may have profound implications for acute and late-occurring cancer-related toxicities and clinical outcome. In this presentation, I will provide an overview of the potential causes of exercise intolerance in cancer patients and the effects of exercise therapy to counteract intolerance in patients with cancer.

**Fri.3****Efficacy of Gemcitabine combined with Hyperthermia therapy in the treatment of unresectable pancreatic cancer : Phase II study**

Satoshi Kokura<sup>1,2</sup>, Takeshi Ishikawa<sup>2</sup>, Manabu Okajima<sup>2</sup>, Tatsuzo Matsuyama<sup>2</sup>, Naoyuki Sakamoto<sup>2</sup>, Yoshito Ito<sup>1</sup>

<sup>1</sup>Kyoto Gakuen University, Kameoka, Japan, <sup>2</sup>Kyoto Prefectural University of Medicine, Kyoto, Japan

**【Background】** Pancreatic cancer is an aggressive malignant tumor. Gemcitabine is the standard first line therapy for pancreatic cancer. Several gemcitabine based chemotherapy combinations were studied for the treatment of pancreatic cancer, but these combination therapies showed no major success over single agent gemcitabine in the treatment of pancreatic cancer. Hyperthermia has been shown to increase the cytotoxic effects of some anticancer agents by facilitating drug penetration into tissue, and Gemcitabine has recently been shown to be a potent hyperthermic sensitizer in preclinical studies. We conducted a phase II study to determine the availability of combination therapy with gemcitabine and hyperthermia in the treatment of unresectable pancreatic cancer.

**【Methods】** Patients who participated in the study had advanced pancreatic cancer and their performance status score were 0-2. The primary end point was one-year survival rate. And the secondary end points were safety and response rate. We set the expectation one-year survival rate to 30%. Gemcitabine(1000mg/m<sup>2</sup>) was given weekly for 3 weeks(day 1,8,15) in four-week cycles, and hyperthermia(40min/once) weekly. This schedule was repeated until disease progression.

**【Result】** From November 2008 to November 2009, 18 patients were enrolled in this study. Median patient age was 64 years old(range 47-78), male/female:10/8. All patients died until September 2011, and the one year survival rate is 33.3%, exceeded the expected rate. Disease control rates (CR+PR+SD) were 61.1% (PR/SD/PD=2/9/7). Median survival times were 6 months. Adverse events (Grade 3/4) were neutropenia(16.7%), anemia(16.7%), anorexia(5.6%), gastrointestinal bleeding(5.6%).

**【Conclusion】** Combination therapy with gemcitabine and hyperthermia is both a safe and effective treatment in patients with advanced unresectable pancreatic cancer. To clarify the effects of sequential combination of hyperthermia and Gemcitabine as compared with Gemcitabine monotherapy, further studies should be performed, particularly prospective randomized trials.

**Fri.4**

### **Local Tumor Ablation plus Immune Stimulation: Towards in situ Cancer Vaccines**

Gosse Adema

*RadboudUMC, RIMLS, Nijmegen, The Netherlands*

**Background:** Local tumor destruction by heating or freezing is used clinically to eliminate tumors difficult to excise by conventional techniques for anatomical reasons. Interest in technologies for minimally invasive and local therapies is increasing rapidly as it may represent a promising alternative strategy for certain types of surgery. Successful local tumor control is often not curative as a consequence of tumor micro-metastases being already present prior to treatment. This indicates the need for additive treatments inducing systemic responses. We are exploring the combination of tumor ablation plus immune stimulation to make use of tumor debris to induce systemic anti-tumor immunity.

**Methods:** Different tumor ablation technologies were tested alone or in combination with different immunotherapy treatments for their ability to create an effective in situ cancer vaccine. Extensive immune monitoring combined with immune cell biological studies were performed to unravel the fundamental mechanisms determining success or failure of tumor ablation immunotherapy in the treatment of cancer.

**Results and conclusion:** We have developed unique murine models for cryo-, radiofrequency and HIFU mediated tumor ablation and reported that tumor ablation by itself can efficiently deliver antigens for the *in vivo* induction of anti-tumor immunity. Yet, tumor ablation alone resulted in only weak immune responses and partial protection against a subsequent tumor-challenge. These results imply that approaches directed at immune stimulation in combination with tumor ablation may be beneficial. Indeed, combining ablation plus immune activation by either immune checkpoint blockade antibodies or Toll Like Receptor (TLR)-Ligands results in strong protection against a subsequent tumor re-challenge and the eradication of untreated metastases in mice. Efficacy was dependent on both tumor ablation and immune stimulation and correlated with the presence of anti-tumor immune cells. These data thus show that tumor debris left behind after *in vivo* tumor destruction can provide the immune system with an effective antigen source for the induction of anti-tumor immunity. Based on these results clinical trials in humans and dogs with cancer have been initiated. Data on the development of optimal tumor ablation plus immune stimulation strategies and the role of the professional antigen presenting Dendritic Cells in this process will be presented and discussed.

**Fri.5**

**Focused Ultrasound Therapy in Radiation Oncology: FUS Foundation Perspective**

Jessica Foley

*Focused Ultrasound Foundation, Charlottesville, VA, USA*

The potential of focused ultrasound has never been more apparent. Effective therapies to treat cancer, Parkinson's disease, epilepsy and brain tumors as an alternative or adjunct to surgery, radiation or chemotherapy are now on the horizon, no longer beyond it.

Furthermore, focused ultrasound research continues to expand into new and exciting therapeutic areas. One such area of research aims to develop focused ultrasound as a tool in radiation oncology - to be used either as a standalone therapy or in combination with radiation and/or drug therapies, to enhance the efficacy of these standard therapies or to reduce their side effects. Early work suggests that focused ultrasound can produce bioeffects beyond thermal ablation, including sensitization to chemotherapy and/or radiation, and immunomodulation.

Despite the significant progress and advancement to develop focused ultrasound therapies for a wide range of clinical applications, clinical adoption remains a hurdle. To this end, the Focused Ultrasound Foundation was established in 2006 to accelerate the development and widespread clinical adoption of focused ultrasound technology. Current and future investments by the Foundation aim to promote this burgeoning area of focused ultrasound therapy in oncology.

This presentation will highlight recent advancements of FUS therapy in oncology, discuss the adoption and development landscape for the field, and share the Foundation's strategy for advancing this field including funding, awareness building, workshops and other opportunities for collaboration.

**Fri.6**

**Magnetic Resonance Guided Focused Ultrasound: Bone Metastases and Beyond**

Mark Hurwitz

*Thomas Jefferson University, Philadelphia, PA, USA*

Magnetic Resonance Guided Focused Ultrasound Surgery (MRgFUS) is an innovative technology for thermal therapy with rapidly evolving applications across medicine. The development of MRgFUS as an anti-neoplastic therapy will be reviewed including presentation of results of a multi-national phase III trial for treatment of painful osseous metastases. Next steps in treatment of bone metastases including recommendations of an international panel of experts convened at the 2013 European Focused Ultrasound Surgery Symposium will be discussed. In addition, opportunities for expanded use of MRgFUS in multi-modality oncologic care beyond treatment of bone metastases will be presented.



**Fri.7**

**Focused Ultrasound Opportunities in Radiation Oncology**

Sunil Krishnan

*MD Anderson Cancer Center, Houston, TX, USA*

An evolving body of recent literature alludes to the potential to sensitize tumors to radiation therapy using metallic nanoparticles for generation of hyperthermia. In preclinical studies, the techniques that hold promise for eventual clinical deployment include those that employ focused ultrasound. This talk will discuss strategies to use nanoparticles to generate hyperthermia and nanoparticles to capitalize on hyperthermia generated by techniques such as focused ultrasound. There are persisting gaps in knowledge relating to the molecular mechanism of action of these radiosensitization approaches – some of these issues will be addressed. Since the literature relating to the diverse disciplines involved in these efforts spans across multiple specialties (clinical radiation oncology, radiation physics, radiation biology, nanotechnology, material science, biomedical engineering, pharmacology, chemistry, and tumor biology) and numerous specialty journals, there is no single compilation of extant research in this arena or forum for merging analogous concepts and paradigms. This symposium will provide such a venue – my presentation will start with familiarizing the audience with the potential applications of metallic nanoparticles in radiation therapy using specific illustrative examples and begin to explore ways to understand the underlying mechanisms of the effects observed.

**Fri.8**

**Therapeutic Ultrasound as an in situ tumor vaccine and other possibilities**

Chandon Guha

*Albert Einstein College of Medicine, Bronx, NY, USA*

Abstract not available at time of printing

**Fri.9**

**MR-guided pulsed high intensity focused ultrasound enhancement of chemo-therapeutic agents combined with radiotherapy for prostate cancer treatment**

Lili Chen

<sup>1</sup>Fox Chase Cancer Center, Philadelphia, USA, <sup>2</sup>Temple University, Philadelphia, USA

This talk presents the results of an animal study on the effectiveness of the increased uptake of docetaxel by pulsed focused ultrasound (pFUS) in combination with radiation (RT) in prostate tumor control *in vivo*. The integrated pFUS system with the MR scanner used for the study is described together with the pFUS parameters, which were optimized for the animal experiment. The enhancement of both [3H]-docetaxel and doxorubicin concentration in tumors treated with pFUS have been evaluated quantitatively with an orthotopic animal prostate tumor model. The study results show that both chemotherapeutic agents increase significantly in pFUS treated tumors. Tumor-bearing mice receiving triple combination therapy of docetaxel + pFUS + RT exhibit highest tumor growth delay compared to all other treatment groups. In addition, tumors treated with pFUS alone also demonstrate the non-thermal therapeutic effects of pFUS. The cell killing mechanisms of non-thermal pFUS, the clinical impact of pFUS + RT, the potential use of nanodroplet-encapsulated chemotherapeutic agents + pFUS and thermal ablation + RT for treatment of prostate cancer are discussed.

**Fri.10**

### **MRI Assessment of Effective Ablated Volume Following High Intensity Focused Ultrasound**

Brett Fite<sup>1</sup>, Andrew Wong<sup>1</sup>, Yu Liu<sup>1</sup>, Lisa Mahakian<sup>1</sup>, Sarah Johnson<sup>1</sup>, Olulanu Aina<sup>1</sup>, Neil Hubbard<sup>1</sup>, Robert Cardiff<sup>1</sup>, Erik Dumont<sup>2</sup>, Katherine Ferrara<sup>1</sup>

<sup>1</sup>University of California, Davis, CA 95616, USA, <sup>2</sup>Image Guided Therapy, Pessac, France

**Introduction:** High intensity focused ultrasound (HIFU) is capable of rapidly and noninvasively delivering a controlled thermal dose for ablative therapies. Under MR guidance, precise temperature measurements can be made in real time. The resulting thermal dose maps can gauge treatment efficacy and determine collateral tissue damage. We sought to examine tumor response to HIFU ablation and determine whether there was a correlation between histological findings and common MR imaging protocols in the assessment of the extent of thermal damage.

**Methods:** An MR compatible therapeutic ultrasound system (IMASONIC SAS, Voray sur l'Oignon, France) was used with a 7T MR scanner (Bruker BioSpin, Ettlingen, Germany). Female FVB mice (n=24), bearing bilateral NDL tumors, were insonated under MR guidance. One tumor per animal was insonated, with the contralateral tumor as a control. Between one and five spots (focal size 1x1x2 mm<sup>3</sup>) were insonated per tumor. Each spot received an approximate acoustic dose of 75J to ensure a minimum CEM43 of 240. MR thermometry measured the temperature change peri-ablation, and thermal dose maps were generated.

Animals were divided into 4 groups: 0, 8, 24 and 48hrs after ablation. Prior to insonation, T<sub>1</sub> weighted (T1w) images were collected in addition to T<sub>2</sub>, T<sub>2</sub><sup>\*</sup>, apparent diffusion coefficient (ADC) maps. Animals were imaged post insonation using the same protocols plus a gadolinium contrast-enhanced (CE) T1w scan. Animals in the 0hr group were sacrificed following these scans while animals in other groups were imaged again at their terminal time point prior to sacrifice. Following sacrifice, treated and contralateral tumors were removed. Of each tumor, half went for NADH-diaphorase and half for haematoxylin and eosin (H&E).

**Results and Discussion:** Tumor necrosis was similar on CE T1w MR and NADH-diaphorase histological images. However, the volume of tumor necrosis (as indicated by NADH-diaphorase staining) and reduced perfusion (indicated by CE T1w images) increased at later time points (non-perfused volume: 13.5 μL at 0 hr, 30.3 μL at 24 hr, 59 μL at 48 hr). Diffusion weighted images underestimated the volume of tumor necrosis, while the region of ablation was not easily discerned on T<sub>2</sub> and T<sub>2</sub><sup>\*</sup> images. An automated CEM43 threshold of 240 overestimated the volume of ablated tissue.

**Conclusions:** The volume and morphology of tumor necrosis were correlated between CE T1w MRI and NADH-diaphorase. The volume of apparent tumor necrosis and the perfusion defect increased dramatically within 24 hours.

**Acknowledgements:** This study was funded by NIHR01CA103828 and NIHR01CA134659.

**Fri.11****Breast Cancer Cell Response to Silver Nanoparticle and Photothermal Therapy**

Edreca Thompson<sup>1</sup>, Michelle Alimpich<sup>3</sup>, Christopher MacNeill<sup>1</sup>, Elizabeth Graham<sup>1</sup>, George Donati<sup>2</sup>, Bradley T. Jones<sup>2</sup>, Nicole Levi-Polyachenko<sup>1</sup>

<sup>1</sup>Wake Forest University Health Sciences, Winston-Salem, USA, <sup>2</sup>Wake Forest University, Winston-Salem, USA, <sup>3</sup>College of Charleston, Charleston, USA

Breast cancer is the most common type of cancer in women worldwide in which over 1.7 million are diagnosed annually. For our study, we developed silver nanoparticles that are tuned to the infrared to create irreversible damage to breast cancer cell lines. In this study, we tailored silver nanoparticles to have triangular and hexagonal shape with an average diameter of 98nm and a positive surface charge. At a concentration of 10ug/ml, in aqueous media, the synthesized silver nanoparticles could generate a 15°C temperature increase, when exposed to 180 J/cm<sup>2</sup> of 800nm light. Three different breast cell lines were evaluated for cytotoxic response to the silver nanoparticles in the absence of infrared light, MCF-7, MCF-10A, and MDA-MB-231. A differential response to silver nanoparticles corresponding to the invasive nature of the cell lines was observed. The response was correlated with the subcellular location of the silver nanoparticles, and the threshold of cellular toxicity was found to be at 50ug/ml. At 50ug/ml, a 40%, 30% and 20% decrease in cell viability was observed in the MCF-7, MDA-MB-231, and MCF-10A cell lines respectively. Interestingly, the benign breast cell line demonstrated resistance to silver toxicity. For photothermal ablation, the same three cell lines were incubated with silver nanoparticles and exposed to 180 J/cm<sup>2</sup> of 800nm light, resulting in a 95%, 75%, and 70% decrease in MCF-7, MDA-MB-231, and MCF-10A MCF cell lines. The subcellular localization of silver in the different breast cancer cell lines appears to be correlated with the differential cytotoxicity and resistance to photothermal therapy. These results demonstrate that the use of silver nanoparticles for photothermal ablation may have a secondary benefit as demonstrated by the differential cytotoxic response of breast cancer cell lines to silver.

**Fri.12**

**A novel theranostic approach to prostate cancer using gold nanoparticle directed photoacoustic imaging and photothermal therapy**

Jung Choi, Eduardo Moros

*H. Lee Moffitt Cancer Center and Research Institute, Tampa, FL, USA*

Background: Prostate cancer is the second most common cancer among men in the U.S. with an estimated 238,000 cases last year. Current methods for detecting prostate cancer (transrectal ultrasound needle biopsy, CT, MRI, nuclear bone scan) each have significant known limitations. This proposal outlines a novel theranostic approach to the detection and treatment of prostate cancer using gold nanoparticle probes (GNPs) targeted to the prostate cancer marker B7-H4. B7-H4 is an immunomodulatory protein overexpressed on prostate tumors that plays a role in suppressing normal host immune responses specific to tumor cells. The theranostic strategy seeks to 1) detect tumor targeted GNPs with real time photoacoustic imaging in a prostate tumor mouse model, and 2) ablate tumors with GNP-enhanced laser-induced photothermal therapy (LITT) in the tumor mouse model.

Methods: Photoacoustic prostate tumor imaging in a mouse model: Anti-B7-H4 monoclonal antibody-GNP conjugates (10x45nm) are intravenously injected into immunodeficient NSG mice bearing B7-H4-expressing PC-3Mluc human prostate cancer cells. Mice are then imaged with a photoacoustic microscopy system (Ti:Sapphire laser; 8-30 nanosecond pulse duration; 10 Hz repetition rate; 3.5 MHz ultrasound transducer). LITT of prostate tumors in a tumor mouse model: The Novilase® NH-ILT001 laser ablation device (Class 4 Diode laser: max power = 8W, wavelength = 805±15 nm) will be used to ablate subcutaneous B7-H4/PC-3Mluc tumors in NSG mice. Post ablation tumor growth is monitored using in vivo fluorescence (luciferase) tumor imaging and 3D sonographic volumetric tumor measurements.

Results: 1) In vivo photoacoustic signal is expected to be significantly higher in prostate tumors bearing B7-H4-specific GNPs compared to tumors exposed to control GNPs and tumors without GNP injection. 2) Prostate tumors injected with B7-H4-specific GNPs are also expected to show greater post-ablation responses (decreased fluorescence activity and tumor volumes) when compared to either control GNP-injected tumor mice or tumor mice lacking GNPs.

Conclusions: This novel theranostic approach to prostate cancer seeks to validate the concept of real time photoacoustic image detection of tumors in the prostate gland followed by LITT-mediated tumor ablation. This strategy may both improve the detection of clinically significant prostate tumors and decrease potential morbidities compared to current methods. This strategy also seeks to affect a clinically significant tumor immune response by combining the general immunostimulatory properties of photothermal ablation with targeted antagonism of B7-H4, a known immune suppressive prostate cancer tumor marker.

**Fri.13**

**CXCR4 Targeted Polymer Nanoparticles for Enhanced Photothermal Ablation of the Brain Metastasis of Breast Cancer *In Vitro***

Elizabeth Graham, Christopher MacNeill, Nicole Levi-Polyachenko

*Wake Forest University, Winston-Salem, NC, USA*

Brain metastasis occurs in approximately 30% of breast cancer cases and only has an estimated one year survival of 20%. Chemokine (C-X-C motif) receptor 4 (CXCR4) is a G-coupled protein receptor that is a key mediator in tumor metastasis, cancer stem cell maintenance, and therapeutic resistance. CXCR4 is overexpressed in a subset of all breast cancer subtypes and is correlated with decreased disease free survival and overall survival. As such, CXCR4 is an ideal target for cancer treatment. Recently, laser interstitial thermal therapy (LITT) has been used as a minimally invasive surgical method to treat deep seated metastatic brain tumors. We hypothesize that it can be improved by targeted nanoparticle (NP) mediated photothermal therapy to localize hyperthermia. Poly[cyclopentadithiophene-*alt*-benzoselenadiazole] (PCPDTBSe) is a donor-acceptor electrically conductive polymer that has been used to form NPs capable of generating heat when stimulated by near infrared (NIR) light. Absorption in the NIR is beneficial as body tissue is most transparent at these wavelengths, and therefore, NIR light without PCPDTBSe NPs present should cause minimal tissue damage. PCPDTBSe NPs can be functionalized through a phospholipid-polymer coating and targeted to cancer cells by conjugation of specific ligands to this coating. Therefore, exposure of targeted PCPDTBSe NPs to NIR light can allow for selective death of cancer cells.

Western blot was used to investigate expression of CXCR4 in murine breast cancer cell line (EO771 parental), brain metastasis selected breast cancer cell line (EO771 BR5), a non-cancerous brain cell line (C8-D30), and cell lines from organs of the reticuloendothelial system, lung (WI-38) and liver (HepG2). Hyperthermia dose-effect survival curves were found for EO771 parental, EO771 BR5 and C8-D30 cells to determine sensitivity to hyperthermia. PCPDTBSe NPs were synthesized by emulsion method and coated in phospholipid-polyethylene glycol-COOH (PL-PEG-COOH). CXCR4 antagonist, AcTZ14011, was covalently conjugated to PCPDTBSe-PL-PEG-COOH NPs through an 1-ethyl-3-(3-dimethylaminopropyl)carbodiimide (EDC) coupled reaction. Both CXCR4 targeted (PCPDTBSe-PL-PEG-AcTZ14011) and untargeted (PCPDTBSe-PL-PEG-COOH) NPs were characterized by ultraviolet-visible spectroscopy, dynamic light scattering, and transmission electron microscopy. The NPs have a polymer core of approximately 30 – 50 nm and a hydrodynamic diameter of about 100 nm. Additionally, the NPs have a narrow absorption peak around 800 nm and generate comparable heat to multi-walled carbon nanotubes when stimulated with 800 nm light. Cytotoxicity and clonogenic assays were performed for PCPDTBSe-PL-PEG-COOH, PCPDTBSe-PL-PEG-AcTZ14011, and AcTZ14011. Finally, ablation studies with both CXCR4 targeted and untargeted NPs were performed to determine photothermal ablation efficiency for future *in vivo* studies.

**Fri.14****Soft Template Synthesis of Donor-Acceptor Conjugated Polymer Nanoparticles: Structural Effects, Stability and Photothermal Studies**Christopher MacNeill, Elizabeth Graham, Nicole Levi-Polyachenko*Wake Forest University Health Sciences, Winston Salem, NC, USA*

Many groups have successfully utilized inorganic-based nanoparticles for nanoparticle-mediated photothermal therapy. Among these, the most widely used are gold- and carbon-based nanoparticles. However, very few groups have developed polymer-based nanoparticles and tested their capabilities as potential nanoparticle-mediated photothermal therapeutics. Some groups have begun to utilize electrically conducting polymer nanoparticles (ECPNs), such as polyaniline, polypyrrole and poly(3,4-ethylenedioxythiophene):poly(4-styrenesulfonate) (PEDOT:PSS), to photothermally treat cancer cells. This may be due to the potentially greater biocompatibility of a polymer nanoparticle compared to its inorganic counterpart. Donor-acceptor conjugated polymers that have a low band gap (1.7 eV - 1.1 eV) can absorb in the NIR window from 700-1100 nm, which could also make them useful cancer therapeutics.

Donor-acceptor conjugated polymer nanoparticles and nanorods, based upon Poly[4,4-bis(2-ethylhexyl)-cyclopenta[2,1-*b*;3,4-*b'*]dithiophene-2,6-diyl-*alt*-2,1,3-benzoselenadiazole-4,7-diyl] (PCPDTBSe), were synthesized using pluronic F127 as a template. The nanomaterials were compared to previously reported, bare PCPDTBSe nanoparticles, which were synthesized without the use of a template. Our goal was to improve on the aqueous stability and photothermal heating efficiency of the previously synthesized PCPDTBSe nanoparticles by decreasing their size and coating them with a biocompatible surfactant. The pluronic wrapped PCPDTBSe (PW-PCPDTBSe) nanoparticles (40-60 nm) showed excellent aqueous stability compared to the PW-PCPDTBSe nanorods ( $d = 40-80$  nm,  $l = 200-600$  nm) and PCPDTBSe nanoparticles (150 nm). Under stimulation from 800 nm NIR light (3W, 1 min), the PW-PCPDTBSe nanoparticles showed greater heat generation ( $\Delta T = 47^\circ\text{C}$ ) compared to bare PCPDTBSe nanoparticles and PW-PCPDTBSe nanorods ( $\Delta T = 35^\circ\text{C}$  for both). Cytotoxicity studies determined that both the PW-PCPDTBSe nanoparticles and PW-PCPDTBSe nanorods displayed no significant cytotoxicity towards either non-cancerous small intestinal cells (FHs 74 Int) or colorectal cancer cells (CT26). Photothermal ablation studies confirmed that both the PW-PCPDTBSe nanoparticles and the PW-PCPDTBSe nanorods can be used as localized photothermal agents to eradicate colorectal cancer cells due to their excellent ablation efficiency (>95% cell death at 15  $\mu\text{g}/\text{mL}$  concentration).



**Fri.15**

**Cyclopentadecanolide Nanoemulsion promotes Heat-Induced Drug and Nanoparticle penetration throughout Tissues and Sensitizes Tissues to Thermal Ablation and Irreversible Electroporation.**

Michael Borrelli, Wolf Heberlein, Jakob Szwedo, Jonah Wu

*University of Arkansas for Medical Sciences, Little Rock, AR, USA*

A stable nanoemulsion (35-60 nm diameter) of the synthetic musk cyclopentadecanolide (CPDL) interacts with cells and tissues to: increase penetration of drugs, macromolecules and nanoparticles (up to 250 nm) throughout solid tissues. Its ability to do is temperature dependent, with an effective temperature range of 20°C to more than 60°C. However, when the temperature exceeds 42°C persistent exposure to the elevated temperature lowers the threshold required to thermally ablate tissues. This was demonstrated in freshly slaughtered liver tissue and in livers from live rats. A 10 min exposure to 50°C in a rat liver treated with a 0.03% CPDL emulsion (w/V) produced a larger ablation lesion than a 10 min exposure to 85°C.

Success with thermal ablation sensitization led to testing the ability of the CPDL emulsion to sensitize cells and tissue to Irreversible Electroporation (IRE). Treatment with CPDL nanoemulsions of 0.01%-0.06% (w/V) sensitized cells and tissues to IRE-mediated tissue ablation, producing an effective, IRE treatment dose enhancement of 1,500 V/cm to 2,000V/cm.

Experiments with liposomes, microbubbles and other particles made from lipids, proteins, or a combination thereof, indicate that CPDL produces its effects on cells and tissues by destabilizing proteins, contrary to initial speculation that it functioned by destabilizing lipids and lipid bilayers. Injection of up to 1.8 mL of a 6% CPDL nanoemulsion into the portal veins of Sprague-Dawley rats produced no detectable toxicity in the liver, lungs, heart, brain, kidneys and other organs. This lack of CPDL toxicity is consistent with the FDA labelling CDPL as a nontoxic chemical and permitting its use in perfumes, soaps, drugs and even foods.

Experiments to date suggest that CPDL nanoemulsions might be useful in a clinical setting for improving thermal targeting of drug delivery and the ablation capacities of Radiofrequency Ablation and IRE. CPDL might also prove effective for promoting combination drug-ablation therapies, especially in hypovascular tissues, e.g. pancreatic cancer, where drug penetration is otherwise minimal and ineffective.

**Fri.16****Novel ultrasound imageable low temperature sensitive liposomes for use with ultrasound-guided high intensity focused ultrasound**

Danny Maples, Ryan Newhardt, Ashish Ranjan

*Center for Veterinary Health Sciences, Oklahoma State University, Stillwater, Oklahoma, USA*

**Purpose:** Objectives of this study were to: 1) develop echogenic E-LTSL, a low temperature sensitive liposome co-loaded with an US contrast agent (Perfluoropentane, PFP) and doxorubicin, 2) determine stability of contrast agent encapsulation and characterize doxorubicin release from E-LTSL and 3) investigate the ability of E-LTSL to report on real-time doxorubicin release in tissue mimicking physiological phantoms in combination with Ultrasound (US)-guided hyperthermia.

**Methods:** E-LTSL was loaded passively with PFP using an innovative 1-step sonoporation method and actively loaded with doxorubicin. Doxorubicin release and PFP imageability from E-LTSL in phantoms was quantified by fluorescence spectroscopy, ultrasound imaging and transmission electron microscopy (TEM) in combination with mild hyperthermia (40-42°C).

**Results:** TEM images confirmed that the PFP emulsion formation is contained within LTSL. Phantom study clearly showed that only E-LTSLs are echogenic. Temperature vs. size increase and drug release kinetics of E-LTSL demonstrated no difference with control. Doxorubicin release in physiological buffer was <5% in 1 hr at baseline (25°C) and body temperatures (37°C), vs. >99% release with hyperthermia (~41°C). Intensity of observed ultrasound image with respect to temperature in the range of 31-40°C correlated strongly to the formation of gas bubbles in E-LTSL, and stabilized to a fixed intensity at the transition temperature. After the transition temperature of E-LTSL reached, the US intensity increased again similar to Dox release. Synthesized E-LTSLs were stable in aqueous environment, with no visual evidence of particle aggregation after 48 hr storage at 4 °C.

**Conclusion:** An US imageable heat sensitive liposome formulation co-loaded with doxorubicin and an US contrast agent was developed. Stability, imageability, and US monitoring of contrast agent and Dox release suggest that US-guided drug delivery from E-LTSL may assist physicians in real-time tumor drug delivery mapping. More detailed in vivo US-guided HIFU studies to determine image guided drug delivery is currently in progress. This technology has potential for clinical translation.

**Acknowledgements:** This work is currently supported by a grant from the Oklahoma Center for the Advancement of Science & Technology, and CVHS seed support.

**Fri.17**

**Increasing ablation times boost local drug deposition during combination therapy with thermo-sensitive liposomal doxorubicin.**

Christian Rossmann, Dieter Haemmerich

*Medical University of South Carolina, Charleston, SC, USA*

Radiofrequency ablation (RFA) is a clinical, image-guided cancer treatment utilizing localized heat delivered via minimally-invasive electrode. Recent studies suggest improved efficacy of combining RFA with localized drug delivery by liposomal drug carriers releasing doxorubicin (DOX) upon supraphysiological temperatures. The purpose of this study was to develop mathematical models for identification of optimal heating strategies to maximize local drug accumulation.

We used three dimensional computer models to simulate RFA for 5 to 60 minutes with target tissue temperatures between 60 and 95<sup>0</sup>C and to predict the amount of DOX in plasma, interstitium and cells considering temperature-dependent liposomal release and tissue DOX uptake. Model results were evaluated via fluorescence image data of DOX concentrations in excised swine livers of equivalent in-vivo experiments (30 min TDOX administration, 5 and 12min ablation).

Total amount of DOX deposited within the tumor tissue increased approx. linearly with total ablation time and was minimal for the 5min and maximal for 60 minute treatment (25 vs. 177ug). Increased delay between drug administration and RFA significantly decreased amount of DOX delivered to the target site due to plasma clearance of liposomal drug carriers (59% DOX reduction for RFA 2h later administration). In both mathematical models and in vivo studies most DOX (80-95%) was delivered just outside the thermal lesion due to temperatures (40-45<sup>0</sup>C) triggering the release of DOX.

Combination of RFA and liposomal DOX may reduce local tumor recurrence as it facilitates increased tissue destruction due to amount of DOX delivered within the margin. The computer simulation model allowed accurate prediction of intratumoral and peripheral drug accumulation and offers promising opportunities to optimize this combination therapy.

**Fri.18**

**Hyperthermia improves drug delivery to solid tumors.**

Timo L.M. ten Hagen

*Erasmus MC, Rotterdam, The Netherlands*

Drug delivery to solid tumors is one of the most challenging aspects in cancer therapy. Whereas agents seem promising in the test tube, clinical trials often fail due to unfavorable pharmacokinetics, poor drug delivery, low local concentrations, and limited accumulation in the target cell. Therefore, improvement of the local delivery of a chemotherapeutic agent is of crucial importance; certainly as these drugs exhibit often steep dose-response kinetics.

Understanding drugs and their behavior enables improvements, which benefit efficacy. Nanocarriers such as liposomes introduce the possibility to alter pharmacokinetics of a compound to favor localization in tumors and evade healthy tissues. Circulation time can be extended while the drug is shield from the body.

Our focus on the drug however neglects other possibilities to improve drug delivery. For instance, the tumor vascular bed has been recognized as a target for therapy, as a direct target, with so-called anti-angiogenic agents, but also as a porte d'entrée for chemotherapeutics. Manipulation of the tumor-associated vasculature to restore its function and appearance, so-called normalization, has been postulated as a way to enhance drug delivery. However, vasoactive agents can be used to utilize and aggravate the aberrant nature of tumor vessels resulting in what we coined tumor vascular abnormalization. By increasing leakiness, restoring fluid pressure equilibrium and favoring fluid flow, we enable drugs to enter the tumor interstitial space and reach target cells. Hyperthermia has the potential to aid to these individual aspects and act as a non-invasive, mild and adjustable method to greatly improve chemotherapy.

Combining nanocarriers, which are tunable by hyperthermia, with specific tumor manipulation, executed by hyperthermia, could very well provide a method overcoming tumor resistance to therapy. Here aspects of this combined approach to improve chemotherapy will be discussed.

**Fri.19****Mechanisms of Cancer Cell Death Following Cryoablation**

John G. Baust<sup>1</sup>, Anthony Robilotto<sup>1,2</sup>, William Corwin<sup>1,2</sup>, Robert Van Buskirk<sup>1,2</sup>, Andrew Gage<sup>3</sup>,  
John M. Baust<sup>2</sup>

<sup>1</sup>SUNY Binghamton, Binghamton, NY, USA, <sup>2</sup>CPSI Biotech, Inc., Owego, NY, USA, <sup>3</sup>SUNY Buffalo, Buffalo, NY, USA

The use of low temperature to destroy unwanted tissue is commonly applied in the treatment of diverse cancers. While the destructive consequences of the lethal stresses attendant to freeze-thaw excursions are long recognized, detail knowledge of the mechanisms of action of the multiple modes of cell death is recent. Essential to this understanding and future optimization of cryoablative treatment is a familiarity with the bio-molecular responses of both cancer and stromal cells contained in and adjacent to the tumor and its microenvironment. Cancer cells have evolved defensive strategies (hallmarks) that assure tumor survival and growth when challenged by “gold standard” monotherapeutic strategies.

Thermal therapies represent unique treatment modalities that typically obviate the need for multiple treatments thereby denying cancer cells the opportunity to develop defensive mutations. Cryoablation induces multiple mechanisms of cell death including physical rupture of those cells experiencing intracellular freezing, apoptosis activation by temperature-dependent mitochondrial (intrinsic) and membrane (extrinsic) cell signaling pathways, primary and secondary necrosis and activation of an unfolded protein response within the endoplasmic reticulum. This review will discuss the post-thaw, delayed on-set cell death mechanisms and chronological sequence that support tumor microenvironment destruction and strategies for ablative optimization.

**Fri.20**

**Arrhenius Models for Cell Death Revisited: Adding a Delay Significantly Improves Predictive Accuracy**

John Pearce

*The University of Texas at Austin, Austin, TX, USA*

Arrhenius models for cell survival curves have been used for many decades and show excellent accuracy at higher temperatures (typically above about 55 C). However, for many cell survival assays that exhibit a significant “shoulder” region in the hyperthermic temperature range (approximately 40 to 50 C) Arrhenius models fail to provide an acceptably accurate prediction. Hyperthermic cell survival curves typically have a slowly developing shoulder region followed by a faster constant-rate region, which an Arrhenius model is not sophisticated enough to represent.

The reason for the failure in the shoulder region is seen to arise from the complex biochemical reactions that characterize intrinsic cell death processes.[1] The classical Arrhenius thermal damage model describes a single step irreversible reaction while intrinsic protein cascades, such as those describing apoptosis, typically involve multiple multi-step reversible reactions, including association and dissociation terms. The primary necessary feature missing from the Arrhenius formulation is some form of time delay. Without such a feature Arrhenius calculations initiate the decay in survival at  $t = 0$  and substantially over-predict loss of signal in the particular assay used for analysis.

Adding a temperature-dependent time delay to the classical Arrhenius method provides an acceptably accurate representation in the constant-rate region in many cases. The shoulder region is not very well represented (as it has been replaced by a delay in the onset of cell death), but this is often much less critical than over-predicting “success”, as it were, by initiating the process at time zero.

To date the time-delay method has been applied to published PC-3, AT-1 and HepG2 cell survival curves with excellent results. The temperature-dependent time delay that provides the improved match is linear in temperature, and most often reaches zero delay time at temperatures between about 55 and 65 C — in concert with typical experimental observations of good classical Arrhenius matches above this temperature range. The results suggest that at higher temperatures the intrinsic cell protein processes are overwhelmed by higher temperature more intense thermal damage processes with a mathematically simpler description.

[1] Pearce JA. Comparative analysis of mathematical models of cell death and thermal damage processes. *International Journal of Hyperthermia*. 2013;29(4):262 - 80.

**Fri.21****Heat shock and endoplasmic reticulum stress-do they enhance the activity of HSP90 inhibitors?**

Michael Graner<sup>1</sup>, Justin Hellwinkel<sup>1</sup>, Jasmina Redzic<sup>1</sup>, Alexandra Graner<sup>1</sup>, Helen Madsen<sup>1</sup>, Alex Lencioni<sup>1</sup>, Laura Epple<sup>1</sup>, Lynne Bemis<sup>2</sup>

<sup>1</sup>University of Colorado Anschutz Medical Campus, Neurosurgery, Aurora, Colorado, USA,

<sup>2</sup>University of Minnesota Duluth, Duluth, MN, USA

We have generated primary tumour cell lines from a canine metastatic lung carcinoma (1st reported in *IJH* 2013;29:390-8) that grow as adherent lines in serum-free medium. These cells, which have a mutated p53 gene, express high amounts of Heat Shock Protein 90 (HSP90, HSP90AA/AB) as well as its endoplasmic reticulum paralog Glucose Regulated Protein 94 (GRP94, HSP90B1, also called glycoprotein 96, or gp96). HSP90 protein amounts increased even further upon heat shock (42°, 2 hr). We wondered if HSP90 inhibitors would be effective against these cells, and if forms of cell stress would enhance or diminish the effects of the drugs. We applied heat shock (42°, 2 hr) or induced the Unfolded Protein Response (UPR, with 1 mM DTT, 4hr) as stressors; control cells were left under standard culture conditions. We then treated cells with the clinically-available HSP90 inhibitors 17-DMAG or 17-AAG (geldanamycin analogs, 5nM, 24 or 48hr) or PU-H71 (a purine scaffold HSP90 inhibitor, 5nM, 24 or 48hr). PU-H71 also targets GRP94, one of the major ER chaperones induced during the UPR. Using the 48hr time point as the endpoint for drug treatment, we found that PU-H71 was the most effective drug under all conditions, but was particularly efficacious during UPR stress. 17-AAG had the next greatest effects under “standard” and heat shock conditions; 17-DMAG had little effect. To determine the impact of the drugs and stresses on key signaling molecules, cells were stressed (or not) and were treated with drugs for 24hrs. Intracellular signaling molecule status (ie, phosphorylation status) was determined by antibody array. We found that under standard conditions, most of the signaling array determinations could be interpreted as beneficial with drug treatments (in terms of drug efficacy). However, under stress conditions, in general, there would appear to be reduced efficacy based on the phosphorylation status of particular intracellular signaling molecules. There were wide variations in terms of signaling molecule indications, with some pathways seemingly activated, and some repressed. Overall the response of cells undergoing the UPR but treated with PU-H71 were the most strongly affected, and generally to the (presumed) detriment of the tumor. These results suggest that under likely conditions of tumor stress for solid tumors (such as the UPR), or in a thermal therapy-based setting, PU-H71 may be a useful anti-cancer drug agent.

**Fri.22****Magnetic Nanoparticle Heating in Cancer Hyperthermia and Cryopreservation Applications**

Michael Etheridge<sup>1</sup>, Katie Hurley<sup>1</sup>, Jinjin Zhang<sup>1</sup>, Seongho Jeon<sup>1</sup>, Yi Xu<sup>1,2</sup>, Jeunghwan Choi<sup>1</sup>, Chris Hogan<sup>1</sup>, Christy Haynes<sup>1</sup>, Michael Garwood<sup>1</sup>, John Bischof<sup>1</sup>

<sup>1</sup>University of Minnesota, Minneapolis, MN, USA, <sup>2</sup>University of Shanghai for Science & Technology, Shanghai, China

Magnetic nanoparticles (mNPs) are being used for a wide variety of imaging and therapeutic applications in biomedicine. One of the most exciting areas of development relates to their ability to generate heat in response to an alternating magnetic field, with great potential for thermal medicine. Here we review our most recent work in two important areas - mNP heating for cancer hyperthermia and thawing in cryopreservation applications.

First, while mNP heating has been extensively characterized in dispersed solutions, very little work has looked at the effects of nanoparticle aggregation on their ability to generate heat. Biological aggregation due to ionic screening and protein adsorption is a known outcome of in vivo application, so understanding its effect on performance is critical for clinical translation of this technology. Here then we systematically characterized the effects of aggregation on heating by creating reproducible populations of iron oxide nanoparticle aggregates in varying concentrations of phosphate buffered saline and fetal bovine serum (ranging in hydrodynamic size from 50 to 700 nm), and comparing their heating in solutions, gels, and prostate cancer cells. We demonstrate up to a 50% reduction in heating versus the dispersed particles (reduced from 243 to 127 W/g Fe at 190 kHz and 20 kA/m), correlating closely with the degree of aggregation observed. More importantly, we demonstrate a concomitant drop in the longitudinal relaxation rate of the aggregate populations through sweep imaging with Fourier transform (SWIFT) magnetic resonance imaging (MRI), providing a potential clinical platform for predicting heating in mNP hyperthermia applications, regardless of their aggregation state.

Second, proof-of-principle experiments and modelling demonstrate the ability of mNPs to overcome current limitations to thawing bulk, cryopreserved biomaterials. While a number of groups have successfully cryopreserved a wide range of biological systems through vitrification, failure due to devitrification and cracking during thaw has limited further development in the field. Here we demonstrate the ability of iron oxide nanoparticles to produce heating rates on the order of 100s of degrees Celsius per minute, which is rapid enough to reduce devitrification in a 6M glycerol solution and prevent it in the case of the "VS55" cryoprotectant. In addition, the combined abilities of nanoparticles to load microscale tissue structures and radiofrequency waves to uniformly penetrate tissue provide a platform for uniformly heating bulk biomaterials, independent of size. This is discussed in the context of scaled heat transfer models, where we investigate the effects of uniformity in heating.



**Fri.23****Lonidamine Induces Intracellular Tumor Acidification and ATP Depletion in Human Melanoma, Breast, Prostate and Ovarian Cancer Xenografts**

Dennis Leeper<sup>1</sup>, Kavindra Nath<sup>2</sup>, David Nelson<sup>2</sup>, Rong Zhou<sup>2</sup>, Jerry Glickson<sup>2</sup>

<sup>1</sup>Thomas Jefferson University, Philadelphia, PA, USA, <sup>2</sup>University of Pennsylvania, Philadelphia, PA, USA

We demonstrate here using noninvasive NMR techniques that the effects of lonidamine (LND, 100 mg/kg in tris-glycine buffer [1], i.p.) are similar for a number of xenograft models of human cancer including DB-1 melanoma (previously reported) [2], HCC1806 breast cancer (ER, PR, HER2 triple negative), BT-474 breast cancer (triple receptor positive), LNCaP prostate cancer, and A2870 ovarian cancer. Each of these tumors exhibits a rapid decrease in intracellular pH to  $6.4 \pm 0.2$ , a small decrease in extracellular pH to  $6.8 \pm 0.1$ , a concomitant monotonic decrease in nucleoside triphosphate, increase in inorganic phosphate and increase in lactate over a 2–3 hr period. Since mitochondrial respiration is reduced so is the rate of oxygen consumption resulting in tumor oxygenation. These effects of LND are discussed in terms of its mechanism of action as an inhibitor of both monocarboxylic acid transporters and the putative mitochondrial pyruvate carrier. No effect of LND was noted in normal tissues including liver, brain or muscle. Because of the induced specific acute tumor acidification, ATP depletion and inhibition of oxygen consumption rate, LND has been shown to be a potent sensitizer of response to hyperthermia [3] and ionizing radiation as well as to N-mustards and anthracyclines. These results suggest that LND could play a critical role in the management of a number of prevalent forms of human cancer. (Supported in part by NIH grants R01-CA129544 and R01-CA172820.)

**References:**

1. Ben-Yoseph O, Lyons JC, Song CW, Ross BD. Mechanism of action of lonidamine in the 9L brain tumor model involves inhibition of lactate efflux and intracellular acidification. *J Neurooncol* 36:149-57, 1998.
2. Nath K, Nelson DS, Ho AM, *et al.* (31) P and (1) H MRS of DB-1 melanoma xenografts: lonidamine selectively decreases tumor intracellular pH and energy status and sensitizes tumors to melphalan. *NMR Biomed* 26:98-105, 2013.
3. Coss RA, Storck CW, Wells TC, *et al.* Thermal sensitisation by lonidamine of human melanoma cells grown at low extracellular pH. *Int J Hyperthermia* 30:75-78, 2014.

**Fri.24**

**Modulation of tumor physiology by exercise: implications for cancer progression and therapeutic response**

Lee Jones

*Memorial Sloan Kettering Cancer Center, NY, NY, USA*

Randomized trials provide promising evidence that supervised aerobic exercise training is an effective adjunct strategy to prevent and/or attenuate chemotherapy-associated toxicity in patients with early-stage cancer. On the basis of the current evidence base, several international agencies have published cancer-specific exercise guidelines for cancer patients both during and following the completion of primary therapy. While the importance of exercise to improve symptom control outcomes in patients receiving cytotoxic therapy is undisputed, a critical corollary to this line of investigation is whether exercise impacts tumor biology and/or interacts with the anticancer efficacy of cytotoxic therapies. In this presentation, I will overview the emerging data investigating the effects of exercise as treatment of cancer in human and mouse models as well as the potential of exercise as combination therapy to improve the therapeutic index of cytotoxic therapy.

**Fri.25****Standard housing conditions elicit cold stress in laboratory mice masking the severity of GVHD in mouse models**

Kathleen M. Kokolus, Nicholas D. Leigh, Jingxin Qiu, George L. Chen, Philip L. McCarthy, Xuefang Cao, Elizabeth A. Repasky

*Roswell Park Cancer Institute, Buffalo, NY, USA*

Allogeneic bone marrow transplants (BMT) are potentially curative treatments for patients with malignant and non-malignant hematologic disorders. A major complication that may arise from this treatment is graft vs. host disease (GVHD), a serious and often lethal side effect. Translational murine models are intended to mimic clinical practice as closely as possible; however, this is not true for BMT models. Specifically, clinical BMT yields lethal GVHD after transplant of un-manipulated bone marrow (BM). This differs from murine GVHD models that typically require addition of T cells derived from spleen or lymph node. Recent work from our lab has revealed that the mandated cool (sub-thermoneutral) temperature (which induces chronic cold stress) results in impaired CD8<sup>+</sup> T cell function and reduced expression of activation including Glut-1 and CD69 as compared to mice at thermoneutrality, an ambient temperature at which cold stress is significantly reduced. In addition to compromised CD8<sup>+</sup> T cell activity, immunosuppressive cells are bolstered. As GVHD depends upon the activation and function of donor T cells we hypothesized that cold stressed mice do not develop GVHD following un-manipulated BMT because the cold stressed host environment blocks the function of effector T cells. We compared GVHD in mice receiving MHC-mismatched un-manipulated BM while housed at standard (22°C) and thermoneutral (30°C) temperatures. In this BMT model, mice housed at 22°C show no signs of GVHD, however, we found weight loss and lethal GVHD in mice housed at 30°C. The same trend was observed with MHC-matched allogeneic BMT. The sympathetic nervous system is activated by cold stress in order to generate additional heat to support body temperature maintenance and is thus a potential pathway by which cold stress could be influencing T cell function. To test this we blocked sympathetic nervous system activation by administering propranolol, a commonly prescribed  $\beta$ -blocker. Following BMT, mice at 22°C treated with  $\beta$ -blocker displayed weight loss and lethal GVHD similar to untreated mice at 30°C. This suggests that T cell responses are dampened by cold stress through a beta-adrenergic pathway which is circumvented by thermoneutral housing. Thus, housing mice at 22°C may mask the full side effects of BMT and reduce the clinical accuracy of murine GVHD models. This study provides insight into translational discrepancies of clinical and murine BMT and demonstrates lethal GVHD in a mouse model generated by un-manipulated BM.

**Fri.26**

**Activation Energy As A System Specific Signature Of Thermal Protein Denaturation At Molecular And Cellular Scales**

Zhenpeng Qin<sup>1</sup>, Saravana Kumar Balasubramanian<sup>1</sup>, Willem F. Wolkers<sup>2</sup>, John A. Pearce<sup>3</sup>, John C. Bischof<sup>1</sup>

<sup>1</sup>University of Minnesota, Minneapolis, MN, USA, <sup>2</sup>Leibniz Universität Hannover, Hannover, Germany, <sup>3</sup>University of Texas at Austin, Austin, TX, USA

Thermal protein denaturation involves molecular unfolding and aggregation and this process is critical to many biomaterial processing applications. In particular, thermal destruction of cancer and other diseases is increasingly performed with laser alone and with nanoparticles. The time scale involved in protein denaturation can occur from minutes, seconds or even to milliseconds depending on the temperature of the system, and a wide range of temperature change can be achieved with nanoparticle laser heating. This leads to a renewed interest in the measurement and prediction of protein denaturation kinetics which will be explored here (50-80°C).

Although protein denaturation can be measured by dynamic heating protocols with calorimetric and/or spectroscopic techniques, the fitting of the measurement to theory can be challenging. The present work focuses specifically on improving the ability to extract parameters from system specific thermal denaturation signatures using the Arrhenius model. Specifically the activation energy,  $E_a$ , is taken as an independent fitting parameter and the frequency factor ( $A$ ) selection is then shown to follow dependently. This relates to a long-standing discussion on the compensation law behavior of the Arrhenius model (linear relationship between  $E_a$  and  $\ln\{A\}$ ). By reviewing data from a wide selection of protein and cellular systems we demonstrate that this compensation behavior also holds for thermal protein denaturation. Based on this we further propose a new correlated parameter fit that leverages this result thereby providing a unique activation energy for protein denaturation that allows comparison and distinction between different systems. We envision that the new correlated parameter method will greatly simplify the measurement and analysis of protein thermal denaturation using controlled heating rate methods thereby allowing further comparison between, and intuition about, protein denaturation within biomaterial systems for a variety of applications.

This work sets the stage for further investigation of protein denaturation kinetics measured at even higher temperatures and short times (millisecond to nanosecond) achievable with high-intensity focused ultrasound or gold nanoparticle laser heating, approaching the time scale that can be studied by molecular dynamic simulations.

**Fri.27****The effects of moderate hypothermia and hyperthermia on microRNA expression**Jeffrey Hasday<sup>1,2</sup>, Ratnakar Potla<sup>1</sup>, Sergei Atamas<sup>1,2</sup>, Mohan Tulapurkar<sup>1</sup>, Ishwar Singh<sup>1</sup><sup>1</sup>University of Maryland, Baltimore, MD, USA, <sup>2</sup>Baltimore VA Medical Center, Baltimore, MD, USA

Our laboratory and others have shown that modest changes in temperature within the physiological range alter expression levels of certain genes with important physiologic and clinical consequences. Most of these studies have focused on transcriptional regulation, but post-transcriptional regulation by small noncoding microRNAs (miRNA) are as important as transcriptional regulation for about 30% of genes. MicroRNA precursors are generated through the same transcriptional processes as messenger RNAs and are then sequentially processed by two RNase III family nucleases, Drosha and Dicer, yielding ~21-nt miRNA duplexes with protruding 2-nucleotide 3' ends, only one strand of which is retained in the silencing complex while the other is degraded. Interestingly the strand with the 5' terminus located at the thermodynamically less-stable end of the duplex is usually preserved as the mature miRNA. However little is known about the effects of physiologic shifts in temperature on miRNA biosynthesis.

Based on previous studies showing that transcription of some messenger RNAs may be temperature-dependent and the importance of thermodynamics to miRNA strand selection, we hypothesized that changes in temperature within physiological range may also alter expression of some miRNAs with impact on expression of some gene products and potential consequences in health and disease. We utilized two complementary methods to analyze miRNA expression profiles in human small airway epithelial cells (SAECs) and HEK293 cells incubated at 32°, 37°, and 39.5°C without or with TNF $\alpha$  and confirmed temperature-responsive miRNA expression by quantitative RT-PCR and the level of a predicted target was analyzed by immunoblotting.

Surprisingly, expression of only 2.2% (11 of 505) of the miRNAs expressed in SAECs were temperature-dependent. Five miRNAs (miR-27a-5p, miR-27b-5p, miR-92a-1-5p, miR-181a-3p, and miR-1260a) exhibited a similar temperature-response pattern with higher expression at 32°C and reduced expression at 39.5°C. TNF $\alpha$  did not modify the temperature effects. Interestingly, most of the temperature-responsive miRNAs detected were the strand that is usually degraded, suggesting the effect of temperature may be on processing as well as transcription. *In silico* analysis demonstrated that the temperature-dependent miRNAs converged on two signaling pathways, PKC $\alpha$  and the Wnt signaling pathway. As expected, we found that hypothermia reduced expression of PKC $\alpha$  protein through its 3'UTR and reduced Wnt signaling. As these signaling pathways are important in homeostasis, injury, and recovery, we expect that the altered expression of miRNA in response to hypothermia or hyperthermia will have important impact on health and disease.

**Fri.28**

**Bioenergetics: Warburg, Apoptosis and Cytochrome C**

John Pearce<sup>1</sup>, Michael Graner<sup>2</sup>

<sup>1</sup>The University of Texas at Austin, Austin, TX, USA, <sup>2</sup>The University of Colorado at Denver, Denver, CO, USA

One prominent hallmark of cancer is the ability to ignore all apoptosis-inducing signals. Also, according to Vander Heiden *et al.* [1] and many others, most cancer cell types utilize only glycolysis to produce ATP and do not engage in oxidative phosphorylation, even in the presence of excess oxygen — the Warburg Effect (although this relationship is complicated in so-called “cancer stem cells”). Apparently, the higher priority for pyruvate in these cells is as a source of carbonaceous building blocks for proteins rather than ATP production. This suggests that these cell types may not even have one or more of the basic elements in the mitochondrial electron transport chain. If the missing components happen to include cytochrome C, then the implications for the apoptotic cascade are significant. Cytochrome C plays an important role in the electron transport chain as a proton pump between complexes III and IV, immediately upstream of ATP synthase. It also constitutes the cleaving tips of APAF-1 arms in an apoptosome, presumably playing a similar role. If cytochrome C is not available, many of the important apoptosis initiator cascades — for example, the p53 pathway — become moot, as an apoptosome will not be able to function.

However, it appears that most cancer cells do indeed express cytochrome C, and in experiments performed in numerous breast cancer and brain tumour cell lines, microinjection of cytochrome C resulted in apoptotic cell death. Thus, the apoptotic machinery are in place, suggesting that cytochrome C release or its sequestration are factors. Cell stress, in particular endoplasmic reticulum (ER) stress, has been heavily implicated in responses to apoptotic stimuli, such as chemotherapeutics. On the other hand, some of our results in brain tumour cells indicate that ER stress prior to, or concurrent with, drug treatments leads to drug resistance. As this form of ER stress results in increased expression of chaperones — and also enhances glycolysis — it suggests that the stress may provide multiple mechanisms of avoiding apoptosis.

[1] Vander Heiden MG, Cantley LC, Thompson CB. “Understanding the Warburg Effect: The Metabolic Requirements of Cell Proliferation.” *Science*. 2009; 324(5930):1029-33.

**Fri.29**

**The William Dewey Award: Lessons learned and passed forward**

Mark Dewhirst

*Duke University, Durham, NC 27710, USA*

I was fortunate to have Dr. Dewey on my graduate committee. In many ways, he served as my mentor as much as my primary mentor, Edward Gillette. However, both shaped my career in significant ways. Over the years, I have mentored well over 70 graduate students, postdoctoral fellows medical students, residents and faculty. In 2011, I was named the first Associate Dean for Faculty Mentoring by the Duke University School of Medicine. Mentoring has been my passion throughout my career and I have been fortunate to be mentor to many students who were involved in studies involving hyperthermia. In this lecture, I will review some of their work, but the emphasis will be on the principles that I have attempted to pass forward to this next generation. I am honored to receive this award and hope to make this lecture something that will be remembered in the future, particularly by the young trainees who will be attending the meeting.

**Fri.30****Regional hyperthermia combined with chemotherapy - from the bench to bedside**Rolf D. Issels<sup>1,2</sup>

*<sup>1</sup>University Medical Center Grosshadern, Munich, Germany, <sup>2</sup>University of Munich Sarcoma Center, Munich, Germany*

The hallmarks of hyperthermia and its pleiotropic effects are in favour of its combined use with chemotherapy. Preclinical research reveals that for heat killing and synergistic effects the thermal dose is most critical. Thermal enhancement of drug cytotoxicity is accompanied by cellular death and necrosis without increasing its oncogenic potential. The induction of genetically defined stress responses can deliver danger signals to activate the host's immune system. The positive results of randomised trials have definitely established hyperthermia in combination with chemotherapy as a novel clinical modality for the treatment of cancer. Hyperthermia targets the action of chemotherapy within the heated tumour region without affecting systemic toxicity. In specific clinical settings regional hyperthermia (RHT) or hyperthermic perfusion has proved its value and deserve a greater focus and investigation in other malignancies. In Europe, more specialised centres should be created and maintained as network of excellence for hyperthermia in the field of oncology.



# **Abstracts for Saturday, May 10<sup>th</sup>**

# **PHILIPS**

**Sat.1****Monitoring and Control of Focused Ultrasound In Thermal Therapy**Emad Ebbini*University of Minnesota, Minneapolis, MN, USA*

The use of high intensity focused ultrasound (HIFU) in forming trackless lesions in soft tissue dates back to the 1950s. Initial speculations about the mechanisms for damage favoured cavitation at first, but later efforts shed light on thermal damage mechanisms with or without (collapse) cavitation. In the 1980s, the application of HIFU in hyperthermia emphasized the avoidance of collapse cavitation while maximizing the focusing gain to achieve localized treatment at depth. Lele's investigation of HIFU for both tissue coagulation and hyperthermia made extensive use of cavitation detection and thermocouple measurements to better describe the nature of tissue response.

Advances in imaging methods and monitoring devices during HIFU exposure have furthered our understanding of the mechanisms of tissue damage in recent years. Several approaches have been proposed during the last decades that utilized cavitation-only (non-thermal) or thermal damage, including cavitation-enhanced thermal damage.

Real-time thermography (both MR and ultrasound) is now a reality and can be synchronized with the application of HIFU to provide instantaneous feedback of tissue response, especially when ultrasound thermography is used). Other forms of linear and nonlinear real-time imaging have been developed for the detection, localization, and characterization of cavitation events. These forms of imaging feedback methods offer the promise of precision control of HIFU treatments in a variety of applications. In this paper, we describe modern methods for monitoring and control of HIFU exposure based on advanced imaging technology. Several examples of HIFU control methodologies that have been recently proposed (e.g. cavitation-enhanced thermal therapy) will be discussed in detail. In addition, high-performance computing architectures allowing for real-time control of HIFU exposure will also be discussed. The presentation will emphasize HIFU systems that are currently in clinical or pre-clinical use with an eye on future trends.

**Sat.2****Can thermotherapy improve radiosensitivity of cancer stem cells?**

Jennifer Yu

*Cleveland Clinic, Cleveland, OH, USA*

Cancer stem cells are a subpopulation of cells that are highly resistant to radiation and chemotherapy. These cells can survive after cytotoxic treatment to re-establish the tumor. Cancer stem cells are preferentially localized in hypoxic and perivascular areas and have the propensity to invade and disseminate. Therapies that can effectively target these cells are needed to improve cancer control. Hyperthermia is one of the most potent radiosensitizers and may restore radiation sensitivity of the cancer stem cell population. We will review evidence to support hyperthermia as an anti-cancer stem cell therapy.

**Sat.3****Clinical Development of Laser Interstitial Thermal Therapy (LITT) For Brain Tumors: Experience and Evidence**

Alireza Mohammadi<sup>1</sup>, Ammar Hawasli<sup>2</sup>, Analiz Rodriguez<sup>3</sup>, Jason Schroeder<sup>1</sup>, Adrian Laxton<sup>3</sup>, Symeon Missios<sup>1</sup>, Paul Elson<sup>1</sup>, Stephen Tatter<sup>3</sup>, Gene Barnett<sup>1</sup>, Eric Leuthardt<sup>2</sup>

<sup>1</sup>Cleveland clinic, Clevelan, Ohio, USA, <sup>2</sup>Washington University, St. Louis, USA, <sup>3</sup>Wake Forest University, Winston-Salem, USA

**Introduction:** The idea of laser interstitial thermal therapy (LITT) for tumor treatment was introduced in 1980s. However, the level of enthusiasm for using LITT in brain tumors had some fluctuations over past decades; mostly because of technical challenges and also the lack of evidence to show clinical benefits outweigh potential risks. In the past few years, advances in technology (e.g. new laser probe design, MR-thermometry sequence) as well as the need for a minimally invasive treatment modality for difficult-to-access brain tumors (typically considered high risk for regular surgery) resulted in resurgence of LITT in different intracranial pathologies. In this study, the impact of LITT on improvement of progression free survival (PFS) in high grade glioma patients is presented.

**Methods:** Thirty-five consecutive high grade glioma patients (24 GBM, 11 anaplastic gliomas) who underwent LITT at the Cleveland Clinic, Washington University in St. Louis, and Wake Forest University during 5/11-12/12 were retrospectively reviewed. LITT was performed using NeuroBlate System (Monteris, MN). Extent of thermal ablation was defined by software as thermal-damage-threshold (TDT) lines including: yellow TDT-line = 43°C for 2 minutes and blue TDT-line= 43°C for 10 minutes (shorter intervals were needed for higher temperatures based on Arrhenius equation). Pre- and post-operative MRI scans as well as TDT-lines were imported into the iPlan software (BrainLAB, Germany) and extent of coverage of tumor volume by TDT-lines was measured. Patient outcomes including PFS were evaluated and correlated with volumetric analysis results.

**Results:** Median age was 56 years and 40% were female. Treatment was upfront in 19 and salvage in 16 patients. Median tumor volume was 10.1cc (0.7-49cc). One patient died because of meningitis and 7 patients had neurological worsening after procedure (temporary in 5 patients). After 7.2 months follow-up, 80% of patients have progressed and 34% died. Median overall-survival was not reached (1-year overall survival is estimated to be 68%±9%). Median PFS was 5.1 months. Thirteen patients who had both ≥99% tumor coverage by yellow TDT-line and <1.5cc residual tumor volume uncovered by blue TDT-line had better PFS than others (9.7 versus 4.6 months; p=0.02) which was still prognostic in the subgroup of 24 GBM patients (p=0.04).

**Conclusions:** This initial report shows that LITT can be used safely and effectively for treatment of high grade gliomas. In addition, more complete coverage of tumor by TDT-lines improves PFS. This can be translated as the extent of resection concept in glioma surgery.

**Sat.4****Analysis of spatial accuracy and precision of a dedicated breast MR-HIFU system during ablation of breast tumors in patients**

Roel Deckers<sup>1</sup>, Gerald Schubert<sup>2</sup>, Laura G. Merckel<sup>1</sup>, Floor M. Knuttel<sup>1</sup>, Thijs van Dalen<sup>3</sup>, Nicky H.G.M. Peters<sup>1</sup>, J.M.H.H van Gorp<sup>4</sup>, Maurice A.A.J. van den Bosch<sup>1</sup>, Chrit T.W. Moonen<sup>1</sup>, Lambertus W. Bartels<sup>1</sup>

<sup>1</sup>Imaging Division, University Medical Center Utrecht, Utrecht, The Netherlands, <sup>2</sup>Philips Healthcare, Vantaa, Finland, <sup>3</sup>Department of Surgery, Diaconessenhuis, Utrecht, The Netherlands, <sup>4</sup>Department of Pathology, Diaconessenhuis, Utrecht, The Netherlands

**Introduction:** Several studies have addressed the feasibility of using MR-guided HIFU ablation techniques for minimally invasive treatment of breast cancer<sup>1,2</sup>. The presented results were promising and the feasibility of this approach was shown. Recently, a dedicated breast MR-HIFU system was developed, in which the breast is sonicated laterally, thereby reducing the risk of heating heart, lungs and ribs<sup>3</sup>. Here, we present the targeting accuracy and precision of the dedicated system as assessed in an on-going clinical phase I study in breast cancer patients.

**Methods:** All experiments were performed on a dedicated breast 1.5-T MR-HIFU system (Philips Healthcare, Vantaa, Finland). Three female patients with histopathologically proven invasive breast cancer were included. Segmented Echo Planar Imaging was performed for PRFS-based thermometry. Online correction of the respiration induced field disturbances was performed by a look-up table based method<sup>4</sup>. The tumor tissue was deliberately partially ablated, to be able to use the remaining tissue for histopathological tumor characterization and staging. At least 48 hours after MR-HIFU treatment the tumor was removed surgically. In total nine ablations (three per patient) were performed. For each sonication the trajectory of the centre of mass of the heating pattern in the focal area in time was calculated. The standard deviation of the distribution of the distance between the centre of mass in time and the mean centre of mass was defined as precision. The distance between the mean centre of mass and the planned treatment position was defined as accuracy. This was done for the sagittal as well as for the coronal slice. Furthermore, we obtained histologic data of the location of tissue necrosis within the tumor.

**Results:** The spatial accuracy was found to be about one pixel and was comparable in the sagittal and coronal slice:  $1.8 \pm 0.9$  mm (sag) and  $1.5 \pm 0.8$  mm (cor). The spatial precision was:  $0.3 \pm 0.1$  (sag) and  $0.3 \pm 0.2$  (cor). Interestingly when three sonications were performed at the same planned treatment position a slightly lower overall spatial precision was found, i.e.  $0.9 \pm 0.5$  (sag) and  $0.6 \pm 0.4$  (cor). Finally, the necrotic areas observed on the histology slides corresponded to the number and location of the sonications performed.

**Conclusion:** The dedicated breast MR-HIFU system allows for the ablation of breast cancer with a high spatial accuracy and precision.

**References:** <sup>1</sup>Huber, 2001, Cancer Res. <sup>2</sup>Gianfelice, 2003, Radiol. <sup>3</sup>Merckel, 2013, CVIR <sup>4</sup>Vigen, 2003, MRM

**Acknowledgement:** CTMM (VOLTA).

**Sat.5****Laser Interstitial Thermal Therapy in Brain Tumors: Predictive Value of Overlap between Hyper-Thermic Field and Corticospinal Tract as Manifested in Post-Op Motor Deficit**

Mandana Behbahani, Jeffrey Mullin, Gene Barnett, Alireza Mohammadi

*Cleveland Clinic, Cleveland, USA*

**Introduction:** Laser interstitial thermal therapy (LITT) has revealed promising results in treatment of difficult to access tumors. There is limited data regarding the predictive role of hyper-thermic field exposure to important white matter fiber tracts in post-op neurological deficit. To that end, we report the clinical relevance of thermal exposure to corticospinal tract (CST) in our LITT series.

**Method:** Thirty-six patients underwent LITT, using NeuroBlate System in Cleveland Clinic (4/2011 to 4/2013). Of those, 24 patients who had pre-op DTI were included (16 glioma, 3 metastasis, 4 radiation necrosis). One patient with post-operative ICH and motor deficit as a direct result was excluded.

Extent of hyper-thermic field is delineated by the software as thermal-damage-threshold (TDT) lines, which include white TDT-line (60 min at 43°C), blue TDT-line (10 min at 43°C), and yellow TDT-line (2 min at 43°C).

Fiber tracking was conducted for motor fibers of upper extremities (UEM), lower extremities (LEM), as well as pre-motor fibers (PM). Pre-operative MRI and TDT-lines were imported to iPlan software for volumetric analysis. The maximum surface area of overlap between fibers of the UEM, LEM, PM as well as the TDT-lines of white, blue, and yellow were analyzed in three planes of axial, coronal, and sagittal imaging.

Clinical review was conducted for post-op motor deficit with either complete or partial resolution. The degree of thermal exposure to the each of the CST correlated with manifestation of post-op motor deficit.

**Results:** Overlap of TDT-lines and CST in number of patients treated were as follows: white (UEM:6, LEM:7, PM:6), blue (UEM:9, LEM:10, PM:2), yellow (UEM:12, LEM:10, PM:10). Median overlap of yellow TDT-lines with UEM, LEM, PM, were 1.9 mm<sup>2</sup>, 1.5mm<sup>2</sup>, 2.6mm<sup>2</sup> respectively, blue TDT-lines with UEM, LEM, PM, were 0.4mm<sup>2</sup>, 1mm<sup>2</sup>, 1.8mm<sup>2</sup> respectively, and white TDT-lines with UEM, LEM, PM, were 0.1mm<sup>2</sup>, 0mm<sup>2</sup>, 0mm<sup>2</sup>, respectively. Deficits with complete resolution of motor movements of arms (3), and legs (3), as well as deficits with partial resolution of arms (2), and legs (1) were evaluated post-operatively. In three occasions with permanent motor deficit, overlap of white, blue, and yellow TDT-lines to corresponding motor-tract were  $\geq 2.2\text{mm}^2$ ,  $\geq 4.6\text{mm}^2$ , and  $\geq 5.9\text{mm}^2$  respectively.

**Conclusion:** Permanent deficit can be noted even in minimal overlap of TDT-lines and motor fibers. Therefore, in pursuing LITT therapy, the goal of treatment is a conformal coverage of tumor volume and minimal overlap of hyper-thermic field with important white matter fiber tracts, to minimize post-op neurological deficits.

**Sat.6**

**Alternative Therapies to Thermal Ablation: Complementary and Competitive Approaches**

Ron Gaba

*University of Illinois Hospital and Health Sciences System, Chicago, IL, United States Minor Outlying Islands*

Many times the clinical presentation of cancer will suggest or even mandate the need for alternative approaches to ablation. Common reasons include large tumor size, inaccessible tumor location, tumor multiplicity, or comorbidities. This presentation will briefly review several interventional transarterial catheter-based treatment approaches and a developing ablative therapy, irreversible electroporation. Among the catheter therapies, bland (no drug) microembolization, chemoembolization using conventional methods and drug-eluting beads, and yttrium-90 radioembolization will be reviewed.

**Sat.7**

**Combinational Oncological Therapies in Interventional Radiology**

Derek West

*University of Texas Health Sciences Center at Houston, Houston, Texas, USA*

Hepatocellular carcinoma is a devastating disease with relatively few treatment options. However, in recent years, transarterial chemoembolization has been introduced as a potential treatment option. At the same time, focal ablative therapy, such as radiofrequency, microwave, cryoablation, or electroporation, have also shown promise in treating HCC. Because of their individual advantages, newer treatment protocols combine both TACE and ablation in the treatment of HCC. This talk will discuss the most recent clinical results of combinational TACE and ablative therapies.



**Sat.8**

**Overview of Image-Based Monitoring of Thermal Therapies**

R. Jason Stafford

*The University of Texas MD Anderson Cancer Center, Houston, TX, USA*

Minimally invasive and non-invasive approaches to energy delivery for techniques such as thermal therapy benefit tremendously from image-guidance. Widening use of thermal therapy techniques for treatment delivery have spurred growth in use of imaging technology to monitor the progress of these treatments. Semi-quantitative as well as quantitative techniques utilizing computed tomography, ultrasound or magnetic resonance imaging for directly monitoring the location of energy deposition as well as changes in tissue state or temperature provides a valuable feedback loop for therapies that can be used for enhancing the safety or efficacy of the techniques. Here, we provide an overview and update of some of these techniques as they pertain to their potential for monitoring of thermal ablative therapy.

**Sat.9****MR-guided Cryoablation of Prostate Adenocarcinoma Recurrences: 6 month follow-up**

Lance Mynderse, David Woodrum

*Mayo Clinic, Rochester, MN, USA*

**Purpose:** To examine the short-term (6 month) follow-up results of MRI guided cryoablation in patients with prior radical prostatectomy (RP) and MRI visualized biopsy proven local recurrence of prostate adenocarcinoma.

**Materials:** Retrospective study of sixteen patients post-prostatectomy patients (mean 64, 51-73yo) with recurrent prostate carcinoma who underwent 18 treatments with MRI-guided cryoablation. All patients had identifiable lesions on multi-parametric MRI with endorectal coil followed by a positive biopsy. Of 16 patients, 5 had a history of additional salvage external beam radiation after surgery with subsequent recurrence. Under general anesthesia and MRI guidance (wide-bore 1.5T MRI), cryo needles were inserted via transperineal approach with cryoablation performed under active MRI monitoring. The cryoablation technique consisted of 0.5cm needle separation with 3 freeze-thaw cycles performed. Follow-up PSA was performed at 1 month, 3 month, and 6 months post-procedure. Follow-up MR imaging was performed at 6 months.

**Results:** For all of these patients, MR imaging was used for needle placement, ablation monitoring, and post-ablation imaging. Average pre-procedure PSA was  $1.22 \pm 1.76$  ng/mL and 6 month post-procedure PSA was  $0.08 \pm 0.11$  ng/mL ( $p < 0.05$ ). Two patients had marginal recurrences at the edge of the ablation zone and four patients had slowly rising PSA with negative pelvic MRI. One patient had an enlarging perirectal lymph node.

**Conclusions:** MRI guided salvage cryoablation for post-RP prostate cancer recurrences demonstrate good treatment stability over 6 month period and provides a viable treatment option for patients with prostate cancer recurrences.

**Sat.10**

**Magnetic nanoparticle hyperthermia cancer treatment: the road from material science to patients.**

Andrew Giustini<sup>1,2</sup>, Alicia Petryk<sup>1,2</sup>, Robert Stigliano<sup>1,2</sup>, Fridon Shubitidze<sup>2</sup>, Jinjin Zhang<sup>3</sup>, Michael Garwood<sup>3</sup>, Thomas Sroka<sup>1</sup>, Lesley Jarvis<sup>1</sup>, Eunice Chen<sup>1</sup>, Lionel Lewis<sup>1</sup>, Peter Kaufman<sup>1</sup>, P. Jack Hoopes<sup>1,2</sup>

<sup>1</sup>*Geisel School of Medicine at Dartmouth, Hanover, NH, USA*, <sup>2</sup>*Thayer School of Engineering at Dartmouth, Hanover, NH, USA*, <sup>3</sup>*Center for Magnetic Resonance Research at the University of Minnesota, Minneapolis, MN, USA*

In spite of preliminary clinical trials in Europe and promising preclinical studies, the successful use of magnetic nanoparticle (mNP) hyperthermia for cancer therapy will depend on many factors, including: 1) A safe and adaptable nanoparticle platform; 2) A non-toxic, targetable, nanoparticle-activating alternating magnetic field (AMF); 3) Non-invasive *in vivo* nanoparticle imaging; 4) Relevant and translatable pre-clinical studies; 5) Thermal dosimetry and *in vivo* validated computational models allowing for nanoparticle-AMF treatment planning; 6) Understanding interactions of mNP hyperthermia with conventional adjuvant therapies; 7) Well planned, early-phase clinical studies in humans.

In this presentation we will address these topics using data from our laboratories. These data will include biodistribution studies in mice, nanoparticle heating characterization *in vitro* and *in vivo*, efficacy studies in mouse tumor models and spontaneous canine oropharyngeal tumors, studies combining nanoparticle hyperthermia with ionizing radiation and chemotherapy and MRI-based nanoparticle imaging. We will also provide preliminary data on computational models predicting nanoparticle hyperthermia dosimetry. Finally, we will address planned clinical trials in humans at Dartmouth, including navigating the Institutional Review Board (IRB) and the Food and Drug Administration (FDA) and the services provided by the FDA/NIH's Nanoparticle Characterization Laboratory.

**Sat.11****Real-time thermography during magnetic nanoparticle hyperthermia and numerical simulations suggest a surface shell like heat source around the tumor**Harley Rodrigues, Francielli Mello, Gustavo Capistrano, Carolina Martins, Sônia Santos, Nicholas Zufelato, Rafael Veloso, Elisângela Silveira-Lacerda, Andris Bakuzis*Universidade Federal de Goiás, Goiânia, Goiás, Brazil*

In magnetic nanoparticle hyperthermia, heating of a tissue containing nanoparticles is achieved by applying an alternating magnetic field. So far, several studies had been focusing on increasing the specific loss power (heating efficacy) of nanoparticles, but mostly at high field amplitude conditions. This work used a magnetic nanoparticle capable of heating at low field amplitude conditions, which has the advantage of avoiding non-specific tissue heating. In general, monitoring temperature during magnetic nanoparticle hyperthermia is usually done using invasive fibre-optic thermometers inside the animal. As a consequence, only few points in the temperature distribution profile can be monitored. One of the objectives of this work was to improve the surface temperature determination using non-invasive infrared thermography, and correlate it to intratumoral temperature distribution. In this work, 30-minute magnetic hyperthermia experiments were performed at 300 kHz with field amplitude in the order of 10 kA/m (130Oe), while the initial murine tumor volume was 586mm<sup>3</sup>, induced by sarcoma S180. In the experiment, 90 microliters of magnetic fluid were injected in three symmetrical tumor positions consisting of around 4 mg of nanoparticles. Prior to hyperthermia procedure the animal was anaesthetized with a solution of ketamine and xylazine. A soft ferrite-based biocompatible magnetic colloid consisting of manganese–ferrite (MNF) nanoparticles surface-coated with dimercaptosuccinic (dmsa) acid was used in the experiments, which was extensively characterized by several techniques (transmission electron microscopy (TEM), X-ray diffraction (XRD), dynamic light scattering (DLS), thermal gravimetric analysis (TGA), vibrating sample magnetometer (VSM)). MTT cytotoxicity studies revealed cell viability around 90% for particle concentration up to 50 micrograms/mL, using the S180 cells. Surface temperature measurements were performed using real-time thermography and fibre-optic thermometers. The precision of this temperature by this non-invasive technique was found to be less than 0.3K. In particular, for a given experiment, maximum temperature at the surface was found to be 48.4 degrees Celsius, while the maximum rectal temperature in the mouse was 35.3 degrees. Numerical simulations using COMSOL multiphysics software taking into account a multilayer skin structure and two nanoparticle distribution configurations (surface and volumetric distribution) were investigated. Finally, the comparison between the surface temperature from the simulations and the real-time thermography data suggests that the nanoparticles are more likely to be distributed around the tumor (surface shell-like configuration). Such conclusion is also supported by fibre-optic intratumoral temperature measurements with citrate-coated MNF nanoparticles.

**Sat.12**

**Magnetic Nanoparticle Hyperthermia for Treatment of Bladder Cancer: A Summary of Large Animal Studies and Remaining Challenges**

Alireza Mashal, Martin Huisjen, Kate McNerny, Karl Frantz, Mike Susedik, Carolyn Adams, Andrew Updegrave, Marvin Ross, Dan McKenna

*Actium Biosystems, Boulder, CO, USA*

Recently, we proposed a novel magnetic nanoparticle-mediated hyperthermia treatment for bladder cancer. In this approach, magnetic nanoparticles are mixed with the chemotherapy drug and directly instilled into the bladder via a catheter. The bladder is then illuminated with a time-varying magnetic field causing the nanoparticles to generate heat and increase the temperature of the bladder wall. A number of recent studies have shown that such combinations of intravesical chemotherapy and hyperthermia reduce the recurrence rates of non-muscle invasive bladder cancer when compared to chemotherapy alone. The advantage of magnetic nanoparticle techniques is the ability to selectively deliver thermal energy to malignant tissue if the parameters of the magnetic field illumination are optimally selected.

As a first step, we completed a round of large animal studies, using eight female pigs, to test the feasibility of achieving therapeutic temperatures in the bladder wall. In these studies, biocompatible magnetic nanoparticles were instilled into the pig bladder via a catheter and illuminated with biologically safe levels of magnetic fields using a custom made human-scale system. Our integrated system precisely controlled the temperature of the nanoparticle fluid to achieve therapeutic temperatures of 39 °C to 41 °C in the bladder interior wall for a duration of one hour.

Here, we will present our results showing the thermal dose delivered to the bladder wall. In addition, we will discuss necropsy and histology results - summarizing the impact of heat and nanoparticles on the bladder and surrounding tissue. Finally, we will discuss challenges that must be overcome before conducting clinical studies.

**Sat.13****Toxicity and genotoxicity in cells of the peripheral blood of Swiss mice exposed to non-uniform magnetic field**

Francielly Mello, Harley Rodrigues, Wanderson Costa, Luis Branquinho, Andris Bakuzis, Elisangela Silveira-Lacerda

*Universidade Federal de GOias, Goiania, Goias/Central, Brazil*

Several studies are conducted to evaluate and determine the toxicity of magnetic nanoparticles used in procedures for magnetic hyperthermia for cancer treatment. However, toxicological and genotoxic effects of the external alternating magnetic field effects *in vivo* are not so much understood. In order to investigate the toxicity profile of the magnetic hyperthermia therapy under non-uniform magnetic field configuration, tumor-free and without injection of magnetic fluid, male Swiss mice were exposed to different alternating magnetic field intensities (AMF). The animals (n = 12) were divided into four groups: 1) Standard (without exposure to AMF), 2) animals exposed to 14.7 kA / m; 3) 17.6 kA / m and 4) 20.6kA / m. Possible behavioral changes and signs of toxicity were checked by Hippocratic screening. The animals were observed after recovery from anesthesia during the first 4 hours and every day for 10 consecutive days, while body weight of the animals was monitored daily. At the end of 10 days of observation, the organs: liver, kidneys, spleen, heart and lungs were excised and examined macroscopically and the relative weight of organs was determined. The genotoxicity was measured by Comet assay. After 24 and 48 h of exposure to AMF, a sample of peripheral blood from the lateral tail vein of the animals were taken to measure DNA damage index (DI). The AMF did not induce behavioral changes in animals or signs of toxicity. The consumption of water and food, and excreta production compared to Standard ( $p>0.05$ ) were not changed. No gross lesions were detected in the organs. The index of relative weight of the organs of animals exposed to 14.7 and 20.6 kA / m AMF showed no statistical difference with the Standard group. The same was found for the 17.6kA/m group after 48h. The results indicate that exposure to AMF does not cause a change in the behavior of the animals and no toxicity, since it does not cause a change in organs associated with important physiological processes such as immune function, metabolic, circulatory and excretion therefore did not alter the supply, ensuring the body weight gain. Furthermore, they do not cause significant damage to the DNA of peripheral blood cells of Swiss mice, and the genotoxic effects observed amenable to repair.

**Sat.14****Influence of *in-vivo* tumor model on outcomes with magnetic nanoparticle hyperthermia**

Robert Ivkov, Anilchandra Attaluri, Sri Kamal Kandala, Jianan Wang, Michele Wabler, Michael Armour, Haoming Zhou, Christine Cornejo, Yonggang Zhang, Theodore DeWeese, Cila Herman

*Johns Hopkins University, Baltimore, MD, USA*

**Purpose:** Hyperthermia with magnetic iron oxide nanoparticles (MIONs) stimulated by alternating magnetic fields (AMFs) is a promising technology to cancer. Understanding intratumor nanoparticle concentration, distribution, and heat propagation is critical for clinical translation. **Methods:** Three human prostate cancer xenograft models (PC3, DU145 and LAPC4; n=40) having volume of  $0.15 \pm 0.02 \text{ cm}^3$  were injected with commercial MIONS (5.5 mg Fe/cm<sup>3</sup> tumor) or PBS. Twenty-four hours after injection tumors were harvested and assessed for total iron with inductively-coupled plasma mass spectrometry (ICP-MS) or for nanoparticle distribution using Prussian blue staining. A second cohort of mice bearing LAPC4 and PC3 tumors (n=50) was treated with AMF (48kA/m,  $160 \pm 5 \text{ kHz}$ ) for 20min, 24hrs after MION injection and followed for tumor growth. A third cohort of mice bearing LAPC4 tumors was used to study the effects of both hyperthermia (HT) and radiation therapy (RT). Mice in this third cohort were randomly assigned to control (MION only), HT (AMF amplitude modulated to achieve  $43.5 \pm 0.5^\circ \text{C}$ ), RT (RT5:5Gy; RT8: 8Gy; RT10:10Gy), RT5+HT groups. Mice were monitored for tumor growth. Kaplan-Meier analysis was performed assuming time to 4X as survival and Log-rank test was used to compare between groups. **Computer model:** Stained tissue sections were digitized and imported into COMSOL to perform 2D heat transfer analysis using the Pennes' bioheat equation. Results were qualitatively compared with experimental data. **Results:** ICP-MS and Prussian blue results showed variable MION retention ( $13.9 \pm 4.7$ ,  $12.4 \pm 1.4$ ,  $19.5 \pm 2.0$   $\mu\text{gFe/mg}$  tumor for PC3, DU145, and LAPC4, respectively), and varied nanoparticle distribution. Computer simulations predicted varied temperature distributions among the models that was consistent with observed tumor temperatures and growth delay. When compared with control group, the 48 kA/m group had a significant tumor growth delay ( $p \leq 0.05$ ) for LAPC4 while PC3 showed no significant tumor growth delay ( $p=0.11$ ). For combinations with RT, CEM43 of  $33.6 \pm 3.4$  and  $25.9 \pm 0.8$  were observed for HT and RT+HT groups. When compared against control all RT, HT, and RT5+HT groups showed significant tumor growth delay ( $p \leq 0.05$ ). RT5+HT showed significant tumor growth delay compared to RT5 ( $p \leq 0.005$ ) and performed slightly better than RT8 (median survival 55 vs. 47 days) but growth curves were not statistically different ( $p=0.21$ ). **Conclusion:** Varied thermal response can be modeled when MION distribution and retention are known. Significant treatment enhancement can be predicted and realized when nanoparticle HT is combined with RT, providing translational motivation.

**Sat.15****Imaging and Treatment Planning for Magnetic Nanoparticle Hyperthermia**

Alicia Petryk<sup>1</sup>, Robert Stigliano<sup>2</sup>, Fridon Shubitidze<sup>2</sup>, Hattie Ring<sup>3</sup>, Michael Garwood<sup>3</sup>, P. Jack Hoopes<sup>1,2</sup>

<sup>1</sup>Geisel School of Medicine, Dartmouth College, Hanover, NH, USA, <sup>2</sup>Thayer School of Engineering, Dartmouth College, Hanover, NH, USA, <sup>3</sup>Center for Magnetic Resonance Research, University of Minnesota, Minneapolis, MN, USA

Magnetic nanoparticle (mNP) mediated hyperthermia has potential for treatment efficacy following direct intratumoral injection, as a tumor bed therapy, and as a systemic treatment of metastatic disease. mNP produce cytotoxicity primarily through the release of energy in the form of heat when exposed to a noninvasive alternating magnetic field (AMF). The biologic effect achieved by heat is dependent on the delivered thermal dose, which is a function of time and temperature. Although thermal dose and tumor effect has been studied in a variety of monotherapy and adjuvant therapy settings for many years, the use of mNP to deliver cytotoxic heat, in either a global tumor or an individual cancer cell situation is not only novel, but affords significant cancer treatment/therapeutic ratio improvement promise that is not possible with conventional hyperthermia techniques (such as microwave, radiofrequency, laser and ultrasound). In spite of very promising recent results, the successful use of mNP hyperthermia in the clinical cancer setting will ultimately depend on the development of sophisticated treatment planning. Such treatment planning must be capable of accurately predicting the optimal use of the mNPs and the activating AMF, with respect to thermal dose in the tumor and relevant normal tissues.

Despite a number of sensitive and accurate techniques for assessing mNP within cells and *ex vivo* tissues, to date an accurate and clinically useful *in vivo* technique for determining (imaging) mNP levels and biodistribution in tumor and normal tissue has not been developed. Researchers at Dartmouth College and the University of Minnesota's Center for Magnetic Resonance Research (CMRR), are collaborating to optimize such a technique. The primary imaging platform will be an ultra-short T2 MRI technique (Sweep Imaging With Fourier Transformation/SWIFT), developed by CMRR Professor Michael Garwood. SWIFT provides a positive iron contrast enhancement and a reduced signal to noise ratio. *In vitro* and *in vivo* (mouse tumor, spontaneous canine tumor, goat breast) results will be discussed.



**Sat.16****Mitigation of eddy current heating during magnetic nanoparticle hyperthermia therapy**

Robert Stigliano, Fridon Shubitidze, Jack Hoopes

*Dartmouth College, Hanover, NH, USA*

**Purpose:**

The purpose of this study was to develop a technique which could be employed to reduce eddy current heating of normal tissue resulting from exposure to an alternating magnetic field (AMF) during magnetic nanoparticle hyperthermia (mNPH) treatment, without decreasing mNP heating of the tumor.

**Methods:**

Tissue mimicking phantoms and *ex vivo* rabbits were exposed to an AMF of various field strengths and frequencies. The AMF was generated by a 25kW induction heating system utilizing a single turn coil with a magnetic core. Experiments were conducted using both a flat treatment table (between the coil and the phantom/animal) and using a modified table surface designed to reduce the induction of eddy currents by displacing noncancerous tissue away from zones of high electric field strength. A plastic tube containing mNP's was embedded into the center of the phantom to evaluate the effect of the modified table surface on mNP heating above the center of the coil. Internal temperature data was collected using eight, single point fiber optic temperature sensors and surface temperature was recorded using a thermal camera. The maximum recorded rate of tissue temperature increase was used to evaluate the effect on eddy current heating in each case.

**Results:**

Eddy current heating was reduced by approximately a factor of two in both phantoms and *ex vivo* rabbits by displacing tissue by a maximum of 2.5 cm from the flat table surface. The phantom data showed that this displacement did not significantly affect mNP heating in the targeted treatment zone.

**Conclusion:**

Our results demonstrate the potential to decrease eddy current heating in normal tissue while maintaining mNP heating in the treatment volume by displacing normal tissue away from zones of high electric field strength. Treatments are limited by the normal tissue toxicity incurred by eddy current heating, thus, by mitigating this non-specific heating more power can be safely coupled to the coil. This has the effect of increasing the maximum treatment depth of the therapy and/or decreasing the concentration of mNP's necessary to achieve an effective thermal dose, which is a major stepping stone toward the treatment of metastatic cancer.

**Sat.17****Integrating Infrared Hyperthermia with Ionizing Radiation in Treatment of Cancer**

Edward Abraham<sup>1,2</sup>, Van Woo<sup>1</sup>, Cheryl Harlin-Jones<sup>1,2</sup>, Mark Pomper<sup>3</sup>, Anja Heselich<sup>4</sup>, Florian Frohns<sup>4</sup>

<sup>1</sup>Artesian Cancer Centers, Claremore, OK, USA, <sup>2</sup>Hyperthermia Associates, Claremore, OK, USA, <sup>3</sup>Horizon Medical Services, Tamarac, Fl, USA, <sup>4</sup>Darmstadt University of Technology, Darmstadt, Germany

**INTRODUCTION:** Patients with bulky and/or aggressive tumors are clinically challenging. To enhance the efficacy of ionizing radiation (photon or electron), we introduce an inexpensive and clinically effective infrared hyperthermia system. We combine longer wavelength black body infrared with halogen infrared spectra and superpose discrete wavelength infrared clinical lasers. The composite infrared spectrum spans far to near infrared with superposed spikes of tissue penetrating coherent 800 nm infrared. We apply hyperthermia immediately before and after (occasionally during) the application of ionizing radiation treatments. Multiple affixed RFID thermal probes were used to monitor surface thermal temperature and in some cases deeper temperatures. This has resulted in excellent patient acceptance and safety, and treatment efficacy.

**MATERIALS:** The far-infrared source: Tempco, CRE10002,. Halogen source: GE 17986, infrared lasers: Thor Corporation: 810 nm or Microlite Corporation 830 nm. Temperature monitoring: Veriteq Corporation RFID thermal monitoring, infrared thermometry, Fluke 63. Patients receive infrared hyperthermia for 20 minutes before the ionizing radiation therapy and 20 minutes after the ionizing radiation therapy with temperatures target 45 degrees centigrade the surface limiting temperature. The fractionated ionizing radiation administered as 1.8 and 2.0 Gy per fraction to up to 70 Gy. Tumor response was documented with direct caliper measurements when possible and photographic documentation. Diagnostic radiologic image monitoring: ultrasound, CT and PET/CT scanning.

**RESULTS:** > 100 patients have been successfully treated with variety of tumors: ranging skin tumors squamous, basal cell, melanoma, cutaneous t-cell lymphoma (mycosis fungoides), head and neck tumors, breast cancers, prostate cancer, anal, rectal cancers and gynecologic cancers.[ Selected breast cancer patients demonstrate statistically significant changes in rates of tumor diameter regression: addition of infrared hyperthermia to the ionizing radiation therapy versus radiation therapy alone. Our data also includes basic science work shows an effect of infrared hyperthermia on increasing double strand breakage beyond that observed with ionizing radiation alone.

**CONCLUSIONS:** Our infrared hyperthermia treatments are applied immediately before, after and in some case during ionizing radiation treatments. Our flexible and user friendly system has proved safe and effective because of patient accepted thermal monitoring. Investigations of effects of infrared hyperthermia on DNA strand breakage in cultured cells and its effect on tumor microenvironment with respect to intra- and extracellular parameters such as ATP and gap junction interconnections. The close collaboration between clinical development and basic science understanding allows rapid refinement and optimization of the combination of infrared radiation with ionizing radiation in the treatment of cancer.

**Sat.18**

**A Preclinical, Dual-Modality System for Focused Microwave Thermal Therapy and Real-Time 3D Microwave Thermal Monitoring**

John Stang, Mark Haynes, Guanbo Chen, Mahta Moghaddam

*University of Southern California, Los Angeles, USA*

The use of focused microwave thermal therapy as an adjuvant to radiation and chemotherapy for breast cancer treatment continues to be an active area of research with the aim of reducing local recurrence, as well as reducing harmful side effects and cosmetic harm of traditional treatments. With it, there is a clinical need for real-time, non-invasive monitoring of subcutaneous heat deposition.

In previous work, we developed a focused microwave thermal therapy system prototype capable of achieving 2 cm focal spot sizes and able to heat phantoms in excess of 55°C in a cavity geometry. Separately, we have demonstrated real-time 3D microwave imaging of differential temperature in simple breast phantoms with 2 cm spatial resolution, 0.5°C temperature resolution. In this work, we combine both modalities into a single system in order to demonstrate focused microwave thermal delivery with simultaneous 3D microwave thermal monitoring.

The dual-modality system is tested in two modes on gelatin breast phantoms: 1) targeted heating of single focal spots, 2) raster scanning to achieve uniform thermal delivery. In addition, numerical breast phantoms are used to evaluate the effectiveness of object pre-imaging on the performance of the real-time monitoring algorithm.

**Sat.19****Real-time Temperature Control using Dual Mode Ultrasound Array System**

Dalong Liu, Alyona Haritonova, Kamlesh Shroff, Mahdi Bayat, Rajagopal Aravalli, Efrosini Kokkoli, Emad Ebbini

*University of Minnesota, Minneapolis, USA*

Modern systems for minimally-invasive thermal therapy increasingly employ imaging for real-time feedback control to achieve the treatment objectives. Temperature control is used directly or indirectly to achieve a desired therapeutic endpoint (e.g. thermal dose in hyperthermia and ablative treatments) or specified levels of controlled release (e.g. thermally-sensitive liposome (TSL) carriers). MRI and ultrasound thermography have been proposed and demonstrated to provide noninvasive temperature feedback, each with its advantages and limitations. Real-time implementation of temperature imaging algorithms with high sensitivity and specificity to temperature change in heterogeneous tissue remains an important goal for most image-guided thermal therapy (IgTT) procedures. We have developed a dual-mode ultrasound array (DMUA) system for imaging and therapy with temperature imaging capability as a form of feedback in IgTT.

In this paper, we present temperature control results from a real-time DMUA system, which includes a custom designed frontend (32Tx/32Rx) and a fully programmable, GPU-accelerated data processing backend. The same DMUA is used for both low temperatures heating and single-transmit focus (STF) imaging. This approach allows for inherent registration between heating and imaging coordinate systems, thus improving the specificity by providing spatially-accurate tissue temperature feedback. The transmit sequencer design allows tight synchronization between heating pulse and imaging pulse. Echo data corresponding to each STF pulse is collected and beamformed on GPU. The post-beamformed frame is then passed to the data processing pipeline in the backend, where temperature estimation algorithm based on thermal strain computation is applied to a selected region of interest (ROI). The temperature data from one or more control point(s) is fed into a proportional-integral-derivative (PID) controller. The output of PID controller is used to directly modulate the subsequent heating pulse. The whole processing chain is capable of operating over 100 fps on a GTX285 GPU (Nvidia, Santa Clara, CA), providing a smooth temperature update at the target control point. We present results from tissue mimicking phantom and bovine cardiac tissue, demonstrating the robustness of temperature control setup in the temperature range that is relevant to hyperthermia and temperature-mediated drug delivery using TSLs. We show that STF imaging can be used to reliably estimate the temperature near the focal location. Robust temperature control based on simple PID controller at frame rates in excess of 100 frames per second is also demonstrated. These results demonstrate the promise of ultrasound thermography as a form of image-guidance and control in drug delivery and other thermal therapy applications.

**Sat.20****Evaluation of tissue-mimicking gelatin phantoms for use with MRgHIFU**Alexis Farrer, Joshua de Bever, Brittany Coats, Douglas Christensen, Allison Payne*University of Utah, Salt Lake City, UT, USA*

A tissue-mimicking phantom that accurately represents human tissue properties is important for both safety testing and for validating new imaging techniques used with MR-guided high intensity focused ultrasound (MRgHIFU) such as MR acoustic radiation force imaging (MR-ARFI). To achieve a variety of desired human tissue properties, we have fabricated and tested several variations of gelatin phantoms. These phantoms have been customized for mimicking acoustic tissue properties important for quality assurance testing as well as MR-ARFI validation, specifically the speed of sound, attenuation, and Young's modulus values.

Gelatin-based phantoms were fabricated from raw powder (Vyse Gelatin Co. and Sigma-Aldrich Corp.) with three different nominal bloom values, 125, 175, and 250 bloom, where a higher bloom value equates to increased stiffness. The speed of sound and attenuation of each phantom were measured using the through-transmission technique. To achieve acoustic properties similar to human tissue (speed of sound ~1550 m/s; attenuation ~0.4 dB/cm/MHz), the gelatin mixtures were made with a concentration of 50% evaporated milk and 50% water. The Young's modulus for each type of phantom was measured using an Instron 5944 single-column testing system at a strain rate of  $0.5 \text{ s}^{-1}$ . All phantoms were fabricated 3 to 18 hours prior to MR-ARFI experimental measurements, acoustic measurements, and Young's modulus testing; all testing was done at room temperature.

The Young's modulus values were derived by taking the mean of six samples per batch, then averaging the means from three separate batches. The Young's modulus intra-batch variation was typically 0.4 Standard Error Mean (SEM). The average attenuation values were calculated from four different phantom batches for each gelatin bloom value ( $0.31 \pm 0.05$ ,  $0.31 \pm 0.08$ , and  $0.36 \pm 0.05$  dB/cm/MHz for the 125, 175, and 250 bloom gelatins, respectively). All values for each bloom came from phantoms fabricated out of the same lot of raw gelatin powder.

The 125-bloom phantom is similar in elastic properties ( $9.5 \pm 1.8$  kPa) to brain tissue in humans, as reported in the literature. The 175-bloom ( $18.8 \pm 2.7$  kPa) and 250-bloom ( $29.4 \pm 4.7$  kPa) measured values were in the range for those reported for human fat and for glandular tissue, respectively.

We can achieve reliable tissue-mimicking phantoms with various representative speeds of sound, attenuations, and Young's modulus values for quality assurance testing and validation of experimental techniques.

**Sat.21**

**A New Energy Source For Thermal Medicine: Convective Thermal Water Vapor**

Michael Hoey<sup>1</sup>, Christopher Dixon<sup>2,1</sup>

<sup>1</sup>*NxThera Inc, Maple Grove, MN, USA*, <sup>2</sup>*Lenox Hill Hospital, NY, NY, USA*

Introduction: Traditional forms of electromagnetic energy have been applied to tissues where they are converted to thermal energy and conducted through tissue. Convective thermal water vapor (steam) is fundamentally different than earlier devices because it is produced externally and only thermal energy is convectively delivered through tissue. This pure thermal energy utilizes the latent heat of vaporization (540 cal/gm water) that is stored during its phase shift to vapor and releases it to the tissues as it condenses. This compares to 1 cal/gm/degree Celsius for hot water.

The purpose of this work was to validate the principles of convective thermal heating.

Methods: Thermal water vapor was produced using radiofrequency (RF) induction in a hand-piece and delivered to the tissue via a needle with small emitter holes. No electromagnetic energy entered the tissue. No ground pads were required and there were no considerations necessary for tissue characteristics. The principles of convective heating were studied in bench-top experiments and in-vivo studies. Initial work was conducted in beef liver and canine prostate followed by extirpated and in-vivo human prostate tissue. The tissues were analyzed by gross observation, vital staining and scanning electron microscopy. In addition, 30 patients with benign prostatic hyperplasia (BPH) were treated using a thermal water vapor device and followed with serial Magnetic Resonance Imaging MRI).

Results: Thermal lesions were produced a minimum 10X faster than RF, focused ultrasound or cryotherapy. Tissue ablation was uniform and controllable. Vital staining confirmed complete tissue ablation within the treatment zone. Serial MRI's demonstrated that vapor was convectively contained within prostate pseudocapsule barriers. Thermal lesions resolved by 93%, and total prostate volume was reduced by 26% at 3 months post procedure.

Conclusions: This is a novel thermal energy source unlike conventional therapies. The latent heat of vaporization makes this a powerful yet controllable treatment. Because the treatment times are short and there is no tissue desiccation, the tissue is almost completely resorbed. Vapor moving through the tissue convectively instead of by conduction is a more efficient thermal therapy and likely to be useful in various clinical applications.

**Author INDEX (by day, Posters are Wed evening)**

|                                 |                                                     |                           |                     |
|---------------------------------|-----------------------------------------------------|---------------------------|---------------------|
| Abi-Jaoudeh, Nadine             | Po.21                                               | Branquinho, Luis          | Po.15, Sat.13       |
| Abraham, Edward                 | Sat.17                                              | Braun, Gary               | Wed.6               |
| Abrams, Scott                   | Wed.25                                              | Buchman, Joseph           | Th.1                |
| Adams, Carolyn                  | Sat.12                                              | Bucsek, Mark              | Th.14               |
| Adams, Matthew                  | Wed.27                                              | Bull, Joan                | Th.25               |
| Adema, Gosse                    | Fri.4                                               | Campos, David             | Th.16               |
| Ahmed, Muneeb                   | Wed.26                                              | Cao, Xuefang              | Fri.25              |
| Aina, Olulanu                   | Fri.10                                              | Capistrano, Gustavo       | Po.15, Sat.11       |
| Ajith, Ashwin                   | Th.14                                               | Cardiff, Robert           | Fri.10              |
| Alimpich, Michelle              | Fri.11                                              | Carp, Stefan A            | Wed.17              |
| Andocs, Gabor                   | Th.15                                               | Caskey, Charles           | Th.4                |
| Aravalli, Rajagopal             | Sat.19                                              | Cattin, Philippe          | Po.11               |
| Argenta, Louis                  | Wed.19                                              | Chaudhari, Rishabh        | Po.24, Po.25        |
| Armour, Michael                 | Sat.14                                              | Chen, Eunice              | Sat.10              |
| Arshad, Hassan                  | Wed.15                                              | Chen, George L            | Fri.25              |
| Arthur, R Martin                | Th.10                                               | Chen, Guanbo              | Sat.18              |
| Atamas, Sergei                  | Fri.27, Po.29                                       | Chen, Lei                 | Th.12               |
| Attaluri, Anilchandra           | Sat.14, Wed.28                                      | Chen, Lili                | Fri.9               |
| Averill, Diana                  | Po.19                                               | Chiang, Jason             | Wed.29              |
| Bakuzis, Andris                 | Po.15, Sat.11, Sat.13                               | Choi, Jeunghwan           | Fri.22, Po.7, Wed.7 |
| Balasubramanian, Saravana Kumar | Fri.26                                              | Choi, Jung                | Fri.12              |
| Balidemaj, E                    | Wed.21                                              | Christensen, Douglas      | Po.17, Sat.20       |
| Ballard, John                   | Po.3                                                | Ciampa, Silvia            | Th.11               |
| Bardati, Fernando               | Th.11                                               | Coakley, Joe              | Wed.16              |
| Barnes, Klressa                 | Po.12, Po.5                                         | Coats, Brittany           | Sat.20              |
| Barnett, Gene                   | Sat.3, Sat.5                                        | Colebeck, Erin            | Wed.18              |
| Barrowes, Benjamin              | Po.22                                               | Conejo-Garcia, Jose       | Th.12               |
| Bartels, Lambertus W            | Sat.4                                               | Cornejo, Christine        | Sat.14              |
| Baust, John                     | Th.19                                               | Corwin, William           | Fri.19              |
| Baust, John G                   | Fri.19                                              | Costa, Wanderson          | Sat.13              |
| Baust, John M                   | Fri.19                                              | Cressman, Erik            | Po.18, Po.3, Wed.8  |
| Bayat, Mahdi                    | Sat.19                                              | Cressman, Erik N K        | Po.16               |
| Bedoya, Mariajose               | Th.16                                               | Crevecoeur, Guillaume     | Wed.31              |
| Behbahani, Mandana              | Sat.5                                               | Crezee, H                 | Wed.21              |
| Bel, A                          | Wed.22                                              | Crezee, Hans              | Th.11               |
| Bel, Arjan                      | Th.11                                               | Crezee, J                 | Wed.22              |
| Bemis, Lynne                    | Fri.21                                              | Dames, Chris              | Po.7                |
| Birla, Sohan                    | Wed.29                                              | Davis, Ryan               | Po.28               |
| Bischof, JC                     | Wed.3                                               | de Bever, Joshua          | Sat.20              |
| Bischof, John                   | Fri.22, Po.2, Po.4, Po.6, Po.7, Th.17, Wed.4, Wed.7 | Deckers, Roel             | Sat.4               |
| Bischof, John C                 | Fri.26                                              | de Kroon-Oldenhof, Rianne | Th.11               |
| Borrelli, Michael               | Fri.15                                              | Demedts, Daniel           | Th.7                |
| Brace, Christopher              | Th.16, Wed.29                                       | Dent, Judy                | Po.20               |
| Braden, Amy                     | Wed.19                                              | DeWeese, Theodore         | Sat.14, Wed.28      |
|                                 |                                                     | Dewhirst, Mark            | Fri.29              |
|                                 |                                                     | Diederich, Chris          | Wed.27              |

|                             |                                     |                              |                                 |
|-----------------------------|-------------------------------------|------------------------------|---------------------------------|
| Dillon, Christopher         | Wed.32                              | Goldberg, SNahum             | Wed.26                          |
| Dixon, Christopher          | Sat.21                              | Gourevich, Lana              | Wed.26                          |
| Donati, George              | Fri.11                              | Goya, Gerardo                | Po.27                           |
| Dumont, Erik                | Fri.10                              | Graham, Elizabeth            | Fri.11, Fri.13, Fri.14          |
| Dupré, Luc                  | Wed.31                              | Graner, Alexandra            | Fri.21                          |
| Dye, Nicholas B             | Po.24, Po.25                        | Graner, Michael              | Fri.21, Fri.28                  |
| Ebbini, Emad                | Sat.1, Sat.19, Th.18                | Griffin, Robert              | Po.12, Po.20, Po.5, Wed.8       |
| Egger, Sam                  | Th.1                                | Griffin, Robert J            | Wed.2                           |
| Elson, Paul                 | Sat.3                               | Guha, Chandon                | Fri.8                           |
| Epple, Laura                | Fri.21                              | Guiriba, Toni-rose           | Wed.28                          |
| Etheridge, Michael          | Fri.22, Po.4, Wed.4                 | Gutschenritter, Tyler        | Po.23, Th.24                    |
| Etheridge, Micheal          | Po.6                                | Haemmerich, Dieter           | Fri.17, Po.8, Th.21             |
| Etheridge, ML               | Wed.3                               | Hagmann, Mark                | Po.14                           |
| Evans, Sharon               | Th.13, Th.14, Wed.25                | Han, Misung                  | Po.28                           |
| Even, Lisa                  | Th.4                                | Hardee, Matt                 | Po.20                           |
| Fahrenholtz, Samuel         | Th.9                                | Haritonova, Alyona           | Sat.19                          |
| Farrer, Alexis              | Po.17, Sat.20                       | Harlin-Jones, Cheryl         | Sat.17                          |
| Feng, Yusheng               | Wed.14                              | Hasday, Jeffrey              | Fri.27                          |
| Ferrara, Katherine          | Fri.10, Th.4, Wed.30                | Hasday, Jeffrey D            | Po.29                           |
| Fiering, Steven             | Th.12                               | Hawasli, Ammar               | Sat.3                           |
| Finkenstaedt-Quinn, Solaire | Th.1                                | Haynes, Christy              | Fri.22, Po.2, Po.6, Th.1, Wed.4 |
| Fisher, Daniel              | Th.13                               | Haynes, CL                   | Wed.3                           |
| Fite, Brett                 | Fri.10, Th.4, Wed.30                | Haynes, Mark                 | Sat.18                          |
| Flynn, James                | Po.23, Th.24                        | Hazle, John D                | Po.16                           |
| Foiret, Josquin             | Th.4                                | Heberlein, Wolf              | Fri.15                          |
| Foley, Jessica              | Fri.5                               | Hedayati, Mohammad           | Wed.28                          |
| Forbes, Natalie             | Wed.6                               | Hellwinkel, Justin           | Fri.21                          |
| Frangineas, George          | Wed.16                              | Herman, Cila                 | Sat.14                          |
| Franken, NAP                | Wed.22                              | Herman, Joseph               | Wed.28                          |
| Frantz, Karl                | Sat.12                              | Heselich, Anja               | Sat.17                          |
| Fried, Nathaniel            | Wed.20                              | Hoey, Michael                | Sat.21                          |
| Frohns, Florian             | Sat.17                              | Hogan, C                     | Wed.3                           |
| Fuentes, David              | Po.18, Th.9                         | Hogan, Chris                 | Fri.22, Wed.4                   |
| Fuentes, David T            | Po.16                               | Holmes, Charles D            | Th.10                           |
| Gaba, Ron                   | Sat.6                               | Hood, Aaron                  | Wed.18                          |
| Gage, Andrew                | Fri.19                              | Hoopes, Jack                 | Po.22, Sat.16, Th.5             |
| Garwood, M                  | Wed.3                               | Hoopes, PJ                   | Wed.3                           |
| Garwood, Michael            | Fri.22, Po.2, Sat.10, Sat.15, Wed.4 | Hoopes, P Jack               | Sat.10, Sat.15, Th.12           |
| Garwood, Micheal            | Po.6                                | Hossann, Martin              | Wed.23                          |
| Geijsen, Debby              | Th.11                               | Huang, Xiao                  | Wed.6                           |
| Georgii, Joachim            | Th.7                                | Hubbard, Neil                | Fri.10                          |
| Giglio, Nicholas            | Wed.20                              | Huisjen, Martin              | Sat.12                          |
| Giustini, Andrew            | Sat.10                              | Hurley, Katie                | Fri.22, Po.2, Po.6, Th.1, Wed.4 |
| Glasmacher, Birgit          | Po.4                                | Hurley, KR                   | Wed.3                           |
| Glickson, Jerry             | Fri.23                              | Hurwitz, Mark                | Fri.6                           |
| Glory, Audrey               | Po.19                               | Hutchens, Thomas             | Wed.20                          |
| Godley, Andrew              | Th.26                               | Iacobuzio-Donahue, Christine | Wed.28                          |
|                             |                                     | Iaizzo, Paul                 | Po.3, Wed.9                     |



|                          |                                 |                          |                                   |
|--------------------------|---------------------------------|--------------------------|-----------------------------------|
| Idiyatullin, D           | Wed.3                           | Leeper, Dennis           | Fri.23                            |
| Iltis, Isabelle          | Wed.7                           | Lee, Yong J              | Po.25                             |
| Ingham, Elizabeth        | Th.4                            | Leigh, Nicholas D        | Fri.25                            |
| Ishikawa, Takeshi        | Fri.3                           | Lencioni, Alex           | Fri.21                            |
| Issels, Rolf D           | Fri.30                          | Leuthardt, Eric          | Sat.3                             |
| Ito, Fumito              | Th.13, Th.14                    | Levi-Polyachenko, Nicole | Fri.11, Fri.13,<br>Fri.14, Wed.19 |
| Ito, Yoshito             | Fri.3                           | Lewis, Lionel            | Sat.10                            |
| Ivkov, Robert            | Sat.14, Wed.28                  | Liapi, Eleni             | Wed.28                            |
| Jamshidi-Parsian, Azemat | Wed.8                           | Li, Li                   | Wed.23                            |
| Jarvis, Lesley           | Sat.10                          | Lim, Sangwook            | Po.10, Po.9                       |
| Jeon, S                  | Wed.3                           | Lin, Yu-Shen             | Th.1                              |
| Jeon, Seongho            | Fri.22, Wed.4                   | Liu, Dalong              | Sat.19, Th.18                     |
| Jeung, Taesig            | Po.10, Po.9                     | Liu, Yu                  | Fri.10, Th.4, Wed.30              |
| Jiang, Chunlan           | Th.17                           | Liu, Yue                 | Wed.28                            |
| Jimenez Lozano, Joel     | Wed.16                          | Lloyd, Bryn              | Po.11                             |
| Johnson, Sarah           | Fri.10                          | Lubner, Sean             | Po.7                              |
| Jones, Bradley T         | Fri.11                          | Maccarini, Paolo         | Wed.18                            |
| Jones, David             | Wed.29                          | MacLellan, Christopher   | Po.18                             |
| Jones, Lee               | Fri.2, Fri.24                   | MacLellan, Christopher J | Po.16                             |
| Jones, Martin            | Po.18                           | MacNeill, Christopher    | Fri.11, Fri.13, Fri.14,<br>Wed.19 |
| Kamal Kandala, Sri       | Sat.14                          | Madsen, Helen            | Fri.21                            |
| Kaufman, Peter           | Sat.10                          | Mahakian, Lisa           | Fri.10, Wed.30                    |
| Keelan, Robert           | Wed.10, Wed.11                  | Maier, Florian           | Po.16, Po.18, Th.9                |
| Kekalo, Katerina         | Po.22                           | Majumdar, Sharmilla      | Po.28                             |
| Kelly, Doug              | Po.23                           | Manstein, Dieter         | Wed.17                            |
| Kelly, Douglas           | Th.24                           | Maples, Danny            | Fri.16                            |
| Kheirrolomoom, Azadeh    | Th.4, Wed.30                    | Martins, Carolina        | Sat.11                            |
| Kim, Donghyuk            | Th.1                            | Mashal, Alireza          | Sat.12                            |
| Kim, Seog-Young          | Po.25                           | Ma, Sunyoung             | Po.10, Po.9                       |
| Knuttel, Floor M         | Sat.4                           | Matsuyama, Tatsuzo       | Fri.3                             |
| Kok, HP                  | Wed.21, Wed.22                  | Maurer-Jones, Melissa    | Th.1                              |
| Kokkoli, Efrosini        | Sat.19                          | McCarthy, Philip L       | Fri.25                            |
| Kokolus, Kathleen M      | Fri.25                          | McGough, Robert J        | Th.6                              |
| Kok, Petra               | Th.11                           | McKenna, Dan             | Sat.12                            |
| Kokura, Satoshi          | Fri.3                           | McNerny, Kate            | Sat.12                            |
| Koning, Gerben           | Wed.23                          | McWilliams, Brogan       | Wed.24                            |
| Koonce, Nathan           | Po.12, Po.20                    | Meggyeshazi, Nora        | Th.15                             |
| Kovago, Csaba            | Th.15                           | Meinken, Almer           | Po.4                              |
| Krishnan, Sunil          | Fri.7                           | Mello, Francielly        | Sat.13                            |
| Kruse, Dustin            | Th.4                            | Mello, Francielli        | Po.15, Sat.11                     |
| Ku, Amy                  | Wed.25                          | Merckel, Laura G         | Sat.4                             |
| Kumar, Gaurav            | Wed.26                          | Metzger, Greg            | Wed.7                             |
| Kurhanewicz, John        | Po.28                           | Mikhail, Andrew S        | Po.21                             |
| Kuster, Niels            | Po.11, Po.13, Wed.12, Wed.13    | Missios, Symeon          | Sat.3                             |
| Kyriakou, Adamos         | Po.11, Po.13, Wed.12,<br>Wed.13 | Moghaddam, Mahta         | Sat.18                            |
| Latimer, Cassandra       | Wed.20                          | Mohammadi, Alireza       | Sat.3, Sat.5                      |
| Laxton, Adrian           | Sat.3                           |                          |                                   |

|                      |                              |                              |                               |
|----------------------|------------------------------|------------------------------|-------------------------------|
| Moonen, Chrit TW     | Sat.4                        | Qiu, Jingxin                 | Fri.25                        |
| Morales, Dean        | Wed.6                        | Quick, Matthew               | Po.20                         |
| Moros, Eduardo       | Fri.12, Wed.13               | Rabin, Yoed                  | Wed.10, Wed.11                |
| Moser, Robert        | Wed.14                       | Ramadhyan, Satish            | Th.3                          |
| Moussa, Marwan       | Wed.26                       | Ranjan, Ashish               | Fri.16                        |
| Mücke, Eike          | Th.7                         | Redzic, Jasmina              | Fri.21                        |
| Muhitch, Jason       | Th.13, Th.14, Wed.25         | Reich, Norbert               | Wed.6                         |
| Müller, Werner       | Th.22                        | Reid, Sean                   | Wed.19                        |
| Mullin, Jeffrey      | Sat.5                        | Remis, RF                    | Wed.21                        |
| Mynderse, Lance      | Sat.9                        | Repasky, Elizabeth A         | Fri.25, Wed.1                 |
| Nakamura, Kosuke     | Po.1                         | Rhee, Juong G                | Po.24, Po.25                  |
| Natesan, Harishankar | Po.7                         | Rieke, Viola                 | Po.28                         |
| Nath, Kavindra       | Fri.23                       | Ring, Hattie                 | Po.2, Po.6, Sat.15            |
| Nau, William         | Wed.20                       | Ring, HL                     | Wed.3                         |
| Nederveen, AJ        | Wed.21                       | Robilotto, Anthony           | Fri.19                        |
| Negussie, Ayele H    | Po.21                        | Rodermond, HM                | Wed.22                        |
| Nelson, David        | Fri.23                       | Rodrigues, Dario             | Wed.18                        |
| Neufeld, Esra        | Po.11, Po.13, Wed.12, Wed.13 | Rodrigues, Harley            | Po.15, Sat.11, Sat.13         |
| Newhardt, Ryan       | Fri.16                       | Rodriguez, Analiz            | Sat.3                         |
| Notter, Markus       | Th.22                        | Roemer, Robert               | Wed.32                        |
| Oakley, Emily        | Wed.15                       | Rossmann, Christian          | Fri.17, Po.8                  |
| Oei, Arlene Leonie   | Wed.22                       | Ross, Marvin                 | Sat.12                        |
| Okajima, Manabu      | Fri.3                        | Rott, Leoni                  | Po.4                          |
| Ota, Satoshi         | Po.1                         | Rudie, Eric                  | Th.2                          |
| Ott, Oliver          | Th.28                        | Sadhukha, Tanmoy             | Wed.5                         |
| Ozhinksi, Eugene     | Po.28                        | Sajjadi, Amir Y              | Wed.17                        |
| Pallaoro, Alessia    | Wed.6                        | Sakamoto, Naoyuki            | Fri.3                         |
| Panyam, Jayanth      | Wed.5                        | Salahi, Sara                 | Wed.18                        |
| Parker, Dennis       | Wed.32                       | Salgaonkar, Vasant           | Wed.27                        |
| Partanen, Ari        | Po.21                        | Santos, Sônia                | Sat.11                        |
| Payne, Allison       | Po.17, Sat.20, Wed.32        | Sauer, Rolf                  | Th.28                         |
| Payne, Michael       | Po.23, Th.24                 | Schnell, Emily               | Wed.24                        |
| Pearce, John         | Fri.1, Fri.20, Fri.28, Th.5  | Schroeder, Jason             | Sat.3                         |
| Pearce, John A       | Fri.26                       | Schubert, Gerald             | Sat.4                         |
| Pereira, Pedro       | Wed.18                       | Schumann, Christian          | Th.7                          |
| Perkins, William     | Wed.20                       | Scott, Serena                | Wed.27                        |
| Peters, Nicky HGM    | Sat.4                        | Sehrawat, Anjali             | Wed.10                        |
| Petryk, A            | Wed.3                        | Seo, Jai                     | Th.4, Wed.30                  |
| Petryk, Alicia       | Sat.10, Sat.15, Th.5         | Shafirstein, Gal             | Po.12, Wed.13, Wed.15         |
| Piazena, Helmut      | Th.22                        | Shetty, Anil                 | Th.9                          |
| Polascik, Thomas     | Th.19                        | Shimada, Kenji               | Wed.10, Wed.11                |
| Pomper, Mark         | Sat.17                       | Shroff, Kamlesh              | Sat.19                        |
| Potla, Ratnakar      | Fri.27, Po.29                | Shubitidze, Fridon           | Po.22, Sat.10, Sat.15, Sat.16 |
| Prakash, Punit       | Th.8, Wed.24                 | Silveira-Lacerda, Elisangela | Sat.13                        |
| Preiswerk, Frank     | Po.11                        | Silveira-Lacerda, Elisângela | Po.15, Sat.11                 |
| Preusser, Tobias     | Th.7                         | Simon, David                 | Po.23, Th.24                  |
| Przybyla, Beata      | Po.12                        | Singal, Ashish               | Po.3                          |
| Qin, Zhenpeng        | Fri.26, Th.17                |                              |                               |

|                         |                               |                              |                      |
|-------------------------|-------------------------------|------------------------------|----------------------|
| Singh, Ishwar           | Fri.27, Po.29                 | van Rhoon, Gerard            | Th.28, Wed.23        |
| Soetaert, Frederik      | Wed.31                        | van Stam, Gerard             | Th.11                |
| Sommer, Graham          | Wed.27                        | Vaupel, Peter                | Th.22                |
| Song, Chang W           | Wed.2                         | Veloso, Rafael               | Sat.11               |
| Soule, Charles          | Po.3                          | Venkatesan, Aradhana         | Po.21                |
| Soullie, Thomas         | Wed.23                        | Vollmers, Manda              | Wed.7                |
| Sprinkhuizen, Sara      | Wed.17                        | von Dresky, Caroline         | Th.7                 |
| Sroka, Thomas           | Sat.10                        | Vujaskovic, Zeljko           | Po.24, Po.25, Th.27  |
| Stafford, Jason         | Po.18                         | Wabler, Michele              | Sat.14               |
| Stafford, R Jason       | Po.16, Sat.8, Th.9            | Wang, Jianan                 | Sat.14               |
| Stalpers, LJA           | Wed.21, Wed.22                | Wang, Yuanguo                | Wed.26               |
| Stalpers, Lukas         | Th.11                         | Ward, Arlen                  | Wed.20               |
| Stang, John             | Sat.18                        | Warren, Warren               | Po.28                |
| Stauffer, Paul          | Wed.18                        | Warzen, Brian                | Wed.15               |
| Steggerda-Carvalho, Eva | Th.11                         | Watson, Katherine            | Wed.30               |
| Stigliano, Robert       | Po.22, Sat.10, Sat.15, Sat.16 | Watts, Edwin                 | Th.24                |
| Subbiah, Jeyam          | Wed.29                        | Weaver, Matt                 | Po.23, Th.24         |
| Susedik, Mike           | Sat.12                        | Werner, Beat                 | Po.13                |
| Szasz, Oliver           | Po.10, Po.9, Th.15            | Wessalowski, Ruediger        | Th.23                |
| Szekely, Gabor          | Po.11, Po.13, Wed.13          | West, Derek                  | Po.26, Sat.7         |
| Szlag, Victoria         | Th.1                          | Wiedmann, Timothy            | Wed.5                |
| Szwedo, Jakob           | Fri.15                        | Wolkers, Willem F            | Fri.26               |
| Taj-Eldin, Mohammed     | Th.8                          | Wong, Andrew                 | Fri.10, Th.4, Wed.30 |
| Takemura, Yasushi       | Po.1                          | Wong, Rosemary               | Tu1                  |
| Tam, Sarah              | Th.4, Wed.30                  | Wood, Bradford J             | Po.21                |
| Tatter, Stephen         | Sat.3                         | Woodrum, David               | Sat.9                |
| Taylor, Oneita          | Po.23                         | Woo, Van                     | Sat.17               |
| ten Hagen, Timo         | Wed.23                        | Wu, Jonah                    | Fri.15               |
| ten Hagen, Timo LM      | Fri.18, Th.20                 | Xu, Yi                       | Fri.22               |
| Thajudeen, Thaseem      | Wed.4                         | Yamada, Tsutomu              | Po.1                 |
| Thompson, Edreca        | Fri.11                        | Yarmolenko, Pavel            | Po.21                |
| Tomitaka, Asahi         | Po.1                          | Young, Christe               | Wed.19               |
| Topsakal, Erdem         | Wed.18                        | Yu, Jennifer                 | Sat.2, Th.26         |
| Toraya-Brown, Seiko     | Th.12                         | Yu, Jesang                   | Po.10, Po.9          |
| Trinks, J               | Wed.21                        | Zasadzinski, Joseph          | Wed.6                |
| Trobaugh, Jason W       | 0048                          | Zhang, Hong                  | Wed.10, Wed.11       |
| Tulapurkar, Mohan       | Fri.27                        | Zhang, J                     | Wed.3                |
| Tulapurkar, Mohan E     | Po.29                         | Zhang, Jinjin                | Fri.22, Sat.10       |
| Turk, Mary Jo           | Th.12                         | Zhang, Yonggang              | Sat.14               |
| Turner, Paul            | Po.14                         | Zhao, Xiaofeng               | Th.6                 |
| Updegrave, Andrew       | Sat.12                        | Zheng, Jinjin                | Po.6                 |
| Utecht, L               | Wed.3                         | Zhong, Yi                    | Wed.28               |
| Van Buskirk, Robert     | Fri.19                        | Zhou, Cliff                  | Wed.14               |
| van Dalen, Thijs        | Sat.4                         | Zhou, Haoming                | Sat.14, Wed.28       |
| van den Berg, CAT       | Wed.21                        | Zhou, Rong                   | Fri.23               |
| van den Bosch, Maurice  | AAJ Sat.4                     | Zufelato, Nicholas           | Sat.11               |
| van Gorp, JMHH          | Sat.4                         | Zum Vorde Sive Vording, Paul | Th.11                |

# Notes

# Notes

***Thanking our sponsors again!***

**Platinum Sponsors**



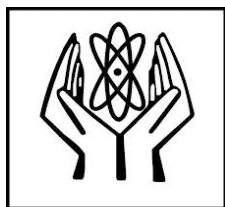
**Gold Sponsors**



**Silver Sponsors**



### Bronze Sponsors



RADIATION RESEARCH SOCIETY



~~~~~

FUTURE MEETINGS:

2015 Annual STM meeting, April 14-18, Orlando, FL

Buena Vista Palace Hotel and Spa



~~~~~

**2016 International Congress of Hyperthermic Oncology  
(ICHO) in the USA**

*Hosted by STM*

**More information coming soon.....**